Modelling peatlands as a complex adaptive systems

Morris, Paul John

MODELLING PEATLANDS AS COMPLEX ADAPTIVE SYSTEMS

Paul John Morris

Thesis submitted for the degree of *PhD* of the University of London, 22nd July 2009.
Following examination, minor corrections submitted February 2010.

Department of Geography,
Queen Mary, University of London,
327 Mile End Road,
London E1 4NS
United Kingdom.

Abstract

A new conceptual approach to modelling peatlands, **DigiBog**, involves a Complex Adaptive Systems consideration of raised bogs. A new computer hydrological model is presented, tested, and its capabilities in simulating hydrological behaviour in a real bog demonstrated. The hydrological model, while effective as a stand-alone modelling tool, provides a conceptual and algorithmic structure for ecohydrological models presented later.

Using **DigiBog** architecture to build a cellular model of peatland patterning dynamics, various rulesets were experimented with to assess their effectiveness in predicting patterns. Contrary to findings by previous authors, the ponding model did not predict patterns under steady hydrological conditions. None of the rulesets presented offered an improvement over the existing nutrient-scarcity model.

Sixteen shallow peat cores from a Swedish raised bog were analysed to investigate the relationship between cumulative peat decomposition and hydraulic conductivity, a relationship previously neglected in models of peatland patterning and peat accumulation. A multivariate analysis showed depth to be a stronger control on hydraulic conductivity than cumulative decomposition, reflecting the role of compression in closing pore spaces. The data proved to be largely unsuitable for parameterising models of peatland dynamics, due mainly to problems in core selection. However, the work showed that hydraulic conductivity could be expressed quantitatively as a function of other physical variables such as depth and cumulative decomposition.

DigiBog architecture was used to build a simple, vertical, ecohydrological model of long-term peat accumulation. As model complexity was increased under a self-organisation approach, model predictions of peat accumulation rates and surface wetness changed dramatically, revealing the importance of feedbacks between peatland hydrological behaviour and peat physical properties. This work may have important implications for palaeoclimatic reconstructions which assume peatland surface wetness to be a reliable climatic indicator. The expansion of the model to include horizontal space altered model behaviour in quantitative and qualitative terms.

Table of Contents

Abstract 2
Table of Contents 3
Chapter 1: Introduction 9
1.1. Peatland Process and Structure 10
1.1.1. Background 10
1.1.2. Rationale part I: peatlands as important global carbon stores 11
1.2. Modelling Peatland Development and Structure 14
1.2.1. The Groundwater Mound Hypothesis 14
1.2.2. The Bog Growth Model 15
1.2.3. Mixed or ecohydrological models 17
1.2.4. Surface patterning models 18
1.2.5. An existing 3-D, dynamic model of peatland ecohydrology? 22
1.3. Complex Adaptive Systems and Emergent Behaviour 23
1.3.1. What are Complex Adaptive Systems? 23
1.3.2. Complexity versus chaos: an issue of scale? 24
1.3.3. Peatlands as Examples of Complex Adaptive Systems 26
1.3.4. Rationale part II: the need for a new conceptual and modelling approach 27
1.4. Thesis Aim and Objectives 28
1.4.1. Model structure 28
1.4.2. Research objectives 29
1.5. Methodological Strategy 31
1.5.1. Construction of DigiBog hydrological model 31
1.5.2. Construction of a model of peatland patterning 31
1.5.3. Predicting hydraulic conductivity in peat soils 31
1.5.4. Modelling peat accumulation over millennial timescales 32
Chapter 2: Modelling Bog Hydrology 35
2.1. Basic Hydrological Concepts 36
2.2. Groundwater Modelling 38
2.3. Hydrological Submodel Description 41
2.3.1. Space, time and heterogeneity in **`DigiBog`** 41
2.3.2. Algorithmic structure 43
2.3.3. Hydrological submodel outputs 44
2.4. Testing `DigiBog_Hydro` 46

2.4.1. Testing background 46
2.4.2. Testing for conservation of mass 46
2.4.3. Testing water-table configurations against analytical solutions 47
2.5. Extended Demonstration of Hydrological Model 52
2.5.1. Experimental setup 52
2.5.2. Demonstration Results 57
2.6. Simulating a Real Bog 60
2.6.1. Site description 60
2.6.2. Model setup, parameterisation 63
2.6.3. Model spin-up 65
2.6.4. Model response to rainfall events 68
2.7. Discussion and Conclusions 70
Chapter 3: Cellular Models of Peatland Patterning 73
3.1. Introduction to Peatland Patterning 74
3.1.1. Background 74
3.1.2. Issues of scale 75
3.1.3. Pattern classification and measurement 76
3.1.4. Models of peatland patterning 76
3.1.5. Chapter aim, objectives 80
3.2. Ponding Model of Peatland Patterning 81
3.2.1. Model description and assumptions 81
3.2.2. Recreating and improving the ponding model 83
3.2.3. Results 85
3.3. Nutrient-Scarcity Model for Peatland Patterning 91
3.3.1. Model description and assumptions 91
3.3.2. Building a water-scarcity model 92
3.3.3. Results 92
3.4. Ecological Memory in Peatland Patterning 95
3.4.1. What is ecological memory? 95
3.4.2. Ecological memory in peatlands 95
3.4.3. Incorporating memory into the ponding model 97
3.4.4. Results 100
3.5. Discussion 103
3.6. Conclusions 108
Chapter 4: Homeostasis in Peat Properties 111

4.1. Introduction 112
4.1.1. Theoretical relationship between peat decomposition and hydraulic conductivity 112
4.1.2. The influence of plant community 115
4.1.3. A mechanism for homeostasis in peatland ecohydrology 117
4.1.4. Chapter aim, objectives 119
4.2. Methodology 120
4.2.1. Study site and peat type 120
4.2.2. Experimental design 122
4.2.3. Core extraction and preparation 123
4.2.4. Measuring peat hydraulic conductivity 126
4.3. Results and Analysis 134
4.3.1. Summary of Results 134
4.3.2. Derivation of a functional relationship for use in ***DigiBog*** 139
4.4. Discussion and Conclusions 143
Chapter 5: Modelling Peat Accumulation in One Dimension 148
5.1. Introduction 149
5.1.1. Background 149
5.1.2. Chapter aim, objectives 154
5.2. A Simple Model of Peat Accumulation 156
5.2.1. Conceptual structure 156
5.2.2. Hydrological submodel 156
5.2.3. Productivity submodel 157
5.2.4. Decay submodel 157
5.2.5. Model testing 158
5.2.6. Demonstration of simple model 161
5.3. Simulating Water-Table-Dependent Peat Formation 168
5.4. Simulating Decay-Dependent Hydraulic Conductivity 174
5.5. Simulating Peatland Lateral Expansion 182
5.6. Conclusions 185
Chapter 6: Modelling Peatland Dynamics in Two Dimensions 188
6.1. Introduction 189
6.1.1. Synthesis 189
6.1.2. Rationale 192
6.1.3. Chapter aim, objectives 192

6.2. Model Description 194
6.2.1. Algorithmic structure 194
6.2.2. Hydrological submodel 194
6.2.3. Productivity submodel 195
6.2.4. Decay submodel 195
6.2.5. Hydrophysical submodel 197
6.2.6. Model time trials 197
6.2.7. Experimental design 198
6.3. Results 200
6.4. Discussion 208
6.5. Conclusions 212
Chapter 7: Thesis Conclusions 215
7.1. Success of Thesis in Addressing Aim and Objectives 216
7.1.1. Hydrological modelling 216
7.1.2. Peatland patterning modelling 216
7.1.3. Laboratory investigation of the controls on peat hydraulic conductivity 217
7.1.4. Modelling peat accumulation in 1-D and 2-D 219
7.2. Agenda for Future Research 221
7.2.1. Hydrological modelling 221
7.2.2. Peatland patterning 222
7.2.3. Controls on peat hydraulic conductivity 223
7.2.4. Modelling peat accumulation 224
Acknowledgements 228
References 229

Researchers have already cast much darkness on the subject, and if they continue their investigations we shall know nothing at all about it.

—

Mark Twain

This thesis is dedicated to my parents.

Chapter 1: Introduction

In this chapter, a literature synthesis is used to introduce basic elements of the peatland system, and a number of important existing models of peatland behaviour are described and evaluated. The concept of complexity is introduced, and peatlands are considered as prototypical examples of Complex Adaptive Systems. A two-part rationale for the thesis identifies: i) peatlands as globally important terrestrial carbon stores, which are potentially at risk from changing climates; and ii) the need for a new approach to modelling peatland system behaviour. A new conceptual model is suggested. Finally, the overall aim of the thesis is formalised, and specific objectives are identified within this aim.

1.1. Peatland Process and Structure

1.1.1. Background

The term 'peatland' covers a diverse range of ecosystem types which develop at most latitudes and at a range of altitudes. Peatlands are the world's largest subset of wetlands, and peatland types include tropical mangrove swamps and tropical swamp forests (see Figure 1.1). As Gorham (1991) notes, however, the vast majority of global deep peat deposits are in the boreal and subarctic zones of the northern hemisphere, as shown in Figure 1.1. Common types of peatlands in these areas, as well as in temperate marine climates such as the British Isles, include upland blanket bogs, minerotrophic fens, heather moorlands and ombrotrophic raised bogs. It is the latter which forms the main focus of the current study.

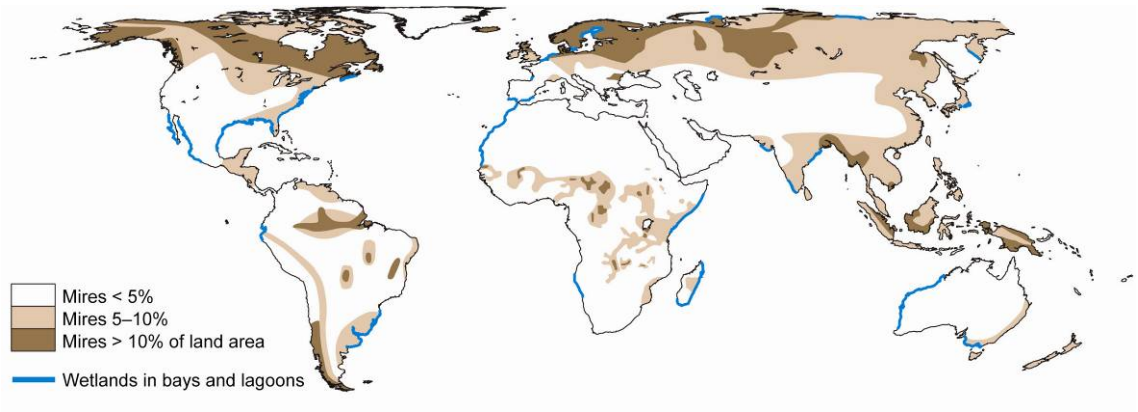

Figure 1.1: Map showing approximate extent and distribution of the world's major peat deposits (not to scale). Redrawn from original maps, copyright International Peat Society; used with permission.

Especially in ombrotrophic raised bogs (rain-fed peatlands, with no minerotrophic groundwater input), soil conditions are commonly cold, acidic, nutrient-poor and perennially waterlogged (van Breemen, 1995). The *Sphagnum* moss species that dominate bogs form the very aquifer upon which subsequent generations grow, by laying down highly porous, yet often poorly-permeable, thermally insulating litter, or peat, which is resistant to decay by micro organisms. While most landscapes studied by Earth scientists are born out of interactions between physical and chemical processes and their influence upon mineral bedrock or soil, thereby priming the area for subsequent biotic colonisation, it is rare that biological processes are responsible for building the very landforms themselves. The latter, however, is the case with peatlands, although it may be more helpful to consider their growth as the result of the

incompetence of certain biological processes, chiefly those of decay. Peat consists of the poorly decayed remains of plants, preserved by virtue of its own inherent recalcitrance and local conditions unfavourable for microbial decomposers.

For any substantial depth of peat to accumulate, vegetation productivity must exceed mass losses via decay over time scales of 10^2-10^3 years. Plant detritus is added to the system in the form of stems, branches and leaves in the zone overlapping with and immediately below the uppermost live vegetation layer (that containing photosynthesising leaves), and from vascular plant root matter several decimetres below this (Frolking *et al.*, 2001). Successive cohorts of vegetation detritus added to the top of the system gradually bury the deposits of previous years. The *Sphagnum* stems that make up the majority of peat dry mass in ombrotrophic bogs remain upright and intact initially, whilst still at shallow depths. As decay progresses, the removal of organic mass and the resultant decrease in structural rigidity, allied to an increasing weight of material above, means that the stems eventually begin to collapse and become horizontally aligned. Below this usually narrow zone of collapse (Clymo, 1992), the stems settle into their new configuration, with the volume and interconnectedness of individual pore spaces greatly reduced (see Chapter 4). Peat decay can occur both aerobically and anaerobically. In the upper, aerated layers of peat above the water-table, aerobic rates of decay are at least an order of magnitude greater than rates in the lower, unaerated layers below the water-table. As such, conditions in the upper, aerated layer above the water-table (often termed the "acrotelm" – *cf.* Ingram, 1978), largely determine the characteristics of the material that is eventually submerged below the water table. This lower layer is often termed the "catotelm" (Ingram, 1978). While the acrotelm-catotelm divide is often defined in terms of lowest annual water-table position, it is often very broadly coincidental with the zone of collapse of *Sphagnum* stems described above. Indeed, a certain degree of confusion surrounds the matter because some authors use the terms acrotelm and catotelm to mean the layers above and below the zone of collapse (rather than the water table), respectively. This issue of terminology is discussed in more detail in section *1.2.2.*, below.

1.1.2. Rationale part I: peatlands as important global carbon stores

The accumulation of peat represents the fact that carbon fixed by peatland plants via photosynthesis is not all released back into the atmosphere by decomposition. For this reason peatlands have been, during the Holocene, net sinks of carbon: Gorham (1991)

estimated that carbon constitutes 51.7% of dry peat mass. In an exploratory modelling study, Hilbert *et al.* (2000) showed how individual peatlands could switch rapidly from being sinks to sources of carbon. When one then considers that the microbial decomposition of peat produces mainly methane and carbon dioxide, the two most important greenhouse gases, the potential importance of peatlands in global climate change starts to become apparent (Moore *et al*., 1998).

Gorham (1991) estimated peatlands in the boreal and subarctic zones of the northern hemisphere alone represent a soil carbon store of 455 Gt (455,000,000,000 t), accounting for one third of the world's soil carbon, the vast majority of which is in the boreal and subarctic zones of North America, Fennoscandia and the former Soviet Union. It is also in these areas where climate change threatens to have the greatest effect on peat accumulating systems (Moore *et al*., 1998). The great expanses of permafrost peat in western Siberia, frozen and biologically dormant for millennia, are beginning to thaw due to rising temperatures. Strong evidence suggests that these peatlands are beginning to provide a large contribution to atmospheric carbon levels as the previously frozen peat there begins to decompose (e.g. Walter *et al*., 2006; Dutta *et al*., 2006). Peatlands in some areas of the world are also under pressure from human interests. Turunen (2008) estimated that, in 1950, intact, undrained peatlands in Finland covered an area of 8.8 M ha, out of a total peatland area in Finland of 10.2 M ha (equivalent to 86.2 %). By 2000, this figure had decreased to 4.0 M ha (38.4 %), with the rest drained for agriculture, pasture or forestry. Klinger *et al*. (1996) even proposed that the drawdown and release of carbon gases by peatlands may impart enough radiative forcing on the Earth's energy budget to act as a control on the glacial-interglacial cycle. Payette *et al.* (2004), however, found that permafrost meltwater in Canada and Fennoscandia provided conditions favourable to terrestrialisation, and that the thawing of such systems led to them becoming local sinks, rather than sources, for atmospheric carbon as peat accumulation reinitiated. The thawing of frozen peat soils also has the effect of releasing large amounts of previously frozen dissolved organic carbon into streams, eventually entering the world's oceans (Frey and Smith, 2005). Such acidification could have severe and far-reaching implications for marine ecosystems. Experimental work by Silvola (1986) suggests that, due to reduced water levels and so increased oxygenation, drained portions of peatlands can release carbon dioxide at three to four times their normal, anoxic rate. Extensive drainage can severely disrupt the mutual dependence of peat accumulation and waterlogged soil conditions,

leading to irreversible damage to the peat accumulating system and, potentially, the oxidation of thousands of years of stored carbon in just a few decades.

It is clear, then, that a detailed understanding of the processes of peat formation, accumulation and decay, including the ways in which peatlands interact with changing environmental conditions, may be crucial to the climate change debate. There is a need to quantify more accurately the potential release of carbon gases from drying, thawing and harvested peatlands. Then, the scientific community can begin to identify the most vulnerable peat accumulating systems, especially any which are close to thresholds of change, so as to inform international policy (Randall *et al.*, 2007) and to help refine the predictions of climate models (Baird *et al*., 2009). Before the true importance of peatlands to climate change can be assessed, however, the scientific community requires a rule-based understanding of the integrated spatio-temporal dynamics of peatland development. Any reliable conceptual model of whole-system behaviour must take account of ecological and hydrological processes and their linkages at appropriate scales and in three dimensions. As argued in the following section, such a modelling approach may currently elude the peatland science community. Its development would appear to require a paradigm shift away from traditional models which consider individual, isolated processes in highly constrained and oversimplified situations.

1.2. Modelling Peatland Development and Structure

There have been many previous attempts to model different aspects of peatland development and structure. Some models have focused almost exclusively on ecological processes such as plant community succession or peat decay, while others have focused on hydrological processes. A small number have attempted to combine both ecological and hydrological processes and their interactions, with varying degrees of success. Some models have been developed as tools for understanding the role of peatlands in the global carbon cycle, while others have been used to help decipher age-depth relationships in peat cores, for the purposes of palaeoenvironmental reconstruction. Some of the most important models of peatland development are discussed below, in an attempt to justify the need for a new model and, more fundamentally, the need for a new approach to modelling peatlands.

1.2.1. The Groundwater Mound Hypothesis

Seemingly developed independently by both Ingram (1982) and Childs and Youngs (1961) (*cf.* Belyea and Baird, 2006), the Groundwater Mound Hypothesis (GMH; Ingram's name for the idea) predicts the maximum size and the shape to which a raised bog will grow, in idealised circumstances. The GMH is described in essence by:

$$\frac{U}{K} = \frac{H^2}{2Lx - x^2} \tag{1.1}$$

where U is net drought-year rainfall (L T^{-1}; total rainfall minus losses due to evapotranspiration and seepage), K is hydraulic conductivity (L T^{-1}) (assumed uniform for an entire peatland), $2L$ is the width of the bog (L), and H is bog height at distance x from one edge (both L). When $x = L$ (*i.e.* at the bog centre), Equation (1.1) simplifies to:

$$\frac{U}{K} = \frac{H_m^2}{L^2} \tag{1.2}$$

where H_m is the height at the centre of the bog (L). The GMH incorporates a simple ecohydrological relationship, in that continued peat growth requires suitably wet conditions (in the form of persistently high water tables), and the fact that a high, domed water table can only exist in a bog of sufficient thickness. For a given combination of

rainfall rate and hydraulic conductivity, the groundwater mound reaches a certain equilibrium height. The high decay rates above the drought water table prevent the bog from growing far beyond that height, and the profile shape of the bog is predicted to follow closely that of the water table. Thus, bog surface elevation is limited by rainfall rates during drought conditions. The characteristics of the anoxic zone are, however, effectively ignored. Ingram (1982) recognised three main assumptions of the GMH: (1) the hydraulic conductivity of catotelm peat is spatially uniform; (2) vertical hydraulic gradients can be ignored, and the horizontal hydraulic gradient is given by the water table gradient (this assumption is known as the Dupuit-Forchheimer approximation: see Chapter 2); (3) during drought conditions, net rainfall flows at a constant rate through the catotelm, and oxic zone seepage is zero. In their detailed mathematical analysis of the GMH and Clymo's (1984) Bog Growth Model (see section *1.2.2.*, below), the main body of which is not repeated here, Belyea and Baird (2006) showed that a fourth assumption implicit within the GMH is: (4) during nondrought conditions, oxic zone transmissivity decreases elliptically with distance from the bog's centre, where transmissivity is the product of hydraulic conductivity and the thickness of flow. The possibility of horizontal variability of peat properties and process rates is an important one, and is used later in this thesis to justify the need for spatially distributed modelling of peat accumulation (see Chapter 6).

1.2.2. The Bog Growth Model

Clymo (1984) presented a simple, closed-form equation, which he called the Bog Growth Model (BGM), to describe peat accumulation in the anoxic zone. In the BGM, oxic-zone processes are effectively ignored, such that input of mass to the anoxic zone is set to a constant. In contrast to the GMH, which uses only hydrological parameters, the predictions of the BGM are based solely on ecological parameter values. In essence, the BGM is given by:

$$x_{an} = \frac{p_{an}}{\alpha_{an}}(1 - e^{-\alpha_{an} t}) \tag{1.3}$$

where x_{an} is peat mass (anoxic zone only) per unit area at time t, p_{an} is the constant addition of mass to the anoxic zone (M L^{-2} T^{-1}) and α_{an} is anoxic specific decay rate (M M^{-1} T^{-1}). The two assumptions of the BGM are, as Clymo (1984) stated: (1) Catotelm decay is nonzero, and is a constant proportion of all catotelm mass; (2) p_{an} is a constant

which implies that the properties and process rates within, the acrotelm (*i.e.* thickness, mass, litter composition, plant productivity and oxic decay rate) are also constant, such that mass is transferred to the catotelm at a constant rate.

The BGM suggests that there is a limit to the height to which a bog can grow because, unlike most authors before him, Clymo (1984) recognised the significance of decay in the anoxic zone. Whilst proceeding at a rate at least an order of magnitude slower than in the aerated zone (Ingram, 1978), anoxic decay cannot be ignored, especially in more mature bogs, simply due to the large thickness of material upon which this slower rate of decomposition acts. Because the BGM recognises the importance of anoxic decay, the thickness of peat upon which decay acts increases as the bog grows. Eventually the rate of loss of mass from the large, slowly decaying anoxic zone will equal p_{an} yielding steady-state conditions: a limit to bog growth, which, in terms of mass per unit area, is equal to p_{an}/α_{an}. In later versions of the BGM, Clymo (1992) partially relaxed the BGM's first assumption and experimented with non-constant rates of decay by allowing α_{an} to decrease as various, simple functions of time. This prevented the model from ever reaching a steady state, so that peat would accumulate indefinitely, albeit at an ever-decreasing rate.

A source of confusion that the BGM serves to illustrate, and which Clymo (1992) himself discussed, is the ambiguity associated with the terms 'acrotelm' and 'catotelm'. If the two are defined in terms of water-table position, such that the acrotelm and the catotelm are the unsaturated and saturated zones respectively, then the BGM requires that water-table position must remain at the same depth from the surface at all times, rising synchronously with bog growth. If, on the other hand, the acrotelm and catotelm are defined in terms of structure, such that the acrotelm is the layer above the zone of collapse, then it is unjustifiable to apply the oxic and anoxic decay rates wholly and exclusively to the acrotelm and catotelm respectively, because water-table fluctuations, and so oxygen availability, are not accounted for under such a rigid scheme. It is proposed that the two terms are discarded in favour of terms that are more descriptive of function and structure within a peat profile, such as 'oxic' and 'anoxic' for the zones above and below the temporally and spatially variable water-table, and 'intact' and 'compacted' for the parts of the peat profile above and below the narrow zone of collapse.

Clymo's (1984) original description of the BGM did not consider hydrological processes explicitly, but the assumption of an oxic zone of constant thickness necessarily requires that water-table rise occurs at the same rate as the growth in height of peat. Belyea and Baird (2006) considered the implications of a growing bog which possesses a groundwater mound according to the GMH, a model that Clymo (1984) advocated. Belyea and Baird (2006) identified a number of logical inconsistencies in the assumptions of the BGM. Again, without repeating their full analysis, Belyea and Baird (2006) showed that in all but one highly constrained situation, oxic-zone transmissivity must change as a bog grows. Whether or not this change in transmissivity is due to a change in the thickness of flow, a change in hydraulic conductivity, or both, is unimportant. A change in the thickness of flow, caused by a difference between water-table rise and growth in peat height, would lead to a change to oxygen availability in the oxic zone, and so a change in decay rates there. Similarly, a change in hydraulic conductivity would in turn be the result of an alteration to rates of compaction or surface vegetation. Thus, Belyea and Baird (2006) demonstrate that the assumption of a steady-state oxic zone and, therefore, a constant value of p_{an} is not reasonable in a growing, developing bog, thereby identifying the second assumption of the BGM as a logical inconsistency. In addition to this finding, Belyea and Baird's (2006) work suggested that current attitudes and approaches to modelling peatland development may be in need of reappraisal. They suggest that the continuous refinement and expansion of existing linear models such as the BGM and GMH which have prevailed for over twenty years in peatland science should be abandoned. Belyea and Baird (2006) argue that a more useful approach to modelling peatland development is that of hierarchical modelling, as described by Werner (1999) and Levin (1998).

1.2.3. Mixed or ecohydrological models

Hilbert *et al*. (2000) are one of the few groups to have developed a model that explicitly considers both ecological and hydrological processes. The first part of their analysis concluded that, in contrast to the approaches used in the BGM and GMH, water balance is likely controlled by a combination of internal (ecohydrological) and climatic factors. Hilbert *et al*. (2000) developed a more sophisticated model than the BGM, consisting of a pair of differential equations to describe changes in bog surface height and water-table depth in terms of a number of parameters, and found that their model produced plausible complex behaviour.

However, the one-dimensional nature of the model of Hilbert *et* al. (2000) means that it is conceptually limited, due to a lack of (principally along-slope) hydrological and hydrochemical interactions. In keeping with Clymo's (1984) approach, Hilbert *et al*. (2000) only considered the centre of a domed bog and their model is therefore unable to represent any change in peat properties in plan dimensions. Evidence suggests, however, that the variation of hydrological and ecological properties and process rates in plan and with depth are an integral feature of bog development (*cf*. Belyea and Baird, 2006; Lapen *et al.,* 2005). Furthermore, alterations to K due to peat decay and compaction are not facilitated, meaning that a single, time-invariant K value is used to represent the hydraulic conductivity of the entire model bog. The model of Hilbert *et al*. (2000) is discussed in more detail in Chapter 5, and the potential importance of the spatial variability of peat properties and process rates is discussed in Chapter 6.

In many bogs there is a distinct surface pattern of microtopographical features, or "microforms", which contain distinct communities of vascular plants and *Sphagnum* mosses. For example, low, wet hollows are often characterised by *Sphagnum cuspidatum*, whereas the higher, drier hummocks, that may protrude more than 50 cm above the surrounding surface, are characterised by *Sphagnum fuscum*, *Calluna vulgaris* and *Erica tetralix*. Evidence is sparse, but it is thought that peat varies in its hydrophysical properties according to the type of microform under which it was formed. Swanson and Grigal (1988) demonstrated that microform distribution could be of key importance to the hydrological behaviour of a bog due to characteristic differences in the hydraulic properties of peat laid down beneath hummocks and hollows. While Hilbert *et al*. (2000) generated some interesting results, it is clear that a significant improvement could be gained by enabling some more realistic feedbacks, chiefly the effect of plant type and decay upon peat hydrophysical properties. It would also be interesting to see what differences, if any, result from the consideration of an extra spatial (horizontal) dimension within such a model scheme.

1.2.4. Surface patterning models

One of the first attempts to model quantitatively the initiation and development of hummock-hollow patterning on raised bogs (for examples, see Figure 1.2) was the work by Swanson and Grigal (1988). They formulated a cellular model to test the theory that patterning could be successfully explained by a simple feedback between hydrophysical and ecological processes. Their model represents a portion of a sloping bog within a

a)

b)

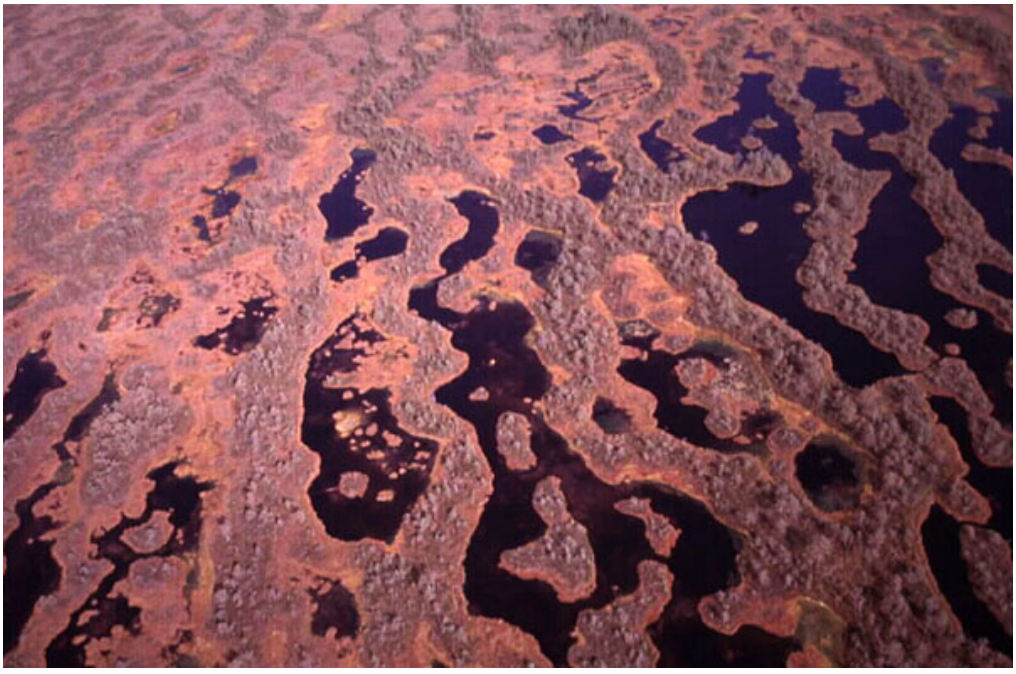

Figure 1.2 Aerial photographs of pronounced ridge-pool striped patterning on Männikjärve bog, Estonia. Note that while there is an obvious contrast between ridges and open pools, there is also a more subtle striping within the vegetation especially in 1.2 (b). For scale, the white boardwalk in (a) is approximately 1 m wide. Photo credit: Aber and Aber (2001), Aber et al. *(2002); reproduced here with permission.*

grid of computational cells, each of which possesses a four-square neighbourhood. In the model, each cell possesses a time-variant water table and may possess one of two possible vegetation microhabitat states – hummock or hollow – for the duration of each timestep. Water flow is facilitated between neighbouring cells using a simple version of Darcy's Law (for an explanation of Darcy's Law, see Chapter 2), but occurs primarily down an imposed slope. Whether a cell is designated as a hummock or a hollow at each timestep is determined by a probability function of the water-table level in that cell during the previous timestep, with the probability of a cell being a hollow equal to 1 when the water table is within a critical distance of the bog surface.

As cells switch from hummock to hollow or *vice versa* they undergo a change in their hydraulic properties. Swanson and Grigal (1988) assumed that the transmissivity of hummocks was an order of magnitude lower than that of hollows, keeping hummocks drier than hollows and thereby facilitating a simple ecohydrological feedback. Due to their low hydraulic conductivity, hummocks acted as barriers to flow, causing water to pond behind (upslope of) dry hummocks, forming hollows there. Strong patterns emerged from this simple ruleset, with alternate, slope-normal stripes of hummocks and hollows developing, even from initial conditions of a random distribution of hummocks and hollows. Given the age and the relative conceptual and mathematical simplicity of this work, it may seem surprising that the underlying principles still form the backbone of one of the two current theories on patterning, although it is argued in Chapter 3 that the model contains a number of important flaws.

A fundamental problem with the model and with Couwenberg's (2005) and Couwenberg and Joosten's (2005) attempts at an improvement upon it (these three models are henceforth referred to collectively as the 'ponding model') is that they consistently predict that hummock-hollow patterns move systematically downslope. While hummocks have been known to move with time (*cf*. Koutaniemi, 1999), there is currently no evidence to support such a systematic downslope migration of entire hummock and hollow complexes and it is hypothesised here that this odd result is attributable to a lack of 'ecological memory'. In the model, a cell that undergoes a switch from a hummock to a hollow, or *vice versa*, also undergoes a complete shift in transmissivity so that the new transmissivity of the cell is that assigned to the type of microform currently occupying the cell. A more realistic situation would be for the model somehow to incorporate previous microform types into the derivation of a cell's

transmissivity at each model timestep, representing the characteristics of peat laid down in the past. This ecological memory effect would mean that if a cell had been a hummock for a long time but then switched to being a hollow, it would still largely behave *hydrologically* like a hummock and would probably soon revert back to being a hummock, thereby providing a negative feedback acting to stabilise patterning. While the ponding model succeeded in demonstrating that complex, patterned behaviour can arise from the simple interactions of lots of small-scale elements, their model is too simple to give realistic results. The ponding model and the concept of ecological memory are explored in more detail in Chapter 3.

The model of Rietkerk *et al*. (2004 a, b) took a different approach to pattern modelling, in developing what is referred to here as the nutrient-scarcity model. Vegetation patterning in the nutrient-scarcity model depends on groundwater movement and associated transfers of dissolved nutrients. However, rather than flow occurring down an imposed slope, water movements are driven by differences in evapotranspiration rates of different vegetation types. The model was able to predict 'islands' of dense vascular vegetation within otherwise sparsely vegetated, moss-dominated landscapes, even on flat ground, which the ponding models could not account for, and it may well prove that inclusion of a nutrient cycling component is necessary to a successful simulation of peatland development. However, there is a substantial body of evidence to suggest that the most important controls on vegetation distribution within peatlands are hydrological parameters, such as water-table behaviour and near surface flux rates, whereas nutrient levels appear to play a secondary role (*cf*. Yabe and Onimaru, 1997; Bragazza and Gerdol, 1996). The nutrient-scarcity model is considered further, alongside the ponding model, in Chapter 3.

The modelling work of Baird *et al*. (2009) demonstrated that the nature or form of peatland patterns, rather than just the relative abundance of hummocks, hollows and pools, may exert a significant control over net rates and directions of peatland-atmosphere exchanges of carbon gases (CO_2 and CH_4). Therefore, for example, a hummock surrounded by pools will behave hydrologically differently from a hummock surrounded by other hummocks. Given the importance of water-table depth to peatland-atmosphere carbon gas exchanges (*cf.* Bubier *et al*, 1995; Bubier, 1995; Bubier *et al*., 1993), an understanding of small-scale pattern dynamics may be crucial to developing accurate carbon budgets for northern peatlands. Efforts to model peatland patterning

may, therefore, shed light on an aspect of peatland system behaviour which is potentially important to the climate change debate.

1.2.5. An existing 3-D, dynamic model of peatland ecohydrology?

Borren and Bleuten (2006) presented a 3-dimesnional, spatially-distributed simulation model of the ecohydrological development of the Backchar Bog complex in western Siberia. In their model, space is discretised in three dimensions, such that the modelled bog is disaggregated into 200 m × 200 m grid squares in plan, forming columns of peat on top of an undulating mineral substrate. The peat columns were further disaggregated into three layers: the 50 cm thick, live plant layer ("acrotelm"); deep peat ("catotelm"); and the underlying mineral soil. Borren and Bleuten (2006) used Modflow to model groundwater movements within the Backchar Bog; surface vegetation class (bog, fen or mixed), the rate of litter production at the top of each column and peat decay rates in each layer were determined by local recent wetness. The model features a relationship between soil wetness and surface vegetation type. Mire community type at each grid square is assumed to depend upon groundwater flux rates through that grid cell. However, only one value of hydraulic conductivity was used for fens and throughflow fens, and this value was halved for bogs. The use of such a scheme implies that the hydrological behaviour of distinct mire types may be accurately summarised by a single value, and that variation in K between individual microforms and their relative abundance and spatial distribution are unimportant. Such an assumption is in sharp disagreement with the analyses of Baird *et al*. (2008) and Baird *et al*. (2009), which suggest that the spatial distribution of K is highly important to an understanding of both peatland hydrology and carbon gas exchanges with the atmosphere. Furthermore, Borren and Bleuten (2006) conducted only a very limited sensitivity analysis, preventing a full understanding of the model's behaviour within parameter space.

Given the potential flexibility afforded by the spatial and algorithmic structure of their model, it is somewhat surprising that Borren and Bleuten (2006) appear to have neglected to take account of a complex linkage between system components which may be important to peatland system function and development. As a result, their model does not give rise to truly emergent behaviour of any kind (*cf*. Abbot, 2006). Borren and Bleuten's (2006) model is described and discussed further in Chapters 5 and 6.

1.3. Complex Adaptive Systems and Emergent Behaviour

1.3.1. What are Complex Adaptive Systems?

A strict definition of what constitutes a Complex Adaptive Systems (CAS) is difficult to come by, and definitions and terminology differ between authors. Gallagher and Appenzeller (1999) note how discussions on complexity have the tendency to dissolve rapidly into semantic debates; thus, it is important to set out clearly and concisely one's adopted nomenclature from the outset. A CAS is defined here as a type of deterministic system composed of multiple, distinct, autonomous, low-level elements participating in local interactions. These interactions may be competitive, cooperative or a mixture of the two. Examples of CAS include biological systems such as the human body, ecological systems such as an ant colony, human systems such as road traffic and economic systems such as the stock exchange. CAS are distinct from other, simpler, types of multiple-agent systems because they exhibit some or all of the following attributes:

- Adaptivity of individual components, as well as the system as a whole. That is, the results of low-level interactions determine which system components are eradicated, modified or replicated. The system and its components therefore 'learn' from their own history or, more formally, exhibit hysteresis.
- Feedbacks across different spatial and temporal scales, such that high-level system behaviour sets the constraints within which lower-level components work, which in turn gradually effect changes at the whole-system scale (Levin, 1999).
- Non-linearity: the reinforcement of chance events causes a drastic reduction in the degrees of freedom with respect to individual component behaviour. This constraint of behaviour leads to pathway-dependent behaviour and the self organisation of system components, leading in turn to;
- High-level (system-scale), emergent behaviour, often unpredictable from isolated observation of individual system components and their low-level interactions. Therefore, system control is dispersed and highly decentralised: coherent behaviour arises from repeated interaction of components and self-organisation rather than from system-scale rule sets.

In the case of the road traffic example above, the low-level components are clearly individual car-driver combinations. These components are autonomous in the sense that, within the high-level constraints of the whole traffic queue, they are free to speed up, slow down and change lanes as they desire, according to a low-level, competitive

rule set which means that each driver aims to progress through the queue to a predetermined destination as quickly as possible. The system components interact with one another by overtaking, allowing one another to change lanes, blocking off spaces and so on. They exhibit adaptivity, as each driver's behaviour is altered by their own history within the queue. Drivers become more tired and so prone to mistakes the longer they drive, they become less likely to give way to others who have cut them up, and their destination may even change depending on the length of time spent in the queue. The system exhibits feedbacks across a number of spatial scales, as the speed of the whole queue is determined by the speed of its component vehicles, whilst each vehicle's speed is constrained by that of its immediate neighbours. At the whole-system scale, waves of congestion and relatively free-flowing traffic move through the queue (e.g. Betró and Ladelli, 1990). There is no universal law of traffic queues, which necessitates the formation of congestion waves. Rather, such phenomena emerge from the repeated interaction of the system's components amongst which system control is dispersed.

Werner (1999) discussed environmental CAS with tangible, spatially referenced components, such as the individual grains of sediment in a riverbed and their collective behaviour in forming a bar, in turn part of a large complex of bars. It is also possible, however, to conceptualise functional system components, where each component is a physical property or a rate of process operation. In contrast to Werner's (1999) examples then, the interactions between system components do not necessarily require the spatial displacement of the components themselves, even if the linkages are still mediated by mass fluxes and energy transfers. As discussed in more detail below, it is believed by some that peatlands, and raised bogs in particular, may be described as complex adaptive systems, a philosophy that provides the contextual setting for this thesis.

1.3.2. Complexity versus chaos: an issue of scale?

The term 'complexity' is the name given to a currently popular approach to systems science which arose in the mid-late 1980s (Lewin, 2000). Complex systems often exhibit emergent behaviour (Abbot, 2006), meaning that the ensemble properties and behaviour of a complex system are not only greater than, but often entirely different from, the sum of its component parts. While the behaviour of complex systems are often describable from low-level, deterministic rulesets, their high-level behaviour is

often surprising or unpredictable when considered holistically. As such, complex systems, for which emergence is an important theme, may be thought of as occupying a domain in-between deterministic order and unordered randomness and so are often said to exist 'on the edge of chaos' (Lewin, 2000). Chaos theory came to prominence amongst system scientists in the mid 1970s, and predicts that large-scale natural systems are highly sensitive to initial conditions and the rules of interaction between elements that exist at even the smallest scale. The result of this extreme sensitivity is entirely unpredictable, seemingly unordered behaviour, as small-scale perturbations combine to generate deterministic chaotic behaviour. Chaos theory's suggestion of sensitive dependence on initial conditions is nicely caricatured by what is popularly known as the butterfly effect. Widely attributed to Edward Lorenz, the butterfly effect suggests that natural systems such as the atmosphere are so highly sensitive that just by flapping its tiny wings, a single butterfly can cause a change in local conditions sufficient to alter entirely the trajectory of global atmospheric behaviour and cause (or prevent) a tornado on the other side of the planet (*cf*. Hilborn, 2004). Stone and Ezrati (1996) set an agenda for detecting and understanding deterministic chaos in ecological systems, while many authors have used simple density-dependent models to predict chaotic behaviour in a wide variety of ecological contexts (for example: Beltrami and Carrol, 1994; Hastings and Powell, 1991; Tilman and Wedin, 1991). However, unambiguous, truly chaotic behaviour has rarely been observed in reality. Rather, natural systems appear to be resilient to small-scale perturbations and tend towards predictable, often stable, patterns (Zimmer, 1999).

Scale is a crucial issue in any consideration of complex systems and emergence, given that complexity attempts to explain phenomena which emerge at level n by a consideration of the interactions of components which exist at level n-1 (or arguably n-2, or n-3) (Abbot, 2006). For example, ecological systems exist at a scale (n) which may be thought of as emergent from biological processes (n-1). Goldenfeld and Kadanoff (1999) recognise how convenient it is that the scales within which the physical laws of the universe hold have both upper and lower bounds. If this were not the case, such that tiny perturbations at the smallest scale were able to affect sweeping changes at the whole-system scale, then chaos would reign. To use Goldenfeld and Kadanoff's (1999) example, in order to model a bulldozer in a truly chaotic universe, one would have to model every quark, photon, graviton and electron involved in that universe. This is clearly not the case: comprehension of a bulldozer requires an

understanding of mechanics rather than particle physics. For many systems, including peatlands, scale appears to be crucial to separating complex understanding from unordered chaos. An inappropriate consideration of scale leads to models which are either linear and trivial, or chaotic and unpredictable. In between lies what may be a narrow domain where order may be comprehended within complex systems (Lewin, 2000).

1.3.3. Peatlands as Examples of Complex Adaptive Systems

The analysis of Belyea and Baird (2006) suggests how peatland system functionality may be conceptualised as a CAS. Low-level system components, including (although not necessarily limited to) groundwater movements, plant community succession, plant/litter productivity, peat decay and compaction interact with each other and with the system's boundaries to give rise to high-level behaviour. The system-scale phenomena which emerge include: peat accumulation; the development of a groundwater mound; the non-random, 3-dimensional distribution of peat properties; and surface patterning at a number of scales. In reference to the key attributes of CAS, identified in section *1.3.1.*, above, peatlands commonly exhibit complex behaviour in a number of ways. Without reproducing her analysis here in full, Belyea (2009) identified non-linear behaviour in a number of aspects of peatland system behaviour, including (but not restricted to) the following: peatland initiation; successional dynamics; ombrotrophication (*i.e.*, fen-to-bog transition); water-table and CO_2-flux dynamics. Self-organisation and emergence are manifest in a number of ways in peatland system behaviour. The non-random, often striped patterns commonly observed on northern peatlands (see section *1.2.4.*, above) are a clear example of this. While the exact natures of the mechanisms that give rise to patterning are contested in the literature (see Chapter 3 of this thesis), the apparent consensus is that peatland surface patterning at a range of scales emerges from the local interactions and self-organisation of small-scale processes. Also, as we shall see in Chapters 4, 5 and 6, peat hydrophysical properties and rates of decay appear to adapt and self-organise so as to maintain a soil-wetness niche suitable for the success of *Sphagnum*. The ability of *Sphagnum* to maintain its own niche in this manner seems likely to be a naturally-selected trait of that genus (van Breemen, 1995).

1.3.4. Rationale part II: the need for a new conceptual and modelling approach

The study of CAS lends itself naturally to a modelling approach, especially computer simulation modelling, which can be used to test our understanding of a complex universe. In keeping with the key CAS theme of emergence, Goldenfeld and Kadanoff (1999) cite the need to build "minimal" models. Such an approach aims to capture the essence of system functionality by considering all of the important system components and their interactions, whilst excluding what is ultimately trivial detail. Again, the most important consideration is that of scale: at what level do the components that give rise to genuinely emergent behaviour operate? A choice of too small a scale when designing a model leads to overly complicated, inefficient simulations, the results of which are often trivial or requiring of laborious analysis, and may lead to models that display inappropriate deterministic chaos. Conversely, a choice of too large a scale leads to an oversimplified and unrealistically constrained model, from which conclusions of only limited use, if any, can be drawn. Almost all existing models represent only limited portions of peatland system behaviour and fail to take account of cross-scale interactions between both ecological and hydrological processes. The few models which do make allowances for complex behaviour are either conceptually limited (Borren and Bleuten, 2006), are still missing potentially important feedbacks such as that between cumulative peat decay and hydraulic conductivity (Borren and Bleuten, 2006; Hilbert *et al*., 2000), or are one-dimensional, thereby failing to take account of potentially important spatial variation (Hilbert *et al*., 2000). No existing models are able to predict all of the types of complex behaviour commonly observed in peatlands, described in section *1.3.3.*, above. Therefore, a new conceptual model was developed that included each of the following: peatland hydrology; peatland vegetation micro-succession; peat dry mass balance (including the formation of fresh peat litter at the surface, and the decay of peat at all depths); the variation of peat hydrophysical properties, such as hydraulic conductivity. The new model is described in more detail in the next section, as is its numerical implementation.

1.4. Thesis Aim and Objectives

The overarching aim of the work reported in this thesis was to build, test and analyse a new suite of models of the spatio-temporal dynamics of the development of raised bogs over long timescales (*i.e.*, 10^2 – 10^3 years). The purpose of the new modelling framework and the individual models therein was to address the limitations of previous peatland models identified earlier in this chapter. In essence, the aim of the work was to produce a model framework and individual models that contain those ecohydrological relationships and feedbacks required to simulate peatlands as CAS. The new model suite is called **DigiBog** and was written in Fortran 95.

1.4.1. Model structure

The conceptual form of **DigiBog** is shown in Figure 1.3. **DigiBog** comprises five submodels, each of which deals with a different aspect of peatland behaviour.

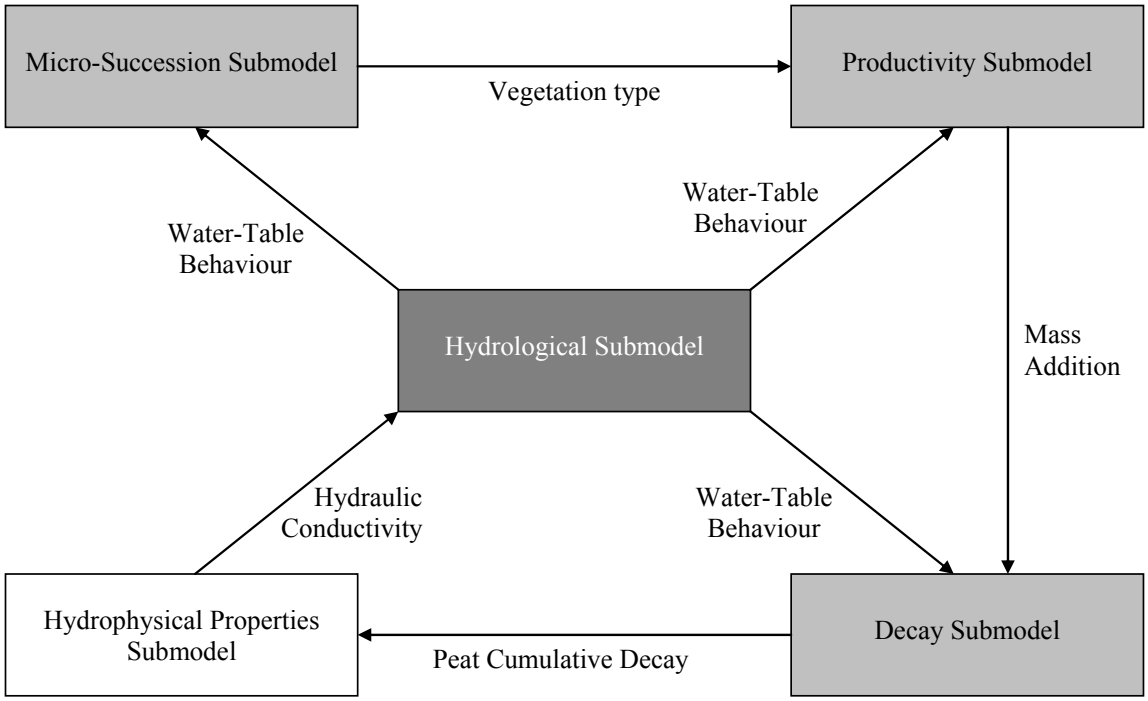

Figure 1.3: Schematic showing **DigiBog** *model structure and internal linkages. Dark grey box represents hydrological submodel; light grey boxes are ecological submodels; white box is hydrophysical submodel. Labelled arrows show the passage of information between submodels.*

The hydrological submodel simulates groundwater movements in response to exchanges of water with the atmosphere and the boundaries of the bog or peatland being simulated (see Chapter 2). The micro-succession submodel simulates annual to decadal changes

in plant community type in response to recent local water-table behaviour (see Chapter 3). The productivity submodel adds freshly formed litter, beneath the live vegetation layer, at a rate dependent upon both local moisture availability and vegetation type (see Chapters 5 and 6). The decay submodel removes peat mass from all depths within the model at a rate dependent on whether local conditions are saturated (anoxic) or not (see Chapters 5 and 6). Finally, the hydrophysical submodel simulates alterations to the hydrophysical properties of peat as a function of the cumulative decay that it has undergone, thereby providing a feedback to the hydrological submodel (see Chapters 4, 5 and 6).

1.4.2. Research objectives

Within the main project aim outlined at the start of section **1.4.**, above, the following four specific research objectives can be identified:

- *(i) Model Algorithm Construction and Testing*

  The first and most obvious task was the construction and testing of the individual submodels identified in Figure 1.3. Prior to the commencement of this PhD, Andrew Baird (unpublished) had already written a 1½-dimensional hydrological model in Fortran 95. As discussed in full in Chapter 2, this existing code was taken up and used as the basis for **`DigiBog`**'s hydrological submodel. All other submodels needed to be designed and written from scratch. Chapter 3 explores the development of the micro-succession submodel and a limited version of the hydrophysical submodel, while Chapters 5 and 6 deal with the productivity and decay submodels and a full version of the hydrophysical submodel. Each submodel needed to be tested in isolation before being incorporated into the linked model, and the results of this testing are included along with the relevant model descriptions.

- *(ii) Exploring the Causes of Peatland Patterning*

  The second objective was to examine cellular models of peatland patterning. As discussed in section *1.2.4.*, above, a number of cellular computer simulation models claim to offer process-based explanations of the causes of peatland patterning. As shown by Baird *et al*. (2009), peatland patterning may be potentially highly influential upon peatland-atmosphere carbon exchange rates, making an understanding of the processes leading to patterning potentially

important to an understanding of the role of peatlands in global climate change. Furthermore, it seems highly likely that peatland patterning is a manifestation of complexity, arising as it does from local-scale interactions between peat properties, hydrology and plant community type.

- *(iii) Examining the Controls on Peat Hydraulic Conductivity*

  As mentioned above, one of the key linkages between **DigiBog**'s submodels is that which governs the effect of peat decay upon hydrophysical properties. This relationship is poorly understood and previous studies have not followed best practice in the measurement of hydraulic conductivity. Therefore, an empirical examination of a quantitative measure of cumulative decay and hydraulic conductivity was undertaken. The aim was to develop a simple empirical model that could be incorporated into **DigiBog**'s hydrophysical submodel in order to predict hydraulic conductivity as some function of peat cumulative decay. This aim is addressed in Chapter 4.

- *(iv) Simulating Emergent Behaviour in Peatland Development*

  Once all submodels have been written, tested and linked appropriately (see Figure 1.3), the resultant ecohydrological version of **DigiBog** should replicate the conceptual model of bog development described above. Thus, the system's low-level components, the individual submodels, should self organise in a manner that gives rise to emergent behaviour at the whole-system scale. Such emergence includes the growth of a peat dome and a groundwater-mound, the development of surface patterning and the prediction of non-random, vertical and horizontal distribution of peat properties. The final objective, therefore, is to experiment with model parameters and the rules of component interaction so as to elucidate the model's sensitivities and its behaviour under a range of situations. At this point the model will take on the role of a hypothesis generating tool, by comparing its predictions of bog system behaviour under a range of circumstances to the behaviour of real-world systems.

1.5. Methodological Strategy

This section describes the various methods that will be used to address the thesis' aim and objectives, identified in section **1.4.**, above.

1.5.1. Construction of DigiBog hydrological model

The first part of the **`DigiBog`** model code to be written will be the hydrological model, which forms a central foundation upon which the rest of the suite will be built. Construction of the hydrological model will necessarily involve creating a scheme within which space, time and interactions between low-level system entities can be represented by the entire **`DigiBog`** suite, not just the hydrological model. The main purpose of the hydrological model will be to act as a submodel within the ecohydrological models in the suite (see sections *1.5.2.* and *1.5.4.*, below), by providing them with information on water-table position. The hydrological submodel will use hydraulic conductivity and porosity to generate steady-state water-table geometries.

1.5.2. Construction of a model of peatland patterning

The first meaningful application of the hydrological model will be as the hydrological submodel within a simulation model of peatland patterning. The model will be called **`DigiBog_EcoHydro1`** (DBEH1), and will be used to experiment with various rulesets for local interaction. It was intended from the beginning of the project that DigiBog should feature a grid-column-layer structure in order to represent discretised space (see Chapter 2 for more details), a scheme which lends itself readily to the representation of peatland patterns (*cf.*, Swanson and Grigal, 1988; Couwenberg, 2005; Couwenberg and Joosten, 2005). While constructed within an ostensibly three-dimensional model scheme, the patterning model will be little more than a two-dimensional representation of a peatland surface. In reference to the schematic in Figure 1.3, DBEH1 includes submodels which represent peatland hydrology, micro-succession, and a somewhat black-box representation of the hydrophysical submodel. However, DBEH1 will not represent the productivity of peatland plants *per se*, or the decay of existing peat. Different rulesets will be assumed to represent the small-scale interactions between grid cells.

1.5.3. Predicting hydraulic conductivity in peat soils

In the schematic shown in Figure 1.3, the hydrological and decay submodels are linked by another submodel, the hydrophysical submodel, which describes the change in peat

hydraulic conductivity on the basis of some measure of peat decay. Before the hydrophysical submodel can be incorporated into the planned models of peat accumulation (see section *1.5.4.*, below), however, the hypothesised link between peat decay and hydraulic conductivity must be investigated using a laboratory-based analyses of peat samples recovered from a suitable location. The work in Chapter 4 uses a field and laboratory study in an attempt to inform the planned hydrophysical submodel which forms part of the subsequent peat accumulation models, by generating an empirically-derived equation to describe hydraulic conductivity on the basis of peat cumulative decay.

1.5.4. Modelling peat accumulation over millennial timescales

Chapters 5 and 6 detail the construction and analysis of 1-D (vertical) and 2-D (profile) models of peat accumulation (DBEH2 and DBEH3, respectively), which include all submodels indicated in Figure 1.3 apart from the micro-succession submodel. Existing models of peat accumulation (e.g., Hilbert *et al*., 2000; Frolking *et al*., 2001) fail to take account of changes in peat hydraulic conductivity (represented in Figure 1.3 by the hydrophysical submodel), a horizontal spatial dimension (which allows spatial interaction via **DigiBog**'s hydrological submodel) or plant community succession (micro-succession submodel). It was therefore deemed desirable to include these extra complexities in an incremental manner so as to allow the observation of the effects of each, thereby allowing greater experimental control. Implementation of the micro-succession submodel was not possible within the time constraints of the current project, but is a desirable objective for future studies.

Table 1.1 (continued on following page): Glossary of algebraic terms used throughout thesis. Baseline values, where given, are assumed in relevant model runs unless otherwise stated:

Symbol	Variable/Parameter Name	Quantity Type	Baseline Value	Chapters
a	Equation 5.4 Coefficient	Constant	8	5, 6
an	Proportion of Layer Below WT	Auxiliary Variable	–	5, 6
α_{an}	Anoxic Specific Decay Rate	0.0001 yr^{-1}	0.0001 yr^{-1}	5, 6
α_{ox}	Oxic Specific Decay Rate	0.015 yr^{-1}	0.015 yr^{-1}	5, 6
	Bog Height	State variable	–	5, 6
b	Equation 5.4 Exponent	Constant	0.001	5, 6
β	Equation 2.7 Exponent	Constant	0.01	2
d	Water-Table Depth	State variable		
Δt_e	Hydrological Runtime	Parameter	–	3
Δt_r	Acrotelm Residence Time	Auxiliary Variable (see Equation 3.1)	–	3
E	Evapotranspiration	Parameter (see Equation 2.2)	–	2
e	Base of Natural Logarithm	Universal Constant	2.718 (3 d.p.)	1, 5, 6
H	Water-Table Height	State Variable	–	2, 3, 5, 6
K	Hydraulic Conductivity	Measured Quantity, Auxiliary Variable	–	2, 4-6
K_{hol}	Hollow Hydraulic Conductivity	Parameter	0.035 cm s^{-1}	3
K_{hum}	Hummock Hydraulic Conductivity	Parameter	0.035 cm s^{-1}	3
L	Peatland Lateral Extent	Parameter	50,000 cm	5
m	Proportional Mass Remaining	Measured Quantity, Auxiliary Variable	–	4, 5, 6

Table 1.1 (continued from previous page): Glossary of algebraic terms used throughout thesis. Baseline values, where given, are assumed in relevant model runs unless otherwise stated:

Symbol	Variable/Parameter Name	Quantity Type	Baseline Value	Chapters
n	Memory Strength	Parameter (see Equation 3.1)	1 Layer	3
ox	Proportion of Layer Above WT	Auxiliary Variable	–	5, 6
P	Total Model Precipitation	Parameter (see Equation 2.2)	–	2
p	Productivity	Parameter	0.0864 g cm^{-2} yr^{-1}	5, 6
ϕ	Discharge Through Pore	Auxiliary Variable (see Equation 4.1)	–	4
Q	Discharge Through Peat Bank	State Variable (see Equations 2.6, 2.8)	–	2
R	Pore Radius	Auxiliary Variable (see Equation 4.1)	–	4
ρ	Peat Dry Bulk Density	Constant	0.1 g cm^{-3}	5, 6
U	Net Rainfall Rate	Parameter	30 cm yr^{-1}	2, 3, 5, 6
s	Peat Effective Porosity	Parameter	0.3	2, 3, 5, 6
	Spatial Step	Grid Resolution	1 m, 10 m, 12 m	2, 3, 5, 6
T	Transmissivity	Parameter	–	3
t	(Model) Time	Auxiliary Variable	–	2, 3, 5, 6
x	Distance from Bog Central Axis	Spatial Index (see Equation 1.1)	–	1
x_{an}	Peat Mass per Unit Area	State Variable (see Equation 1.3)	–	1
z	Height above Impermeable Base	Auxiliary Variable (see Equations 2.5 – 2.7)	–	2

Chapter 2: Modelling Bog Hydrology

This chapter describes the theory, design, testing and application of the **DigiBog** hydrological submodel, **DigiBog_Hydro** (DBH), the need for which was identified in Section *1.3.4*. While DBH may be used as a stand-alone hydrological modelling tool, it has been constructed with the primary objective of utilising it as one of the central components in the ecohydrological models detailed in Chapters 3 and 6. The Fortran 95 code for DBH can be found as two separate text files on the supplementary CD.

2.1. Basic Hydrological Concepts

Groundwater movements within bogs occur in response to hydraulic head gradients caused by transfers of water between the bog and its boundaries and between the bog and the atmosphere (in the form of precipitation and evapotranspiration). Groundwater movements are mediated by the spatial pattern of peat hydrophysical properties. The most important hydrophysical properties are hydraulic conductivity, or permeability, K (with dimensions of L T^{-1}), and effective porosity, s (dimensionless). K is defined by Darcy's Law as the specific discharge q (L T^{-1}) that occurs under a unit hydraulic gradient (*cf.* Freeze and Cherry, 1979):

$$q = -K \frac{dH}{dx} \tag{2.1}$$

where H is the hydraulic head (L), x is distance in the direction of water flow (L), and dH/dx is the hydraulic gradient (dimensionless). Because flow is described as occurring in the direction of a negative hydraulic gradient, a minus sign is introduced to the right-hand side of Equation (2.1) to make q positive.

A key hydrological concept is that of the water table, which is defined as the surface at which groundwater is at atmospheric pressure. It is common to describe conditions below the water table, where groundwater experiences pressures greater than atmospheric, as being saturated, meaning that all void spaces are occupied by water and there is no free-phase gas present. However, there is strong evidence that the decay of organic matter at all levels below the water table within a peat soil leads to the production of methane bubbles, possibly in significant quantities (Tokida *et al*., 2004), meaning that, even below the water table, conditions might not necessarily be truly saturated. Conversely, conditions above the water table (lower than atmospheric pressure) may be thought of as unsaturated, except when a capillary fringe forms (*cf.* Belyea and Baird, 2006). The Richards equation, sometimes known as Darcy's Law for unsaturated flow, is a variant of Equation (2.1) which assumes that K in the unsaturated zone is some function of soil wetness and suction (Freeze and Cherry, 1979). While bog surface vegetation may draw upon water from primarily within the shallow unsaturated store (*cf.* Malmer and Holm, 1984), a full consideration of unsaturated flux and storage would greatly complicate **`DigiBog`**'s hydrological submodel. Instead,

water-table depth (relative to the bog surface) is used as the main measure of wetness within the hydrological submodel, and conditions below the water table are assumed to be fully saturated, or at least any deviation from truly saturated conditions are assumed uniform throughout the peat profile below the water table. Moisture distribution in the zone above the water table is often closely related to water-table depth (Hayward and Clymo, 1982; Kettridge and Baird, 2007). It was deemed satisfactory, therefore, to use some description of water-table depth as a predictor of surface ecological processes, because the added complications necessitated by a full consideration of conditions above the water table would add little to the model suite. Thus, processes in this zone are considered no further within this thesis.

It is often assumed that subsurface water flow in a shallow aquifer, such as a raised bog, can be described satisfactorily by a consideration of horizontal flows alone; in such situations vertical hydraulic gradients are so small as to be negligible. The assumption that flow in shallow aquifers may be described mathematically as predominantly horizontal is known as the Dupuit-Forchheimer (D-F) approximation (*cf*. Freeze and Cherry, 1979). Reeve *et al*. (2000) simulated a range of hydrological scenarios in order to examine the importance of vertical groundwater flow within raised bogs. Their work showed that vertical hydraulic gradients within shallow peat aquifers are negligible when the underlying substrate is much less permeable than the peat. An assumption common to all **DigiBog** simulations reported in this thesis is that of an impermeable mineral substrate. It was judged, therefore, that the D-F approximation was reasonable for **DigiBog**'s purposes, so that a hydrological submodel which considers only horizontal hydraulic gradients and flux would suffice.

2.2. Groundwater Modelling

The main purpose of the hydrological submodel is to calculate the spatio-temporal dynamics of water-table behaviour within the modelled bog in order to inform **DigiBog**'s other submodels, which are outlined in Chapter 1. There are a number of so-called 'off-the-shelf' groundwater model software packages available that could have been used to compute **DigiBog**'s water-table behaviour, by far the most widely used of which is Modflow from the United States Geological Survey (McDonald and Harbaugh, 2005; 2003; 1984).

Modflow is perhaps the industry-standard groundwater hydrological modelling software used by scientists and engineers in different disciplines all over the world, and has gone through a number of redevelopments since it was first released in 1984 (McDonald and Harbaugh, 2003). As such, the program is reliable and well-tested, with a large and diverse user community able to offer advice and support. The program was designed so as to be as flexible and as future-proof as possible, with a modular structure which allows the user to choose which types of hydrological features (e.g. wells, lakes, rivers, etc.) are to be simulated. The choice of possible program modules also allows the user to select the most desirable from a number of methods for solving Modflow's groundwater flow equations in order to optimise computational time. While Modflow may be configured so as to adopt the Dupuit-Forchheimer (D-F) approximation, it is also capable of genuinely 3-dimensional simulations of groundwater problems. As such it is able to simulate vertical hydraulic gradients and their effects upon groundwater flow and water-table behaviour (McDonald and Harbaugh, 2005; 2003; 1984).

The open-source nature of the Modflow code allows experienced users who possess sufficient programming skills to alter the code as they see fit for their own applications (McDonald and Harbaugh, 2003). Furthermore, Modflow is written in Fortran, a programming language with which I am familiar and in which the rest of the **DigiBog** model suite is written, meaning that it could have been possible to integrate the code for **DigiBog**'s other submodels directly into the existing Modflow code. However, the option of using an existing groundwater model software package was rejected in favour of developing from scratch a new, bespoke model, called **DigiBog_Hydro** (DBH). Given the widespread use of Modflow and all of its advantages listed above, a robust argument is necessary in order to justify the time and effort required to build a new model from scratch.

DigiBog was not conceived with the aim of simulating specific situations involving hydrological features such as drains, lakes, wells, rivers and the like. Rather, **DigiBog** is intended to be used as a tool for generating and testing hypotheses regarding peatland system behaviour in the general – and often idealised – sense. The general applicability of the D-F approximation in shallow aquifers such as bogs would also mean that full 3-D capability is not required. The D-F approximation is attractive for modellers because it leads to simpler flow equations than those in which vertical flow is considered. Furthermore, advanced numerical techniques for solving groundwater flow equations more quickly are simply not necessary for **DigiBog**'s purposes, meaning that many of Modflow's advanced features would have been redundant. Repeatedly scanning though the lines of code associated with these redundant features could increase model run times, possibly significantly. Perhaps more troublesome is the fact that code familiarisation would have been made much more difficult by all of Modflow's advanced features and flexibility. Learning and understanding such a large volume of industry-standard code, to the point where the code for **DigiBog**'s other submodels could have been confidently incorporated, would have been highly labour intensive and coding would have been prone to mistakes.

The main reasons for rejecting Modflow, however, involved a lack of flexibility in its spatial and conceptual structure. The ecohydrological modelling described in Chapters 3 and 6 require the small-scale spatial variation of peat hydrophysical properties such as hydraulic conductivity, effective porosity and bulk density, and ecological properties such as peat botanical composition and cumulative decomposition. Modflow was originally designed for use in simulating regional scale aquifers. Various packages have been developed to enable Modflow to represent ever smaller scales of groundwater problems, although representation of individual layers of peat, each of which may be only millimetres thick, is likely to be inappropriate and prone to error.

The original DBH code was written by A. J. Baird (*cf*. Baird, *et al*., 2006) (but only for one plan dimension) with a grid-column-layer structure that allows peat properties (e.g. hydraulic conductivity, but also ecological properties such as peat quality) to vary vertically, horizontally and through time. An important advantage that this facility affords DBH over Modflow is that DBH's algorithmic structure has been designed so as to be able to deal easily with fine-scale variation in hydraulic properties which may be

important to accurate description of the hydrological behaviour of peatlands (Beckwith, *et al*., 2003b; Almendinger and Leete, 1998; Ivanov, 1981). Doherty (2001) noted the tendency for computational cells in Modflow simulations to become "dry", and discussed a number of problems associated with this phenomenon. A Modflow cell is said to by "dry" when the hydraulic head in that cell is lower than the base of the cell. Once dry, a cell is automatically designated by Modlfow as inactive and does not rewet in an easy or uncomplicated manner. Furthermore, as Doherty (2001) observed in mining applications, while MODFLOW performs well in cases of falling water levels, when head starts to rise and successively higher cells need to be rewetted, "extreme difficulty" is often encountered in solution convergence. The algorithm governing the drying and rewetting of cells often produces numerical instability, with cells in certain locations oscillating between wet and dry states during successive iterations. While Doherty (2001) presented a somewhat cumbersome fix to overcome drying-rewetting difficulties, the structure of DBH means that no such difficulties are ever encountered in the first place. Doherty's (2001) fix assumes that no cell ever completely dries out and that, even when head is below the base of a cell, that cell still conducts small amount of water in a saturated manner. Such an assumption is clearly problematic in situations where head is several cells below the cell under consideration, and the simpler conceptual structure of DBH does away with the need for such inelegant fixes.

To summarise, DBH is conceptually and algorithmically simpler than Modflow. As a result, it is unable to simulate such a large range of hydrological scenarios but it has been purpose built for its task and it is easier to work with. Specifically, Modflow makes it difficult to simulate situations in which hydrophysical properties vary over small spatial scales, as required by **DigiBog**, and can become unstable in situations where water tables frequently rise and fall through multiple layers.

2.3. Hydrological Submodel Description

2.3.1. Space, time and heterogeneity in **DigiBog**

The hydrological submodel, in common with all other **DigiBog** submodels, utilises a grid-column-layer arrangement similar to that of Modflow. This means that a bog represented in **DigiBog** is disaggregated into many square-sectioned columns of peat arranged in a lattice framework in the *x*-*y* (horizontal) plane. The plan dimensions of columns are equal for all columns and in both horizontal directions (*i.e.*, unlike Modflow, columns must always be square in plan). The length of each column's sides is referred to as the model's spatial step. Each column is further split into a number of slab-like layers, as shown in Figure 2.1, with each layer possessing its own values for *K*, *s*, thickness and any other property which must vary in three dimensions (e.g. peat ecological properties required by other submodels). Such an arrangement allows for peat properties to vary not only in plan dimensions but also with depth, and also allows for the easy addition of discrete cohorts of peat at the top of each column. Both of these are necessary requirements for the ecohydrological versions of **DigiBog** reported in later chapters.

DigiBog's grid-column-layer structure allows any plan shape of bog to be defined within the lattice framework. Any column may be assigned as a Dirichlet boundary column, in which water-table level does not alter from initial conditions, although a situation in which boundary water tables changed throughout model time would be easy to represent with only minor code amendments. A marginal stream or ditch of constant water level can therefore be represented by a string of such boundary columns (for example, see Figure 2.1). Columns that fall outside of the boundaries are effectively deactivated during a model run and take no part in the simulation. Furthermore, the height of each peat column is not prescribed independently from the thicknesses of its constituent layers. Rather, the height of a column is equal to the sum of the thicknesses of the layers which comprise it and, unlike in Modflow, layer heights need not be contiguous between columns. This is of key importance to **DigiBog** and an important advantage over Modflow, because the ecohydrological model version that allows peat decomposition to occur at varying rates in three dimensions will alter the thicknesses and elevations of each layer independently, meaning that layers will not be contiguous between columns. Setting appropriate initial values for individual layer thicknesses therefore allows a heterogeneous surface topography to be defined. Thus a bog of any 3-D shape can be modelled, such as a simple dome or other basic geometric shape; by

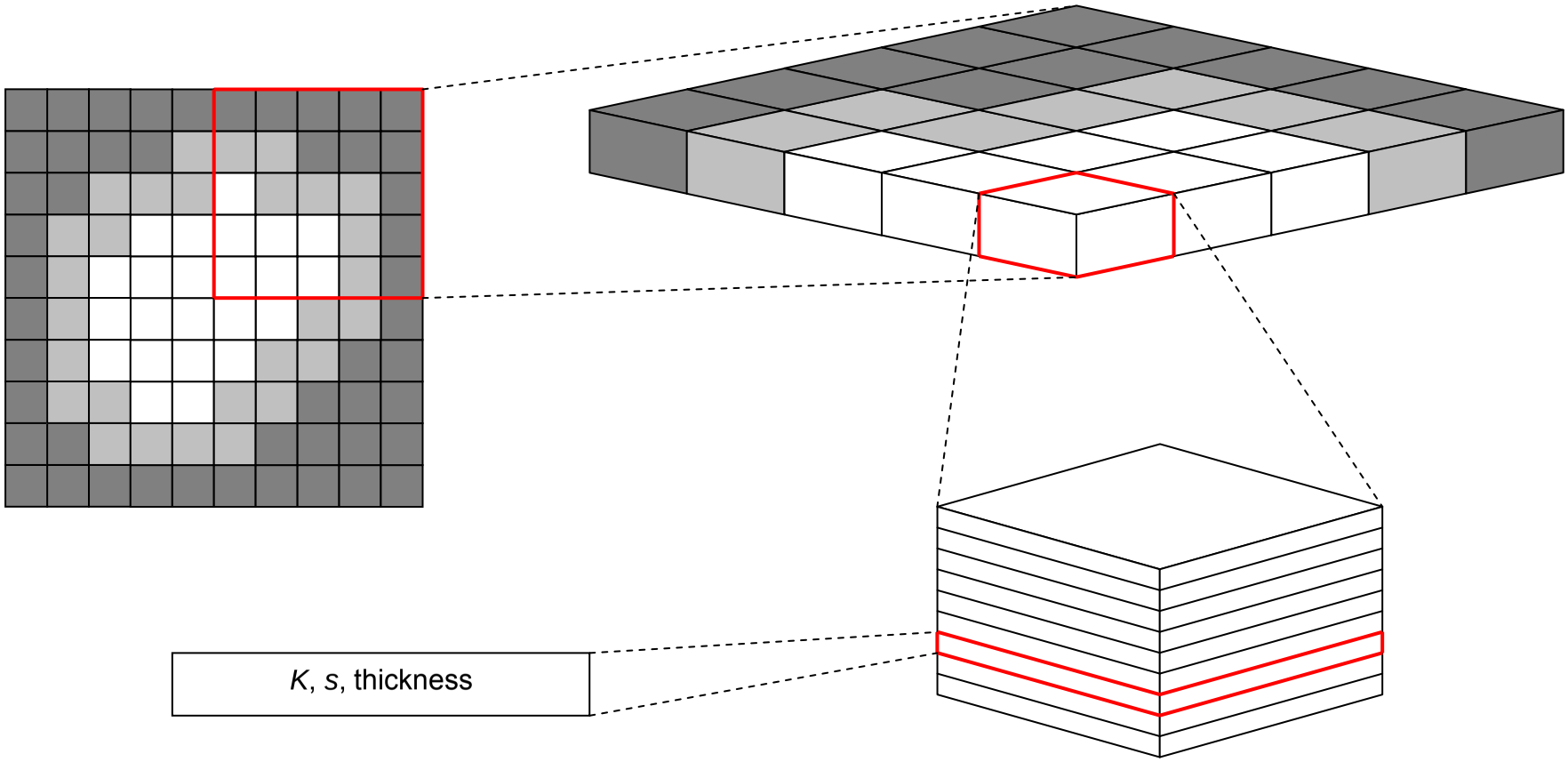

Figure 2.1: example schematic to illustrate the way in which a bog in **DigiBog** *takes the form of a square grid in plan (top left – dark grey squares are deactivated columns, light grey squares are boundary columns, white squares are active columns). The lattice is formed by a matrix of adjacent columns (top right), each column being composed of layers (bottom right) and each layer possessing its own properties (bottom left).*

using an appropriate Digital Elevation Model (DEM), the complex shape of a real-world bog may be defined.

The partitioning of time and space that is necessary within numerical models means that each model store – an individual peat layer in the case of **DigiBog** – is internally homogeneous in terms of properties, process rate operation and storage levels. So, while variation is facilitated between layers and between timesteps, the quantities assigned to any given layer at any given timestep are applied uniformly to the entire layer and for the duration of the timestep. Changes in storage levels between timesteps are therefore given by integrating rates of process operation with respect to timestep length.

2.3.2. Algorithmic structure

As noted above, DBH assumes that the D-F approximation holds for groundwater flux in bogs. A key feature of the D-F approximation is that, unlike in genuinely 3-D simulations, the hydraulic gradient is given by the gradient of the water table. If this change to equation (2.1) is made, flow in both horizontal dimensions (x, y) is considered, and the flow equation is combined with a storage equation (*cf*. Freeze and Cherry, 1979), the following variant of the Boussinesq equation is obtained:

$$\frac{\partial H}{\partial t} = \frac{\partial}{\partial x}\left(\frac{K(H)}{s(H)} H \frac{\partial H}{\partial x}\right) + \frac{\partial}{\partial y}\left(\frac{K(H)}{s(H)} H \frac{\partial H}{\partial y}\right) + P - E \qquad (2.2)$$

where H is now the water-table height above a datum; s is effective porosity, defined as the volumetric proportion of a soil that is available for flow (dimensionless); P is addition of water to the water table due to precipitation (L T^{-1}) and E is losses from the water table due to evapotranspiration (L T^{-1}). It can be seen from equation (2.2) that K and s are functions of water table height and also may vary with position in the x-y plane. As noted above, however, vertical hydraulic gradients are ignored, so DBH is said to be a 2½-D, rather than a truly 3-D, model. DBH adopts a finite-difference approach to solve Equation 2.2. Note that the quantity P-E may be thought of as net precipitation, *i.e*., that which is not lost back to the atmosphere and which is assumed to be added to the water table. A full representation of evapotranspiration would greatly complicate DBH, and so model precipitation $U = P$-E (L T^{-1}) was assumed to be net of

evapotranspiration. As such, all subsequent references to "net rainfall" throughout the thesis should be taken to be net of evapotranspiration.

Flow occurs between adjacent columns according to equation (2.2). The value of K appropriate for flow between adjacent columns is calculated in the following manner. Depth-averaged K for each column is given by the arithmetic mean of the K of all layers which are beneath the water table, weighted by layer thickness. Where the water table falls between layer boundaries (as is almost always the case), this is also accounted for. The K value appropriate for the calculation of flux between two columns is then given by the harmonic mean of the depth-averaged K values of those columns.

DBH assumes that flow between columns must occur through a finite wetted contact, *i.e*. through column walls. Thus, each column's neighbourhood is a four-square one (a von Neumann neighbourhood), meaning that flow does not occur diagonally within DBH's grid. Once flux rates have been calculated between each column and its four neighbours, and integrated with respect to the length of the hydrological timestep, water tables are updated in all active columns. The model's main hydrological loop then begins again, by recalculating hydraulic gradients and depth-averaged K. This process continues until either: (i) model runtime exceeds a certain predefined value; or (ii) the model exhibits steady-state behaviour. For DBH's purposes, steady-state is defined by the proportion of all active columns exhibiting absolute water-table change of less than a critical amount during a hydrological timestep. At this point in the standalone hydrological model, descriptive data are written to file and the program terminates. In the ecohydrological versions of **`DigiBog`**, control passes to the ecological and/or hydrophysical submodels, some of which are informed by recent water-table behaviour, before another hydrological loop begins.

2.3.3. Hydrological submodel outputs

As a submodel within the larger **`DigiBog`** ecohydrological model suite, DBH was required to be able to produce a number of different measures of water-table behaviour in order to inform other submodels. These measures are:

- Steady-state/timeout water-table elevation, $H(x, y)$. This is the elevation of the water table above the impermeable base within each column at the end of a hydrological loop, whether the model has timed out or attained its steady-state criterion. Water-table elevation above an arbitrary datum is not a particularly

useful output for the purposes of informing ecological submodels, as it gives no indication of surface moisture availability, nor does it take account of time-averaged behaviour. Rather, H is merely the final position of the water table. However, H was a useful output for testing the hydrological model's solutions, as discussed in section **2.4.**, below.

- Steady-state/timeout water-table depth, d (x, y). As above, but water-table position for each column is expressed as a depth relative to the peat surface, which is not necessarily – indeed, rarely – contiguous between neighbouring columns. Such a quantity is the simplest measure of moisture availability at the surface of a given column, and is arguably of relevance, therefore, to processes such as vegetation succession and productivity. In common with H, however, d fails to take account of the behaviour of the water table throughout the duration of a hydrological model run.
- Steady state/timeout layer wetness, w (x, y, z). The decay submodel (see Chapters 5 and 6) operates on a layer-by-layer basis: that is to say that each layer within any given column loses mass at the end of an ecological timestep at a rate determined by that layer's peat quality and oxygen availability. w expresses time-averaged water-table behaviour as the proportion of each layer which is below the steady-state water table at the end of a hydrological loop.

2.4. Testing `DigiBog_Hydro`

2.4.1. Testing background

One of the main trade-offs of building DBH from scratch, as opposed to using an off-the-shelf package such as Modflow, was the loss of a guarantee that the model solutions work correctly. Two potential problems are associated with numerical models and are often caused by too coarse a spatial or temporal resolution. These are: (i) numerical instability, when the model solution fluctuates indefinitely between a number of unrealistic values or breaks down completely, and; (ii) numerical diffusion. Despite these problems, a numerical model is desirable for the construction of **`DigiBog`**. It simply would not be possible to develop analytical solutions for situations with spatial geometries and temporal variation as complex as the ones which **`DigiBog`** must deal with, because an analytical method would require all properties to be defined as functions of time and 3-D space. Numerical models use powerful computers to cycle many thousands or millions of times through large sets of much simpler equations in order to approach the solutions to much more complex situations than can be dealt with by analytical models. For simple situations for which an analytical solution does exist, individual **`DigiBog`** submodels can be tested by observing their deviation from the exact solutions as given by closed-form equations, and this forms the first type of testing to be performed on DBH in an attempt to falsify its predictions. While such exact-solution testing cannot strictly prove that a model is working as it should, a consistently close correspondence between model outputs and the exact solutions for a range of situations can be taken as strong evidence that the model is working correctly. Comparisons with exact solutions are also highly effective ways of finding 'bugs' in the code that might otherwise go unnoticed and could cause problems later in model development or analysis. In all tests described below, a timestep of 500.0 s and a spatial step of 100.0 cm were used.

2.4.2. Testing for conservation of mass

Before model outputs were compared against exact solutions from the literature, two simple tests were made on a 10 × 10 column grid, in order to check the conservation of mass in the transfers of water between columns and at the boundaries. The outer 36 columns were set as external to the boundary and effectively deactivated, bounded from the inner 36 active columns by 28 boundary columns. Flow was enabled in both the x and y directions, and water-table elevation H in all boundary columns was held constant through time at 1.0 cm above the impermeable base, while the 36 active columns had an

initial water-table elevation 100.0 cm above the base. Peat properties were uniform in all directions, with K = 0.005 cm s^{-1} and s = 0.5; evaporation and rainfall were set to zero. The active columns were allowed to drain to the boundary for 100,000 s. Firstly, a transient test was run, yielding a result of zero error (as represented by the double-precision representation of real numbers used in **DigiBog**), with the volume of water lost across the boundary exactly matching the total volume lost by all columns to full double precision. The test was repeated except that a constant net rainfall rate (P - E) of 5.0×10^{-7} cm s^{-1} was assumed and the model was allowed to run until a steady-state was reached. In order for steady-state conditions to occur, the model must lose water to the boundaries at the same rate that it receives rainfall. At steady state, time-integrated losses to the boundary underestimated rainfall input by 0.000034 % of the total depth of rainfall received. For the model tests presented in this chapter, percentage errors were calculated by deducting the value of the true solution from the value predicted by **DigiBog**, and then dividing this difference by the value of the true solution, thereby giving a standardised difference. This proportion was then multiplied by 100 in order to express it as a percentage.

In summary, both of the mass-balance checks were highly successful, suggesting that mass is indeed being conserved during transfers between columns and at the boundaries.

2.4.3. Testing water-table configurations against analytical solutions

The remaining tests performed on the hydrological submodel's output involved comparison of DBH's predictions of water-table configurations against exact solutions to specific, simple situations documented in the literature. Youngs (1990) gives the height H of a steady-state water table at any point in a bank of earth between two parallel ditches of constant water heights H_1 and H_0 such that $H_1 > H_0$ and where the D-F approximation is assumed:

$$H = H_1 \sqrt{1 - \left(1 - \frac{H_0^2}{H_1^2}\right)\frac{x}{L}} \tag{2.3}$$

where x is horizontal distance from the higher ditch and L is the horizontal separation between the ditches (*i.e.* the width of the earth bank). The hydrological submodel was set up to simulate this situation with time-invariant water levels in the ditches set at H_1 = 200 cm and H_0 = 100 cm and with the distance between the ditches set at L = 10,000

cm. Flow was deactivated in the *y* axis because Youngs' (1990) solution describes a strictly one-dimensional situation. At steady-state, the hydrological submodel's output water-table profile for any transect along the active columns of the *x* axis correlated well with the predictions of Equation (2.3). After 500,000,000 s of simulated time, **DigiBog** = 1.0 (Equation (2.3)) - 2×10^{-9} and $R^2 = 1.0$. The sum of absolute errors in all columns overestimated the predictions of Equation (2.3) by 1.49×10^{-9} %, so demonstrating exceptional performance within **DigiBog**'s normal expected operating domain. The same test was then rerun with a much steeper hydraulic gradient across a very coarse spatial resolution such that H_1 = 1,000 cm, H_0 = 100 cm and L = 1,000 cm, the kind of situation that is likely to occur only rarely in the full version of **DigiBog**. Again, after 500,000,000 s of simulated time, **DigiBog** = 0.9627 (Equation (2.3)) + 1.239 with $R^2 = 1.0$. The sum of absolute errors in all columns overestimated the predictions of Equation (2.3) by 2.83 % and so demonstrated acceptable performance even for situations well beyond **DigiBog**'s normal expected operating domain.

Ingram (1987) reproduced an equation that gives the height H of a water table within a cylindrical body of earth that is circular in plan. This vertical cylinder of earth has radius L and is fed by a steady rainfall of rate U (L T^{-1}). The cylinder drains to a peripheral ditch which contains an infinitesimally small depth of water. Both the cylindrical aquifer and the peripheral drainage ditch are immediately underlain by a flat, impermeable base material. The exact solution to this situation, again assuming the D-F approximation, is:

$$H = \sqrt{\frac{U(L^2 - x^2)}{2K}} \tag{2.4}$$

where K is the uniform hydraulic conductivity of the cylindrical aquifer and x is the radial distance from the central vertical axis of the cylinder. To replicate this situation using **DigiBog**, a finite depth of water in the ditch is necessary and a value of 1.0 cm was used. The cylinder of earth was assumed to possess a diameter (equal to $2L$) of 9,600 cm and was represented in **DigiBog** by 6,833 columns, each 2,000.0 cm high so as to ensure that in no column did the water table reach the top of the column, thereby ensuring that water was not lost from the model solution. K was set to 5.0×10^{-5} cm s^{-1} and U to 5.0×10^{-7} cm s^{-1}. A comparison of equation (2.4) with **DigiBog** for a transect from the centre of the cylinder to the peripheral ditch gave a regression result of

DigiBog = 0.9951 (Equation (2.4)) + 1.87, with R^2 = 0.999. Figure 2.2 shows **DigiBog** – Equation (2.4) for all grid locations, giving deviation of model outputs from the predictions of Equation (2.4) for all points in the model. The model overestimates Equation (2.4) at the northern, eastern, southern and western edges and underestimates it at the north-eastern, south-eastern, south-western and north-western edges, with error increasing with proximity to the boundary. These errors are due to the fact that a digital cylinder is used (so the boundary will not be a perfect circle in plan) and because a finite depth of water in the ditch is needed in the **DigiBog** solution. The sum of absolute errors in all active columns reveals that **DigiBog** overestimates the total amount of water in the model, according to the predictions of equation (2.4), by 0.102 % of the true value, representing excellent performance.

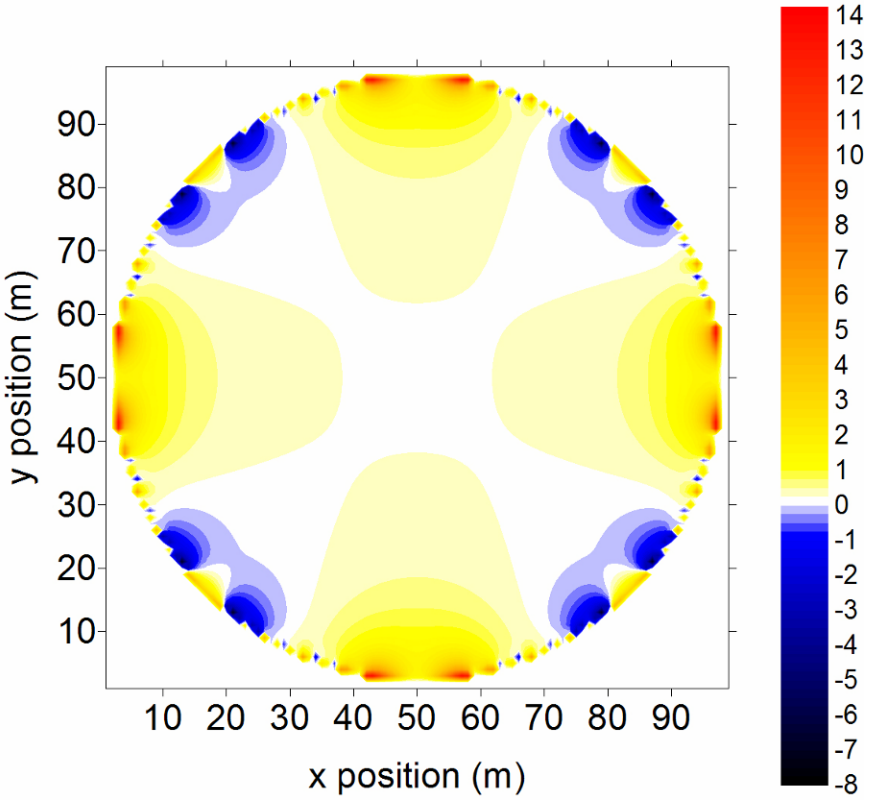

Figure 2.2: Model error, calculated as **DigiBog** *minus Equation (2.4), illustrated using coloured contour plot. Note colour scale legend on right of plot indicates error in cm.*

For the final test of the hydrological submodel a spatially-variable *K* was considered. Youngs (1965) offers solutions for a number of situations where the D-F approximation

holds and where hydraulic conductivity K is some function of elevation z above the impermeable base:

$$K = f(z) \tag{2.5}$$

Thus, K varies with vertical distance from the base, but is uniform in any horizontal plane. In the steady-state case of the flow of water through a bank of earth between two ditches that extend vertically to an impermeable base, and where the water levels in each ditch are constant but the level in one is higher than in the other, Youngs (1965) shows that:

$$QL = \int_{H_w}^{H_e} \left[\int_0^H K(z)\,\mathrm{d}z \right] \mathrm{d}H \tag{2.6}$$

where Q is discharge per unit width of the bank ($L^2\ T^{-1}$), L is the distance between the ditches (L), H_e is the constant water level at the upstream end of the bank (L), H_w is the constant water level at the downstream end of the bank (L) and H is water table level above the impermeable base (L). If equation (2.5) has the form:

$$K = K_0 \mathrm{e}^{\beta z} \tag{2.7}$$

where K_0 is hydraulic conductivity at $z = 0$ ($L\ T^{-1}$) and β is a constant, then hydraulic conductivity increases exponentially with elevation above the impermeable base and the solution to equation (2.6) is:

$$QL = \frac{K_0}{\beta}\left[H_w + \frac{\mathrm{e}^{\beta H_e}}{\beta} - H_e - \frac{\mathrm{e}^{\beta H_w}}{\beta} \right] \tag{2.8}$$

DigiBog was configured so as to represent the situation described by Equation (2.8), with the parallel ditches assumed to be separated by 97,000 cm. The area between the ditches was therefore represented by 96 columns. Each column consisted of 100 layers of thickness 1.0 cm and s was set to 0.5. K varied between layers according to equation (2.7), with the elevation, z, for each layer taken to be the height of the layer's mid point (meaning that no layer possessed K_0). The water level in the upstream ditch (representing H_e) was set to 100.0 cm, while in the downstream ditch (H_w) the water

level was set to 50.0 cm. For $K_0 = 0.0000005$ cm s^{-1} and $\beta = 0.01$, equation (2.8) yields the prediction that $Q = 2.93588 \times 10^{-7}$ cm^2 s^{-1}. **DigiBog** yielded a steady discharge along the transect of $Q = 2.9350 \times 10^{-7}$ cm^2 s^{-1}, equivalent to an absolute error of 0.03%. Yet again, this error is well within acceptable limits for the hydrological submodel.

2.5. Extended Demonstration of Hydrological Model

In this section, four different scenarios are simulated in order to demonstrate more comprehensively the ability of the hydrological model to simulate water-table behaviour in a range of situations of varying realism. Specifically, it was desirable to demonstrate the capabilities of the hydrological model in simulating situations for which analytical solutions do not exist. This demonstration uses model aquifers that have relatively simple geometric shapes.

2.5.1. Experimental setup

The four simulated scenarios used to demonstrate the capabilities of the hydrological model are:

(i) Water-table drawdown in an aquifer which is kidney-shaped in plan, underlain by a flat, impermeable mineral soil/bedrock layer. The modelled aquifer had a flat, featureless surface and sheer, vertical sides which extended 300.0 cm above the impermeable base. In plan, the aquifer had a long axis of 132 m and at its widest point was 100 m across (see Figure 2.3). The aquifer had homogeneous hydraulic properties, with hydraulic conductivity = 0.005 cm s^{-1} and effective porosity = 0.3. The aquifer was surrounded on all sides by a Dirichlet boundary which consisted of a 0.5 cm thick wetted contact, representing a shallow peripheral stream into which the aquifer drained. Net rainfall rate was assumed to be zero and the initial water table of 300.0 cm above the base (*i.e.* the initial water table was at the surface) was allowed to drain to the boundary ditch.

(ii) As (i) above, except that hydraulic conductivity increased with elevation above the impermeable base according to Equation (2.7) with K_0 = 0.0005 cm s^{-1} and β = 0.018 (see Figure 2.7).

(iii) As (i) above, but the modelled aquifer had a plan shape of two overlapping circles. The aquifer had a long axis of 132 m and at its widest point was 74 m across (see Figure 2.5).

(iv) As (iii) above, except that hydraulic conductivity increased with elevation above the impermeable base according to Equation (2.7) with K_0 = 0.0005 cm s^{-1} and β = 0.018 (see Figure 2.7).

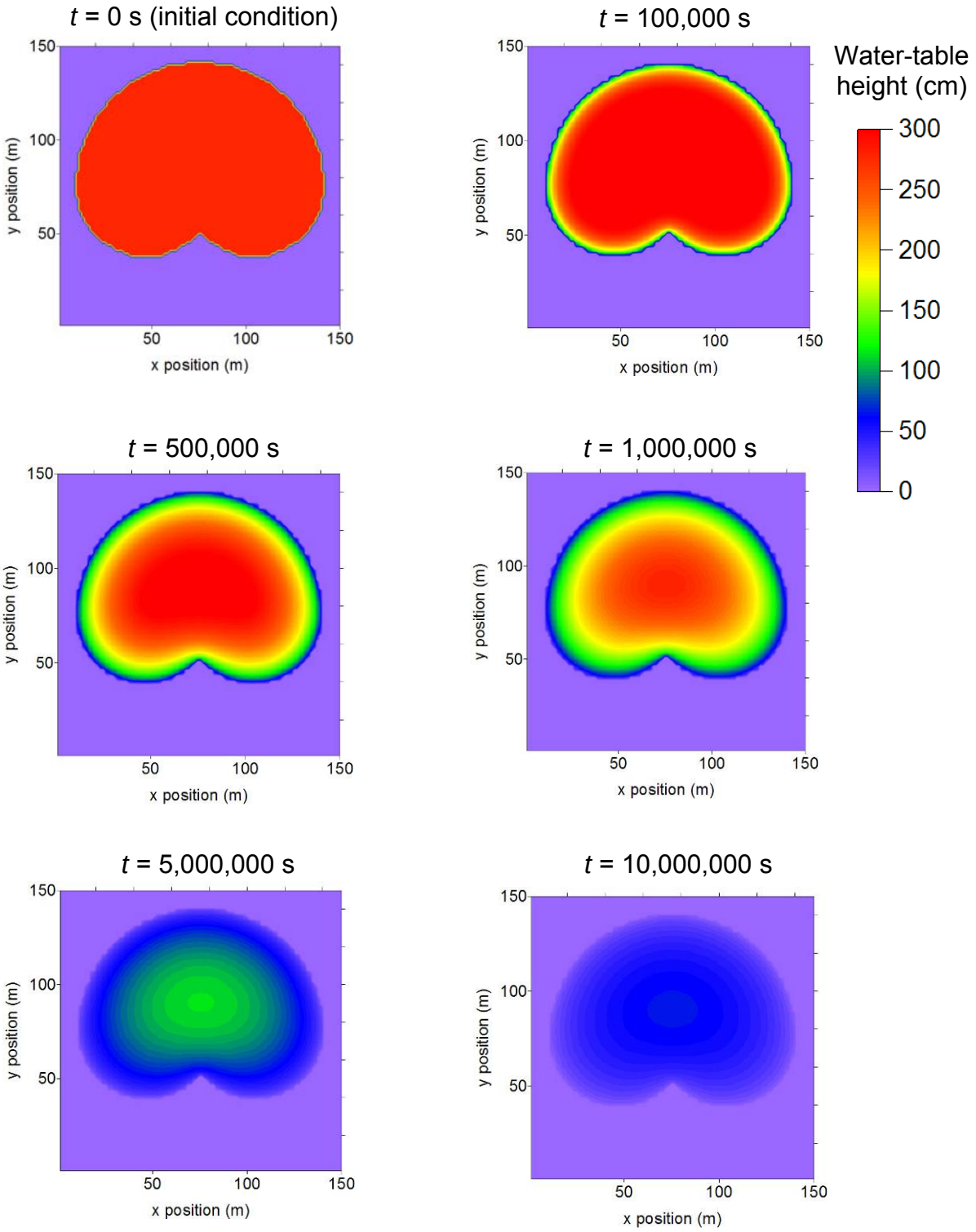

Figure 2.3: Water-table height maps through time in a kidney-shaped aquifer, as predicted by DBH. Hydraulic conductivity is homogeneous. t *is simulated model time in seconds. Water-table heights given as height above impermeable base.*

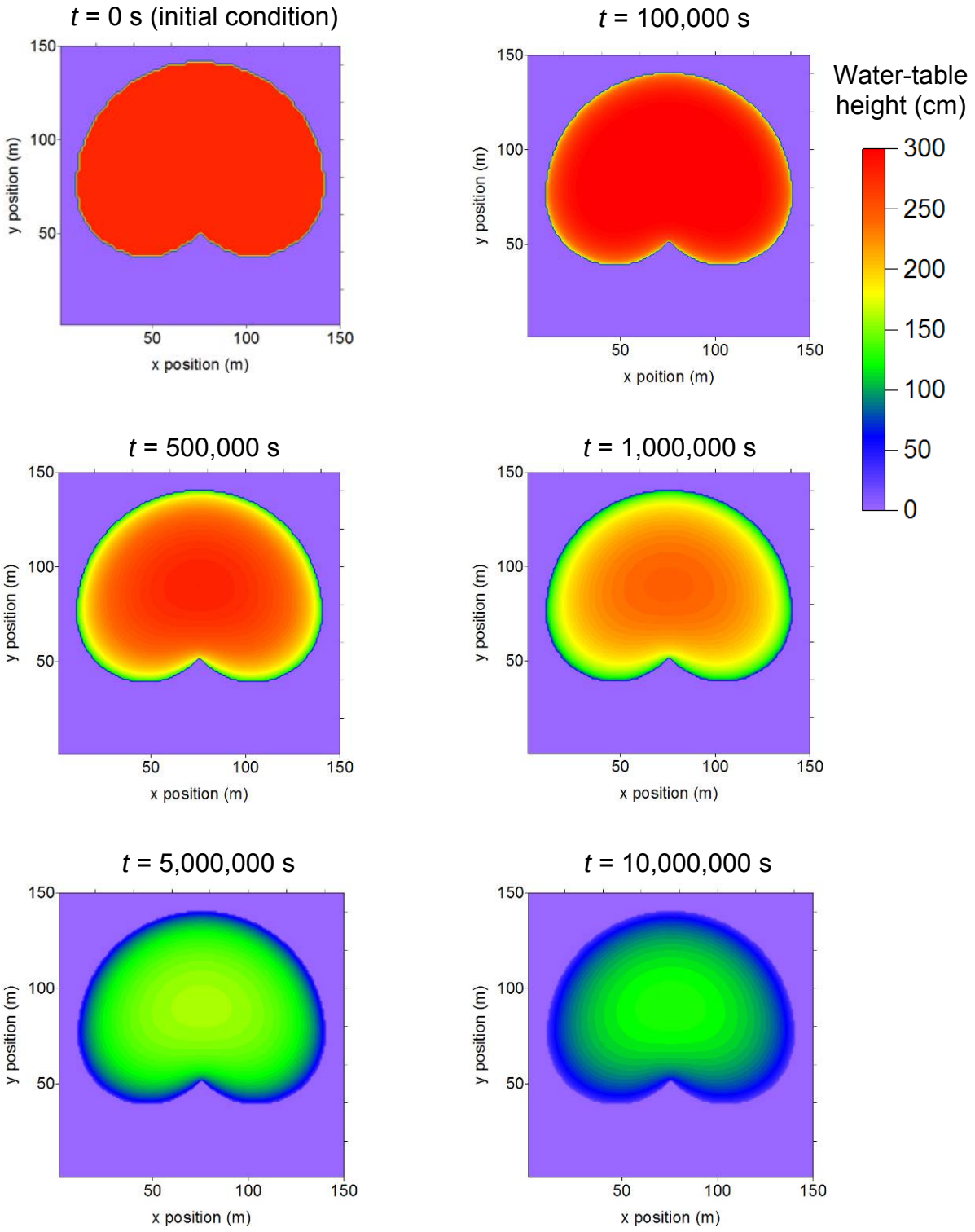

Figure 2.4: Water-table height maps through time in a kidney-shaped aquifer, as predicted by DBH. Hydraulic conductivity varies with depth according to equation 2.7. t *is simulated model time in seconds. Water-table heights given as height above impermeable base.*

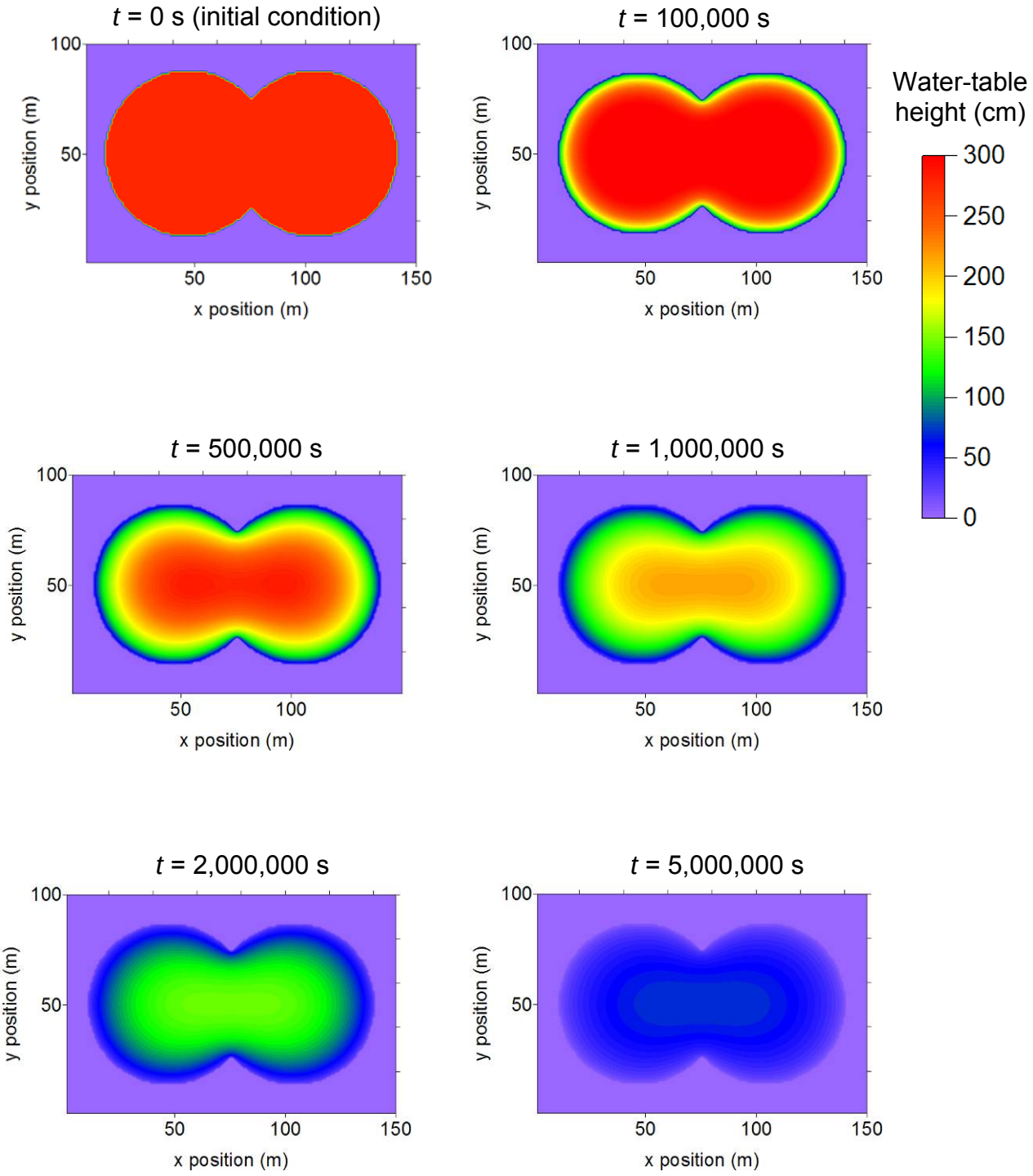

Figure 2.5: Water-table height maps through time in a figure-of-eight-shaped aquifer, as predicted by DBH. Hydraulic conductivity is homogeneous. t *is simulated model time in seconds. Water-table heights given as height above impermeable base.*

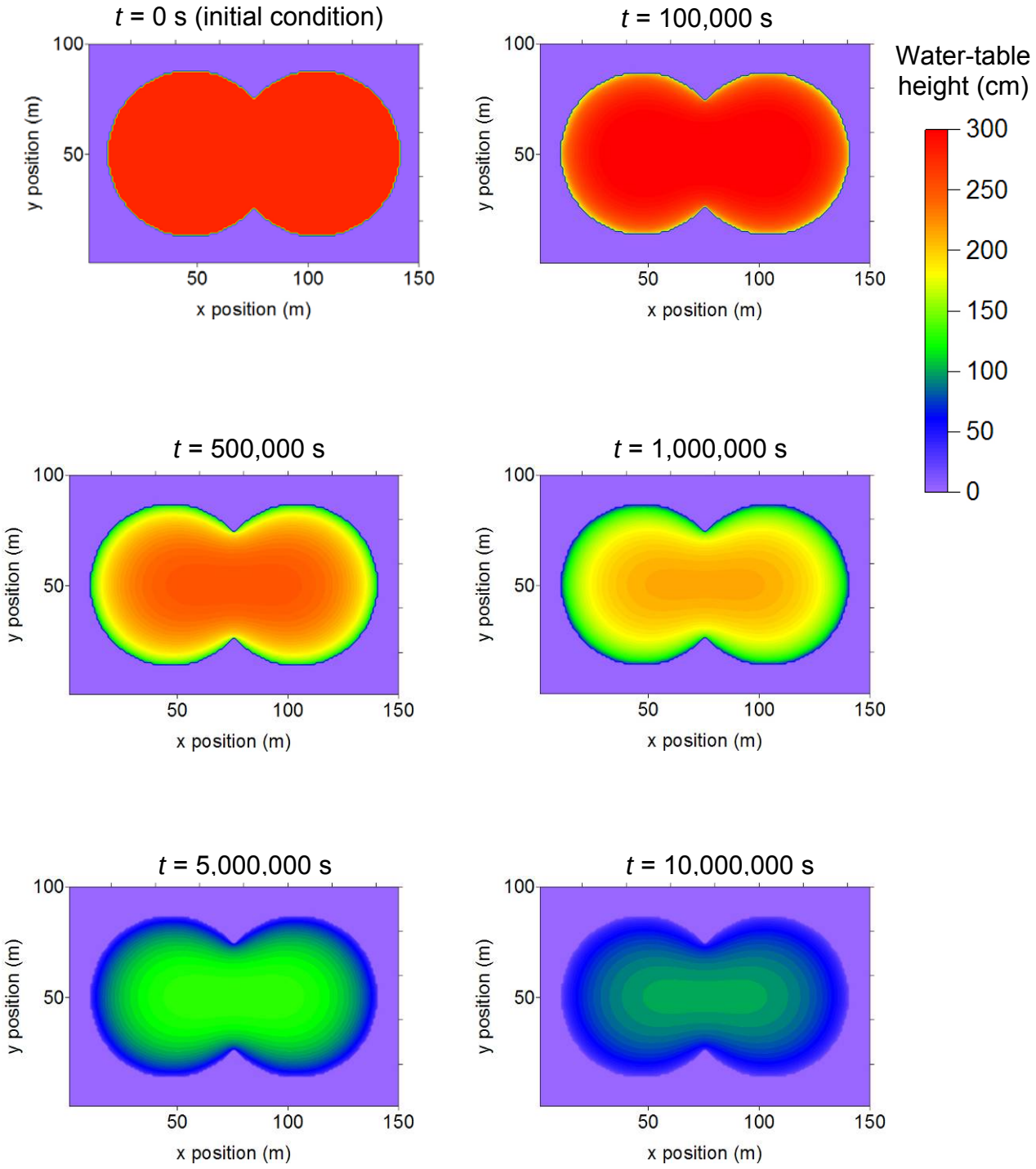

Figure 2.6: Water-table height maps through time in a figure-of-eight-shaped aquifer, as predicted by DBH. Hydraulic conductivity varies with depth according to equation 2.7. t *is simulated model time in seconds. Water-table heights given as height above impermeable base.*

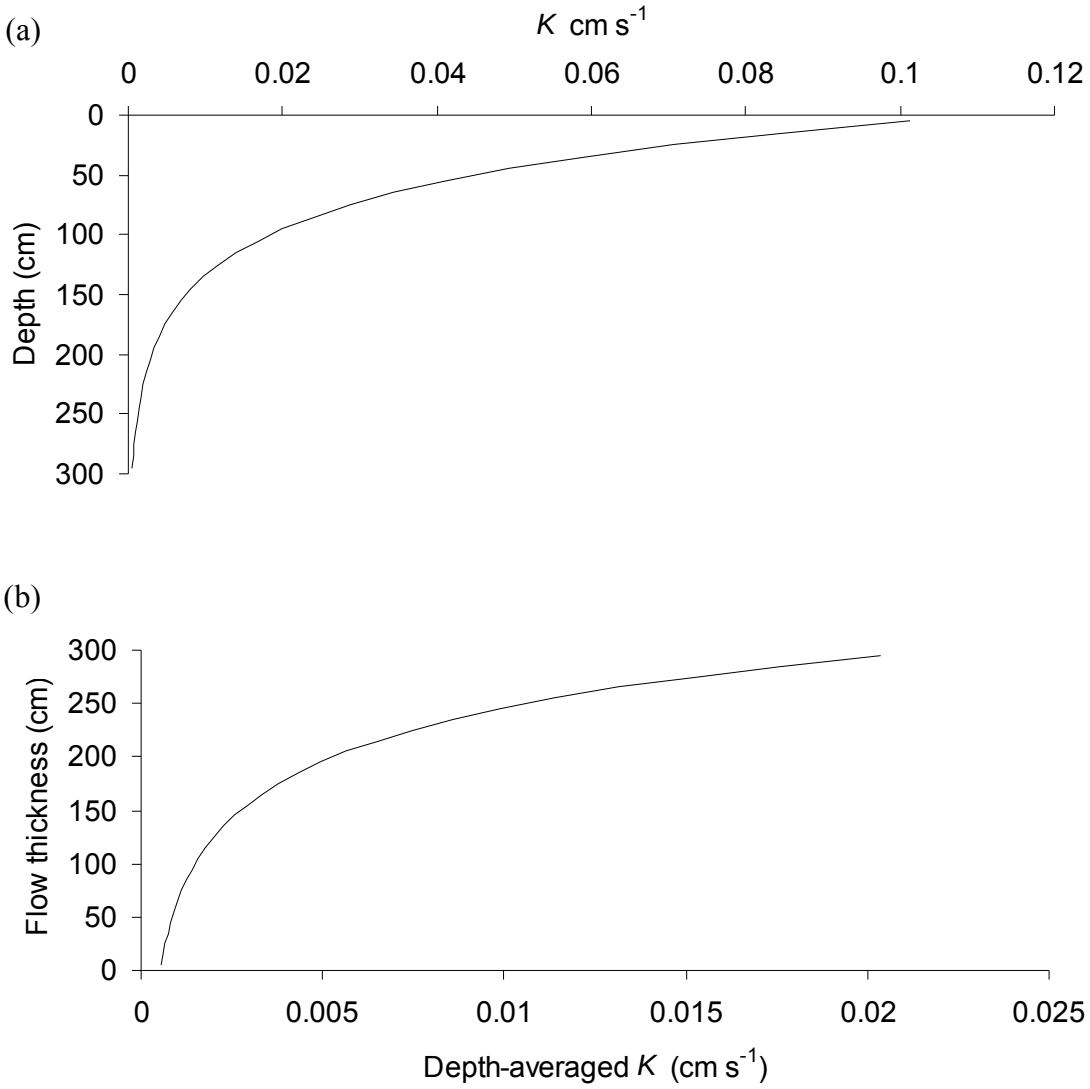

Figure 2.7: (a) hydraulic conductivity and (b) depth-averaged hydraulic conductivity profiles for simulations (ii) and (iv).

2.5.2. Demonstration Results

Figures 2.3 through 2.6 show time series of water-table drawdown for simulations (i) through (iv). In all cases, initially steep hydraulic gradients at the aquifers' boundaries were allowed to drain to the peripheral ditches, and each plot shows change in water-table position with time. Regardless of aquifer shape, homogeneous and heterogeneous *K* distributions produced distinctive, characteristic patterns in water-table drawdown. As can be seen in Figures 2.3 and 2.5, when *K* was homogeneous, the water table initially drew down steeply near the boundary, whilst the water-table levels near the centre remained high until 500,000 s (iii) or 1,000,000 s (i). This led to a strongly convex-upwards curvature to the water-table shape in the simulations with homogeneous *K*. By contrast, the very high *K* values in the shallow layers of the

heterogeneous aquifers (Figures 2.4 and 2.6) caused water tables to drain more evenly at first, resulting in a lower, flatter central area than in the homogeneous simulations. As water-table levels fell with time, however, flow was increasingly restricted to layers of low *K*. This resulted in water tables becoming more curved as most flow occurred near to the boundary where hydraulic gradients were steep. The low *K* in the deepest peat layers means that water table levels by the end of the 10,000,000 s runs were higher in the heterogeneous runs than in the homogeneous. Indeed, the homogeneous aquifers had all but completely drained by the end of the simulations whereas the heterogeneous runs still showed distinct curvature to the water table, with central water-table heights of over 100 cm.

Furthermore, the pattern of drainage in each case is clearly influenced in a plausible manner by the shape of the aquifer. For instance, in Figures 2.3 and 2.4, the water table draws down much more steeply near the centre of the southern edge of the aquifer, where the shape of the aquifer is pinched. Similarly, the same effect occurs in Figures 2.5 and 2.6 where the water table draws down more steeply at the centre of the northern and southern edges, where the aquifer is again narrower.

Figure 2.8 shows the change through time in the total volume of water held in each aquifer. It is clear that for both aquifer shapes, a homogeneous *K* distribution led to a quicker overall drainage than a heterogeneous distribution where *K* decreased with depth. Even though depth-averaged *K* at the start of the simulations was higher in the heterogeneous aquifers (see Figure 2.7), drainage losses to the boundaries were reduced by the relatively low *K* in the deepest peat layers (for the bottom layers, $K = 0.00055$ cm s^{-1} in the heterogeneous aquifers as opposed to 0.005 cm s^{-1} in the homogeneous aquifers).

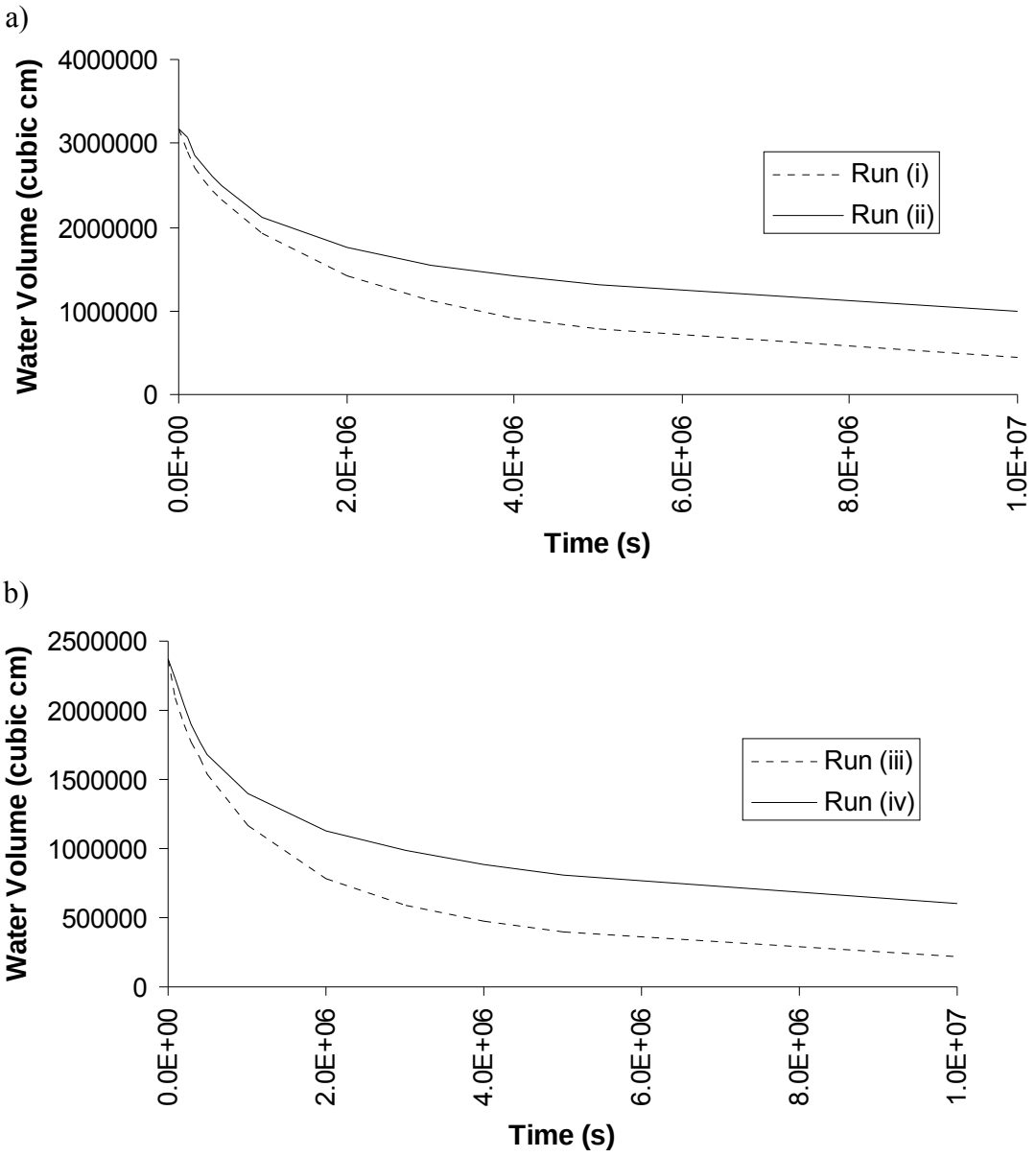

Figure 2.8: Plots showing change through time of total water volume stored in a) kidney-shaped aquifers and; b) aquifers with plan shape of overlapping circles.

2.6. Simulating a Real Bog

In order to demonstrate the ability of DBH to simulate water-table behaviour in a real raised bog, a Digital Elevation Model (DEM) of Cors Fochno, West Wales, with a horizontal resolution of 12 m, was converted into a DBH model in order to judge whether the model predicted plausible water-table behaviour across the bog. After demonstrating the model's ability to simulate water-table behaviour in aquifers with simple geometric shapes in section **2.5.**, above, the wider utility of the model was demonstrated during consultancy work contracted by the Countryside Council for Wales (CCW); some of that work is presented here in order to illustrate the ability of DBH to represent real aquifers with highly complex geometries.

2.6.1. Site description

Cors Fochno is a partially cutover, estuarine raised bog in West Wales (52° 30'N, 4°0'W), the dome of which is at a mean elevation of approximately 5-6 m above sea level. Mean annual temperature is 9.9 °C and mean annual net rainfall is approximately 122 cm yr^{-1}. At its thickest the peat deposit is approximately 6.5 m thick (A. J. Baird, personal communication). Cors Fochno and other, smaller peat domes in the vicinity were cut extensively for fuel and for land reclamation between 1820 and 1970. The smaller domes have all but disappeared as a result of the cutting, but a large, central dome of peat remains, covering an area of 653 ha, tightly bordered on all sides by agricultural and residential land (Baird *et al*., 2006). In terms of ease of model setup, Cors Fochno offers a more attractive proposition than many uncut sites because it is almost entirely surrounded by open-water ditches which are regularly monitored by CCW (see section *2.6.2.*, below).

As part of the monitoring and management scheme implemented at Cors Fochno by CCW, dipwells containing pressure transducers with automatic data loggers have been installed by A. J. Baird at five locations along a 250-m long transect running approximately north by north-west from the Pwll Ddu, a former lagg stream which has since been deepened to form a large agricultural drainage ditch on the site's southern margin (see Figure 2.9). The pressure transducer in the downslope-most dipwell was malfunctioning during the monitoring period, meaning that only four dipwells have provided useable data. Table 2.1 shows the time-averaged water-table depths in the four dipwells with working pressure transducers. Water-table depth measurements were taken every two hours during two separate periods, covering a total of 32 days between

December 2005 and February 2006. The data show the response of water tables to rainstorm events and were used to assess the plausibility of model behaviour.

Table 2.1: Locations and time-averaged water-table depths for the four dipwells near the Pwll Ddu.

Dipwell name	Distance from Pwll Ddu (m)	Time-averaged water-table depth (cm)
PDPT1	246.4	4.43
PDPT2	155.7	1.75
PDPT3	101.5	18.79
PDPT4	58	5.87

The coarse grid resolution of 12 m means that it would have been inappropriate to try to assign columns in the Cors Fochno DBH model to the locations of the four dipwells for direct comparison of water-table behaviour. Rather, a transect of model columns in the closest possible vicinity to the location dipwell transect may be identified, and the shapes of water-table profile compared. The fact that no data were available from the downslope pressure transducer is problematic, however, because it means that the shape of the drawdown in water table at the boundary cannot be seen.

Baird *et al*. (2008) used extensive piezometer measurements to assess the 3-dimensional distribution of K at Cors Fochno. They found strong, interrelated controls upon K exhibited by both plan position and depth. Particularly, their measurements showed strong evidence of (i) a central area where K declined in a non-linear manner with increasing depth from the surface, and (ii) a marginal rand, distinct from the central zone and approximately 300-400 m in width, where K values were generally observed to be lower than in the central area. As with the central area, K in the marginal areas decreased with depth, apart from at the greatest depths (nominally '400 cm' according to the categorical depth classification of Baird *et al*., 2008), which exhibited the highest K values of all depths in the marginal zone. Depth distributions of median K values for both central and marginal areas, as measured by Baird *et al*. (2008) are summarised in Table 2.2.

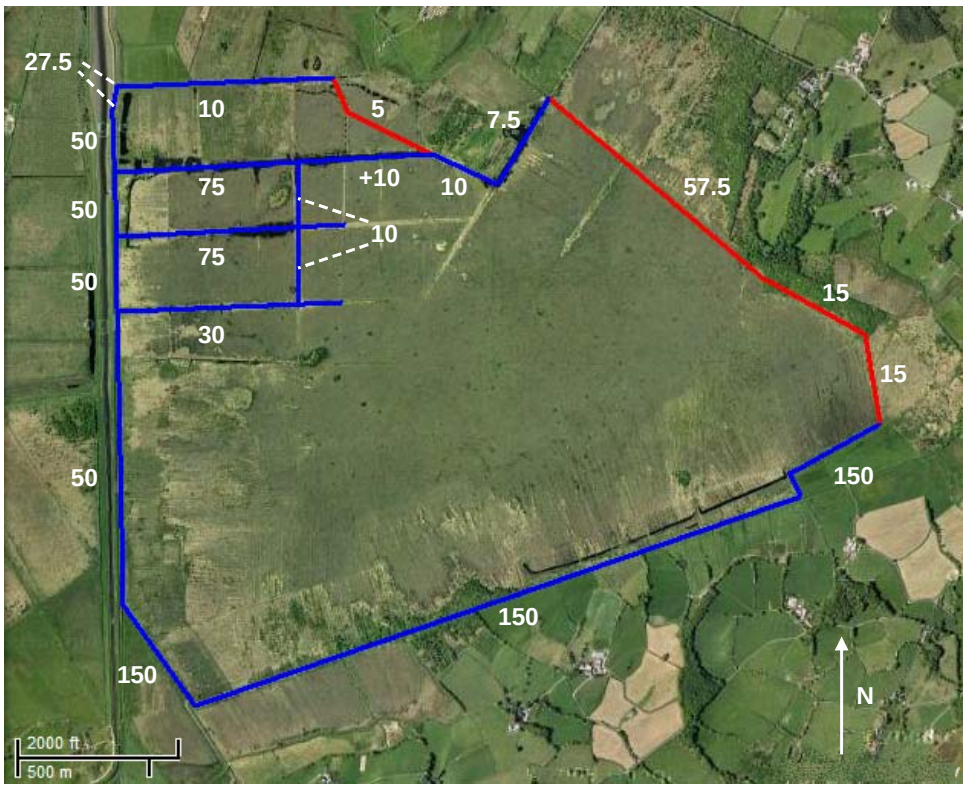

Figure 2.9: Aerial photograph showing positions and water-table depths of both internal and external boundaries within Cors Fochno site. Blue lines represent open-water ditches where water levels have been measured, red lines are boundaries where average water-table depth below surface has been estimated. Numbers indicate assumed water-table depths (cm below surface) in adjacent boundary sections. Note that the boundary with the + 10 level is elevated above the surrounding bog surface by peat bunds. Note also that the Pwll Ddu drainage ditch, which features prominently in the storm simulations, is the ditch oriented WSW-ENE at the southern edge of the site, labelled with a water-table depth of 150 cm. Image adapted from Google Maps.

Table 2.2: profiles of median K *values at Cors Fochno as measured by Baird* et al. *(2008). The marginal zone may be thought of as all areas within 100 m boundary ditches, as illustrated in Figure 2.9.*

Depth (cm)	Central Zone K (cm s^{-1})	Marginal Zone K (cm s^{-1})
50	0.000467	0.000144
90	0.000823	0.000046
130	0.000614	0.000098
200	0.00349	0.000051
400	0.000096	0.000608

Some of the peat in marginal areas at Cors Fochno – particularly along the Pwll Ddu where large peat bunds have been built – shows evidence of degradation and cracking although the extent of these cracks is not clear (Baird *et al*., 2006). An extensive network of cracks in dried peat might provide highly preferential pathways for groundwater flux. Piezometer measurements taken in or very near to cracks would overestimate the true K of a peat soil, whereas measurements between cracks would underestimate K. As such, any modelling of hydrological behaviour based on piezometer measurements of cracked peat is likely to be highly prone to errors. However, with no alternatives available, the only option is to accept with caution the measurements of Baird *et al*. (2008)

2.6.2. Model setup, parameterisation

High-resolution LIDAR data provided by Environment Agency (Wales) gives elevation above sea level for the Cors Fochno site and the area immediately surrounding it, and were aggregated by Baird *et al*. (2006) to give a resolution of 12 m. A 300 × 300 grid square subset of these data, which covers what remains of the main bog dome and the peripheral ditches to which it drains, was used as a digital elevation model (DEM) and converted into input files for DBH. The boundaries illustrated in Figure 2.9 were implemented: those marked in blue are open-water ditches, which are either purpose-built drains or inundated former peat cuttings, where the Cors Fochno site manager for CCW, Mike Bailey, was able to measure a representative depth below surface for the water in the ditches. The boundaries marked in red, however, are not open-water ditches. Rather, they are topographically lower areas of the landscape where Mr Bailey was able only to estimate an annual average depth to water table.

Again in the absence of evidence to the contrary and for the sake of parsimony, a flat, planar impermeable base layer was assumed, 650 cm below the top of the column with the greatest elevation. The DEM data were smoothed using a purpose built algorithm, the details of which are not given here, so as to remove small-scale ‘spikes’ and other oddities within the dataset which likely represent trees and bushes that have been detected by the LIDAR beam. The smoothed DEM is illustrated in Figure 2.10.

For all runs, each model column consisted of four layers representing the intact zone, which was assumed to have a total thickness of 35 cm (the uppermost layer, assumed to represent live vegetation, was 5 cm thick, and the three layers below were 10 cm thick

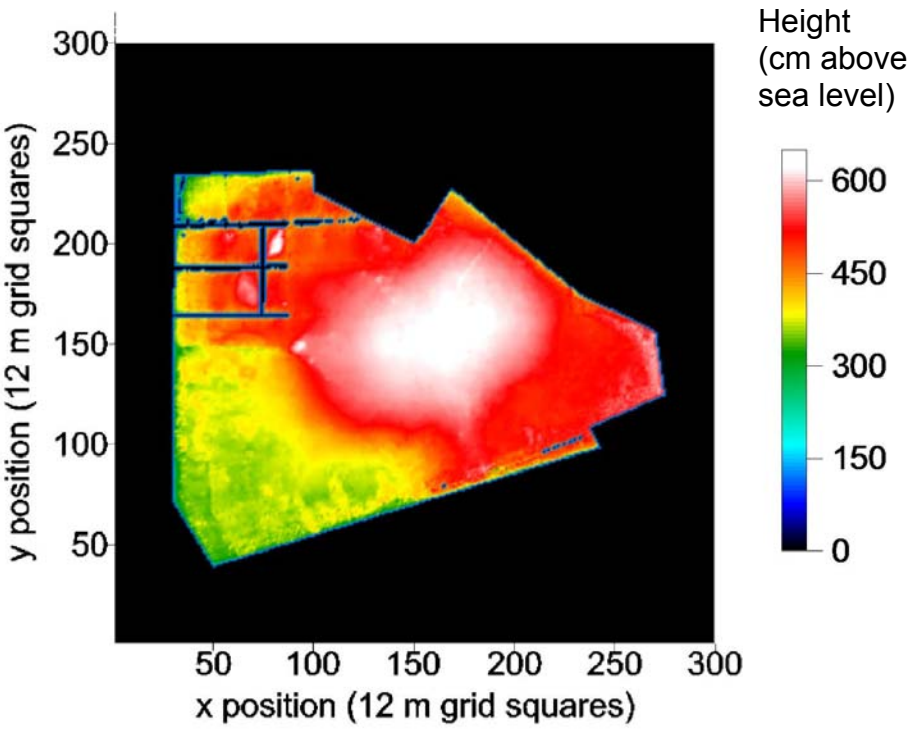

Figure 2.10: Digital elevation model of Cors Fochno raised bog, with 12 m horizontal resolution, after smoothing. Colour shading indicates height above impermeable base. See text for full description of smoothing. N.B., black shading denotes areas external to model boundaries.

each), underlain by a single layer to represent the compressed zone, which extended from the base of the intact zone down to the impermeable base. All active columns within 100 m of a boundary were assumed to possess a depth distribution of *K* representative of that measured by Baird *et al*. (2008) in the marginal areas of Cors Fochno. The *K* distributions assumed for both marginal and central areas are shown in Table 2.3. While the assumed values for very near-surface peat are substantially higher than any of the median values observed by Baird *et al*. (2008), they are below the maximum values observed and are plausible values for fresh, oxic-zone peat, for which Baird *et al*. (2008) did not take measurements. Below depths of 35 cm, hydraulic conductivity was assumed to be uniform and equal to 0.001 cm s^{-1} (central zone) or 0.0001 cm s^{-1} (marginal zone). Shallow layers in the model exhibit large variations in *K*, whereas deep layers assumed uniform *K* with depth. This represents the fact that shallow peat layers are the hydrologically most important (Ingram, 1978), and the model was deemed likely to exhibit the greatest sensitivity to their *K* values. The reader is reminded that all *K* values assumed here should be taken as being only broadly

representative of the properties of peat at Cors Fochno. This reflects the fact that the point of the current exercise is to demonstrate the capability of DBH in representing plausible behaviour at a real bog, rather than to conduct a full and accurate sensitivity analysis.

Table 2.3: Assumed K *and* s *profiles in central and marginal areas of the Cors Fochno model.*

Depth Interval (cm)	Central Zone K (cm s^{-1})	Marginal Zone K (cm s^{-1})
0 – 5	Variable (see *2.6.3.*, below)	0.01
5 – 15	0.1	0.01
15 – 25	0.0058	0.001
25 – 35	0.0015	0.001
> 35 (catotelm)	0.001	0.0001

Depth Interval (cm)	Central Zone s (-)	Marginal Zone s (-)
0 – 5	0.45	0.2
5 – 15	0.25	0.2
15 – 25	0.2	0.15
25 – 35	0.175	0.15
> 35 (catotelm)	0.15	0.1

2.6.3. Model spin-up

Comprehensive empirical data giving water-table depth distributions across Cors Fochno are not available, meaning that generating a realistic and defensible initial condition is not a trivial task. In the absence of evidence to the contrary, it was deemed reasonable to use a 'spin-up' period to generate initial conditions, a similar manner to that employed in global atmospheric oceanic circulation models (e.g., Merlis and Khatiwala, 2008; Johns *et al*.,1997). At the start of the spin-up, all model columns had initial water-table elevations equal to bog surface elevation, *i.e.* all columns were fully saturated, and the model was then allowed to drain. Net rainfall rate was set to zero and the model was run for 30 simulated days, allowing model water tables to drain to the boundaries. Five different spin-up treatments were experimented with, each assuming a different spatial distribution of K, so that the results of the spin-up could be assessed and a set of suitable initial conditions chosen:

- Spin-up run 1: K distribution as per Table 2.3, with the 0-5 cm interval in the central zone assumed to possess K = 1.0 cm s^{-1}.

- Spin-up run 2: K distribution as per Table 2.3, with the 0-5 cm interval in the central zone assumed to possess $K = 5.0$ cm s^{-1}.
- Spin-up run 3: K distribution as per Table 2.3, with the 0-5 cm interval in the central zone assumed to possess $K = 10.0$ cm s^{-1}.
- Spin-up run 4: K distribution in central zone was as per Table 2.3, with the 0-5 cm interval in the central zone assumed to possess $K = 5.0$ cm s^{-1}. This same depth distribution of K was also applied to the marginal zone; *i.e.*, the marginal and central zones both possessed the same K distribution.
- Spin-up run 5: identical to the setup for spin-up run 2, except that the lowest layer (> 35 cm depth) in the marginal zone was assumed to possess $K = 0.0006$ cm s^{-1}.

As well as the spin-up runs serving to generate initial conditions for the simulation runs, the different K setups also allowed a partial consideration of the effects of K distribution upon drainage. While the model clearly has almost limitless degrees of freedom when it come to selecting appropriate K values, those given above are within reasonable limits suggested by Baird *et al*. (2008), and describe a non-linear decrease in K with depth.

Figure 2.11 shows final water-table depths for the eight columns in the transect running N-NW from the Pwll Ddu after the 30-day spin-up runs. The plot also includes empirical data showing time averaged water-table depths from the four dipwells. Because the downslope dipwell provided no usable data, water-table depth at the southern end of the transect is assumed to be 150 cm, equivalent to Mike Bailey's estimate for water level in the Pwll Ddu. Spin-up run 1 appears to have provided the closest approximation of the dipwell data, with a shallow up-slope water table and a steep draw down at the down-slope end of the profile, and the final water-table distribution from this run (see Figure 2.12) was taken as the initial water-table condition for all subsequent simulation runs (see section *2.6.4.*, below). Runs 2 and 3, which assume higher near-surface K in the central zone, produced slightly deeper water tables near the up-slope end of the profile, but their predicted draw down to the Pwll Ddu are all but identical to that of run 1. In runs 4 and 5, K distributions in the central zone were assumed to be identical to that in the central zone of spin-run 2. These runs showed very similar behaviour in the central zone to spin-up run 2 but were, predictably, much drier

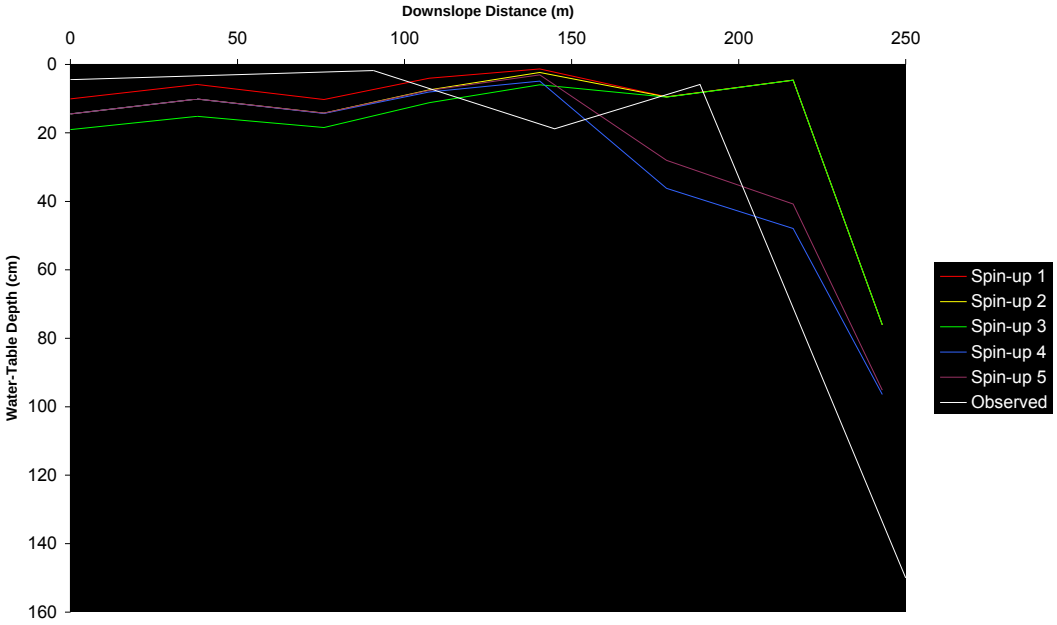

Figure 2.11: Water-table depth profiles in the five spin-up runs and observed time-averaged water-table depth observed in the four dipwells.

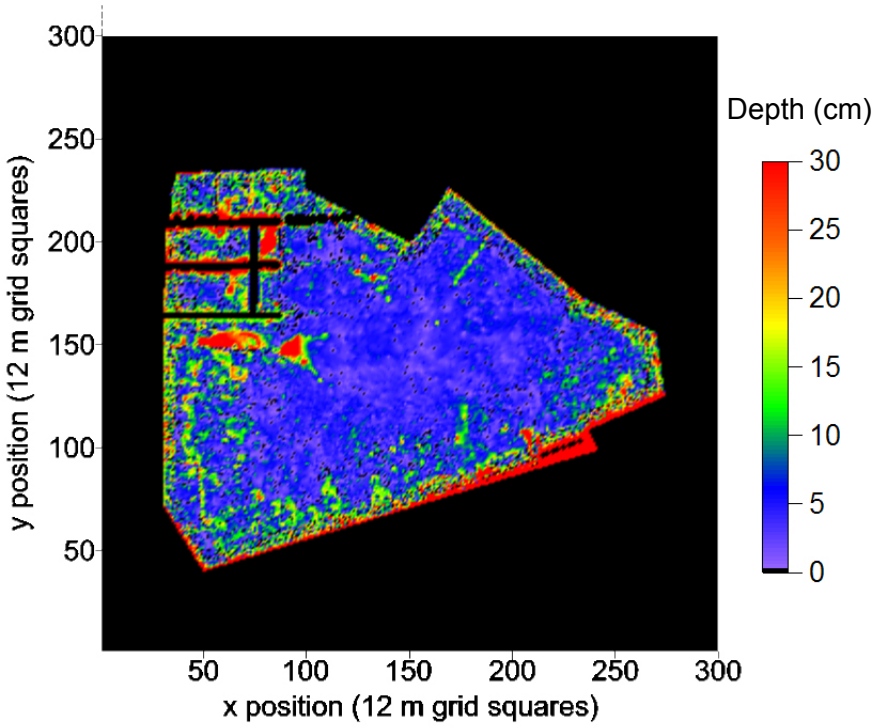

Figure 2.12: Map showing water-table depth distribution after 30-day spin-up period, used as an initial condition for the four subsequent experimental runs.

in the marginal zone. Runs 4 and 5 gave a better approximation of the dipwell data near the boundary, but it was deemed more important to use the distribution that gave the

best approximation of shallower, upslope water tables, which apply to the majority of the spatial extent of the bog. The results of the spin-up runs suggest that, over short-medium timescales such as 30 days, the effects of differential *K* values upon DBH model behaviour are highly localised. The model appears to be sensitive to marginal-zone *K* values, as even a small increase in marginal *K* produced much steeper drawdowns.

2.6.4. Model response to rainfall events

Four simulation runs were performed in order to examine the response of the DBH representation of Cors Fochno to simulated storm events. While the effects of storm events of different magnitudes were to be examined, an experimental design including a range of possible *K* distributions was not used, for two reasons. Firstly, the purpose of this experimental work was to demonstrate the capability of DBH in simulating water-table behaviour in a real bog, rather than to provide a full sensitivity analysis. Secondly, the spatial and temporal extent of available quantitative empirical data against which the model could be tested was extremely limited, meaning that it would have been difficult to evaluate meaningfully subtle variations in predicted water-table positions. Therefore the *K* and *s* distributions, boundary conditions and spatial and temporal resolutions used were identical to those in spin-up run 2. The only alterations to the setup for the simulation runs were that rainfall was assumed to be non-zero and time-variant, and model runtimes were reduced to eight hours. Each of the four simulation runs assumed rainfall events of different magnitudes, with: (a) 1 cm; (b) 2 cm; (c) 5 cm; and (d) 10 cm of net precipitation delivered over six hours, after which the model was allowed to drain for a further two hours under zero net rainfall conditions. The four treatments represent storm events which range from the modest – treatment (a) – up to the extremely, probably unrealistically, severe – treatment (d).

Differences in final water-table depth distributions between treatments were striking. The final water-table depth maps in Figure 2.13 generally show increasing wetness, as one would expect, with increasing magnitude of storm event. The most striking differences are between treatments (a) and (b), and between treatments (b) and (c). Treatment (a) has very few columns in which water tables are at the bog surface, whereas in treatment (c) many columns are completely saturated, all over the model grid. Water-table depths close to boundaries also noticeably decrease with increasing rainfall. The final water-table depth maps for treatments (c) and (d) exhibit much less

difference to one another, because both are almost entirely saturated. It seems likely that the rainfall events in both simulations caused water tables in most columns to rise to the surface of the model, after which further rainfall would have caused water to have been lost from the model solution. While this 'excess' water is not strictly accounted for in the model's mass balance equation (see Equation 2.2), it may be taken to represent overland flow losses during an extreme storm event. The two hours of drainage in treatments (c) and (d) have barely allowed water-table depths to increase beyond 2 cm in the majority of model columns, although water tables in columns close to the south-eastern and north-western boundaries are noticeably deeper for run (c) than for run (d). In run (d) almost all columns, including those adjacent to deep boundaries, are completely flooded.

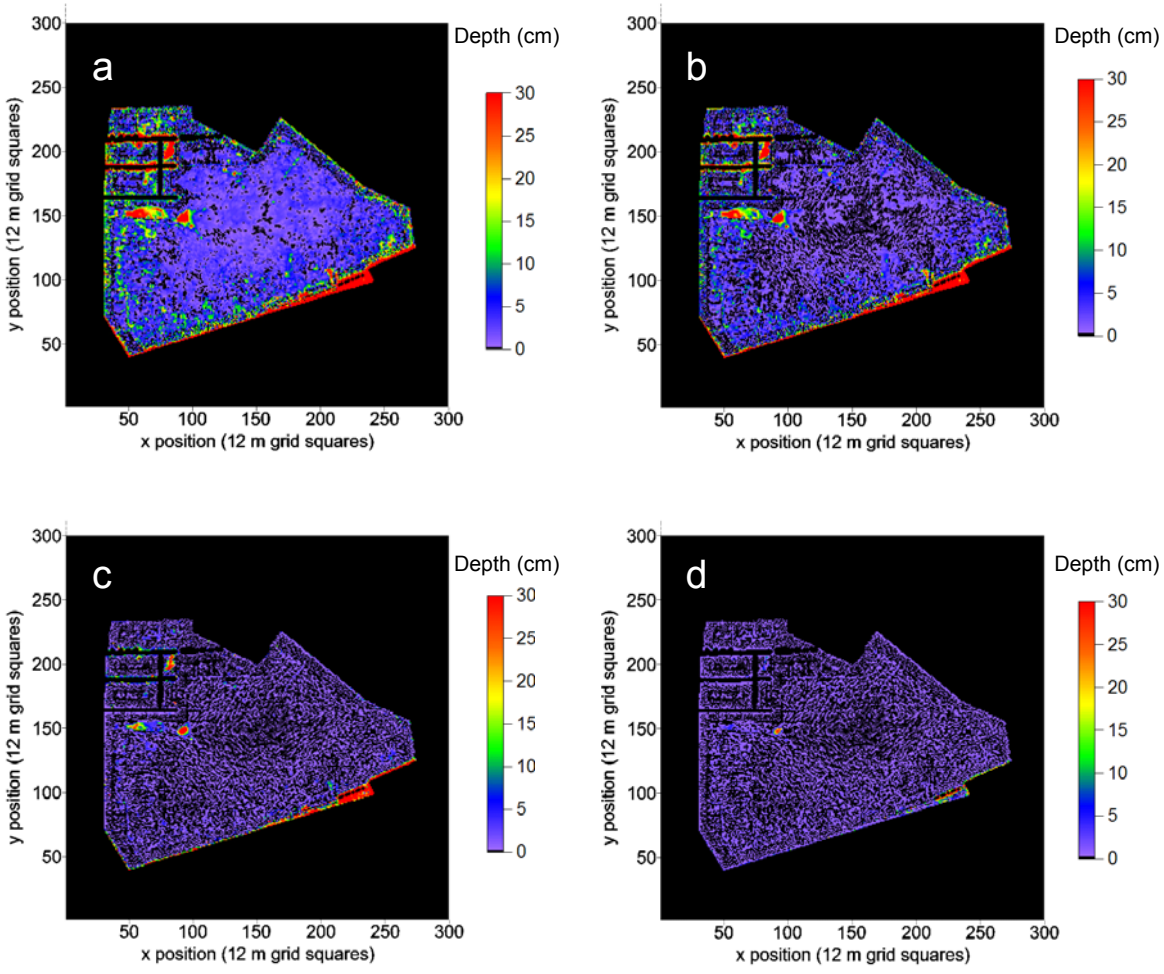

Figure 2.13: Maps showing water-table depth distributions after 6-hour storms which delivered rainfall depths of (a) 1 cm; (b) 2 cm; (c) 5 cm; and (d) 10 cm.

2.7. Discussion and Conclusions

The hydrological testing was highly successful, offering strong evidence that **DigiBog_Hydro** is functioning correctly. The largest error observed in any test was 2.83 %, in a situation well outside of **DigiBog**'s normal expected operating domain. Estimates could be further improved in all cases, if necessary, by using a finer spatial or temporal resolution or by setting a more stringent definition of what constitutes steady-state behaviour (*i.e.* by allowing the model to run for longer). Water mass appears to be conserved correctly during transfers between columns, at the boundaries and as input from rainfall. The model performed well when simulating situations both inside and outside of its anticipated normal operating domain. Furthermore, the extended demonstration of the hydrological model successfully illustrated the model's capability in dealing with groundwater problems in irregularly-shaped aquifers with heterogeneous hydraulic properties and non-constant rainfall. Analytical solutions to such problems do not exist, so DBH provides an important tool for modelling water-table behaviour in the ecohydrological simulations described in later chapters. On the basis of such successful testing results, the hydrological model was judged to be a reliable means of simulating dynamic water-table behaviour in shallow aquifers, and so was used as a submodel in the ecohydrological versions of **DigiBog** described in Chapters 3 and 6.

The extended model demonstration and the Cors Fochno simulations successfully demonstrated the model's ability to produce plausible water-table behaviour in complex, realistic situations, including drawdown in aquifers with complex geometries and subtly different responses to differential rainfall rates. These results gave the author further confidence in accepting DBH for use as a hydrological submodel in the ecohydrological models which are reported in Chapters 3 and 6.

Using a spin-up period to generate usable initial conditions for simulation runs seems to be reasonable, and is cautiously advocated for future use of DBH when large, real world aquifers are to be simulated. The Cors Fochno simulations demonstrated DBH's sensitivity to K values in deep layers in the marginal zone (where hydraulic gradients are large) and, to a lesser degree, the model's sensitivity to near-surface K in the central zone. Given that the model may be sensitive to marginal-zone K, the inability of DBH to simulate features such as soil pipes and cracks within its grid-column-layer structure may prove a limiting factor to the model's applicability to peatlands which are highly cutover, drained or otherwise degraded. One possible solution might be to represent

cracks in peat in a similar manner to the representation of ditches in the Cors Fochno simulations reported in section **2.6.**, above. Such a scheme would require very high spatial resolution so that individual cracks could be defined as distinct boundaries, and would likely be highly computationally intensive and difficult to parameterise.

One limitation of DBH which may preclude its efficacy at simulating high latitude peatlands is that there is currently no subroutine which deals with the addition of groundwater via snowmelt. The thermal insulation afforded by a thick snow layer to near-surface peat, live vegetation and seed capsules are commonly held to be a highly important contributory factor important as well as the large and often sudden seasonal addition of water to groundwater stores (*cf.* Cook *et al*., 2008). An additional subroutine to simulate variable rates of atmospheric water exchange could quite easily be constructed, if and when the need arose, so as to represent snowmelt.

A further limitation of DBH was brought to the author's attention during parameterisation for the Cors Fochno simulations but is not evident from the results presented above. The lack of an integrated pre-processing tool or graphical user interface necessitates the manual creation of input data files, a task which is laborious and highly prone to mistakes when attempting to model large, real-world aquifers. Indeed, an entirely separate piece of code was written in order to convert the original LIDAR data into a set of input files which could be read by **`DigiBog`**. Such input generator programs must also be fully checked and tested in order to ensure that the data that they produce are what the user expects. It seems highly unlikely that the input generator program used to create the Cors Fochno input files would be readily portable for use with other systems. Rather, such a program would need to be written for each simulated aquifer in response to the particular geometry, nature and extent of source data and other specifics of the situation under consideration, making the model less portable. Partly as a result of this difficulty in parameterising the model to represent real aquifers, the bogs simulated by the ecohydrological versions of **`DigiBog`** in Chapters 3, 5 and 6 take the form of simple geometric shapes.

As for future work on **`DigiBog_Hydro`**, the model may prove to be a useful tool in its own right. It was been commissioned by CCW in order to simulate the hydrological consequences of different management strategies at Cors Fochno, and the simulations presented in section **2.6.**, above, were developed as part of that work. Certainly, when

one is interested in water-table movements in shallow aquifers in which hydrophysical properties are thought to vary on small spatial scales as well as change through time, **DigiBog_Hydro** is able to provide a solution where models such as Modflow might struggle. A full sensitivity analysis is desirable in order to aid with future model parameterisation. Possible future additions to the existing **DigiBog_Hydro** code, to simulate seasonal snowmelt and unsaturated flux and storage could greatly improve the model's scope for use as a specialist hydrological tool, both within peatland science and beyond.

Chapter 3: Cellular Models of Peatland Patterning

This chapter introduces the phenomenon of bog surface patterning and reviews the main theories regarding its formation. Peatland patterning, in addition to being an interesting, widespread and poorly understood phenomenon, may exert a control over peatland-atmosphere carbon gas exchanges. Two cellular models of bog patterning from the literature are then replicated, modified and analysed using a model called **`DigiBog_EcoHydro1`** (DBEH1). Bog patterning represents both a complex system, where large-scale behaviour emerges from local interactions and simple rulesets, and a system with elements of adaptivity, whereby system components retain a memory of their previous behaviour. Also, through ecohydrological feedbacks, surface patterning may play an important role in the ability of peatlands to self-organise, another theme which is central to research on complex adaptive systems. The unorthodox structure of this chapter reflects the unusual, sometimes frustrating path by which the research proceeded and the often surprising sequence and nature of the findings that were made. The Fortran 95 code for DBEH1 can be found as two separate text files on the supplementary CD.

3.1. Introduction to Peatland Patterning

3.1.1. Background

Northern peatlands commonly feature strong, non-random patterning of plant communities and microtopography at a range of spatial scales (see Figure 1.2). Patterns commonly take the form of sub-parallel, anastomosing, across-slope stripes or concentric rings on the flanks of bogs. Excellent examples of such patterning from Mannikjärve bog in Estonia can be seen in the aerial photography of Aber *et al.* (2002).

Previous authors have identified peatland patterning in terms of various characteristic environmental variables, such as microtopographical variation (Nungesser, 2003), plant communities (Foster and Fritz, 1987), nutrient availability (*cf.* Eppinga *et al.*, 2008) and water-table depth (Belyea and Lancaster, 2002). It is notable that particular peatland plant communities are often closely associated with characteristic local water-table depths, due to different *Sphagna* and other peatland species occupying narrow and predictable niches along a water-table gradient (Rydin and McDonald, 1985a, b). Furthermore, different peatland plant communities are commonly closely associated with characteristic microtopographies. Botanists agree that *Sphagnum* species act as ecosystem engineers (*cf.* van Breemen, 1995), naturally selected in such a way as to maintain their own water-table niches. For example, *Sphagnum fuscum* forms raised hummocks, several decimetres above surrounding lawns and hollows (Nungesser, 2003). Hummocks form from tightly-packed bundles of moss stems which provide water to live moss capitula via capillary rise. In contrast, species such as *Sphagnum papillosum* and *Sphagnum cuspidatum*, which form 'lawns' and 'hollows' respectively, are out-competed by hummock species under conditions of high water stress, and so maintain lower elevations above the water table where they are subject to lower water stress (*cf.* Rydin and McDonald, 1985a, b). Hollow species are able to outcompete others when water tables are very shallow. As such, they are naturally selected to produce loose, low density moss with large pore spaces. The inherent structural weakness of this type of moss ensures that it is not able to grow up above the water surface, where it would have to support its own weight without the aid of buoyancy. The resulting association of particular plant communities with characteristic water-table depths and microtopographies means that the current author is reluctant to define patterning solely in terms of any one of these three variables. As such, for the rest of this chapter, peatland patterning should not be taken to mean patterning in terms of

plant-communities, microtopography or water-table position in isolation, but an idealistic combination of the three.

3.1.2. Issues of scale

As noted in Chapter 1, a key characteristic of CAS is cross-scale feedbacks, meaning that any discussion of complexity and adaptivity in peatlands necessitates the identification of components operating at different system levels, as well as the links between these levels. Problematically, however, the literature contains a confusing and incongruous mixture of terminology used to describe entities at different levels within patterned peatlands. For example, it would appear that the 'microforms' of Swanson and Grigal (1988) and Couwenberg and Joosten (2005) are equivalent to the 'patches' of Peterson (2002) and Wu *et al*. (2000). Similarly, the 'strings' of Swanson and Grigal (1988) and Koutaniemi (1999) are equivalent to the 'ridges' of Belyea (2007), while the 'flarks' of Swanson and Grigal (1988) are equivalent to the 'pools' of Koutaniemi (1999). In order to avoid any potential confusion, I present my own nomenclature for the different scale levels within a patterned peatland landscape. The smallest, most fundamental unit of size of relevance to this work is referred to as Scale Level One (SL1), and is equivalent to the 'microforms' which occupy a single grid square within the model of Swanson and Grigal (1988). An appropriate and convenient size for SL1 is 1 m × 1 m in plan (Nungesser, 2003). Units at SL1 are fundamental in that they are the smallest scale at which distinct plant communities can be identified. Whilst individuals and species are identifiable at much smaller scales, plant communities cannot be defined at scales much smaller than SL1. Although SL1 units may be identified by their characteristic plant communities, they are also often distinct from one another in terms of mean annual water table (or other hydrological metrics), microtopography and biogeochemical regime (Belyea and Clymo, 2001).

At a larger spatial scale on the order of tens of metres, which shall be termed Scale Level Two (SL2), aggregations of SL1 units form distinctly non-random structures, often apparent on a mire surface as elongated or otherwise patterned areas of plant communities. By this description, SL2 units are equivalent to the 'flarks' and 'strings' of Swanson and Grigal (1988), or the 'pools' and 'ridges' of Belyea (2007).

At a still larger scale of hundreds of metres to kilometers, which is termed Scale Level 3 (SL3), non-random aggregations of SL2 units delineate the whole mire surface into

broadly wetter or drier patches. For instance, it is commonly observed that the centre of a domed bog is dominated by an abundance of generally wetter habitats such as large pools and hollows, whilst the outer flanks are commonly concentrically patterned with stripes of alternately wet and dry SL2 units (Ivanov, 1981).

3.1.3. Pattern classification and measurement

In order to identify, analyse and discuss patterns and processes in complex, continuous landscapes, many previous authors have found it convenient to classify plant communities at the SL1 and SL2 scales into discrete categories. Notwithstanding section *3.1.2.* and the stated need for new terminology to differentiate between pattern entities at different spatial scales, the terms 'hummock' and 'hollow' are still used in the current work in order to distinguish between different types of SL1 unit. That is to say, while the terms SL1, SL2 and SL3 are used to describe the spatial scale of pattern entities, each SL1 unit may be thought of as occupying one of two binary states: hummock (raised microtopography, deeper water table) or hollow (low microtopography, shallow water table). It is the combination and distribution of these binary types at the SL1 scale which forms patterns at the SL2 and SL3 level. Such an approach is essentially identical to that of Swanson and Grigal (1988), Couwenberg (2005) and Couwenberg and Joosten (2005), although it contrasts with the continuous-biomass scheme of Rietkerk *et al*. (2004a, b; see section *3.1.4.*, below).

3.1.4. Models of peatland patterning

A number of models, both conceptual and mathematical, have been developed in order to explain the phenomenon of peatland patterning. Some of the most important ones are discussed and evaluated here.

Comas *et al*. (2004, 2005) developed a conceptual model of patterning on the Caribou Bog Complex in Maine, USA. Their model essentially involves the locations of small-scale (SL2 and even SL1) surface pattern features being controlled by the 'bottom topography' of underlying mineral sediments. Using geophysical techniques, they identified a spatial (plan) correlation between various sub-surface sedimentary features and certain surface patterning features. Open water pools were thought to have developed in an area above an esker ridge where the peat surface was lower and so water-table depths shallower. According to the model of Comas *et al*. (2005), the esker ridge formed a natural boundary between adjacent peat domes which initiated in the

lower areas either side of the ridge. Because the ridge formed a drainage divide, the growing peat domes either side of it drained (and sloped) down towards it. Once the domes had grown sufficiently large, they bulged up above the top of the ridge and eventually coalesced and merged above it, burying it in peat. However, the initially low rate of peat formation near the esker ridge meant that it now represented a topographic low, encouraging pool development. Comas *et al*. (2005) even speculated that the locations of individual pools may be controlled by the location of sub-surface esker bead deposits. This seems highly improbable given that the glacio-marine deposits and the peat above are separated at Caribou Bog by several metres of lacustrine sediment, although the current author knows of no evidence to contradict directly such a theory. While Comas *et al.* (2004, 2005) presented circumstantial evidence to support their theory that patterning at Caribou Bog is influenced by the geometry and composition of sub-organic layers, it is difficult to imagine that such a mechanism would operate in the general case, especially where the necessary undulation in the suborganic material is absent. It seems more likely that some kind of autogenic mechanism, rather than a climatic or geologic control, is responsible for peatland patterning in the general case.

In order to explain field and laboratory data from their broad and detailed empirical study of peatlands in central Sweden, Foster and Fritz (1987) developed a simple conceptual model. They assumed that small differences in peat accumulation rates caused by subtle variations in species composition, water-table height and microtopography are exaggerated and maintained over time. While such a theory might predict clumped, patchy patterning, it would appear to be unable to account for the persistent across-slope orientation of striped patterning that they observed. Foster and Fritz (1987) claimed that they were able to rule out the possibility of surface patterning being controlled by the geometry or geochemical properties of the sub-organic sediments at their site in Sweden, thereby providing evidence against the later claims of Comas *et al*. (2004, 2005). Foster and Fritz (1987) observed that peat botanical, biochemical and physical properties varied little in plan and did not reflect characteristics of the suborganic mineral layers. Such a finding would appear to add weight to the suggestion that the model of Comas *et al*. (2004, 2005) is not applicable in the general case.

The model of Nungesser (2003) was not dissimilar to that of Foster and Fritz (1987) in that it cited inherent inter-specific differences in rates of growth and decomposition

between three *Sphagnum* species as the cause of peatland topographic patterning. The model is 1-dimensional, *i.e.* it considers the vertical thickness and density of peat below individual hummocks and hollows, but fails to take account of horizontal space. As such, it seems likely that Nungesser's (2003) model, like that of Foster and Fritz (1987), would predict directionless clumping of plant communities, but would fail to predict the highly directional nature often seen in peatland patterning, commonly evident as across-slope (or, in some cases, along-slope: *cf*. Larsen *et al*., 2007) stripes at SL2 – see Section *3.1.2*., above.

Larsen *et al*. (2007) sought to explain the large areas of slope-parallel striped patterning, which they referred to as ridge and slough landscapes (RSL), commonly observed in the peatland swamps of the Everglades, Florida. Their model predicted that ridges and sloughs developed at SL2 from dense networks of pre-existing, low-energy, anabranching streams which drain the Everglades. Their numerical model involved feedbacks between rates of peat accumulation and streamflow regimes. RSL patterning and the processes believed by Larsen *et al*. (2007) to be responsible for their formation are quite different from those observed in temperate raised bogs. The development of raised bogs requires a gradually growing groundwater mound (*cf*. Ingram, 1982), often superimposed with patterns formed by feedbacks between ecological processes and local water-table regime (*cf*. Swanson and Grigal, 1988; Rietkerk *et al*., 2004a, b; Couwenberg and Joosten, 2005). By contrast, RSL peatlands develop in fluvial environments, and the location, size and shape of individual ridges and sloughs are dictated by feedbacks between peat production and fluvial erosion and deposition. As such, RSL peatlands fall outside of the remit of the current work and so are considered here no further.

Swanson and Grigal (1988) developed a simple cellular simulation model, for brevity referred to here as the 'ponding' model, which predicted across-slope striped patterning, based on feedbacks between peatland water tables, plant community composition and peat hydrophysical properties. The later versions of the model presented by Couwenberg (2005) and Couwenberg and Joosten (2005) corrected a small error in the original model's groundwater flux equation but led to similar findings to those of Swanson and Grigal (1988); *i.e.*, the model still predicted across-slope stripes at SL2 and SL3. The ponding model is explored in more detail in section **3.2.**, below.

Drawing on the reaction-diffusion work of Alan Turing, Rietkerk *et al*. (2004a, b) hypothesised that the cause of peatland patterning relies upon the scarcity of nutrients required for plant growth and their increased concentration in the vicinity of vascular plants due to evapotranspiration. Rietkerk *et al.* (2004a, b) used a cellular model to discretise three partial differential equations, representing the state variables – hydraulic head, vascular plant biomass and groundwater nutrient concentration – at all points in the model landscape. From random initial conditions, Rietkerk *et al.* (2004a, b) used the nutrient-scarcity model to generate maze patterns similar to those commonly seen in the tundra of Siberia in flat model domains, and contour-parallel striped patterning on sloping model grids. Grimm *et al.* (2005) demonstrated how models of complex systems which predict only realistic patterns in space and/or time are likely to be more mechanistically accurate than those which predict some realistic patterns and some unrealistic ones. Unlike the ponding model, the nutrient-scarcity model predicts patterns which become stable with time. The available empirical evidence is sparse, but points to stable patterns in real bogs, suggesting greater reliability of the model's mechanistic basis than that of the ponding model. This issue is discussed in more detail in section *3.2.1*., below.

Couwenberg (2005) and Couwenberg and Joosten (2005) disputed the mechanistic accuracy of the nutrient-scarcity model on the basis that the available evidence suggests that depth to water table is the principal control upon succession between peatland plant communities (*cf*. Rydin and McDonald, 1985a, b; Yabe and Onimaru, 1997; Robroek, 2007a, b) and that availability of nutrients varies very little across bogs. Eppinga *et al*. (2008), however, set out to falsify the assumptions of the nutrient-scarcity model. Their field study in Siberia revealed higher groundwater nutrient concentrations beneath hummocks than beneath hollows, providing compelling empirical evidence in favour of the nutrient-scarcity model. What is not clear from the work of Rietkerk *et al*. (2004a, b), however, is the degree to which two of their model's three state variables, hydraulic head and groundwater nutrient concentration, spatially co-vary with one another. Their nutrient-cycling submodel includes terms which describe diffusion of nutrients along concentration gradients and the recycling of plant detritus, processes which are not governed solely by water-table position, but there is clearly a strong association between low hydraulic head and high nutrient concentrations, because this is the stated mechanistic basis for the model. It may be, therefore, that the approach of Rietkerk *et al*. (2004a, b) was not a strictly minimalist one, and that the so-called 'nutrient-scarcity'

model is, in essence, little more than a transpiration-driven, 'water-scarcity' model. If this were the case, then it should prove possible to reproduce the realistic, stable patterns predicted by the model of Rietkerk *et al.* (2004a, b) using a similar model but which ignores nutrient concentration. Again, the nutrient-scarcity model is explored in greater detail later in this chapter, in section **3.3**.

3.1.5. Chapter aim, objectives

The aim of this chapter is to use a coupled ecohydrological cellular model to investigate the causes of peatland patterning. As discussed in section *1.2.4.* (see Chapter 1), models which seek to elucidate the causes and mechanisms of peatland patterning may yield important insights into structures which influence peatland-atmosphere carbon gas exchange (*cf.* Baird *et al*., 2009). The study of peatland patterning may arguably be viewed, therefore, as important to understanding the role of northern peatlands within the climate change debate. Furthermore, peatland patterning is an interesting and poorly understood phenomenon, and one which seemingly represents an emergent phenomenon resulting from peatland ecohydrological feedbacks, and is therefore an interesting and worthy research pursuit in its own right. Within the broad aim identified above, three specific objectives have developed from the synthesis above, the rationales for which are discussed in the relevant sections later in this chapter. Objectives:

(i) To demonstrate the sensitivity of a revised version of the ponding model to the stringency of the hydrological steady-state criterion assumed to predict SL1 succession. This objective is further discussed and addressed in section **3.2.**

(ii) To investigate whether stable, realistic peatland patterning can be predicted by a transpiration-driven model which does not include a nutrient-cycling routine. This objective is further discussed and addressed in section **3.3.**

(iii) To test the hypothesis that the inclusion of an ecological memory effect would stabilise the SL2 patterning predicted by the ponding model. This objective is further discussed and addressed in section **3.4.**

3.2. Ponding Model of Peatland Patterning

3.2.1. Model description and assumptions

The ponding model may be thought of as a reduced version of the conceptual model of peatland development presented in Chapter 1, and assumes that steady-state water-table position is the principal predictor of local patterning. Each of the model's grid squares (SL1) possesses one of two states, hummock or hollow, during each model timestep, determined by a probabilistic function (see Figure 3.1a) of steady-state water-table depth during the previous timestep. As steady-state water-table depth in any given grid square increases from zero (*i.e.*, water table is at the surface) to 5 cm below the surface, the probability of that square being designated as a hollow declines linearly from certainty to zero. This assumption meant that deeper water tables are more likely to lead to the prevalence of hummocks, although it also has the rather odd corollary that even when the steady-state water tables are just a few mm below the surface, there is still a chance (albeit a small one) of that square being designated as a hummock.

Despite using Ingram's (1982) GMH (which assumes a permeable catotelm; see Chapters 1 and 2) to generate the gross dimensions of their model bog, Couwenberg and Joosten (2005) paradoxically assumed, like Swanson and Grigal (1988) before them, an impermeable catotelm for their ponding model. All flow was assumed to occur through the thin, surficial acrotelm layer. The model uses a simple hydrological submodel based on Darcy's Law (see Chapter 2) to calculate what Swanson and Grigal (1988), Couwenberg (2005) and Couwenberg and Joosten (2005) describe as a hydrological 'steady state'. While the ponding model has been used by previous authors to predict striped SL2 patterns similar to those observed on real bogs, the model has two main flaws, only one of which was noted by previous authors and neither of which have been resolved. Each of these two issues is discussed in the rest of this section.

Swanson and Grigal (1988), Couwenberg (2005) and Couwenberg and Joosten (2005) demonstrated that, assuming appropriate parameter values, the ponding model can be used to predict realistic SL2 patterns. These same authors note, however, that these patterns are not stable ones, and that they migrate consistently, and sometimes rapidly, downslope with successive timesteps. This curious model prediction is well illustrated by Couwenberg (2005; page 659, Figure 6). There is, to the current author's knowledge, no reported empirical evidence that could serve either to confirm or

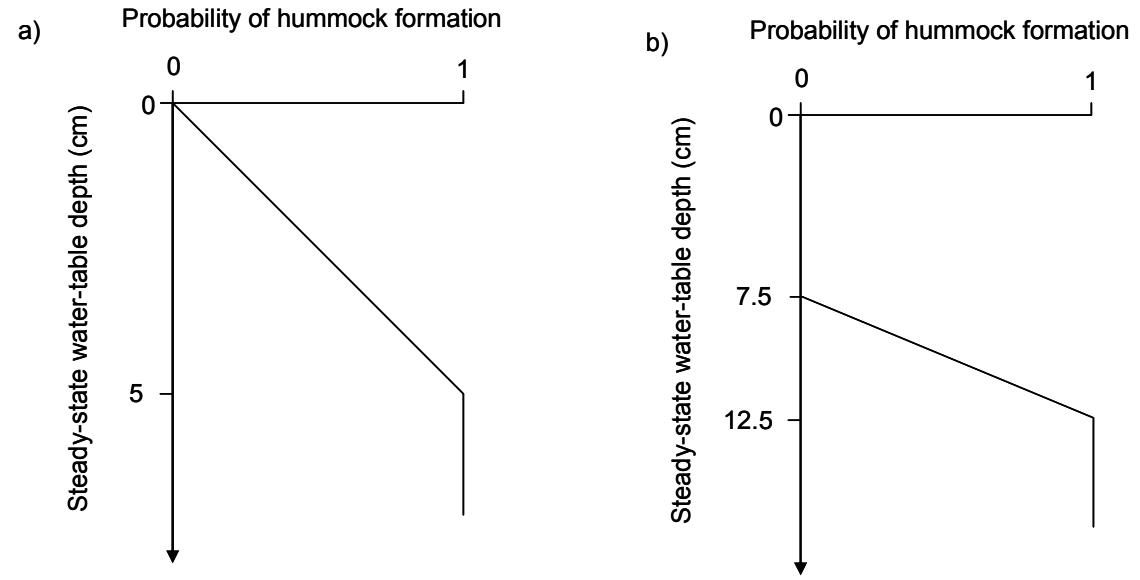

Figure 3.1: plots showing probability functions used to predict SL1 transitions, based on calculated steady-state water table depths, a used in: a) original ponding model, as reported by Swanson and Grigal (1988), Couwenberg (2005), and Couwenberg and Joosten (2005); b) the revised ponding model, as reported in the current work.

contradict the prediction of downslope movement of SL2 stripes. Koutaniemi (1999) observed a cyclic movement of ridges that he deduced was caused by freeze-thaw cycles on a peatland in Finland, but to the current author's knowledge there is no recorded account of systematic downslope migration, and the few long-term mapping studies that exist appear to show highly stable patterns which change little, if at all, over decadal timescales (*cf*. Backéus, 1972). Grimm *et al*. (2005) present a protocol for assessing the predictive strength of what they term agent-based models, such as the ponding model. Grimm *et al*. (2005) state that, while different models of the same system may be able to predict certain realistic patterns, the model with the greatest predictive ability and mechanistic insight is likely to be one which predicts more than one pattern in space and/or time. The downslope migration of SL2 as predicted by Swanson and Grigal (1988), Couwenberg (2005) and Couwenberg and Joosten (2005), while recognised by those authors as an oddity, was left as an unresolved matter. It was this odd prediction that alerted the current author to the possibility that the model's mechanistic basis may be in error, and prompted attempts to recreate it for further investigation. Preliminary experimentation suggested that the types of SL2 patterning

predicted by the ponding model were highly sensitive to the stringency of the steady-state criterion which was adopted for the hydrological model.

3.2.2. Recreating and improving the ponding model

In order to examine the sensitivity of the ponding model to hydrological steadiness, a revised version of Couwenberg's (2005) model was created. This model was called **`DigiBog_EcoHydro1`** (DBEH1). Ingram's (1982) Groundwater Mound Hypothesis (GMH) was used to generate the profile shape of a section of raised bog, assuming a drought-year net rainfall (P - E) of 15 cm yr^{-1} and a K in the anoxic zone of 0.00125 cm s^{-1}. Model plan dimensions of 200 m (along-slope) × 70 m (across-slope) gave a maximum acrotelm thickness of 397 cm, thinning elliptically to 28.2 cm. The model aquifer was discretised into a horizontal (x, y) grid of square-sectioned columns with plan dimensions of 1 m × 1 m. Groundwater movement within the aquifer was simulated using DBH (see previous chapter). Model time proceeded in developmental steps. During each developmental step, steady-state water-table positions were calculated in all columns using DBH, before SL1 unit types and acrotelm K were updated in all columns. During each developmental step, DBH was allowed to run for a predetermined length of time, Δt_e, in order to calculate steady-state water-table positions. High values of Δt_e therefore give steady water-table positions, whereas shorter run times lead to more transient positions with steep local gradients. Columns in which steady-state water-table depth was deeper than 12.5 cm below the ground surface were designated as hummocks, and those in which steady-state water-table depth was shallower than 7.5 cm below the ground surface were designated as hollows. Columns in which steady-state water-table depth was between 12.5 and 7.5 cm had their SL1 designation predicted by a linear probability function of water-table depth, illustrated by Figure 3.1b. This scheme is similar to that of Swanson and Grigal (1988), Couwenberg (2005) and Couwenberg and Joosten (2005) except that the zone of probabilistic consideration was assumed to be 7.5 cm lower, meaning that hummocks were no longer able to develop when water-table depths are barely below the ground surface.

Each column consisted of two vertically stacked layers of peat, the lower layer representing the less permeable catotelm, the thickness of which was determined for each column using the GMH. Above the catotelm was a more permeable layer, 20 cm thick in all columns, representing the acrotelm. K in the acrotelm for each column was

determined by that square's SL1 designation (*i.e.*, hummock or hollow). Effective porosity was assumed to be spatially invariant in all directions and equal to 0.3. The peat deposit was assumed to sit above an impermeable mineral substrate, and the model's upslope and lateral boundaries were assumed impermeable (reflective). The downslope boundary to which the model therefore drained was assumed to exhibit a Dirichlet condition, whereby water-table elevation at the boundary was held constant at 38.2 cm above the impermeable base.

The use of unscaled units by Swanson and Grigal (1988), Couwenberg (2005) and Couwenberg and Joosten (2005) proved problematic for the current author when it came to choosing values of K and Δt_e for DBEH1 that would allow direct comparison between studies. Those previous authors assumed canonical values of transmissivity, T, rather than K, for hummocks and hollows. However, it was not possible to discern what absolute values of T were used, because those authors gave only ratios between hummock and hollow transmissivity. It is impossible to tell, therefore, how the combinations of K assumed here compare directly to those of Swanson and Grigal (1988), Couwenberg (2005) and Couwenberg and Joosten (2005). The choice of K values for DBEH1 was constrained, however, by the need to maintain water tables within the zone of probabilistic consideration for as much of the model grid as possible. Three combinations of values were assumed for acrotelm K of hummocks (K_{hum}) and hollows (K_{hol}): (i) $K_{hum} = 0.005$, $K_{hol} = 0.1$; (ii) $K_{hum} = 0.0095$, $K_{hol} = 0.095$; (iii) $K_{hum} = 0.035$, $K_{hol} = 0.035$. These values served, during preliminary experimentation, to maintain water tables within the 5 cm zone of consideration for sufficiently large areas of the model grid, and represent a maximum K differential between hummocks and hollows of 20 times. In the third combination, K_{hum} is equal to K_{hol}, allowing the observation of steady-state water-table configurations under conditions of no K differential, and may be thought of as a control treatment. The combinations of K_{hum} and K_{hol} values assumed for DBEH1 are realistic ones (*cf.* Ivanov, 1981), and were combined factorially with four values of Δt_e: 10 hours, 24 hours, 30 days and 365 days, representing a range of hydrological conditions from transient to steady. It should be noted that the very small values of Δt_e do not mean that SL1 succession is assumed to occur on the timescale of hours or days; rather these values should be thought of as a simple means by which to introduce small-scale spatial variability to water-table positions, by curtailing each developmental step before steady state is reached. The

experimental design of twelve treatments was intended to allow the observation of the interaction between hydrological transience and *K* differential, and their effects upon patterning. The choice of *K* values helped to maintain water-table positions within the zone of probabilistic consideration for as many columns as possible in the mid-slope region of the model domain. Thus, a somewhat artificial balance was imposed between net rainfall rate and hydraulic conductivity, which ensured that the model did not become uniformly too wet or too dry for striped patterning to develop.

3.2.3. Results

Before results had been fully collated, it had been the intention of the current author to use a number of techniques, of varying sophistication, to measure the strengths of patterns predicted by different model runs and to gauge the spatial scales at which patterns were strongest. Upon initial summary inspection of data, however, it was deemed unnecessary to employ such techniques, because the strength and scale of patterning was, in almost all cases, entirely self-evident from a visual inspection of the patterning maps produced. As we shall see in this section, differences in pattern configurations between model runs were stark rather than subtle, and the employment of quantitative measures of pattern strength and configuration would only have served to reiterate what the human eye can see immediately and more easily.

In general, results appear to confirm suspicions, aroused during preliminary work not reported here, that the strength and configuration of SL2 striped patterning is sensitive to hydrological transience. Figure 3.2 shows that distinctive, across-slope patterning develops near the downslope end of the model grid under conditions of differential *K* (for both non-control *K* combinations) when Δt_e is equal to 10 hours or 24 hours. When Δt_e is increased beyond 24 hours, the realistic striping is replaced by thicker, more widely spaced stripes, and patterning is only evident at SL3.

There were four treatments which predicted realistic striped patterning: the runs in which Δt_e was equal to 10 or 24 hours, and for which acrotelm *K* differentials were 10 and 20 times. In these four runs, striped SL2 patterning develops within a small area at the downslope end of the model domain, with the larger upslope area containing seemingly random mixtures of hummocks and hollows not organised into SL2 or SL3 units. The spatial extent of the patterned areas, as well as the apparent strength of the

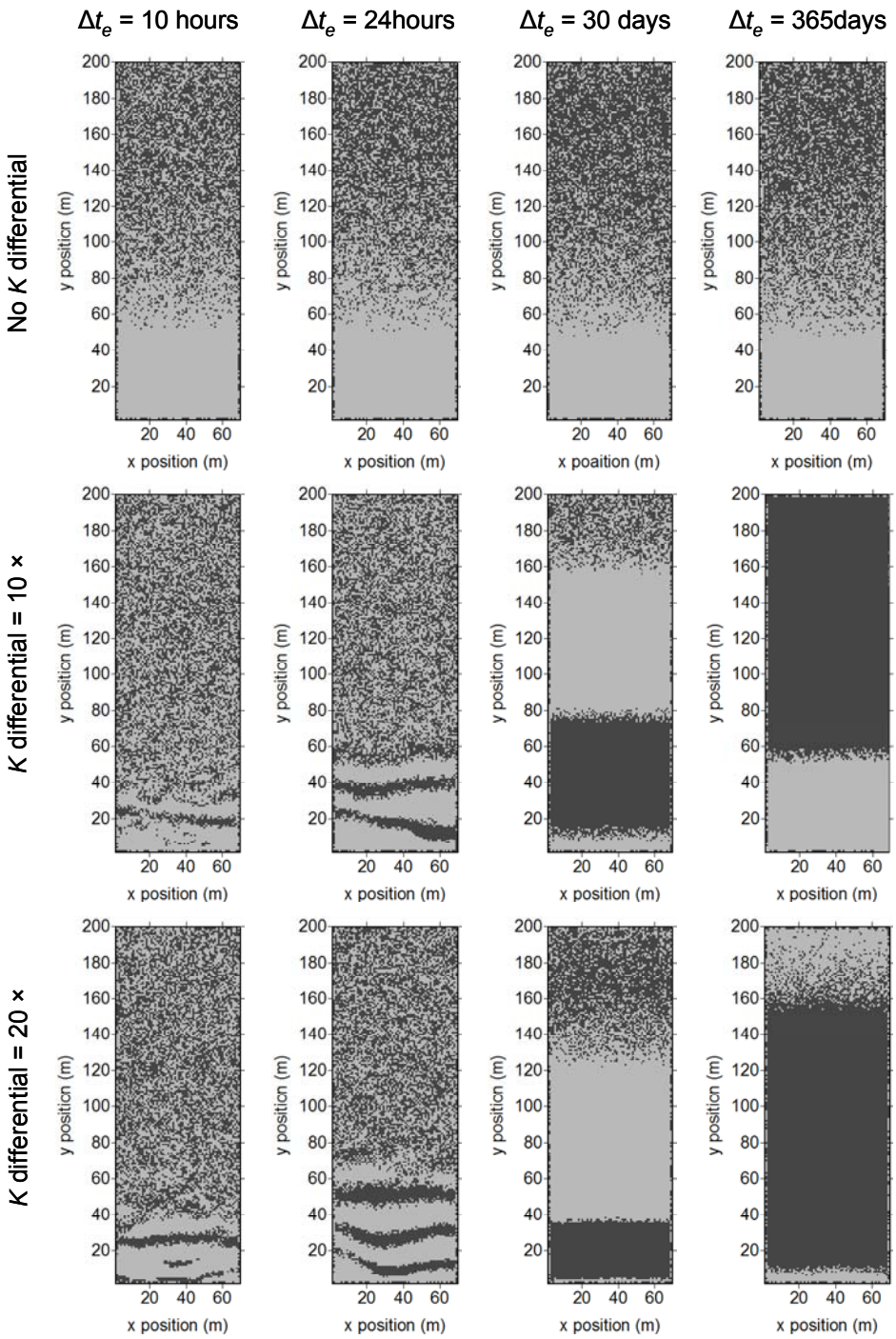

Figure 3.2: Maps showing SL1 distribution after 100 developmental steps under 12 treatments of revised ponding model. Light pixels are hummocks, dark pixels are hollows. Model domain slopes from high to low values of y, i.e. *water flow is generally down-page.*

stripes, appear to increase from Δt_e = 10 hours to 24 hours, and also increases with increasing *K* differential, as reported by Swanson and Grigal (1988). That the strongest

and most extensive patterning observed here occurs under neither the longest nor the shortest Δt_e is suggestive that an optimum value of Δt_e exists, for which patterning is strongest.

Figures 3.3 and 3.4 illustrate the development of two model runs, both with K differentials of 20 times, and one with Δt_e = 24 hours, the other with Δt_e = 365 days. When Δt_e = 24 hours, both the proportion of the model domain covered by hummocks and the SL1 turnover rate both stabilise at approximately 0.5. SL1 turnover is defined as the proportion of model columns which undergo a transition from hummock to hollow, or vice-versa, during a given developmental step. Such trends are also similar to those observed for Δt_e = 10 hours. By contrast, when Δt_e = 365 days, model behaviour appears to become cyclical, switching rapidly between very hummock-dominated and hollow-dominated states. Periodic cycling such as this between wet and dry states has, to the author's knowledge, never been reported in the literature. However, both Belyea and Malmer (2004), and Barber (1981) recognised the potential for abrupt changes in peatland plant communities to occur in response to threshold hydrological changes. Concerns that such behaviour was a reflection of the hydrological submodel having become numerically unstable appear to be unfounded, because the output water-table maps (not reproduced here) show no signs of instability, suggesting that this cyclic behaviour appears to be a 'genuine' prediction of the steady-state ponding model.

In model runs where across-slope SL2 stripes do develop, these stripes migrate consistently downslope in the same manner as observed by Swanson and Grigal (1988), Couwenberg (2005) and Couwenberg and Joosten (2005) (see Figure 3.5). The upslope portion of the model domain remains dominated by a random mixture of hummocks and hollows, the downslope end of which appears alternately to issue forth wet and dry SL2 units which then migrate downslope through the patterned area.

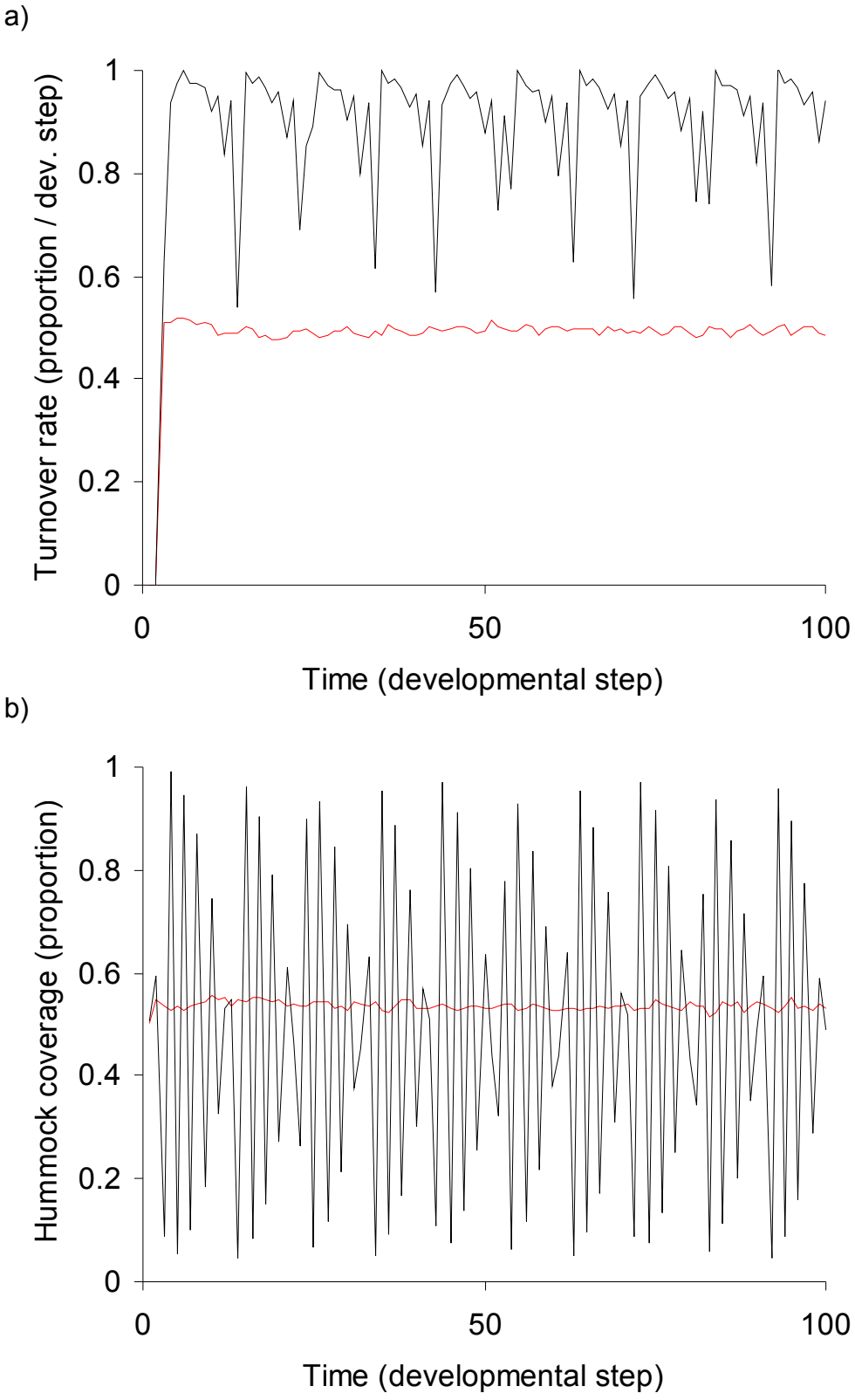

Figure 3.3: Plots showing changes in a) SL1 turnover rate, and; b) proportional hummock coverage over 100 developmental steps of ponding model. Two treatments are illustrated here, both with a K *differential of 20, and one with* Δte *= 24 hours (red line), the other with* Δte *= 365 days (black line).*

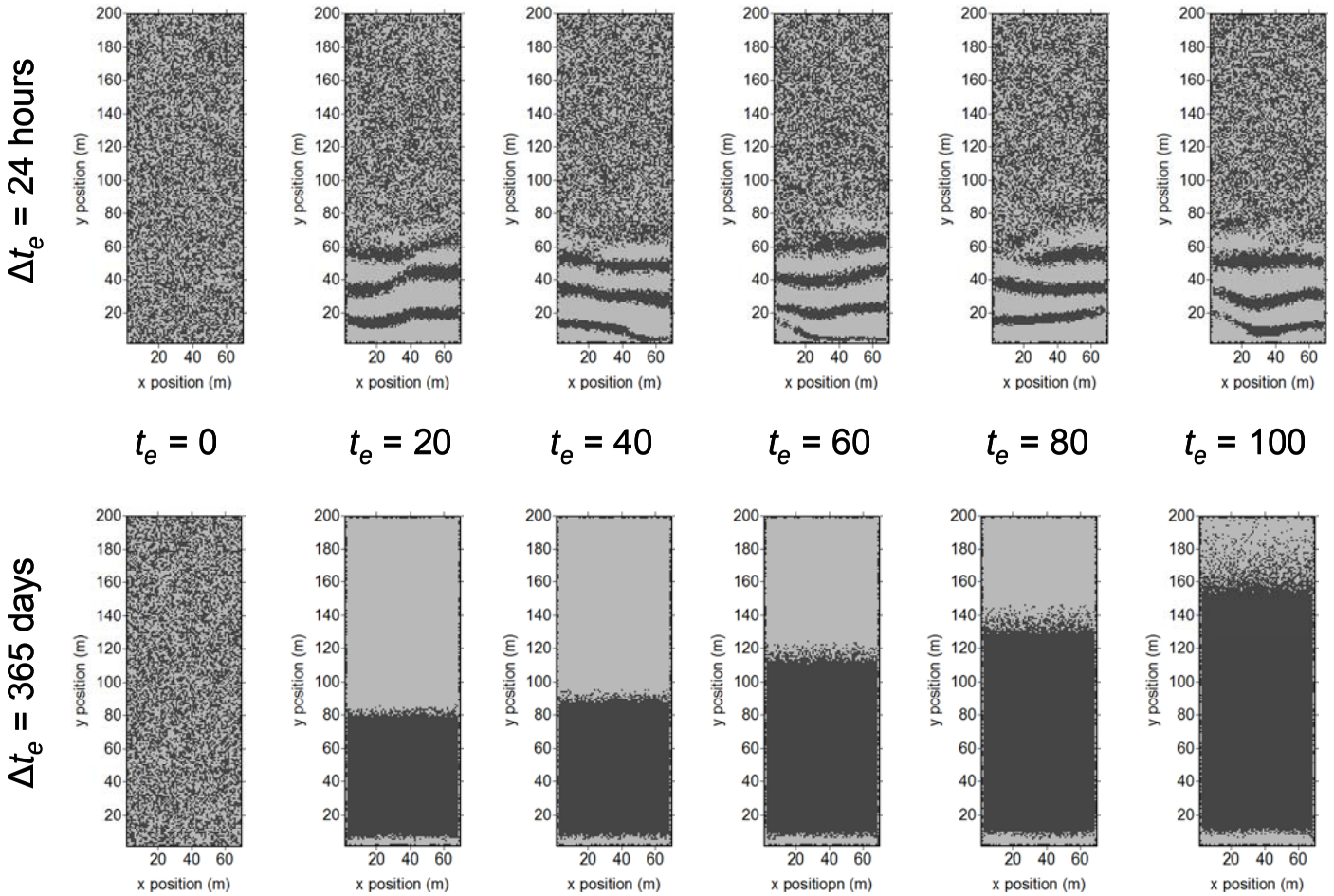

*Figure 3.4: Maps showing development through time of SL1, SL2 and SL3 patterns for two ponding model runs, one with Δ*te *= 24 hours and one with Δ*te *= 365 days. In both cases,* K *differential between hummocks and hollows was equal to factor of 20 (*Khol *= 0.1 cm s-1,* Khum *= 0.005 cm s-1).*

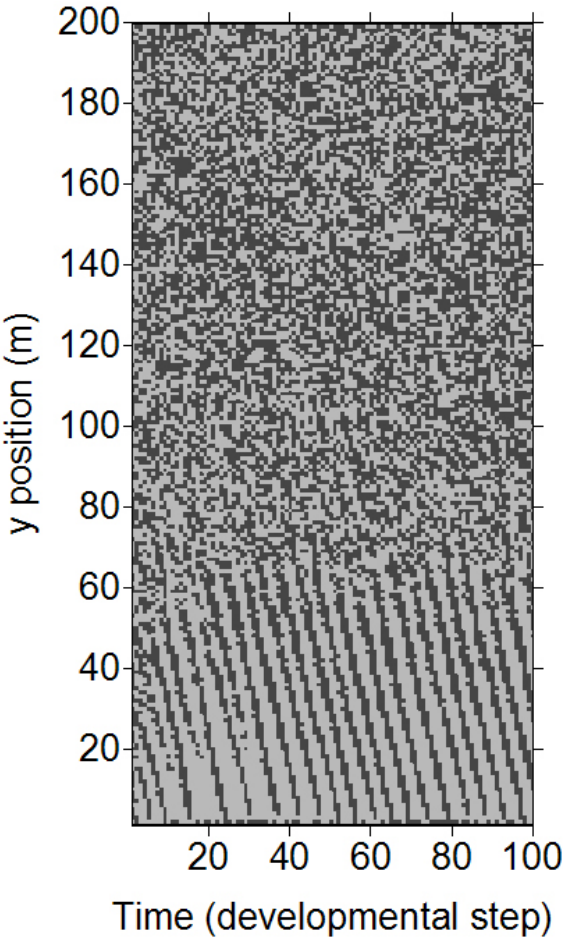

Figure 3.5: Spatio-temporal plot showing apparent downslope migration of SL2 units along a central, along-slope transect of the revised ponding model, with Δt_e *= 24 hours,* K_{hum} *= 0.005 cm* s^{-1} *and* K_{hol} *= 0.1 cm* s^{-1}.

3.3. Nutrient-Scarcity Model for Peatland Patterning

3.3.1. Model description and assumptions

In the nutrient-scarcity model of Rietkerk *et al.* (2004a, b), vascular plant biomass at each grid location was determined by a function of water stress and groundwater nutrient concentration. Nutrient concentrations were increased locally by high biomass, based on the assumption that a certain proportion of the useful nutrients in plant detritus is returned to the groundwater store by decomposers.

Most available reports suggest that plant-community succession, and so SL1 distribution, are controlled by water-table depth behaviour rather than nutrient concentrations. Furthermore, Rietkerk *et al*. (2004a, b) did not discuss the level of covariance between hydraulic head and nutrient concentration in their model. It is not clear, therefore, whether the nutrient-scarcity model is a strictly minimalist one. It may be that similar patterns are predicted by a model in which SL1 distribution is predicted by water-table behaviour (as in the ponding model) rather than groundwater nutrient concentrations and in which different SL1 unit types receive different amounts of net rainfall. Such an assumption is justifiable from first principles when one considers that:

(i) Hummocks are topographically raised above the level of surrounding lawns and hollows, meaning that they extend further into the local airstream, and so experience greater evaporative losses.

(ii) Hummocks are also likely to contain greater amounts of vascular plants than hollows, leading to higher transpirative losses.

Alternatively, it may be that, by removing the submodel which simulates the behaviour of limited nutrients, an important negative feedback is lost from the model. That is, it seems likely that, in the new water-scarcity model, a prevalence of hummocks will lead to lower water tables (due to lower net rainfall on hummocks) generally, thereby further encouraging hummock formation. Conversely, hollows will encourage wetter conditions and so beget hollows. Without the in-built 'cut-off' provided by a limited nutrient supply, it may be that the model is sensitive to net rainfall rate and will tend towards wet or dry attractors, possibly in the form of uniformly wet or dry landscapes, depending on net rainfall rate. Furthermore, increasing the differential in net rainfall received by hummocks and hollows may increase the model's sensitivity to base net rainfall rate and could cause it to converge on a wet or dry attractor.

3.3.2. Building a water-scarcity model

Another new model was built in order to test the hypothesis that patterning of the type predicted by the models of Rietkerk *et al*. (2004a, b) could be generated by a similar evapotranspiration model which did not consider groundwater nutrient concentrations. The new model was essentially a minor reworking of the DBEH1 model described in section *3.2.2.*, above. The same model grid and aquifer geometry as before were assumed, as well as the same anoxic zone K (0.00125 cm s^{-1}), boundary conditions, and the same probabilistic function for determining SL1 transitions. However, unlike the ponding model and the version of DBEH1 used in section **3.2**, K in the oxic zone was held constant at 0.05 cm s^{-1}, irrespective of SL1 type. Two 'base' net rainfall rates were assumed, 30 cm yr^{-1} and 35 cm yr^{-1}. Based on the above discussion (see section *3.3.1.*), each grid point was assumed to receive a net rainfall which depended on its SL1 status (*i.e.*, hummock or hollow). Two control runs were performed, one for each base rainfall rate, in which there was no difference in net rainfall between hummocks and hollows. A further three treatments were also performed for each rainfall rate, where net rainfall received by hummocks was decreased by 2.5, 5 and 10 per cent, with hollow rainfall being increased by the same amounts. This design resulted in a total of eight treatments, including the two controls. It seems highly unlikely that transpirative losses from hummocks and hollows could vary by as much as ± 10 % from the base net rainfall rate, but the use of this value is justified by an attempt to understand the sensitivity of the water-scarcity model.

3.3.3. Results

It is clear from Figure 3.6 that SL2 striping has not occurred under any parameter combination. Under the control treatments, SL3 patterning has developed with a wet central area and dry downslope area, delineated by a narrow band within which SL1 units undergo a steep transition from hollows (upslope) to hummocks (downslope). In the control run with higher net rainfall, the zone of transition between wet and dry patches is noticeably further downslope and the control run with 35 cm yr^{-1} rainfall consistently predicts approximately 30 % more hollows than the control run with 30 cm yr^{-1}.

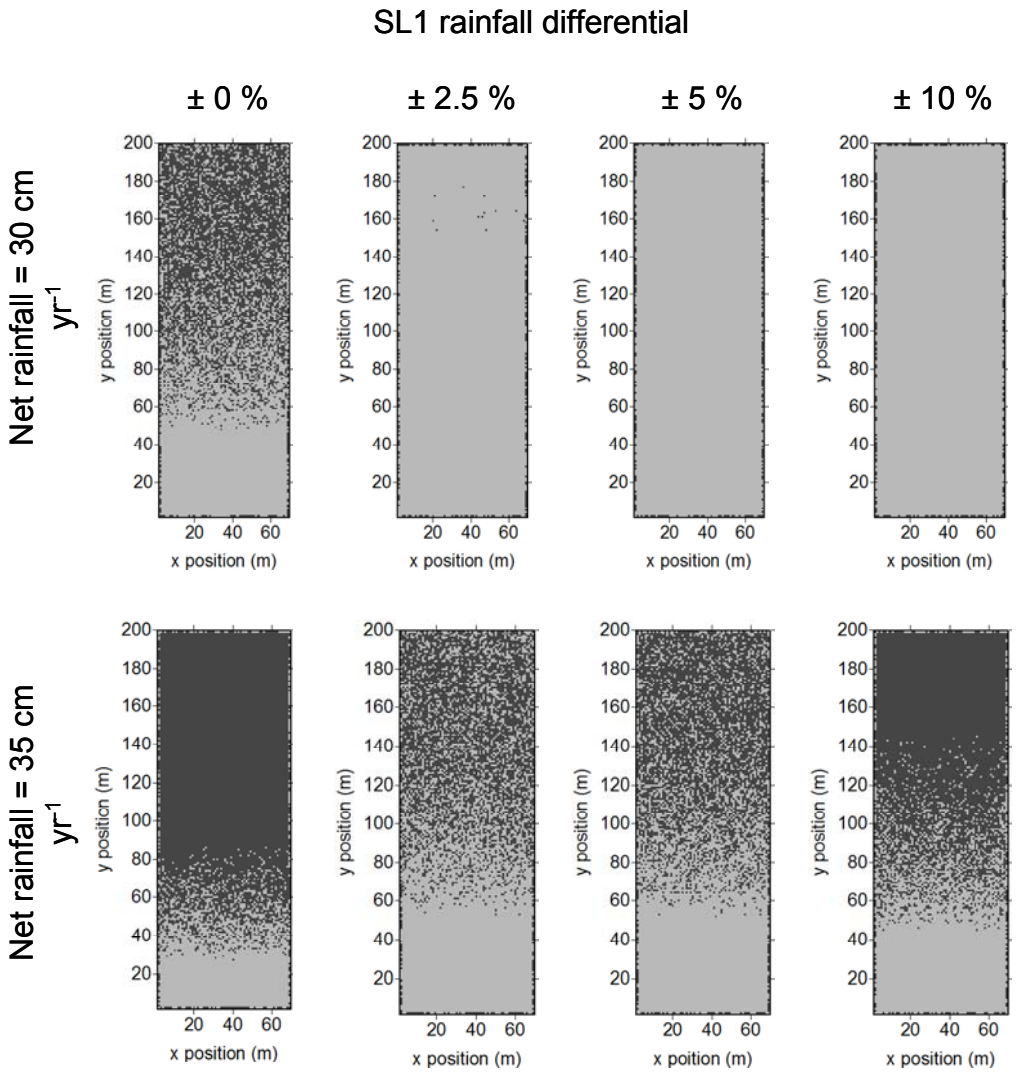

Figure 3.6: maps showing SL1 distribution 100 developmental steps for six treatments in water scarcity model after. As before, light pixels are hummocks, dark pixels are hollows and model domain slopes down from high to low y (i.e., flow is generally down-page).

For the runs with a base net rainfall of 30 cm yr^{-1}, implementing even the smallest rainfall differential of ± 2.5 % has caused the model to 'run away' to an almost completely dry state. After 100 developmental steps, all model runs with a net rainfall of 30 cm yr^{-1}, other than the control, possessed more than 99 % hummocks. Given that the control run possessed 65.5 % hummock coverage, it is evident that the implementation of a rainfall differential has caused the model, as suspected, to converge upon a dry attractor. By contrast, however, the model runs with a base net rainfall of 35 cm yr^{-1} did not converge upon a wet attractor. From 26.8 % hummock coverage in the control run, rainfall differentials of ± 2.5, ± 5 and ± 10 % led to final proportional

hummock coverages of 62.1 %, 58.8 %, and 40.6 %, respectively, a non-monotonic decrease in wetness from the control. This indicates that for runs with base net rainfall rates of 35 cm yr^{-1}, contrary to expectations, the implementation of a rainfall differential has caused drier, rather than wetter, models to develop, although this increase in dryness is not a simple one.

3.4. Ecological Memory in Peatland Patterning

3.4.1. What is ecological memory?

In a cellular modelling study of forest vegetation pattern development and its response to fire events, Peterson (2002) offered the following, broad definition of the term 'ecological memory':

> *"The degree to which an ecological process is shaped by its own history"*

It is arguable that, while Peterson's (2002) definition is not an unreasonable starting point, it is so broad as to be of only limited application. Surely, almost all natural processes, ecological or otherwise, exhibit some form of hysteresis and therefore satisfy the above definition. The only kinds of systems in which contemporary behaviour is entirely independent of past events are quantum-scale processes or highly artificial, engineered systems, such as the toss of a coin. As such, it is argued here that ecological memory according to the above definition is somewhat trivial. In the models of Swanson and Grigal (1988), Couwenberg (2005) and Couwenberg and Joosten (2005), SL1 unit distribution during any given developmental step t is dictated by water-table behaviour during t-1, which is in turn constrained by the SL1 unit distribution during t-1. Thus, the system state during any timestep is influenced by the system state during the previous timestep, and indeed all previous timesteps. If one takes Peterson's (2002) definition of ecological memory, then it is difficult to argue against the notion that the original ponding models do indeed incorporate a memory effect. However, it seems highly unsatisfactory to describe what we observe in the ponding model as genuine 'memory'.

3.4.2. Ecological memory in peatlands

We might term the type of memory exhibited by the ponding model as 'weak memory'. It is possible, however, to identify two potentially important mechanisms through which ecological memory, or adaptivity, may operate in peatlands and which were neglected by the authors of the original ponding model. These mechanisms are described and discussed immediately below, and are henceforth referred to as 'strong memory' and, unlike weak memory, are suggested as genuine manifestations of adaptivity.

The original ponding models assumed that all groundwater flux occurs through the acrotelm layers and that once peat has been compressed and buried sufficiently to be considered part of the catotelm, it is no longer permeable enough to be influential upon flow. The models are presented with unscaled units, such that units of space, time and rates of process operation are not specified. An assumption implicit within the ponding models, however, is that the length of time for which peat resides within the acrotelm is equal to the length of time required for the complete transition of a peatland plant community covering a unit area from hummock to hollow, or vice versa, given appropriate hydrological conditions. Swanson and Grigal (1988) suggested in their original model description that 1 m × 1 m was a justifiable size for the planimetric dimensions of each grid cell, a scheme which Couwenberg (2005) and Couwenberg and Joosten appear also to have adopted, although no scales are explicitly given for any properties in any of the three papers which describe the ponding model. While evidence is sparse, studies such as those by Aaviksoo *et al*. (1993), Barber (1981) and Walker and Walker (1961) would appear to suggest that individual hummocks and hollows may persist in a particular location for hundreds or even thousands of years. However, these same studies also suggest that when conditions are favourable, a transition from a hollow-type community to hummock-type, or vice-versa, is likely to occur on a timescale of decades. The available evidence suggests that peat is likely to reside in the acrotelm for significantly longer periods, on the order of 10^1 to 10^2 years (El-Daoushy *et al*., 1982; Malmer and Wallén, 1999; Weider, 2001). Thus, in areas which have undergone a number of recent SL1 transitions, the hydraulic properties of the peat in the near-surface zone are likely to be dependent on more than just the current plant community type. A plant community which has recently undergone a transition from hummock to hollow, for instance, might still behave hydrologically like a hummock, because most of the peat beneath it has been formed from hummock plants. Through the preservation of old peat types in an important functional layer (the hydrologically-active acrotelm), peatlands may exhibit a form of strong ecological memory. This type of adaptivity is here termed Type 1 Strong Memory. It was hypothesised here that the downslope migration of SL2 stripes, as predicted by the steady-state ponding model (Swanson and Grigal, 1988; Couwenberg, 2005; Couwenberg and Joosten, 2005; and section **3.2.**, above) will be slowed or halted entirely by the inclusion of Type 1 Strong Memory. It was expected that the memory effect would lead to more gradual temporal changes in inter-column depth-averaged hydraulic conductivity, thereby acting to

stabilise water-table behaviour and so SL1 configurations. The work presented in this chapter stemmed from an original intention to include Type 1 Strong Memory in a version of the ponding model, in order to assess its effectiveness in slowing the downslope migration of SL2 stripes. This aim was decided upon long before it had become apparent that, in steady state, the ponding model does not predict SL2 stripes.

Another mechanism by which ecological memory may operate in peatlands, and which is not considered by the ponding model, involves changes in gross peatland dimensions, both in plan and in profile. It is common for even large, well developed peatlands to initiate as small patches of minerotrophic fen in topographic depressions. If conditions remain favourable to peat accumulation then these small, dispersed patches of proto-fen will grow up out of their depressions and coalesce with neighbouring patches (*cf.* Anderson, *et al*., 2003). The eventual result may be large complexes of coalesced bog domes covering thousands of square km, such as the Endla complex in Estonia (see Figure 1.2). Thus, changes in plant-community type and productivity, rates of decomposition and external climatic factors are likely to be preserved not only in peat properties as discussed above, but also in the overall morphometry of the bog complex. Gross bog dimensions, in particular the locations and configurations of drainage divides and hydrological boundaries, are likely to be highly influential upon groundwater movements and so upon micro-succession between peatland communities. This type of adaptivity is termed Type 2 Strong Memory. Consideration of such ecological memory in peatlands is not taken until Chapters 5 and 6, because the inclusion of such a phenomenon within the algorithmic structure of DigiBog constitutes a full CAS treatment of peatland modelling, according to the conceptual model outlined in Chapter 1.

3.4.3. Incorporating memory into the ponding model

The model setup for this part of the experimental work differed little from that used in section **3.2.**, except that the 20-cm thick acrotelm no longer consisted of a single layer, but was assumed to be represented by n vertically-stacked layers. When n is equal to one, the acrotelm consists of a single layer in the same way as the original ponding models, and the model does not possess Type 1 Strong Memory. In the simulations which examined the effect of adaptive SL1 units, however, a multi-layered acrotelm was necessary. With regards to parameters, the following values were assumed:

catotelm K = 0.00125 cm s^{-1}, acrotelm = 0.005 cm s^{-1} (hummocks) and 0.1 cm s^{-1} (hollows), and net rainfall = 30 cm yr^{-1}. Furthermore, the same boundary conditions, randomised initial conditions, and rules governing SL1 transitions were assumed as in section **3.2.**, above. The combination of acrotelm K values chosen are the same as the first set used in section **3.2.**, above, and represent the largest differential in K between hummocks and hollows. As noted by Swanson and Grigal (1988), a greater assumed difference in permeability between hummocks and hollows is likely to lead to stronger, more widespread predicted patterning. A high K differential between hummocks and hollows was therefore chosen so as to give the model the best possible chance of developing patterning.

To facilitate Type 1 Strong Memory within DBEH1's algorithmic structure, each column's K represents not only the current SL1 designation, but also that column's recent history of SL1 transitions. Thus, if a computational column is currently occupied by a hummock, but was recently occupied by a hollow, we might expect the K of the acrotelm to reflect the type of litter/peat found under hummocks but also the type found under hollows. However, the longer the column remains a hummock the closer one would expect the depth-averaged K of the acrotelm to accord with the 'canonical' hummock K. This approach differs from that of Swanson and Grigal (1988), Couwenberg (2005) and Couwenberg and Joosten (2005) in that they assumed a wholesale change in acrotelm transmissivity upon SL1 transition. Thus, in those previous versions of the ponding model, the acrotelm transmissivity T of a column, when a transition from a hollow to a hummock occurred, changed immediately and completely to the canonical T value of a hummock. This meant that all columns with hummocks, regardless of how long they had possessed hummock status, had identical acrotelm T values.

Such an assumption also implies that the length of time required for the transition from one SL1 unit type to another, Δt_e, is exactly equal to the residence time Δt_r of peat in the acrotelm. Given that existing evidence suggests that Δt_e is generally equal to or greater than Δt_r (see section *3.4.2.*, above), it seems reasonable to assume that the hydraulic properties of the acrotelm reflect not just the peat being laid down by the current plant community but also that associated with previous SL1 unit types which occupied the column over the previous n-1 developmental steps, where:

$$n = \text{int}\left(\frac{\Delta t_r}{\Delta t_e}\right), \quad \Delta t_r \geq \Delta t_e \tag{3.1}$$

and where *int* is a function that returns the closest integer value to a real number. In DBEH1, n is a parameter and may be thought of as the strength of the Type 1 Strong Memory, or simply 'memory strength'. The value of n is always an integer greater than zero and each column in DBEH1 is composed of $n + 1$ layers: a single layer to represent the well-decomposed and compressed peat of the catotelm, and n layers to represent the acrotelm. The thickness of each layer in the acrotelm is given by D/n where D is the total thickness of the acrotelm. Given the above argument that SL1 transition occurs on timescales of the order of decades, and that t_r is of the order of 10^1 to 10^2 years (again, see section *3.4.2.*, above), values between 1 and 100 are justifiable as reasonable estimates of n. At the start of each developmental step, the top layer in each column is assigned the canonical K representative of the current SL1 unit type. The K of each of the other layers in the acrotelm is moved downward one position, while the K of the bottommost layer is 'lost' from the model, representing burial within the catotelm (assumed to be homogeneous) of peat older than n developmental steps. As illustrated in Figure 3.7, acrotelm layers other than the uppermost layer represent peat laid down during previous developmental steps and the SL1 unit type that was present at the time the layer was formed. The downward movement of layer properties that occurs during each developmental step is a loose approximation of what has been observed to happen in reality (*cf*. Belyea and Baird, 2006).

An experimental design with twelve treatments was used to test the effects of memory strength upon pattern development. Four hydrological runtimes (Δt_e = 10 hours, 24 hours, 30 days and 365 days) were combined factorially with three memory strengths (n = 1, 10 and 100 developmental steps). The rationale for examining the effects of memory under a range of hydrological conditions is as follows. The inclusion of memory may have slowed or stopped the migration of patterns under transient conditions (low values of Δt_e). Additionally, memory may have caused patterning to develop, where previously it did not, under steady hydrological conditions (high values of Δt_e).

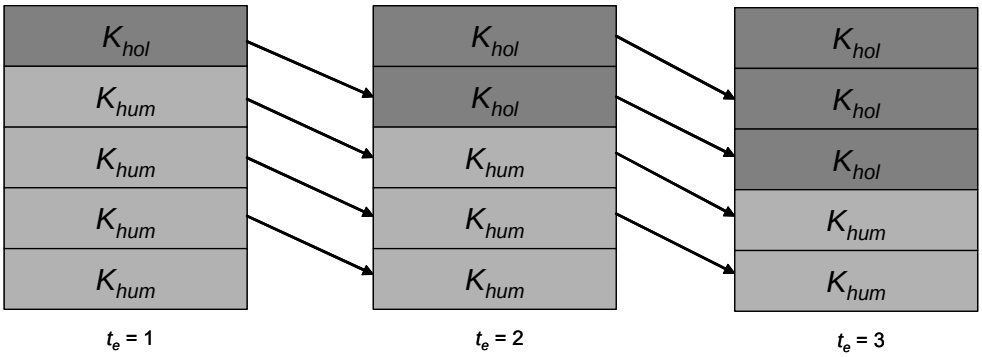

Figure 3.7: Cross-section schematic illustrating the simulated burial of old peat within a single column for DBEH1's multi-layered acrotelm. The column in question possesses five acrotelm layers. At each developmental step t_e, the properties of each acrotelm layer are assumed to move downwards one layer. The properties of the top layer are determined by the current SL1 designation for the column, and the properties of the bottom layer are assumed lost from the system, as the oldest acrotelm peat passes into the catotelm. In the example situation here, at t_e = 1, a previously persistent hummock is replaced by a hollow. As that new hollow persists for the next two developmental steps, so more of the acrotelm peat for that column takes on the canonical hollow K.

3.4.4. Results

Under transient hydrological conditions (Δt_e = 10 and 24 hours), the strong patterning previously observed (see section **3.2.**, above) is still evident when n is equal to 1 and 10, but is altered by the very strong memory of n = 100 such that across-slope stripes no longer develop. Instead, the modelled landscapes still feature a large, upslope area of randomly mixed SL1 units, but the lower area consists of a single, dry SL3 patch. As Δt_e is increased to 30 days and 365 days, the large-scale, thickly-spaced stripes are altered little by the inclusion of memory, compared to the runs with n = 1 developmental step. Certainly, the memory effect does not appear to have induced more realistic, closely-spaced SL2 striping such as that observed under transient hydrological conditions.

For all values of Δt_e, a memory strength of 10 developmental steps has reduced SL1 turnover rate compared to the runs with n = 1 (see Figure 3.8). For the runs with Δt_e = 10 hours and 24 hours, in which strong, across-slope SL2 stripes develop, it can be seen that this reduction in turnover rate is manifest as a slower

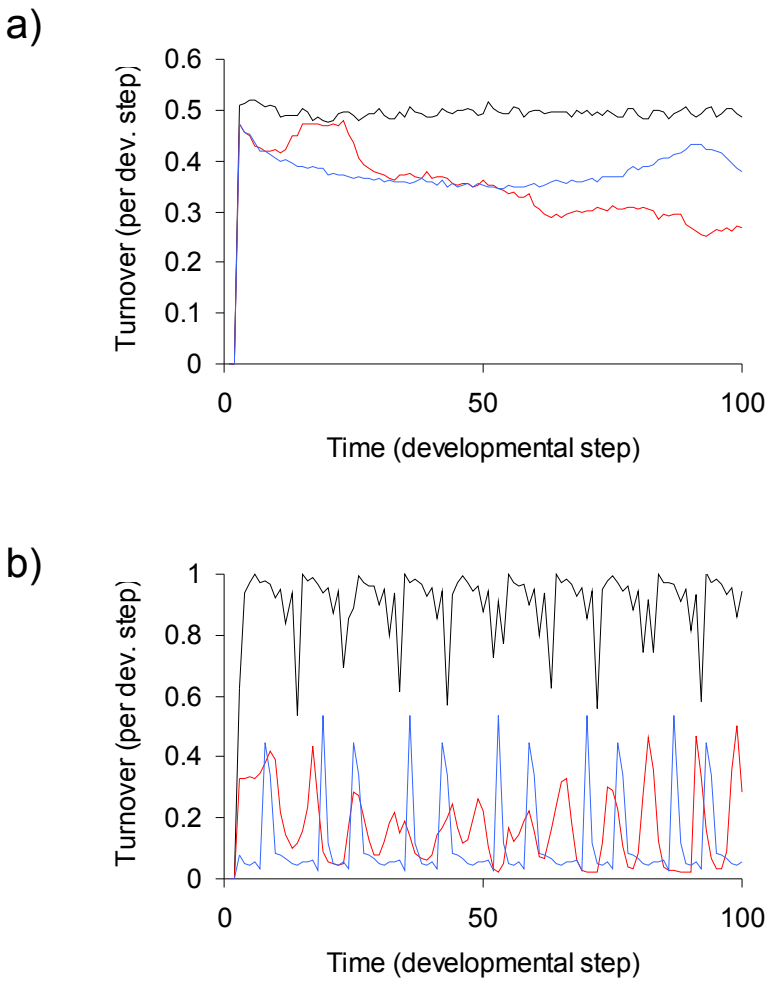

Figure 3.8: Plots showing turnover of model columns under differing memory strengths (black line shows n *= 1, red line shows* n *= 10, blue line shows* n *= 100 developmental steps) and hydrological runtimes: a)* Δt_e *= 24 hours; b)* Δt_e *= 365 days.*

migration of SL2 units (see Figure 3.9). In the runs with Δt_e = 365 days, the frequency of cyclical switching between wet and dry states has been reduced in runs with $n > 1$. Further increasing memory strength to 100 developmental steps appears to have a mixed effect upon model stability. For Δt_e = 24 hours, turnover rate is initially lower for n = 100 than for n = 10, but after approximately 50 developmental steps, turnover rate for n = 100 appears to increase to a level above that for n = 10. Certainly, turnover rates are lower with memory than without, but there does not appear to be a simple relationship between memory strength and turnover rate.

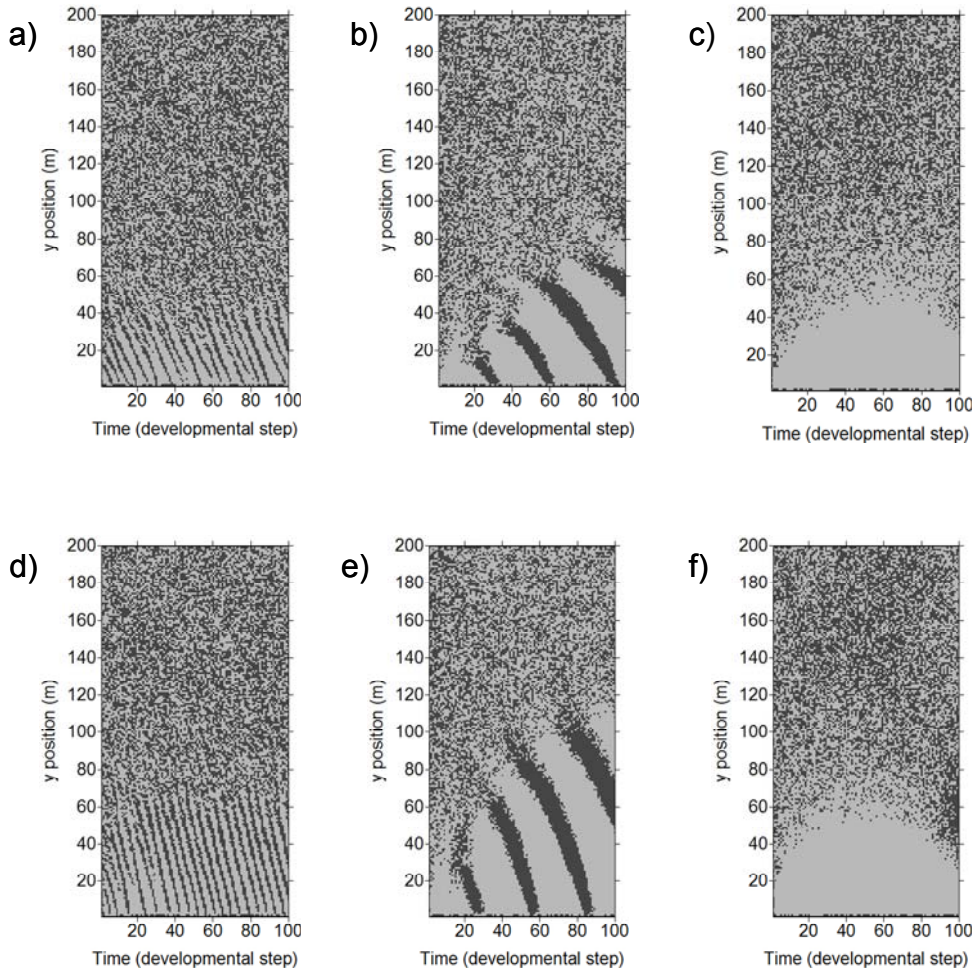

Figure 3.9: Spatio-temporal plots showing downslope migration of SL1 and SL2 units along a central, longitudinal transect. Dark pixels represents hollows, light pixel are hummocks. In each panel, the model domain slopes from high to low values of y, i.e.*, flow occurs down-page. Treatments are as follows: a) n = 1, Δt_e = 10 hours; b) n = 10, Δt_e = 10 hours; c) n = 100, Δt_e = 10 hours; d) n = 1, Δt_e = 24 hours; e) n = 10, Δt_e = 24 hours; f) n = 100, Δt_e = 24 hours.*

3.5. Discussion

It is clear from the experimental work presented in section **3.2.**, above, that the ponding model is highly sensitive to hydrological steadiness. Without a comprehensive sensitivity analysis it is not possible to deduce that the ponding model is unable to predict patterning in steady state, but if an area of parameter space exists in which this is possible, it appears to be a much narrower one than for transient hydrological conditions. Rather than representing a system prone to patterning and which is robust to small perturbations in climatic conditions, the ponding model, when run to a genuine hydrological steady state, appears to be controlled largely by hydrological boundary conditions. Only a relatively narrow area of parameter space was explored here, so caution must be adopted. It may be that an area of parameter space, as yet undiscovered, exists within which the steady-state ponding model does predict SL2 stripes, although the model fails to predict patterning under a range of realistic parameter values. The fact that striped patterns on peatlands are very common and form from a range of plant communities and under a range of climates indicates that any suggestion of high sensitivity is in error. In work not presented here, the zone of probabilistic consideration was narrowed from 5 cm to 1 cm. This assumption gave rise to stronger, more visibly striking patterning in the transient runs, covering a greater extent of the model domain, but still no parameter set was found that led to SL2 stripes under steady-state hydrological conditions. It would appear that, by running the hydrological model to a conservative steady state, some crucial feedback or other effect, present in the transient runs, is lost. One likely explanation involves an increasing spatial range of hydrological influence on individual SL1 units with increasing runtimes. That is, as the hydrological model is allowed to run for longer, so the local variation in SL1 K values becomes less influential, water-table position becoming increasingly determined by its boundary conditions (including net rainfall rate). When hydrological runtimes are shorter, however, small-scale variations in K cause locally-variable water-table geometries which are not smoothed out by flow at the larger scale. The long-range, boundary-condition-dominated flow in steady-state runs means that SL2 stripes never have the chance to develop from random initial conditions.

The cyclic behaviour predicted by the steady-state ponding model appears to be an artefact of a mechanistically unsound model, rather than a genuine prediction worthy of further investigation. As the model grid becomes dominated by hummocks, for example, so average values of K across the whole model are reduced sufficiently to cause significantly higher steady-state water tables during the next developmental step, leading to prevalence of hollows. Conversely, during the next developmental step, the high proportion of hollows and accompanying high K leads to lower water tables and so a prevalence of hummocks in the subsequent developmental step, and so on. In this way the model appears to have predicted high-frequency cyclical behaviour, switching between wet and dry states almost every developmental step. While there is some evidence for peatland plant communities undergoing dramatic alterations in plant community composition over relatively short periods of time (*cf*. Belyea and Malmer, 2004; Barber, 1981), the current author knows of no empirical evidence in support of such dramatic, rapid and regular switching as predicted by the steady ponding model. The rapid, cyclical behaviour observed here is suggestive of a chaotic system. The ponding model may, therefore, be missing an important negative feedback, such as the long-range inhibition of the nutrient-scarcity model, which acts to counterbalance intrinsic sensitivity, stabilising patterning.

In reality, SL1 succession clearly occurs on timescales longer than a few hours or days, and complete replacement of hummock communities with hollow communities, for example, is likely to take at least several years (Rydin and Jeglum, 2006), even when conditions are favourable. The hydrological timescales employed in this work cannot be taken literally as representative timescales for succession, which begs the questions of what they should be taken to represent. Some aspect of the real system which leads to patterning appears to have been inadvertently captured by the hydrological transience, although it is difficult to envisage what aspect this is. The fact that the model makes erroneous predictions about downslope pattern movement suggests that the model does not represent the true mechanisms by which patterns form (Grimm *et al*., 2005). The representation of hydrological transience using short runtimes is an obvious culprit when it comes to identifying unreasonable assumptions or spurious mechanisms within the model. Although realistic spatial patterns are predicted, they are not steady in time and appear to be

generated by spurious mechanisms. Thus, while it appears that the steady-state ponding model must be discounted as a viable theory on peatland pattern formation (see above), it is also difficult to justify the transient model. The unstable nature of the patterning predicted, manifest in its consistent and sometimes rapid downslope migration, should help to ease anxieties over dispensing with the non-steady ponding model (*cf*. Grimm *et al*., 2005). That none of Swanson and Grigal (1988), Couwenberg (2005) or Couwenberg and Joosten (2005) reported the model's sensitivity to hydrological steadiness is surprising indeed.

Contrary to reports by previous authors, the steady-state ponding model did not predict slope-normal stripes, and so there appears to be little to be gained from a detailed discussion of the effects of memory upon this model. Nonetheless, two main points are still worth making. Firstly, ecological memory, represented by a layered acrotelm, did not cause the steady-state ponding model to predict SL2 stripes. Although ecological memory is justifiable from first principles (see section *3.4.2.*), it is clearly not this particular omission which causes the ponding model to fail to predict stripes, indicating that the model is still flawed in other crucial respects. Indeed, a very high memory strength (n = 100 developmental steps) appears to prevent SL2 stripes developing even under transient hydrological conditions.

Secondly, an ecological memory strength of n = 10 developmental steps was only partially effective at stabilising pattern migration in the transient version of the ponding model. SL1 turnover rates were reduced, indicating a more stable system than without memory. Migration of SL2 units was slowed, but not halted entirely. If SL2 units are conceptualised as gliders in the sense used in the cellular automata literature, then this finding fits with the work of Alonso-Sanz (2007), who similarly found that memory slows, but does not entirely halt, glider movement. It may be that SL2 stripes on real peatlands do, indeed, migrate consistently downslope, on a timescale which is slower than that of human observation. Such a prediction is made by the ponding model when n = 1 and 10 developmental steps, and could be tested in future through macrofossil analyses of cores from patterned peatlands. If SL2 units do indeed move consistently downslope in some peatlands then

they would likely leave a three-dimensional record of this movement within the peat profile.

The 'water-scarcity' model did not succeed in replicating the SL2 stripes predicted by the nutrient-scarcity model of Rietkerk, *et al*. (2004a, b). For the lower of the two assumed net rainfall rates, even a small net rainfall differential caused the model to predict a uniformly dry landscape, as hypothesised. The lower of the two assumed net rainfall rates, which gave rise to a majority of hummocks in the control run, has initiated a positive feedback in the runs with a net rainfall differential. A majority of hummocks leads to a drying of the model due to the receipt of less total net rainfall, which in turn stimulates further hummock development. The opposite case, convergence upon a wet model state, did not occur under a base net annual rainfall rate of 35 cm yr^{-1}, indicating that the model possess more stable areas of parameter space, and is not so sensitive as to be described as chaotic.

For runs with base net rainfall rate of 35 cm yr^{-1}, rainfall differentials of ± 2.5 % and 5 % between hummocks and hollows have allowed hummocks to persist in the midst of the otherwise wet area at the upslope end of the model domain, where they would otherwise have been eradicated by shallow water tables; likewise, for hollows in the dry downslope area of the model. Unlike the nutrient-scarcity model, however, these isolated SL1 units did not coalesce and self-organise to form recognisable SL2 units. There does not appear to be a stable state for which SL2 stripes develop, although a full sensitivity analysis would be required to be certain. While a full sensitivity analysis has not been undertaken, the model fails to predict such patterns under a range of realistic parameter sets. As with the steady-state ponding model, it may be that the water-scarcity model does predict patterning under a limited, and potentially unreasonably narrow, range of realistic parameter values.

It is not entirely clear whether the inability of the water-scarcity model to predict the kinds of patterns given by the nutrient-scarcity model is due to the lack of a nutrient-concentration submodel or other differences between the two models. The water-scarcity model may be missing a certain feedback or set of feedbacks, as a result of it not featuring a nutrient concentration submodel, which causes the nutrient scarcity model to predict

patterns. That is, it may be that the nutrient-scarcity model, with its three differential equations, is in fact a minimalist model of peatland patterning. Alternatively, the nested time loops, the binary SL1 classification (as opposed to the continuous biomass state variable of Rietkerk *et al*., 2004a) and the lack of a nutrient-concentration submodel in the water-scarcity model may all have played a part in its inability to predict stripes. It may be possible that SL2 patterning would develop in a version of the model of Rietkerk *et al*. (2004a), complete with its congruous submodel time loops and continuous biomass state variable, modified in such a way that no nutrient concentration submodel was included and in which biomass growth rate depended solely upon water-table positions. Building such a model appears to be the next logical step in the pursuit of a minimalist cellular model to explain peatland patterning.

Rietkerk *et al*. (2004a) discussed the possibility of a model which incorporates their nutrient-scarcity mechanism and the differential K of the ponding model, something which is not investigated here. Given that is has been possible to justify such things from first principals, it may be desirable in future to develop a patterning 'super model', which incorporates differential K and transpiration rates as well as a memory effect. The counter argument is that, in the interests of minimalism (*cf*. Goldenfeld and Kadanoff, 1999), it is unnecessary to build such a complex model when the much simpler, existing version is already able to predict stable, realistic patterns. The previous point is only strengthened by the field study of Eppinga *et al*. (2008), which served to corroborate the mechanistic basis of the nutrient-scarcity model. It is the current author's personal view that the research group of Max Rietkerk are to be commended for this rigorous attempt to falsify their own theoretical work using primary field data.

3.6. Conclusions

A number of modifications, all based on first principles, were made to existing models of peatland patterning, but none was able to predict the stable, across-slope stripes seen in reality. In this respect none of the models presented here is able to offer an improvement on the model of Rietkerk *et al*. (2004a, b), meaning that the nutrient-scarcity model cannot currently be discounted as the cause of peatland patterning. The ponding model was shown to be highly sensitive to the stringency of the hydrological steady-state criterion adopted and, contrary to the findings of Swanson and Grigal (1988), Couwenberg (2005) and Couwenberg and Joosten (2005), the model did not predict SL2 stripes when run to a true steady state. The fact that the model does predict strong SL2 patterning under a range of transient hydrological conditions, suggests that the lack of patterning under steady hydrology is a genuine model prediction rather than merely a failure to exploit a sensitive area of parameter space. Given the ponding model's odd prediction of downslope migration of SL2 units and its high sensitivity to hydrological steady-state criteria, it is here suggested that the steady-state ponding model, as described by previous authors, be discarded as a viable theory for the formation of peatland patterning.

It seems likely that the steady-state water tables used by DBEH1, and in the ponding model as described in the literature, are an inappropriate quantity by which to predict peatland community succession. Part of the apparent success of the nutrient scarcity model may well lie in the congruous timescales of its three submodels, whereby changes in biomass and nutrient concentrations respond in "real" (model) time to water-table behaviour and to one another. In the nutrient scarcity model, the hydrological submodel runs on the same time loop as the submodels which represent nutrient concentration and plant biomass, and so all submodels are run to steady state.

Furthermore, it appears that a submodel which describes the distribution of a finite resource, such as growth-limiting nutrients, may well be a necessary component of the larger model of Rietkerk *et al*. (2004a, b). Concerns that, with no limit to the supply of nutrients, the model may 'run away' to wet or dry attractors, appear to be well placed, at least for low rainfall rates, on the evidence of the water-scarcity model work presented in

this chapter. However, short of using a model algorithmic structure which is closer to that of Rietkerk *et al*. (2004a), so as to relax the assumption of a probabilistic SL1 transition ruleset, it is not possible to tell whether the water-scarcity model's inability to predict patterns is attributable to the probabilistic transition ruleset or the lack of a nutrient-concentration submodel. Building a new version of the water-scarcity model which uses the continuous state-variable approach of Rietkerk *et al*. (2004a, b) seems to be the next obvious step towards developing an insightful and minimalist model of peatland patterning. Such a model would ignore the role of nutrient cycling, instead predicting vegetation biomass solely on the basis of hydraulic head. Additionally, it remains to be seen whether SL2 patterning would be successfully predicted by a version of the nutrient-scarcity model which, as Rietkerk *et al*. (2004a) advocate, includes the transpiration-driven nutrient scarcity of their own model (or, perhaps, transpiration-driven water scarcity) and combines this with the differential K values of the ponding model. In the interests of parsimony, however, and in light of the apparent success of the nutrient scarcity model as reported by Rietkerk *et al*. (2004a, b), it is arguable that construction of such a model is unnecessary.

Alternatively, it may be that the essentially two-dimensional, cellular models such as those discussed in this chapter are inherently unsuited to the task of representing the complex and three-dimensional nature of peatland spatio-temporal dynamics. None of the models discussed in this chapter, including the nutrient-scarcity model, constitute a full CAS treatment of peatland development according to the conceptual model advocated in Chapter 1 (see Figure 1.3). Understanding and simulating emergent phenomena is, by definition, always likely to provide a number of challenges and surprises to even the most diligent of researchers, but progress on the work on DBEH1 presented in this chapter was particularly slow and frustrating. Much of the difficulty arose in trying to constrain K (in both the acrotelm and catotelm), rainfall, bog dimensions and SL1 transition rules in order to give sensible behaviour. The inability of these various system elements to adapt during the course of model time may be a reason for DBEH1's cumbersome nature, and so a full CAS treatment which includes peat accumulation and decay is advocated for future modelling studies. Without a full CAS treatment, individual model agents (such as DBEH1's peat layers) are unable to adapt or self organise in the manner prescribed by the conceptual

model presented in Chapter 1 and their properties must therefore be prescribed in a highly constrained manner. In particular, the linkage between peat decay, compression and a reduction in hydraulic conductivity may be crucial. This hypothesised relationship is explored empirically in Chapter 4, and is incorporated into models of bog landform development in Chapters 5 and 6.

Chapter 4: Homeostasis in Peat Properties

This chapter reports an empirically-derived relationship to describe peat hydraulic conductivity as a function of depth, cumulative decay, SL1 type and proximity to bog margin. The relationship was derived using data from sixteen shallow peat cores, recovered specifically for this purpose, from a Swedish raised bog. The relationship represents an important mechanism by which peatlands, and raised bogs in particular, may achieve a certain ecohydrological homeostasis. It is also an important and previously undocumented linkage in the conceptual model of peatland development advocated in the first chapter of this thesis. Chapter 3 demonstrated the limitations of cellular models of peatland patterning which arise from the inability of those models to self-organise in the manner described here, thereby justifying the scientific need for the work in this chapter.

4.1. Introduction

4.1.1. Theoretical relationship between peat decomposition and hydraulic conductivity

The formation of thick peat deposits, especially raised bogs, reflects a mutual dependence of saturated soil conditions (thereby causing anoxic conditions and slowing decay) and the preservation of old, deep peat (which provides a poorly-permeable medium which retains rainwater). Deep peat is often highly compressed and poorly permeable (Ivanov, 1981); values of hydraulic conductivity as low as 10^{-4} cm s^{-1} are not uncommon (Ingram, 1982; Rycroft *et al*., 1975; although *cf*. Surridge *et al*., 2005). Once compressed by overlying peat layers, *Sphagnum* moss, in particular, is highly effective at retaining water, leading to shallow water-table depths in which the genus is able to out-compete most other plants. This trait of the *Sphagnum* genus seems likely to be naturally selected, and van Breemen (1995) noted that it may be thought of as a part of the *Sphagnum* toolbox in its role as an "ecosystem engineer". Similar behaviour is exhibited by other peatland plants, such as the *Eriophorum* genus (*cf*. Hughes, 2000). A more subtle mechanism by which *Sphagnum* and other peat-forming plants may influence their environment involves a theorised linkage between the state of cumulative decay of peat, and its hydraulic conductivity. As argued in the coming paragraphs, empirical and modelling evidence, as well as physical first principles, appear to support the notion that older, more highly decomposed peat is likely to exhibit lower values hydraulic conductivity.

Physical first principles indicate that, generally speaking, older peat will present a less permeable medium for groundwater movements. Assuming that deeper peat is older than that at shallow depths, cumulative decay (the proportion of a peat sample's original mass lost through decay) is likely to increase with increasing depth. Cumulative decay will be inversely associated with the structural rigidity of individual stems and of the peat matrix as a whole. With increasing age, peat is increasingly likely to be compressed by the increasing weight of younger, overlying peat (Price *et al*., 2005), particularly near the bottom of the unsaturated zone, where the effective stress is greatest because the weight of porewater and overlying peat is not buoyed by saturated conditions (*cf*. Clymo, 1992). As flow pathways become narrower and more tortuous, so hydraulic conductivity decreases.

Poiseuille's law (*cf*. Pfitzner, 1976) describes the rate of flow ϕ (L^3 T^{-1}) of a Newtonian fluid through a cylindrical tube of constant radius R (L) such as an idealised soil pore:

$$\phi = \frac{\pi R^4}{8\eta} \frac{|\Delta P|}{L} \tag{4.1}$$

where all terms other than ϕ and R may be taken to be constants. Equation (4.1) predicts, therefore, that flow rate per unit area (equivalent to hydraulic conductivity) varies with the square of pore radius, so that even a small increase in peat compaction is likely to produce a large decrease in hydraulic conductivity. In a study of the compressibility of peat, Price *et al*. (2005) observed an inverse relationship between peat bulk density and compressibility. That is, young fresh peat has a low dry bulk density due to large pore spaces in-between the stems and branches, meaning that it is highly compressible. As peat becomes compressed, the pore spaces close between the solid stems and branches, leading to a lower compressibility and a higher bulk density. Once pore spaces have been mainly closed, further compression of peat is highly limited and further increases in bulk density and closure of pore spaces is likely to occur much more slowly. Given that hydraulic conductivity seems likely to be strongly related to compression, it seems reasonable to theorise that K will vary as a sigmoid (s-shaped) or step-like function of proportional remaining mass (that proportion of the original mass of a peat sample which has not been lost through decay), because compression of peat occurs in a narrow zone of collapse once a critical ratio of overlying weight to stem strength is exceeded (*cf*. Clymo, 1992).

Many previous studies have examined the relationship between the degree of peat decomposition and hydraulic conductivity, and the majority suggested a decrease in hydraulic conductivity with increasing depth or degree of decomposition (see, for example: Boelter, 1969; Hoag and Pice, 1997). As Beckwith *et al*. (2003a) observed, however, many of these studies have used measurement techniques for hydraulic conductivity which are potentially flawed, which therefore calls into question the reliability of many of their findings. Most of the studies mentioned above also used crude, subjective or qualitative methods for estimating the degree of decomposition of peat samples. For instance, the von

Post technique (*cf.* von Post and Granlund, 1926), while commonly used by many peatland researchers (e.g., Boelter, 1969; Rycroft *et al*., 1975), provides an estimate of peat cumulative decomposition that is subject to errors in the form of imprecise user interpretation of the scale. Ivanov (1981) observed a curvilinear relationship between what he termed the degree of peat humification, given as a dimensionless percentage, and hydraulic conductivity. While it is difficult to tell exactly how Ivanov (1981) calculated degree of humification for his samples, it seems likely that he too used the von Post scale.

While the von Post technique assigns a numerical designation to peat samples, the method is in effect little more than ordinal, meaning that it should not be treated as a continuous variable in analytical or modelling studies. Because the von Post scale is not physically based, it would be difficult for a model such as **DigiBog** to predict peat decay and the resultant changes in hydraulic conductivity on the basis of the scale. Other measures of decay, such as fibre content (e.g. Boelter, 1969), are similarly problematic for a modelling scheme such as **DigiBog**. The **DigiBog** decay submodel (see Chapters 5 and 6) predicts proportional remaining mass as a result of decay losses, based on a scheme similar to that of Clymo (1984). The **DigiBog** hydrophysical submodel predicts changes in peat hydraulic conductivity as a function of cumulative decay (again, see Chapters 5 and 6). While the model could be parameterised so as to predict hydraulic conductivity on the basis of fibre content, for instance, this would require a much more sophisticated decay submodel which could predict fibre content on the basis of proportional mass loss. What is required in order to inform **Digibog**, therefore, is a relationship between reliable measurements of proportional mass loss and hydraulic conductivity. Clearly, while decomposition weakens the structure of peat, it is compression rather than cumulative decay *per se* which is mechanistically responsible for the closure of pore spaces and, therefore, for any reduction in hydraulic conductivity of older peat. It may be, however, that cumulative decay exhibits substantial covariance with compression, and may be a good predictor of K.

The empirical study of Baird *et al*. (2008) and the modelling of Lapen *et al*. (2005) both suggested the existence of rands of low-K peat, up to 200 m in width, which act as barriers to drainage in their study sites, and which may be important to the retention of groundwater

in raised bogs in general. Evidence is limited, but if low-*K* boundaries are common features of raised bogs, they may be artefacts of higher rates of decay in the partially-oxic drawdown zone near the edges of large peat deposits. The theoretical study of Belyea and Baird (2006) suggested that accurate modelling of peatland developmental dynamics should consider temporally- and spatially-variable hydraulic conductivity, while the empirical study by Belyea and Malmer (2004) also suggested temporal shifts in hydraulic conductivity, in response to plant community composition and decay regime.

4.1.2. The influence of plant community

Ivanov (1981) observed a control of plant community type upon peat hydraulic conductivity, suggesting that different SL1 types (e.g. hummock, hollow) produce peat of differing permeability. More than a few decimetres below the surface, hummock peat becomes highly impermeable, forming barriers to flow, whereas hollow species produce much more highly permeable peat, with large, open pore spaces. This idea has been taken up in a number of modelling studies, such as those by Swanson and Grigal (1988), Couwenberg (2005) and Couwenberg and Joosten (2005), as well as the experimental work presented in Chapter 3 of this thesis. However, rather than simply influencing the value of hydraulic conductivity of peat, the type of plant community which formed the peat may have another, more subtle affect on peatland hydrology. That is, the shape of the relationship between cumulative decay and hydraulic conductivity may differ between peat types of contrasting botanical composition, due to differences in physical structure and biochemical properties of the litter, as well as differences between soil moisture and biogeochemical (decay) regimes between hummocks and hollows (*cf*. Belyea and Clymo, 2001).

Hummocks such as those formed of *S. fuscum* litter may often be elevated above surrounding lawns and hollows by up to 60 cm (Nungesser, 2003), and the live moss layer relies on capillary action in narrow but intact pore spaces to draw up water for photosynthesis (Rydin and Jeglum, 2006; Robröek *et al*., 2007b). Litter at shallow depths near the surface of hummocks is usually well preserved and retains a high structural integrity. Empirical observations suggest, however, that hummock peat undergoes a rapid

transition at a certain depth, whereupon stems collapse, structural integrity and permeability decreases and humification increases greatly (Clymo, 1992). Therefore, it seems reasonable to expect hummock peat to exhibit a sigmoid or step-like relationship between cumulative mass loss and hydraulic conductivity, with poorly-decayed peat exhibiting relatively high permeability and a rapid decline in *K* occurring at intermediate levels of cumulative decay. At shallow depths, hollow *Sphagna* such as *S. cuspidatum* are, by contrast, often loosely-packed, structurally weak and subject to almost constantly saturated conditions (Ivanov, 1981). The structurally-weak nature of the peat formed by hollows might reasonably be expected to lead to an initially rapid collapse of stems and decrease in hydraulic conductivity at low levels of cumulative decay. Once the original stem structure has collapsed, whether peat was initially weak (as in hollows) or strong (as in hummocks), further reductions in pore size and connectivity seem likely to occur more gradually with increasing cumulative decay. Below the zone of collapse, individual stems and branches have been compressed so far that there remains little void space for further compression (Kennedy and Price, 2005; Johnson *et al.*, 1990). While hummocks seem likely to exhibit a rapid decline in hydraulic conductivity over intermediate degrees of decomposition, for hollows this decline seems likely to occur in much younger, fresher peat. As such, the hypothesised relationship between cumulative decay and hydraulic conductivity may take more of a logarithmic relationship for peat formed by hollows, and the hypothesised sigmoid nature of the relationship may only be apparent in hummock peat.

The maintenance of high structural integrity at shallow depths in hummocks is likely attributable to rapid decay occurring over a narrow depth range several decimetres below the surface, which in turn may be attributable to water-table behaviour. Belyea and Clymo (2001) observed that the highest decay rates occurred in the zone of water-table fluctuation (sometimes referred to as the "mesotelm"; *cf*. Clymo and Bryant, 2008), which is typically several decimetres below the top of tall hummocks, leading to low decay rates at perennially-oxic shallow depths. The close spacing of stems in hummock peat means that, in the zone of water-table fluctuation, effective porosity (those pore spaces through which flow can occur, as a volumetric proportion of the entire peat sample) is likely to be lower than in comparably fresh peat formed by hollows, causing water-table position to fluctuate

over a greater range, and thereby subjecting a greater depth-range of peat to the high, periodically-oxic ("mesotelmic") decay rates. By contrast, effective porosity of fresh peat formed by hollows is much higher than in hummocks, leading to less dramatic fluctuations in water-table depth (Ivanov, 1981), and so little deviation from fully saturated, anoxic conditions, where decay rates are very slow. This fact, combined with the low microtopographic position of hollows (Nungesser, 2003) and the tendency for the live moss layer to effectively "float" (Strack *et al*., 2004; Schlotzhauer and Price, 1999; Dise *et al*., 1993) in response to varying water tables, means that even surficial layers of peat formed by hollows are rarely far from complete saturation (*cf*. Robröek *et al*., 2007b). As such, hummocks seem likely to exhibit a greater range of decay rates than hollows. This may be represented in hummocks by an abrupt increase in cumulative decay within the zone of water-table fluctuation. By contrast, perennially-saturated hollows may exhibit a more gradual increase in cumulative decay with depth. If there is a strong mechanistic relationship between peat cumulative decomposition and hydraulic conductivity, then the form of this relationship may well differ between the SL1 types from which the peat was formed.

4.1.3. A mechanism for homeostasis in peatland ecohydrology

In keeping with the title of this thesis, it appears that the hypothesised relationship between cumulative peat decay and hydraulic conductivity may be of key importance to the role of raised bogs as CAS. In contrast to models such as those by Hilbert *et al*. (2000) and Frolking *et al*. (2001), a conceptual model generated here suggests that peatlands appear to be largely resistant, at least over short (annual to decadal) timescales, to hydrological perturbations. Let us consider in combination a number of basic empirical and theoretical models of: groundwater hydrology (*cf*. Ingram, 1982); peat decay (*cf*. Clymo, 1984); the formation of new peat litter (*cf*. Belyea and Clymo, 2001); hydraulic properties (*cf*. Boelter, 1969); and plant community succession (*cf*. Couwenberg and Joosten, 2005). All of these models were developed from either basic first principles or from empirical data, but when considered together they allow us to develop a conceptual model which may exhibit a certain homeostasis in response to varying rainfall rates. Under a given distribution of peat hydraulic properties, rising rainfall rates are likely to lead to an increase in water-table

height (Ingram, 1982). Under the acrotelm-catotelm scheme of Clymo (1984), this situation would lead to a greater amount of peat material being captured by the catotelm, and that peat would possess a higher proportional remaining mass. According to the conceptual model advocated in sections *4.1.1.* and *4.1.2.*, above, this would in turn lead to higher hydraulic conductivity in the catotelm (*cf.* Boelter, 1969), increased drainage from the peatland and lowering of the water table. The converse would apply to a drying climate, where falling water tables would lead to greater decay in the thickening acrotelm, reduced hydraulic conductivity and so reduced drainage, again possibly inducing conservative water-table behaviour. If such a mechanism for homeostasis exists, it is possibly a naturally-selected trait of *Sphagnum*; not only does *Sphagnum* create peat which retains water, thereby maintaining its own waterlogged, acidic niche, but the permeability of that peat may also be able to adjust to changing climates in order to maintain water levels suitable for optimum growth (or at least suitable for *Sphagnum* to out-compete other plants) (*cf.* van Breemen, 1995). The possibility of peatland ecohydrological homeostasis via the mechanism described here is a fascinating one and fits with the Gaian theory of homeostasis (*cf.* Watson and Lovelock, 1983). Furthermore, it seems that some SL1 units – particularly hollows – may be further resistant to hydrological perturbations due to a tendency to "float" in response to changing water-table positions (Strack *et al.*, 2004; Schlotzhauer and Price, 1999; Dise *et al.*, 1993). While this mechanism is an intriguing one, it is outside the scope of the current work and was not considered during experimental design.

A number of models of peat accumulation represent cross-scale feedbacks and complexity in peatland system behaviour (e.g., Hilbert *et al.*, 2000; Borren and Bleuten, 2006). Given the potential importance of decay-dependent hydraulic conductivity, as argued above, it is surprising that no existing model represents this mechanism. A full consideration of the influence of decay-dependent hydraulic conductivity on peatland behaviour is given for simple 1-D peat accumulation models in Chapter 5.

4.1.4. Chapter aim, objectives

The aim of this chapter is to establish what kind of relationship, if any, exists between peat hydraulic conductivity and the proportion of original peat mass remaining, and to consider how any such relationship may be affected by the SL1 type from which the peat was formed and its position on the bog. Within this aim, two specific research objectives may be identified:

i) To provide a first approximation of the form of the relationship between proportional mass remaining and hydraulic conductivity.
ii) To take into account the effects of SL1 type and/or proximity to bog margin upon the form of the relationship between peat mass loss and hydraulic conductivity identified under (i), above.

Sixteen shallow (30-50 cm) peat cores were recovered from a raised bog site in Sweden and analysed in the laboratory in order to address these two objectives.

4.2. Methodology

4.2.1. Study site and peat type

In order to address the aim and objectives identified in section *4.1.4.*, above, a raised bog site was sought from which to take a number of cores for laboratory analysis of hydraulic conductivity and proportional mass remaining. There were a number of key requirements which greatly narrowed the choice of field site. Firstly, the site was required to be safe and easily accessible by road, for the transportation of equipment and samples. A British mainland site would have been the most convenient choice in order to minimise the cost and logistical effort required to transport equipment and samples. Failing this, a site within the European Union was a necessity, so that equipment and samples could be transported to the laboratories at Queen Mary with a minimum of expense and difficulty. The international transportation of soil samples within the European Union is permitted, but transportation into the EU is highly restricted, therefore making areas such as Canada or Russia much more logistically difficult and expensive for fieldwork. Also, it was deemed desirable to perform the field work at a site that had seen as little anthropic disturbance as possible, thereby discounting many sites in the United Kingdom and the Republic of Ireland which have been cut extensively for fuel, and drained for agriculture. A pristine site would allow the study of a raised bog in as natural a condition as possible, and would ensure that factors such as the cutting and subsequent regrowth of surficial *Sphagnum* layers did not cause complications and unconformities in the peat profile. Ryggmossen is an ombrotrophic raised bog in the Uppland region of Sweden (60°03'N, 17°20'E), approximately 25 km north by north-west of the city of Uppsala and at an elevation of approximately 60 m a.s.l. (see Figure 4.1). The Ryggmossen raised bog is also a nature reserve administered by Uppland County Council, who granted the author permission to work on the site. Despite the site's easy access and proximity to a large urban conurbation, Ryggmossen has been subject to only very limited cutting near the site's northern margin, where there are also the remains of a small number of tracks used to move timber sleds during the mid 20th century (Rydin *et al*., 2002). Håkan Rydin, of the bryophyte research group at the Centre for Evolutionary Biology at Uppsala University, provided logistical support during the fieldwork and allowed the author use of laboratory facilities, including refrigerators for storage of cores before transit to the UK via commercial courier.

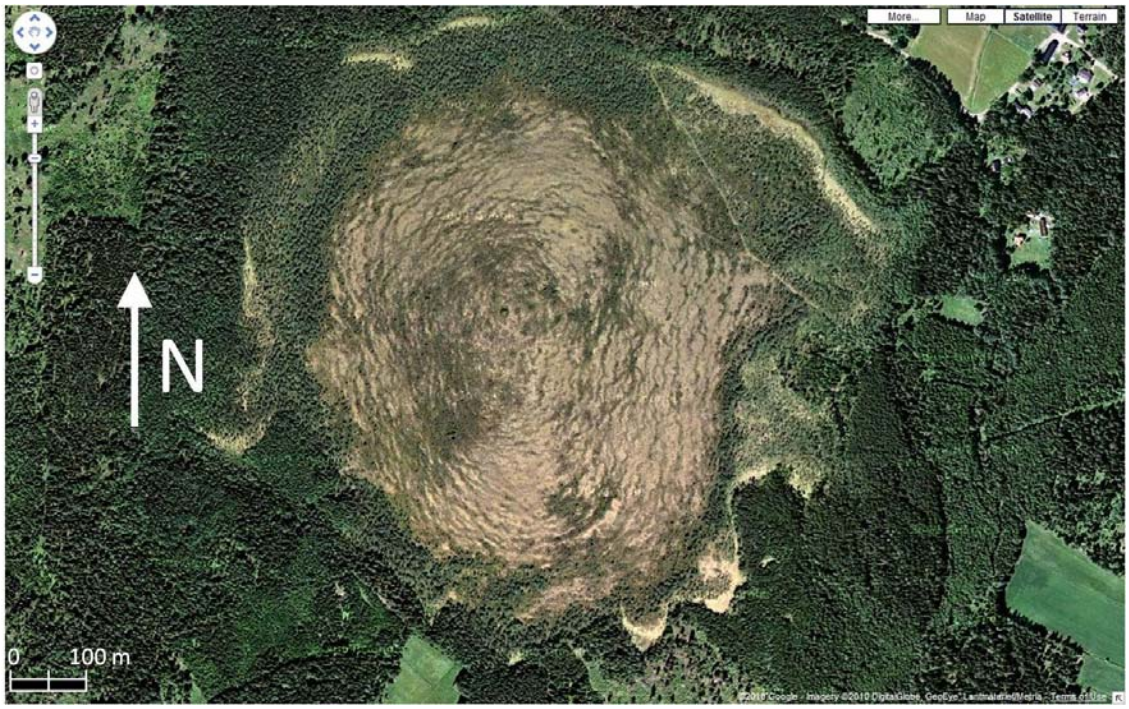

Figure 4.1: Aerial photograph showing distinct, concentric hummock-hollow patterning on Ryggmossen raised bog. Adapted from Google Maps.

The Ryggmossen raised bog extends over an area of approximately 60 ha and is sub-circular in plan. Mean annual rainfall is approximately 550 mm and mean annual temperature is 5.6 °C. The sub-circular central portion of the bog dome (diameter of approximately 400-500 m) is free of the pine trees that feature on the surrounding flanks. At it deepest, peat extends to a depth of approximately 4.6 m and the peat surface there is elevated approximately 3.5 m above the marginal lagg fen. The slope in the open, central area is very shallow, leading to low hydraulic gradients and acidic conditions which favour *Sphagnum* mosses. The central area is characterised by broken, concentric patterns of plant communities, chiefly hummocks or ridges of *Sphagnum fuscum*, *Sphagnum rubellum, Calluna vulgaris* and *Polytrichum strictum* in amongst a matrix of lower lawns and hollows of *Sphagnum balticum*, *Sphagnum cuspidatum* and *Eriophorum vaginatum*. Surrounding the central area is a drier, more steeply-sloping annular zone on the flanks of the main bog dome where hydraulic gradients are steeper and conditions are more favourable for the growth of coniferous species including *Pinus sylvestris* and *Picea abies*. In this zone the average height of trees and the abundance of dry-favouring, hummock-forming moss

species (e.g. *Sphagnum angustifolium, Sphagnum fuscum*) generally increases with distance from the bog centre, whilst wetter microforms become scarcer. A full description of the site is given by Rydin *et al*. (2002).

4.2.2. Experimental design

In order to examine any such effect, as required by research objective (ii) in section *4.1.4.*, above, eight of the sixteen cores were taken from the central area of the bog while the rest were taken from near the margins. Furthermore, four of the marginal cores and four of the bog-centre cores were taken from hummock locations characterised by *Sphagnum fuscum*, while the rest were taken from hollow areas characterised by *Sphagnum balticum*, in order to test for the effect of vegetation microhabitat type, again as required in order to address research question (ii). Thus, a 2 × 2 factorial experimental design (hummock vs. hollow and centre vs. margin) was used to address research objective (ii), with four cores in each treatment.

The structure of the dataset provided by the experimental design described above contains a number of dependencies, thereby violating one of the assumptions of standard regression modelling. For instance, all data for upslope hollows are independent from data for downslope hummocks, but are not independent from data for upslope hummocks. Data points from different depths within any given core are clearly also dependent upon one another. Such a design was justifiable, however, in order to examine the possibly interacting effects of both SL1 type and position on the bog, but the lack of independence in the dataset reduced the possibilities for regression modelling. The statistical analysis of the Ryggmossen data is described in full in section *4.3.2.*, below. More problematic than the lack of independence, however, was that the sites from which cores were extracted were chosen in pairs. Thus, eight sites were chosen, four from upslope locations and four from downslope location, and two cores were taken from each site, one from a hummock and the other from an adjacent hollow at the same site. The original intention for such a dataset was that paired measurements would facilitate statistical tests such as two-sample t-tests, Chi-squared tests, and other analyses which examine differences between categorically grouped data. For example, one of the original intentions for the dataset was to calculate

depth-averaged hydraulic conductivity for all samples, and to compare the effects of binary treatments such as SL1 type and position on the bog via the use of t-tests or Chi-squared tests. Not until after sample collection was it realised that regression modelling could be used more effectively to generate a predictive model of *K* as a function of proportional mass remaining, and that a lack of independence between data points would make this substantially more difficult. While the lack of independence in data due to the categorical treatments (position and SL1 type) was accepted as a necessary limitation and allowed fieldwork to be carried out in an efficient manner, the problems caused by taking cores in pairs represents an unjustifiable weakness in the dataset arising from an oversight by the author. Section *4.3.2.*, below, describes how the problems associated with dependencies at various levels within the dataset were overcome using a hierarchical regression modelling approach.

The fieldwork at Ryggmossen was conducted less than a year after the beginning of the author's studies, and the experimental design was therefore developed even earlier than this. As a result of the author's own inexperience, combined with a lack of confidence and flexibility in the field, meant that the resultant data structure contained a number of limitations. While the limitations described above necessarily limit the use of the empirical data in this chapter, the exercise nonetheless provided a very useful learning experience. A full discussion of the learning outcomes from this chapter, including the measures the author would take in future were the work to be repeated, is given in section **4.4.**, below.

4.2.3. Core extraction and preparation

A 60 cm long cylindrical steel corer (diameter 10 cm), supplied by N. Malmer, was used to extract the peat cores. The corer is open at both ends and has large, curved saw teeth at the bottom end. A split along the cylinder's side allows it to be opened in order to clean it between extractions and to remove samples. A handle bar can be inserted through two openings in the top end of the corer and another handle which curves over the top of the corer also acts as a clamp to hold the cylinder together during use (see Figure 4.2). Any tough, fibrous surface vegetation that may have become entrained in the corer's teeth and damaged the sample was carefully cut away before the corer was slowly and carefully

worked into the peat. So as to reduce compression of the sample as far as possible, the corer was worked into the peat just a few cm at a time before fibrous material at the cutting edge was weakened by snipping into it with kitchen scissors. Then the corer was worked in a little further and the scissors used again, and so on, until a sufficiently deep core had been cut. Some compression of samples was unavoidable, however, and compression was measured once the corer had been fully inserted by using a ruler to measure the difference in elevation between the peat surfaces inside and outside of the corer. Compression caused by the coring process was no greater than 5 cm in any sample. Before cores could be extracted, a long, serrated kitchen knife was used to cut away a section of the surrounding peat, leaving the corer and the core within standing unmoved and upright in a shallow pit. This allowed the corer and its contents to be lifted out of the bog more easily and reduced the risk of damage to the core. Once a core had been extracted from the bog, the corer was opened by removing its clamp and the sample transferred immediately into a section of PVC pipe, before being wrapped in thick PVC sheeting and sealed with waterproof tape ready for transport to the laboratory. The cores will have suffered inevitable damage during the insertion of the corer, extraction from the ground, transferral to the plastic drainage pipes, and transit. The extent of such damage and its effect upon measurements of hydraulic conductivity are difficult to assess, although the loose, poorly decomposed peat from hollow locations is likely more susceptible to compression, disaggregation and other damage than is the firmer peat from hummocks, and this should be kept in mind when interpreting results.

Before any laboratory analyses could be performed, the Ryggmossen cores had to be removed from the sealed plastic pipes in which they were transported from the field. Like the corer, the pipes have a split along their side which allows them to be prised open when inserting or removing a sample, again in order to reduce the amount of damage suffered by the samples.

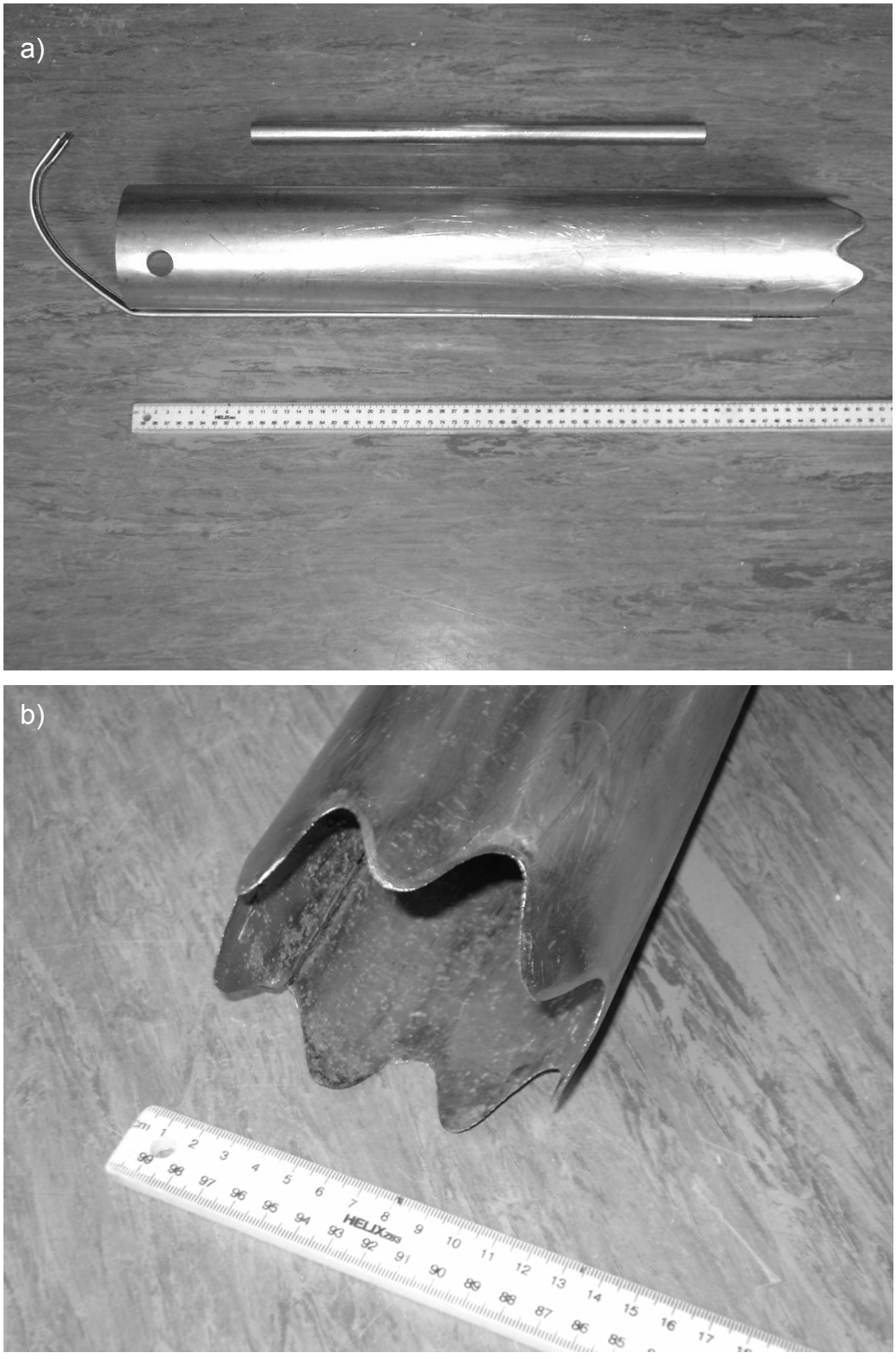

Figure 4.2: photographs showing Lund corer used for extraction of samples at Ryggmossen: (a) profile view; and (b) detail of the cutting edge.

Each core was cut up into depth intervals of 6 cm and trimmed into cubes with dimensions of 6 cm × 6 cm × 6 cm. A very sharp, non-serrated knife was used to cut the samples so as not to snag or entrain any fibrous material which might have damaged the sample and biased the results by creating preferential pathways for flow. Each cube was then analysed for hydraulic conductivity and for proportional mass loss due to decomposition (see sections *4.2.4. and 4.2.5.*, below, for descriptions of these methods). Although an effort was made to cut cores at regular depth intervals of 6 cm, any obvious changes in colour, texture or other indicators of decay along the core were used as natural boundaries for subsamples. Given that research objective (i) (see section *4.1.4.*, above) concerns the form of any relationships between cumulative peat decay and hydraulic conductivity, it would have made little sense to have included, knowingly, different levels of decay within a single cube. The depth interval z (dimensions of L) of each sample relative to the top of the live capitula was recorded in all cases.

4.2.4. Measuring peat hydraulic conductivity

The modified cube method (MCM) of Beckwith *et al.* (2003a) was used to measure horizontal hydraulic conductivity, K_h, of each cuboid subsample. Vertical hydraulic conductivity, K_v, was not measured, because **DigiBog** only takes account of horizontal flux (see Chapter 2). After cutting, the outer surfaces of each cuboid were first gently dabbed dry with paper tissue in order to remove excess water before the cuboid was sealed by repeatedly dipping its sides into molten paraffin wax. The reason for dabbing the outer surfaces dry was to remove any continuous film of water that may otherwise have become trapped between the peat and the inside of the wax casing, thereby creating a void that may have acted as a preferential flow pathway during hydraulic conductivity tests. The wax casing was built up to approximately 5 mm on all sides of the cubes so as to create an effective seal.

After coating with wax, each cube was placed into a wooden mould. Molten wax was then poured into the mould, forming a high collar of wax around one side of the sample. When the wax had cooled, the samples were removed from the moulds and the wax carefully removed from the two opposing faces surrounded by the collars. The cubes were orientated

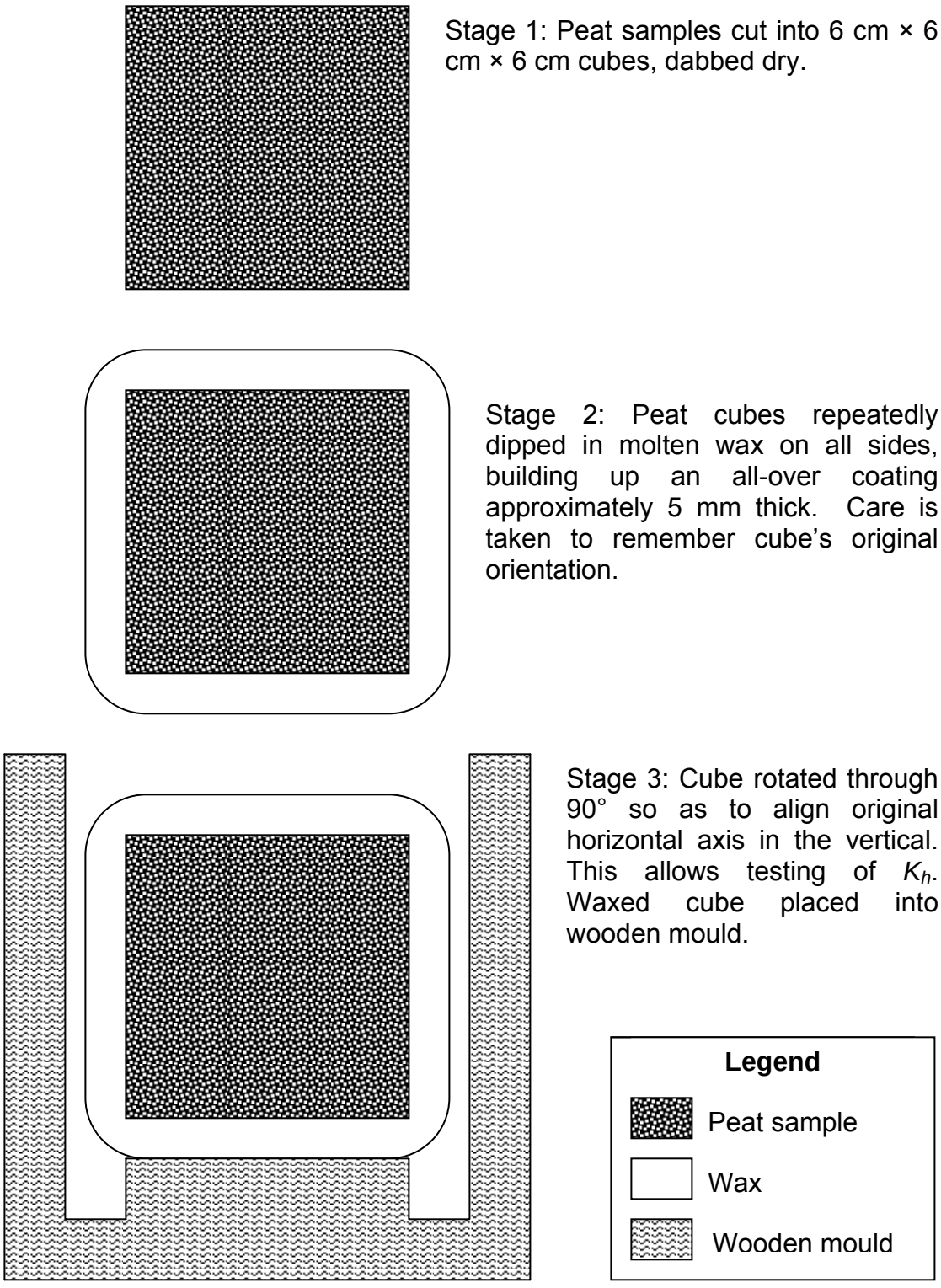

Figure 4.3: Cross-sectional diagram illustrating stages of creation of wax casing around peat cubes in order to perform constant-head tests of hydraulic conductivity using modified cube method (continued overleaf).

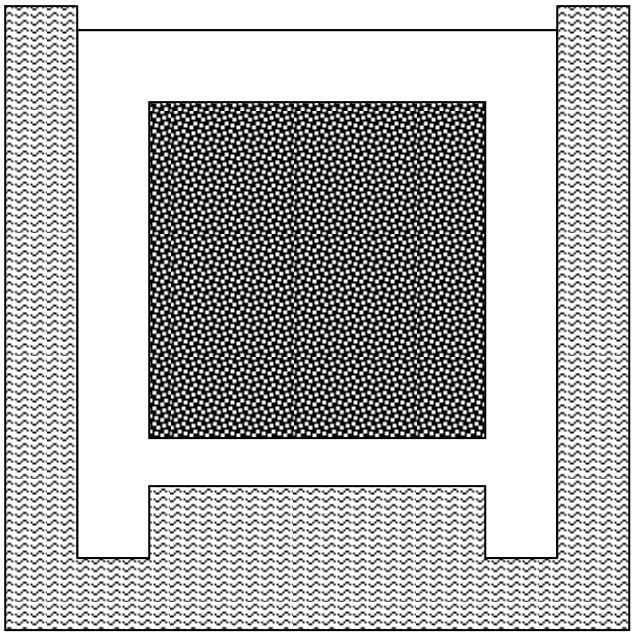

Stage 4: Mould filled with molten wax, forming collars around two opposing ends of the cube, one of which is particularly high. Wax left to cool, but sample and its casing are removed from mould before having fully cooled, so that wax is still slightly soft, thereby reducing risk of breaking the casing or collars.

Stage 5: Cube removed from mould and rotated through 180° so that highest collar is at top of sample. Opposing thin faces of wax carefully removed with sharp knife, again preferably while wax is still warm, so as to expose peat faces surrounded by the two collars. Sample is now ready for MCM testing of K_h.

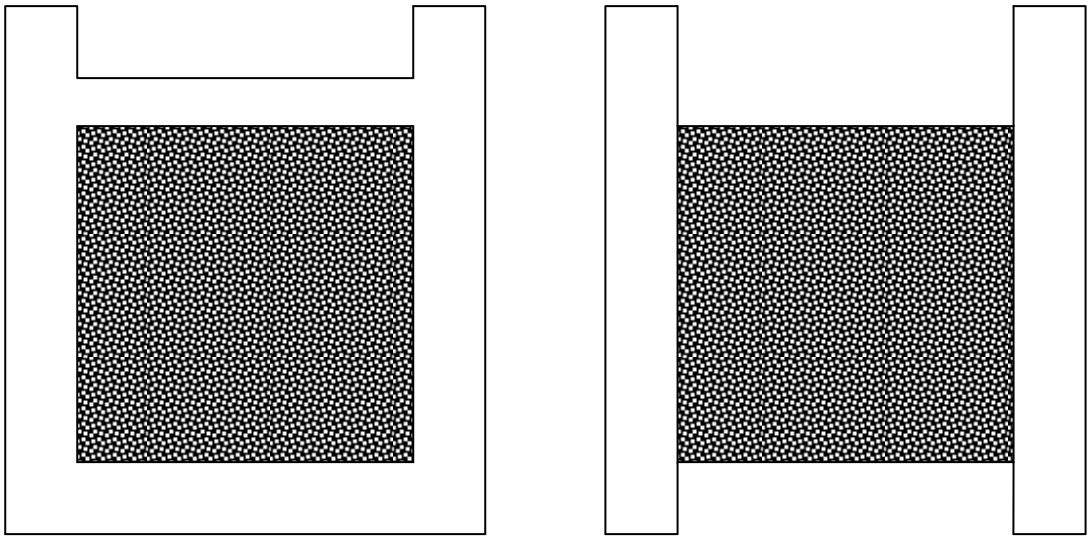

Figure 4.3: Cross-sectional diagram illustrating stages of creation of wax casing around peat cubes in order to perform constant-head tests of hydraulic conductivity using modified cube method (continued from previous page).

such that the highest collar was at the top. See Figure 4.3 for full explanation of the preparation of samples for the MCM. Next the cubes were wetted up in deep baths of deionised water for 24 hours in order to give as near to saturated conditions as possible. After wetting, the samples were placed onto permeable mesh supports in shallow baths, with an overflow pipe near the bottom of the peat sample. Maintenance of a constant and steep (approximately equal to unity in most cases) head gradient through the peat sample was facilitated by ensuring that the upper collar was kept full of water, causing flow through the sample, into the bath and out through the overflow pipe (see Figure 4.4). Once steady-state flow had been achieved, K_h was estimated using the constant-head method (see, for instance, Khan, 2005, p. 47):

$$K_h = \frac{Q}{A} \cdot \frac{\Delta h}{\Delta x} \tag{4.2}$$

where K_h is estimated horizontal hydraulic conductivity (L T^{-1}), Q is the steady-state rate of flow through the sample (L^3 T^{-1}), A is the cross-sectional area of the peat sample through which flow occurs (L^2), Δh is the head difference across the sample (L), and Δx is the length of the sample in the along-flow direction (L).

For each cube, five measurements of K_h were taken. While Beckwith *et al*. (2003a) demonstrated for their samples that K measurements using the MCM are repeatable for a given cube and are not sensitive to any potential unclogging of pores caused by repeated flushing from repeated measurements, the measurements taken here appeared to exhibit a trend in which values increased through time. In all cases, the first repetition of K was used because it was for this test that any effects due to: i) the dilution of peat porewater with distilled water, possibly leading to a change in fluidity (*cf*. Ours *et al*., 2007); and ii) flushing of pores due to unrealistically large hydraulic gradients, thereby dislodging large particulate matter (*cf*. Beckwith *et al*., 2003a, b), would be least.

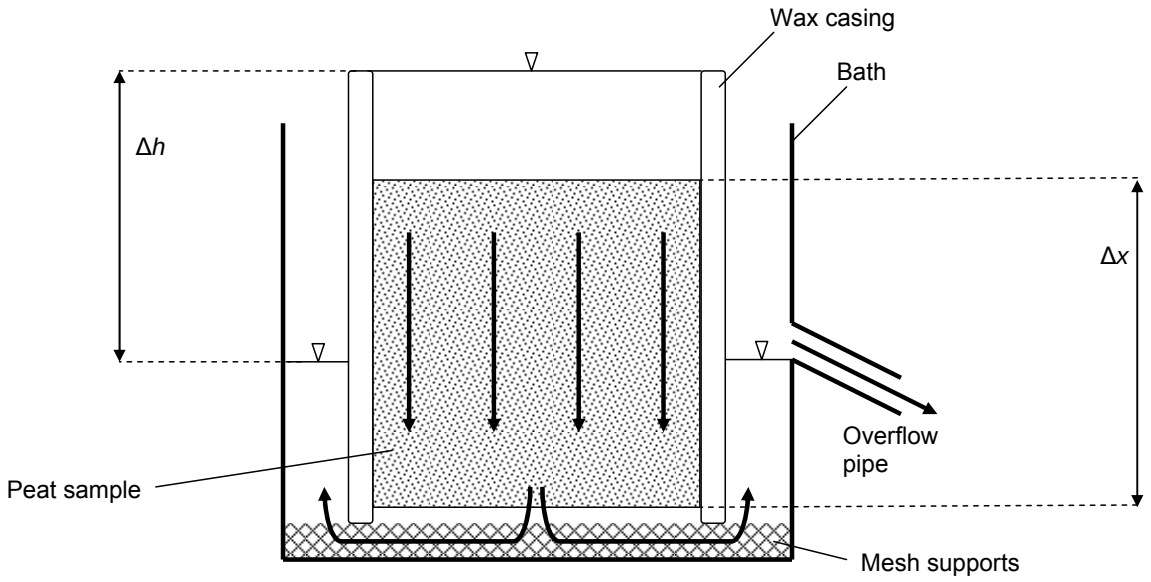

Figure 4.4: Cross-sectional diagram illustrating experimental setup for modified cube method (constant-head variant) to test hydraulic conductivity of peat soils. Thick arrows denote general directions of water flow, thin arrows indicate lengths.

4.2.5. Estimating decay losses

Johnson *et al*. (1990) devised a simple but labour-intensive method for estimating the proportional mass lost via microbial decay from a sample of *Sphagnum* peat. The full details of the method are not reproduced here, but it requires the measurement of the cumulative length of all *Sphagnum* stems within a known volume of peat. Measurement of peat dry bulk density facilitates a compensation for compaction, thereby theoretically allowing the estimation of cumulative mass loss as long as *Sphagnum* stems can be identified (preferably to species level) and measured. The method of Johnson *et al*. (1990), henceforth referred to as the 'stem-length method', had originally been chosen as the most suitable one by which to estimate proportional mass loss for the current study. After approximately one third of all measurements had been completed, however, it had become apparent that the method was not yielding meaningful results, and estimates of mass loss varied drastically and seemingly randomly between successive depth intervals. The failure of the stem-length method in this instance is attributed to a combination of: i) highly variable contents of non-*Sphagnum* species, which introduce an error to measurements; ii) my own poor species-identification skills; and iii) the inherent unsuitability of the method –

recognised by Johnson *et al*. (1990) themselves – for highly-decomposed peat. While the stem-length method is surely a useful one when plant remains are poorly decomposed and therefore reasonably intact, it becomes increasingly difficult to apply accurately further down a profile. Thinning, broken stems and branches and an inability to identify species confound attempts to apply the method accurately in highly decayed peat. Thus, the stem-length method was abandoned and results are not presented here. An alternative method for estimating decay losses was sought.

Both Belyea and Warner (1996) and Malmer and Holm (1984) used an alternative method to estimate cumulative decay, by taking the ratio of concentrations of total carbon to nitrogen (C:N) per unit mass to suggest a value for proportional mass loss. The method assumes that nitrogen mass is conserved and that carbon mass is lost down-core, via microbial respiration, as peat decays aerobically (leading to CO_2 production) and anaerobically (leading to CH_4 production). Given the assumption that nitrogen is conserved, the C to N concentration ratio should decrease with peat age and could be reasonably expected to be closely associated with the proportion of original mass remaining in a decaying sample.

There are, however, a number of arguments against the assumption of conservative N. In particular, nitrogen is assimilated by vascular plant roots and is consumed by denitrifying bacteria in the top few dm of the peat column (Malmer and Holm, 1984). Despite these flaws, the assumption of conservative N was nonetheless adopted. If the assumption of conservative N were to be relaxed then an alternative model for the down-core behaviour of N would be required. In the absence of such a model to suggest otherwise, the assumption of conservative N was adopted, albeit in the knowledge that this approach may lead to biased estimates of proportional remaining mass. In particular, C:N ratios from samples deeper in the peat profile, which may have experienced substantial losses of N, are likely to overestimate the true proportion of remaining mass, a fact which must be borne in mind when interpreting results.

In order to measure C to N concentration ratios for the Ryggmossen samples, three 1 cm × 1 cm × 1 cm subsamples were cut from each depth interval and were tested for C:N using a Thermo Electron soil elemental analyser. In order to avoid any contamination bias from the paraffin wax, the subsamples tested for C:N were taken from the offcuts of peat that were removed in order to form the cubes for K_h analysis (see section *4.2.2.*, above). All cubes were oven dried at 105 °C for 24 hours, in keeping with the protocol prescribed by Givelet *et al*. (2004), before being ground and homogenised in an automated mechanical mill. A test subsample was used to examine the sensitivity of C:N measurements from the elemental analyser to the weight of sample tested. The high C to N concentration ratios in bog peat, typically in the range of 50 to 150, meant that too low a sample weight may have led to a failure of the instrument to detect any nitrogen at all. Conversely, too great a sample weight may have prevented the instrument from being able to distinguish between carbon and nitrogen. Sample weights for this preliminary test ranged from 2 mg to 15 mg. Results suggested that a sample weight of 5 mg was sufficient to allow accurate measurement of nitrogen concentration, so all subsequent C:N measurements reported in this Chapter were made from 5 mg of dried, ground, homogenised peat material.

Proportional mass remaining *m* (*i.e.*, that portion of a peat sample which has not been lost via decay) was calculated for all samples in the following manner. For each core, the ratio of carbon to nitrogen concentration was calculated for fresh (live) material at the top of the core. Based on the assumption that nitrogen was conserved down-core, *m* was calculated for each depth interval as the quotient of C:N ratio at that depth over C:N ratio for the surface of that core. For cores in which peat botanical composition exhibited dramatic downcore variation, the C:N ratio method is likely to introduce errors to estimates of *m*. That is, if the live vegetation layer in a core is dominated by *Sphagnum*, for example, but deeper layers are dominated by *Eriophorum* remains, then the C:N method assumes that typical C:N ratios for fresh *Sphagnum* are indistinguishable from those for fresh *Eriophorum*, an assumption which seems highly unlikely given the inherent biochemical differences between species, let alone genera (Rice, 2000). This issue might have been resolved by taking account of the proportional contribution of each species to each sample. Rather than comparing the C:N ratio for each depth interval to the surface C:N ratio, *m*

would be calculated for each species present in a sample as a ratio of its C:N ratio to that representative of fresh material of the same species. The final value of *m* for each depth interval would then be calculated as the mean of all its constituent, species-specific *m* values, weighted by the proportional mass contribution of each species. Early attempts to implement this scheme were confounded, however, by the same problems of species identification which hampered efforts with the stem length method, with plant remains in poorly decomposed samples being almost impossible to identify with any confidence. Therefore, it was assumed for the purpose of the current work that peat botanical composition was uniform with depth within each core, and *m* was calculated simply as the C:N ratio for that sample divided by the C:N ratio of fresh material at the top of the core, with no attempt made to differentiate between species.

For one of the cores with the (*upslope*, *hollow*) treatment, an error test was conducted in order to assess the reliability of the C:N method. Seven subsamples were taken from the uppermost depth interval (nominal mid-point depth of 6 cm), and another seven were taken from a sample at 18 cm depth. The C:N ratio was calculated for each subsample. The upper depth interval exhibited mean C:N ratio of 115 with a standard deviation of 19.9, while the lower depth interval exhibited a mean of 73.9 and a standard deviation of 2.27. Two sample, one-tailed t-test (assuming unequal variances) indicates that mean C:N ratio is significantly ($p = 0.001$) greater for the upper depth interval than for the lower depth interval. This result suggests that the C:N method may reasonably be expected to distinguish between old and young peat samples.

4.3. Results and Analysis

4.3.1. Summary of Results

Due to errors in laboratory procedures, data from two out of the sixteen cores were not available. Data are missing for one core with the (*hummock*, *downslope*) treatment, and another with the (*hollow*, *downslope*) treatment. For the remaining fourteen cores, both hydraulic conductivity and *m* generally declined with increasing depths within individual cores (see Figure 4.5), as would be expected. Tables 4.1 shows summary statistics for the hydraulic conductivity data, and indicates that K_h was generally higher in hummocks than hollows, an initially surprising result given the argument in section **4.1.**, above.

Table 4.1: Summary of mean K_h *measurements for factorial combinations of SL1 unit type and slope location.* N.B. *As with Table 4.2, below, this table contains data for all 14 cores for which data were available, including three data points which were deemed to be outliers (see section* 4.3.2*., below).*

	Upslope		*Downslope*	
K_h (cm s^{-1})	Mean	n	Mean	n
Hummock	0.418	16	0.526	10
Hollow	0.041	13	0.032	12

Surprisingly, and unlike the results of Malmer and Holm (1984) and Belyea and Warner (1996), the C:N data did not appear to exhibit a shallow subsurface peak, which would have represented nitrogen loss in shallow peat layers (see *m* plots in Figure 4.5). This absence of a near-surface peak may be due to the coarse spatial sampling window of 6 cm, but could also represent errors in measurements of carbon and nitrogen. Caution must therefore be adopted when interpreting results of the elemental analysis. Some cores exhibited large peaks in both *m* and K_h at around 20-30 cm from the surface, the abrupt nature of these peaks suggesting that they do not represent decreasing nitrogen content through assimilation or denitrification. Rather, they seem more likely to be indicative of operator or instrumental error, down-core changes in peat botanical composition or, in the case of K_h measurements, slumping and cracking of peat. The variability in hydraulic conductivity

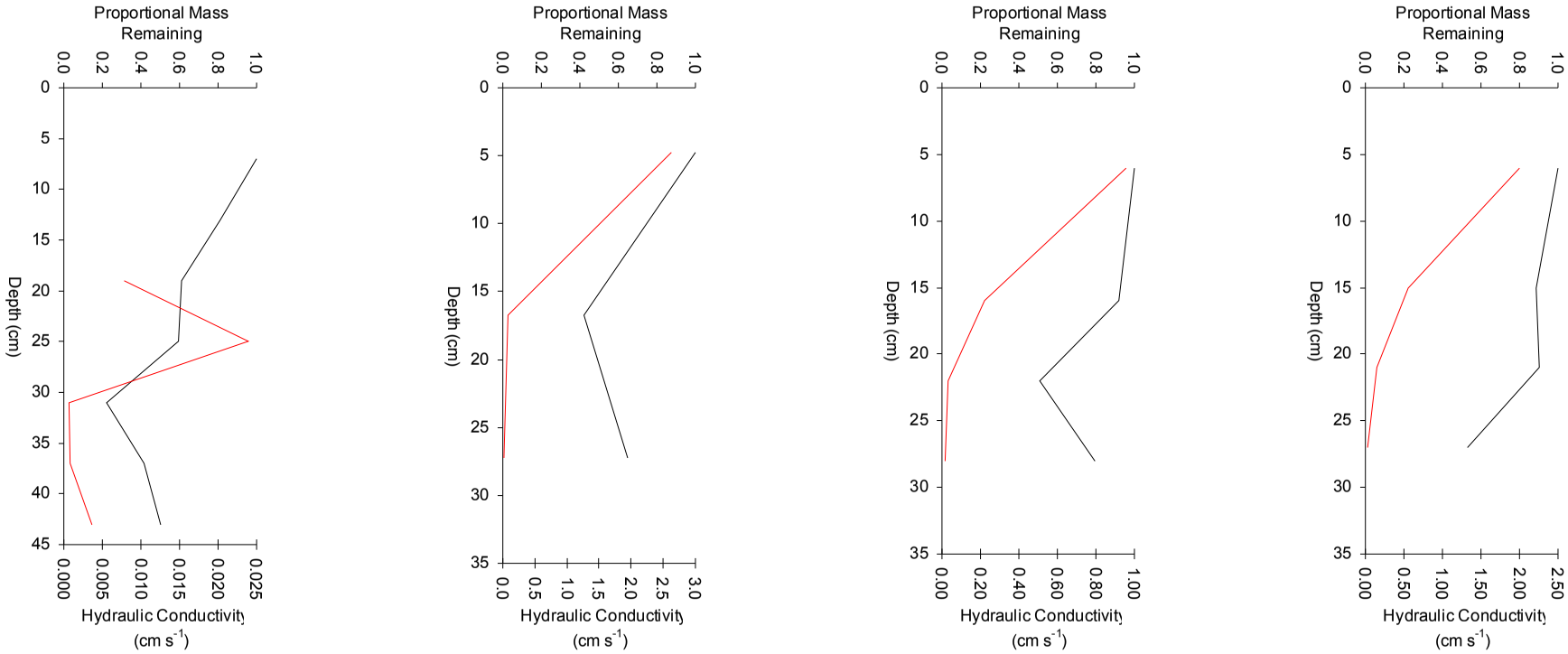

Figure 4.5a: Variation of proportional mass remaining (in black; estimated by proxy from C to N ratios) and hydraulic conductivity (in red) with depth the cores in the upslope hummock treatment. Note differences in axis scales between plots.

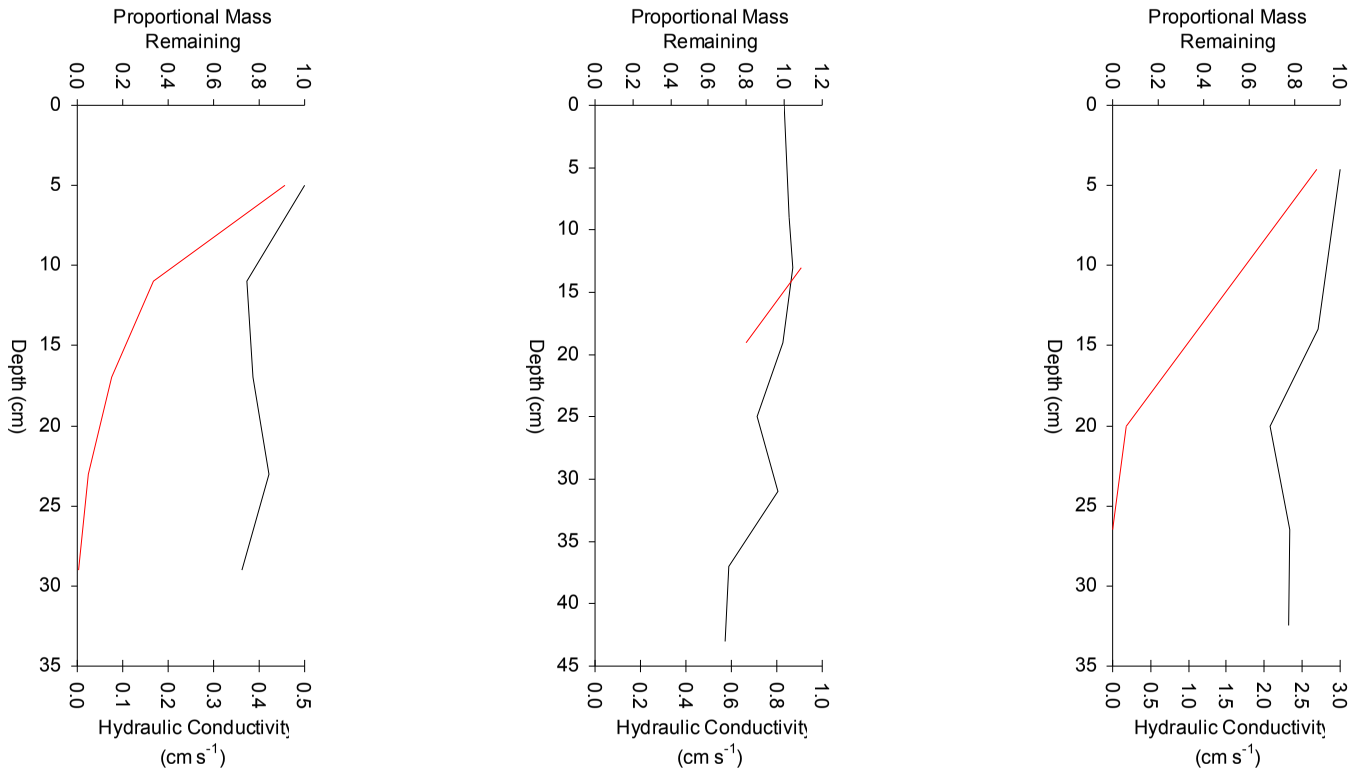

Figure 4.5b: Variation of proportional mass remaining (in black; estimated by proxy from C to N ratios) and hydraulic conductivity (in red) with depth the cores in the downslope hummock treatment. Note differences in axis scales between plots.

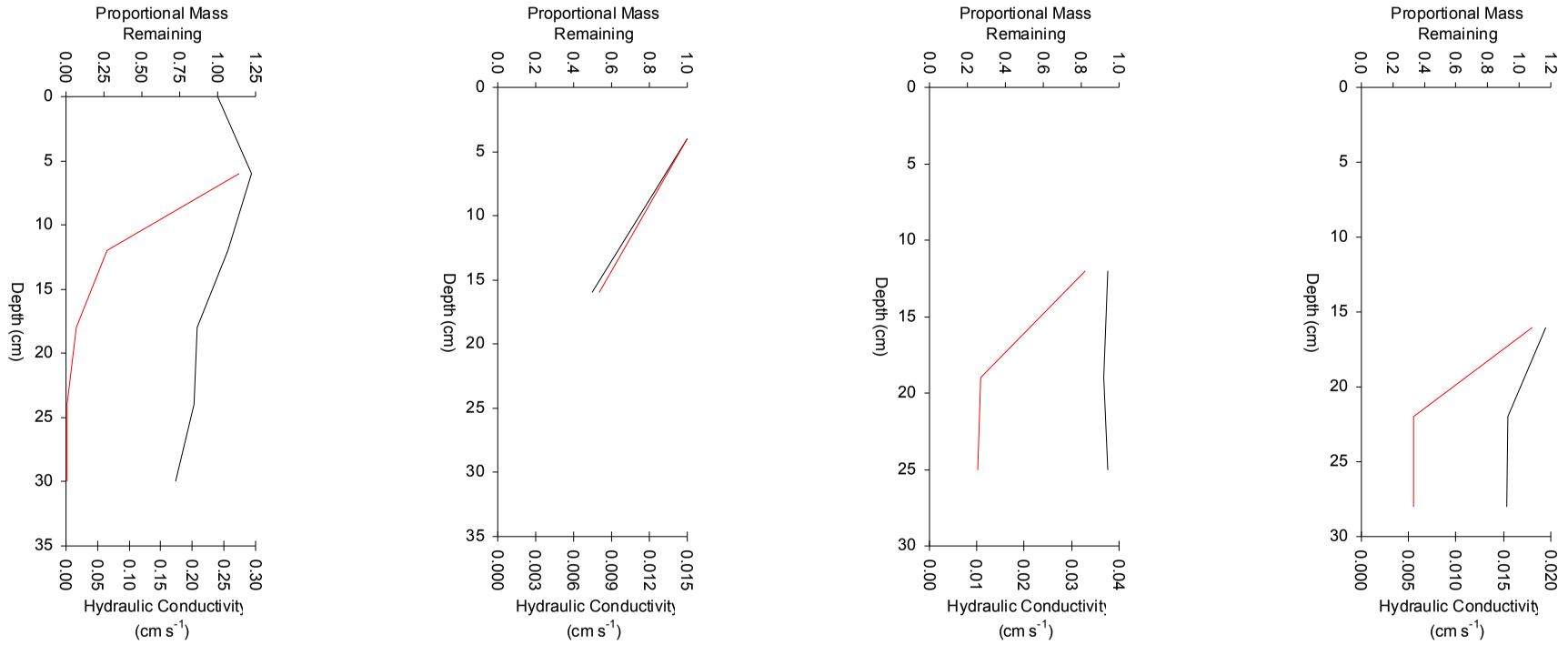

Figure 4.5c: Variation of proportional mass remaining (in black; estimated by proxy from C to N ratios) and hydraulic conductivity (in red) with depth the cores in the upslope hollow treatment. Note differences in axis scales between plots.

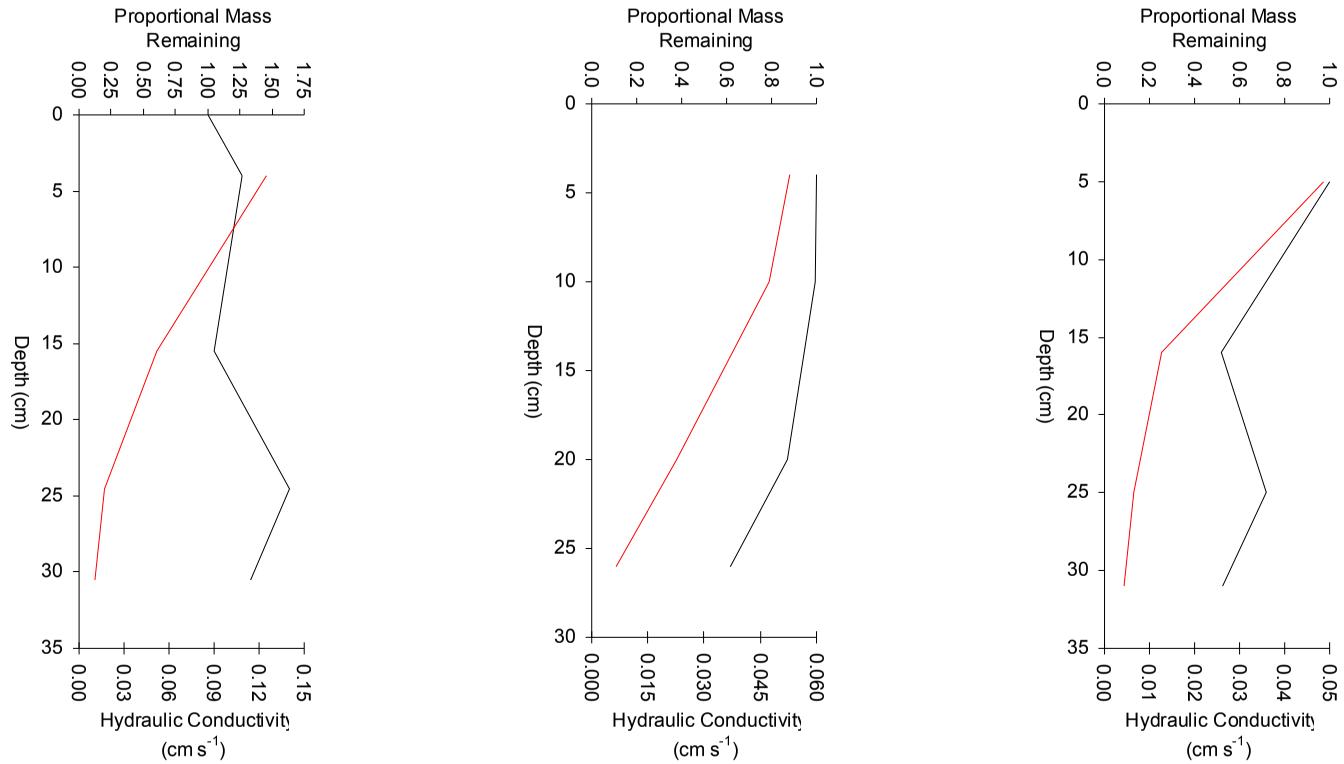

Figure 4.5d: Variation of proportional mass remaining (in black; estimated by proxy from C to N ratios) and hydraulic conductivity (in red) with depth the cores in the downslope hollow treatment. Note differences in axis scales between plots.

may be due in part to compression and slumping of samples during extraction, transport, storage and analysis.

For two cores, no surface C:N data were available, so *m* for those cores was calculated using the average surface C:N ratio for other cores with the same treatment of SL1 type and slope position. Concerns that differences in calculation of *m* between cores may have led to biases in the data set appear to be unfounded. The statistical analyses described in section *4.3.2.*, below, were performed both including and excluding the two cores in question, and no qualitative differences were apparent between the statistical models generated (*i.e.*, the inclusion of data from the two cores in question did not cause otherwise significant variables to become non-significant, and *vice versa*). As such, the data from the two cores in question are confidently included in the analyses described in the rest of the current chapter. The *m* data are summarised in Table 4.2, below, and in Figure 4.5. Hollow samples exhibited higher mean values of *m* than did hummocks, reflecting the fact that hummocks possess much thicker oxic and periodically-oxic zones, causing a greater loss of mass before peat is 'captured' by the anoxic zone.

Table 4.2: Summary of mean m *measurements for factorial combinations of SL1 unit type and slope location.* N.B. *As with Table 4.1, above, this table contains data for all 14 cores for which data were available, including three data points which were deemed to be outliers (see section* 4.3.2*., below).*

	Upslope		*Downslope*	
m (-)	Mean	n	Mean	n
Hummock	0.709	18	0.854	17
Hollow	0.925	13	0.962	12

4.3.2. Derivation of a functional relationship for use in ***DigiBog***

The fact that both *m* and K_h were measured quantities means that, for the purposes of regression analysis, both the dependent and independent variables are subject to error, thereby violating one of the fundamental assumptions of standard linear regression modelling. As such, Type I regression was not appropriate for the prediction of K_h as a

function of *m*; an alternative approach was required so as to allow for errors in the independent variable (*m*). Furthermore, and as described in section *4.2.2.*, above, the Ryggmossen dataset contains dependencies at a number of levels. Such dependency between data points required a hierarchical regression modelling approach in order to establish a predictive relationship. This task was outsourced to a professional statistical consultant, Islay Gemmell of Remstat Consultants, Manchester, who conducted all statistical analysis described below, including the development of the regression models. Random-effects models were used to analyse the data in order to establish the controls on K_h. Random effects modelling allows the estimation of the effect of each variable (SL1 type, slope position, depth and m) upon K_h, whilst taking into account the fact that the data are clustered within cores, but without explicitly estimating the effects of core. For an introduction to multi-level regression modelling such as this, see Austin *et al*. (2001) and Gelman (2005).

The fourteen cores which yielded usable data provided a total of 51 data points, although three of these were identified as outliers because of K_h values greater than 2.0 cm s^{-1}. The constant-head version of the modified cube method becomes increasingly unreliable for very high K_h values such as 2 cm s^{-1}. In order to maintain a constant elevation head acting upon the test sample, water had to be poured manually from a container into the top of the sample's collar. With the extremely rapid drainage occurring through the highly permeable surface samples, it was almost impossible to be sure that a constant head had been maintained, or that the sample remained entirely saturated throughout the test period. These problems with experimental procedure seem likely to lead to conservative errors in estimation of *K* for highly-permeable samples, suggesting that they should not have been identified as outliers. However, Equation 4.2, above, assumes that the only force motivating flow is a hydrostatic head gradient and that no dynamic forces are involved. This assumption seems unlikely to hold, however, for the samples with the highest *K*, for which distilled water had to be poured manually from a bucket onto the top of the sample in order to keep the headspace in the wax collar full of water, which in turn was intended to maintain a constant hydraulic gradient. The force of the water falling from the bucket will

have added momentum to the flow through the sample, causing a possible overestimation of K. A summary of the model, excluding the three outliers, is shown in Table 4.3, below.

The random-effects model indicates that K_h is significantly associated with SL1 type and depth of sample but not with slope position or m (the latter is marginal, with a p-value of 0.069). Hydraulic conductivity is significantly lower in hollows compared to hummocks and is significantly negatively correlated with the depth of the sample.

Table 4.3: Summary of Random effects model (see text below Equation 4.3 for explanation of variable names):

Variable	*Coefficient*	*Standard Error*	*Z*	*p*
constant	0.220	0.145	1.51	0.130
habitat	-0.275	0.085	-3.22	0.001
position	0.041	0.085	0.49	0.625
depth	-0.008	0.003	-2.96	0.003
m	0.232	0.128	1.82	0.069

The model provided the following regression equation to describe K_h:

$$K_h = 0.22 - 0.275habitat - 0.041position - 0.008depth + 0.232m \qquad (4.3)$$

where *habitat* is a binary variable representing the SL1 unit type from under which the sample was taken (a value of 0 represents a hummock, 1 represents hollow); *position* is another binary variable, representing the location on the bog from which the sample was taken (value of 0 represents upslope location, 1 represents downslope); and *depth* is the mid-point depth of the sample, relative to the bog surface, in cm. The model predicts values of K_h between -0.1522 and 0.461 cm s^{-1} for the Ryggmossen dataset.

The surprising result of no significant association of K_h with m prompted further investigation of the dataset. A new random effects model was generated, excluding depth

as a variable. The new model is summarised in Equation 4.4 and Table 4.4, and suggests that, if depth is not considered, *K* is significantly associated with *m*.

$$K_h = -0.085 - 0.277 habitat + 0.036 position + 0.407 m \quad (4.4)$$

Table 4.4: Summary of random effects model which excludes depth.

Parameter	Coefficient	Standard Error	Z	P
constant	-0.085	0.109	-0.78	0.434
habitat	-0.277	0.088	-3.14	0.002
position	0.036	0.087	0.41	0.683
m	0.407	0.123	3.30	0.001

Finally, a further regression analysis was performed on all data points together, and indicated that *m* and depth covaried highly significantly ($p < 0.001$) with one another, as described by Equation 4.5:

$$m = 1.048 - 0.012 depth \quad (4.5)$$

This apparently close association of *m* with depth is not surprising, and reflects the fact that deeper peat is older and generally more highly decomposed than shallow peat. Clearly then, *m* is closely associated with K_h, significantly so when depth is not considered. However, K_h exhibited a stronger association with depth, when included, than with *m*.

4.4. Discussion and Conclusions

The findings presented in section **4.3.**, above, contained two initially surprising results. The first was that K_h was not significantly associated with m (even though the p value of 0.069 represents marginal significance) when depth is also used as an explanatory variable. However, some light is shed on this situation by the fact that K_h and m were both very strongly associated with depth. The data seem to reflect the facts that deeper peat is: i) generally older and more highly decomposed than shallow peat; and ii) more highly compressed by the weight of overlying layers, causing low hydraulic conductivity at depth. These two findings, in isolation, are reconcilable with the literature synthesis in section **4.1.**, and an obvious corollary is that K_h is likely to be strongly associated with m. For this particular dataset from Ryggmossen, however, depth appears to exhibit a stronger control over K_h than does m.

The second surprise was that hummocks exhibited higher mean K_h values than did hollows, a finding which again disagreed with the arguments developed in section **4.1.** and with existing empirical evidence (e.g. Ivanov, 1981). According to Equations 4.3 and 4.4, above, hydraulic conductivity was highly significantly associated with SL1 unit type (represented by the variable *habitat*), as predicted in section **4.1.**, above. However, the direction of this relationship was the opposite of that expected. This finding is easily explained by a consideration of contrasting microtopography between hummocks and hollows. The shallow nature of the cores recovered from Ryggmossen (no core was deeper than 50 cm) means that the majority of hummock peat sampled is from the oxic zone. In this area, stems and branches are very poorly decomposed and are almost completely structurally intact, resulting in very highly permeable peat. However, the water table rarely, if ever, rises into the upper layers of hummocks, meaning that the high K_h values there are likely never to be utilised for saturated flow. Below the zone of collapse, hummock peat has commonly been shown to be very highly compressed and poorly permeable (Clymo and Hayward, 1982; Hayward and Clymo, 1982; Ivanov, 1981). A lack of flexibility in the method used to extract cores as well as the author's own inexperience in the field meant that the samples from hummock locations were not as deep as they needed to be in order to enable a more direct comparison with hollow samples. The fact that most

hummock peat sampled was from the unsaturated zone necessarily means that that peat is not subject to saturated flow, making the measurement of its saturated hydraulic conductivity of slightly less relevance than that of hollow samples. An examination of saturated peat from contiguous depths between hummocks and hollows would likely have shown hummock peat to possess low K_h values than hollows. Furthermore, hollow samples are particularly likely to have suffered compression and slumping, offering further partial explanation for low K_h measurements from hollow samples. If the work here were to be repeated, the author would ensure that deeper samples were taken, particularly from hummocks, so as to ensure that saturated peat was being examined.

Position on the bog, with respect to proximity to the margin, did not exhibit a significant association with hydraulic conductivity, and no trend is apparent in mean values of either K_h or m between upslope and downslope locations. If bogs such as Ryggmossen do indeed possess marginal areas of low K, such as suggested by Baird *et al*. (2008), then this is likely to be due largely to differences in proportional coverage of SL1 types. That is, in the marginal zone of drawdown where water tables are likely to be deeper than in the centre of a bog dome, conditions are likely to be favourable to the development of hummocks rather than hollows. This certainly appears to be the case at Ryggmossen, where the flanks of the bog are dominated by hummocks which, as discussed earlier in this section, seem likely to lay down peat of low hydraulic conductivity in the saturated zone. The sampling strategy used here meant that proportional coverage of hummocks and hollows was not taken account of, and equal proportions of both SL1 types were sampled in both upslope and downslope locations. As such, the results do not reflect any differences in K between upslope and downslope locations which are attributable to plant community composition gradients. However, the approach allowed the isolation of the parameter *position*, which does not appear to exert its own, independent control over K.

There are a number of problems associated with the elemental analysis method used to estimate m, which may have contributed to the poor data quality and the surprising nature of some of the findings. The method relies on the assumption that nitrogen is conserved downcore, although studies by Belyea and Warner (1996) and Malmer and Holm (1984)

have shown that this is not necessarily a valid assumption at shallow depths in peat soils. In the absence of an alternative model to describe the downcore behaviour of nitrogen, the assumption of conservative N allowed for the hypothesised relationship between *m* and *K* to be examined, although the findings here should be treated as a first approximation. Sweden is situated downwind of major industrial atmospheric pollution sources in the UK, has been subject to acid precipitation through much of the 20th and early 21st centuries (*cf.* van Dam, 1988; Gorham *et al*., 1984). Nitrogen deposition via acid precipitation may also have had an effect upon the measured C to N ratios in this study, and may have biased estimates of *m* for shallow layers.

The study succeeded in part in its aim of developing a first approximation of the relationship between the state of cumulative decay of peat and hydraulic conductivity. The evidence presented here does not suggest that hydraulic conductivity may reasonably be described as anything other than a linear function of depth and/or *m* in models of peat accumulation, although a number of limitations in the dataset appear to inhibit the general application of Equations 4.3 and 4.4 to this purpose. The data presented here represent only a single raised bog site and certainly should not be taken as necessarily being representative of peatlands in general. The applicability of Equations 4.3 and 4.4 for use in **DigiBog** is further limited by: i) the shallow extent of samples, and the failure to take account of deep peat; ii) compression and slumping of cores, particularly those from hollows, which may have introduced a bias into results for those samples; and iii) high apparent errors in C:N measurements and the failure of the method to detect a shallow subsurface peak in the C to N ratio. The latter may be partly attributable to the coarse depth resolution of samples necessitated by the modified cube method used for *K* measurements, and partly due to the failure to take account of changes in peat botanical composition with depth. Evidence from the literature is strongly suggestive that *K* may reasonably be predicted as a curvilinear function of depth and/or *m*, even though the current work did not support this notion. Studies such as those by Ivanov (1981), Rycroft *et al*. (1975), and Boelter (1969) all found hydraulic conductivity to decrease exponentially with estimates of increasing peat cumulative decomposition or humification. Those authors used the von Post scale to estimate cumulative decomposition, which does not necessarily possess a linear association

with cumulative decomposition, making it difficult to assess how reliable those estimates of the relationship between cumulative decomposition and hydraulic conductivity really are. As such, there is an argument for using either a linear or curvilinear relationship to describe K as a function of m in the modelling work in Chapters 5 and 6.

The limitations of the current work may be used to suggest obvious targets for future work on the topic. The first of these would be to extend the work into deeper peat. No cores were deeper than 50 cm, meaning that all data presented in this chapter represent relatively fresh peat. This fact may also have contributed to the surprising finding of lower K in hollows than in hummocks. Most measurements of K_h in hummocks were from fresh, very well-preserved peat, probably from well above the average water-table position by virtue of the raised relief of *S. fuscum* hummocks. As such, most of the high K measurements are likely to be unrepresentative of the deeper, well decomposed peat through which the majority of saturated flux occurs. If, as Clymo (1992) suggested, compaction occurs over a relatively small depth interval, it seems logical that cumulative decay would exhibit an s-shaped relationship with K_h. It may be, then, that the results presented in this chapter represent only the beginning of a step-like or s-shaped relationship. Deeper studies would likely shed more light on this situation.

Secondly, the techniques adopted here for the extraction and storage of cores may also have had an undesirable effect upon results. In order to reduce any damage to samples in future studies, cores could be taken from high-latitude sites during winter, when the structurally-weakest, near-surface peat is frozen. While this would make core extraction more difficult, samples would be much less prone to collapse. Samples could be maintained at sub-zero temperatures during transport to the laboratory and storage, and could even be cut and prepared for K_h measurements while frozen, using powered tools. Once encased in wax, samples would be allowed to thaw before being fully wetted.

Thirdly, the estimation of m proved highly challenging in this study and deficiencies in the method used appear to have been the primary factor which confounded attempts to develop a predictive relationship between m and K_h. This suggests that future efforts should be

directed towards developing a more reliable method to estimate *m*. Proportional mass loss could be estimated using tomographic methods such as those currently being employed by Nick Ketteridge and Andrew Binley at Lancaster University, UK (*cf.* Kettridge and Binley, 2008). Stem lengths could potentially be measured using a tomographic scanner and appropriately trained software, thereby eradicating observer error associated with the manual stem-length method. This work is currently only at a concept stage, although enough of the samples from Sweden have been conserved for it to be trialled in future. Another exciting possibility for future work in this area would be to adopt the approach of Turetsky *et al*. (2008), who examined the ratio of metabolic to structural carbohydrates in a range of moss types, and the change in this ratio during the course of decay. Very generally, metabolic carbohydrates present decomposers with a more labile source of carbon than do structural carbohydrates, and are removed from peat litter more quickly. Therefore, the ratio of metabolic to structural carbohydrates in a peat sample might be used as an indicator of its state of decay.

Despite its limitations, the current work represents, to the author's knowledge, the first attempt to assess the form of the relationship between a continuous, quantitative measure of peat cumulative decomposition and hydraulic conductivity using reliable methodological protocols (*cf*. Surridge *et al*., 2005). The prediction of a linear relationship, at least in shallow peat layers, is an interesting one which disagrees with most of the existing literature, although it remains to be seen whether this prediction is a result of using a continuous estimate of *m* (as opposed to the categorical von Post scale as used by previous authors), or whether the samples analysed here show a near-linear portion of what is in fact a curvilinear relationship.

Chapter 5: Modelling Peat Accumulation in One Dimension

In this chapter, a literature synthesis is used, in combination with the findings from Chapter 4, to argue for a new approach to modelling peat accumulation. This new approach allows for self-organisation of key components within the conceptual peatland system. The algorithmic architecture of **DigiBog** is then used to build a simple, 1-dimensional (vertical) model of peat accumulation in raised bogs, similar to existing models. This simple model is then expanded using the self-organisation approach. Unlike previous models of peat accumulation, the new model, **DigiBog_EcoHydro2** (DBEH2), constitutes a CAS treatment by allowing peat accumulation rates, peat properties, and bog hydrology to self-organise in a realistic manner, informed by empirical work from various sources. The Fortran 95 code for DBEH2 can be found as two separate text files on the supplementary CD.

5.1. Introduction

5.1.1. Background

As discussed in Chapter 1, peatlands represent highly concentrated and potentially fragile terrestrial stores of organic carbon. Improved understanding of the production of peatland plant litter (*i.e.*, the formation of new peat) and peat decomposition will lead to more accurate estimates of the size of the global peat store and the amounts of labile carbon contained therein. Modelling the response of peat accumulating systems to climatic influences will also provide a clearer picture of how stable peat deposits are likely to be under a changing climate, particularly in the temperate and boreal zones of the northern hemisphere, where the largest peat deposits are situated and where the greatest changes in climate are expected. Although heavily cited in the peatland science literature, the best available estimates of the extent of the global peat store and its likely response to changing climate, such as those of Gorham (1990) and Turunen *et al*. (2002), are subject to large errors, which those authors recognised. Available empirical data are sparse and, in the case of much of the former Soviet Union, often unreliable (although see Smith *et al.*, 2004). As a result, the best available estimates of the size of the world's peat deposits and their likely response to changing climates (Moore *et al*. 1998) are based on extrapolations using simple and somewhat basic models and tentative estimates of parameters such as peat types, depth, extent, and accumulation rates.

Most existing models predict the 1-dimensional (vertical) accumulation of peat in idealised circumstances. One of the earliest and most widely-cited, the BGM by Clymo (1984, 1992; see Chapter 1 of this thesis), was intended for use in interpreting age-depth relationships in peat cores for the purposes of environmental reconstruction. The original version of the BGM (Clymo, 1984) predicts that peatlands approach an equilibrium state in terms of peat mass per unit area and, if constant peat bulk density is assumed, in terms of the thickness of the peat deposit generated by long-term accumulation; the equilibrium state results from an assumed constant rate of addition of peat to the anoxic zone being balanced by a constant rate of loss of peat via decay from the anoxic zone. In other words, as model time advances, peat mass per unit area ($M\ L^{-2}$) predicted by the BGM approaches an asymptotic limit, given by the ratio of the production of fresh peat ($M\ L^{-2}\ T^{-1}$) to anoxic specific decay

rate (T^{-1}). In a later version of the BGM, Clymo (1992) allowed for a reduction in the decomposability of ageing peat due to the increasing proportion of recalcitrant compounds (*cf.* Ågren and Bosatta, 1996). This assumption of decreasing peat decomposability caused the revised BGM to predict bogs which continued to grow indefinitely. Of the greatest relevance to the current argument, Clymo (1984, 1992) assumed a constant rate of passage of peat from the oxic to anoxic zone. As discussed in Chapter 1 of this thesis, Belyea and Baird (2006) showed that a steady-state oxic zone with constant water-table depth and decay rate is not a reasonable assumption for a growing bog and that, as a consequence, the BGM contains a number of logical inconsistencies. Belyea and Malmer (2004) noted at their study site in Sweden that a changing water-table position with respect to the bog surface had led to temporally-variable net rates of peat accumulation (where net accumulation may be defined as the addition of fresh plant litter minus decay losses of all peat), and dismissed models which assume a constant rate of peat addition as oversimplified.

The Peat Accumulation Model (PAM) developed by Frolking *et al*. (2001) provides an expansion upon the BGM by considering two litter types, representing vascular and non-vascular plants, as well as above- and below-ground litter addition. Vascular plants are assumed to deliver oxygen and fresh litter below ground, within the rooting zone. Furthermore, the PAM accounts for the decomposability of peat, representing increasing recalcitrance with age. Frolking *et al*. (2001) also accounted for groundwater nutrient status in order to model peatlands of a range of different trophic states, from rich fens to ombrotrophic bogs. While this scheme makes for a more detailed model of peat decomposition, both peat production and water-table depth were still assumed by Frolking *et al*. (2001) to be constants. As such, the PAM's algorithmic structure contains the same limitations as that of the BGM. A similar model by Gilmer (2001), called PORTACH, represents the passage of peat material from the oxic to anoxic zone on the basis of peat bulk density, a scheme which Gilmer (2001) claimed represented the structural collapse of peat. Nonetheless, PORTRACH does not feature a genuine hydrological submodel to distinguish the oxic/anoxic divide, and the rate of addition of new peat is assumed constant. Frolking *et al*. (2001) noted that their model is highly sensitive to the depth chosen for the

oxic-anoxic divide. A thicker oxic zone means that less peat is transferred into the anoxic zone, due to it being exposed to aerobic decay rates for a longer time. The high sensitivity to water-table position suggests that a hydrological submodel should be as realistic as possible, and provides further evidence that the assumption of a constant water-table depth is insufficient for accurate modelling of peatland development.

The rate of addition of fresh litter immediately below the live plant layer has commonly been conceptualised in peat accumulation models as a constant. As noted above, authors such as Clymo (1984, 1992), Frolking *et al*. (2001), and Gilmer (2001) assumed that a single, temporally- and spatially-invariant value of fresh litter productivity could be taken as representative of a given type of peatland. However, there is extensive empirical evidence that such an assumption is unreasonable. A strong dependency of peatland vegetation productivity upon water-table depth is commonly observed across a range of peatland and SL1 unit types (for example: Rydin and McDonald, 1985; Riutta *et al*., 2007b). In particular, Belyea and Clymo (2001) observed a humpback relationship between water-table depth and vegetation productivity at an ombrotrophic bog in south-western Scotland, with a maximum productivity of approximately 9.0×10^{-2} g cm^{-2} yr^{-1} occurring at an 'optimum' water-table depth of 30 cm. Furthermore, under controlled laboratory conditions, Robröek *et al.* (2007a) found the direction and strength of the relationship between water-table levels and *Sphagnum* productivity to be species-dependent. This finding of inter-specific variation in response to water levels is not surprising given the distinct niches occupied by different *Sphagnum* species, although it may serve to add an extra level of complexity to spatially-distributed models of peat accumulation.

The Peat Decomposition Model (PDM) of Hilbert *et al*. (2000) was a refinement of the BGM and features what those authors described as a dynamic water table, which was allowed to vary in response to an assumed net rainfall rate and the hydraulic gradient between the centre and margin of the bog. The PDM's dynamic water table means that the boundary between the zones of aerobic and anaerobic decay can move in relation to the bog surface as the peatland develops. That is, the thickness of the oxic zone and the passage of

material from it to the anoxic zone are variables in time, thereby relaxing one of the logically-inconsistent assumptions of the BGM and the PAM. As peatland height increases in the model, so does the rate of drainage of groundwater. Furthermore, the PDM assumes that the rate of addition of fresh peat is described by a humpback function of water-table depth (*cf*. Belyea and Clymo, 2001). These two assumptions lead to a negative feedback between the two state variables, peat accumulation and water-table depth, and cause the model solution to converge on one of two possible stable equilibria. Depending on net rainfall rate, the PDM predicts either a thick peatland with a deep water table, or a shallower, wet peatland with water-table position close to or at the surface.

Hilbert *et al*. (2000) recognised that their model is highly sensitive to assumed rainfall rate, and that it requires arguably unreasonably high rainfall rates in order to predict substantial peat accumulation. Indeed, when net rainfall (equivalent to P - E in Equation 2.2) is assumed to be less than 20 cm yr^{-1}, the PDM fails to predict any peat accumulation at all. Hilbert *et al*. (2000) suggested that this behaviour may reflect a genuine sensitivity of real peatland systems to long-term rainfall rates, although the fact that peatlands develop in a broad range of rainfall regimes suggests that their model's mechanistic basis may be flawed, at least in part. The PDM seems to be unable to retain enough water, particularly at low rainfall rates, for peat to develop. Nonetheless, the PDM offers a partial treatment of self organisation by allowing a feedback between peat growth and peatland hydrological processes, and produces interesting and complex behaviour. As such, it certainly represents an improvement over other accumulation models in terms of their mechanistic bases. However, perhaps the most important omission from the model of Hilbert *et al.* (2000), in light of the evidence presented in Chapter 4, is that no allowance is made for a reduction in the permeability of peat with increasing depth or cumulative decay. A number of existing models of peat accumulation feature hydrological models (Hilbert *et al.*, 2000; Borren and Bleuten, 2006), but very few assume K to be anything other than a constant. Certainly, none affords a satisfactory treatment of the continuous, non-linear variation in K as a function of depth or cumulative decomposition, such as observed in Chapter 4 (*cf.* Boelter, 1969). Again, a discussion of depth or decay-dependent hydraulic conductivity as a mechanism for homeostasis in peatlands is given in Chapter 4.

To the author's knowledge, no existing simulation model of peat accumulation allows for the lateral expansion of the modelled peatland (although see Belyea and Baird, 2006). The lateral expansion of a peatland may occur via either the paludification of surrounding mineral soils or via the terrestrialisation of water bodies such as lakes, which have been colonised by peat-forming plants and gradually infilled by their detritus (Anderson *et al*., 2003). Lateral expansion may represent a key mechanism by which peatlands are able to self organise: for instance, the lateral extent of a domed peatland affects the overall hydrological gradient, a key determinant of the height of the groundwater mound (Ingram, 1982). If peatlands are liable to expand laterally during the course of their development, the result is likely to be a lowering of hydraulic gradient, thereby allowing an increase in water-table height through time. A change in water-table position would lead in turn to an alteration to surface plant communities, peat botanical composition, rates of decay and peat hydraulic properties (see Chapter 4), thereby providing a feedback between gross bog dimensions, ecological processes and peat hydrophysical properties. Therefore, the lateral expansion of peatlands may represent another important mechanism by which they are able to self organise (Belyea and Baird, 2006; Almquist-Jacobson and Foster, 1995). Allowing models of peat accumulation to include peatland lateral expansion may prove to have a profound effect upon their predictions as well as model stability, although the rulesets by which lateral expansion might be represented are not clear.

Borren and Bleuten (2006) developed a spatially-distributed model to predict the accumulation of carbon in peatlands in Western Siberia, Russia. The model uses Modflow as its hydrological submodel and simulates peat accumulation rates and mire-type transitions within a raster grid, based on water-table position. However, the model assumes a very simple conceptual structure which calls into question its reliability as a generally-applicable model of peat accumulation. Hydraulic conductivity for all but surficial layers is assumed constant, and does not take into account depth below the surface or cumulative peat decay. Furthermore, the model does not allow for the lateral expansion of the modelled bog. The use of a spatially-distributed grid for the modelling of peat accumulation would appear to have allowed for a number of interesting opportunities for

Borren and Bleuten (2006) to experiment with complex behaviour in peatland development which, given the stated aims of that paper, were overlooked. More comprehensive discussions of Borren and Bleuten's (2006) model are given in Chapters 1 and 6.

To summarise, to the current author's knowledge, no existing accumulation model allows for true self organisation in peatland developmental dynamics. Models which are highly constrained and which neglect cross-scale feedbacks are liable to make erroneous predictions and cause misinterpretation of field data; a good example is provided by the BGM and the problems associated with its assumption of constant rate of transfer from the oxic to anoxic zone. Similarly, the models which provide a partial treatment of self-organisation and complexity are either highly sensitive to allogenic influences such as rainfall rate (e.g. Frolking *et al.*, 2000) or do not feature enough algorithmic flexibility so as to be able to represent northern peatlands in general (e.g. Borren and Bleuten, 2006: see discussion in Chapter 1 of this thesis). It remains to be seen, therefore, whether a full CAS treatment of peatland developmental dynamics, including self organisation via the mechanisms discussed above, will prove to be more satisfactory.

5.1.2. Chapter aim, objectives

The aim of this chapter is to use the **`DigiBog`** model framework to construct a simple model of peat accumulation in a single spatial dimension (vertical) over millennial timescales, similar to that of previous authors, and then to improve that model so as to allow it to self organise in a realistic manner. Within this aim, four specific objectives have been developed from the literature synthesis above:

i) To explore the behaviour of the simple model under a range of realistic parameter combinations. In particular, behaviour in response to varying net rainfall rates will be investigated.

ii) To expand the simple model so as to incorporate a dynamic, empirically-informed relationship between water-table behaviour and the rate of formation of fresh peat. It is hypothesised that this mechanism of self organisation will reduce the sensitivity of the peat accumulation model to external factors such as

rainfall rate, and allow peatlands to develop under a greater range of conditions than other models suggest.

iii) To expand the model further so as to incorporate depth or decay-dependent hydraulic conductivity, as observed in Chapter 4. Again, it is hypothesised that this mechanism of self organisation will lend further stability to models of peatland development.

iv) To examine the effects upon bog development of various simple rulesets to describe lateral expansion. It is hypothesised that this mechanism of self organisation will lead to differences in long-term rates of peat accumulation compared to comparable models with a constant lateral extent, due to changes in overall hydraulic gradient.

5.2. A Simple Model of Peat Accumulation

5.2.1. Conceptual structure

In this section, a simple model of peat accumulation is developed using the **DigiBog** algorithmic architecture, in keeping with objective (i) identified in section *5.1.2.*, above, and is henceforth referred to as **DigiBog_EcoHydro2** (DBEH2). For reasons of simplicity, a bog represented in DBEH2 may be conceptualised as an infinitely long strip of peat which is hemi-elliptical in cross-section, such as that in Ingram's (1982) GMH. The model simulates peat accumulation and water-table behaviour for a single column of peat, of unit cross-sectional area, through which the central axis of the bog passes. In the simple model presented here, again as with Ingram's (1982) model, lateral expansion of the peat deposit is assumed to be constrained by parallel streams to which the bog drains. While the lateral extent of the bog (*i.e.*, the distance between the two parallel streams) is specified within the model algorithm, horizontal water movements and the profile shape of the bog are not explicitly represented, and the model is essentially one-dimensional (vertical) in nature. Such an assumption means that there is no need to complicate the hydrological model by incorporating radial divergence of flow, as would be required for a circular bog.

5.2.2. Hydrological submodel

The 1-dimensional version of DBEH2 utilises a modified and highly simplified version of **DigiBog_Hydro** (see Chapter 2) as its hydrological submodel. Water-table height H during any timestep Δt is given by:

$$H_t = H_{t-1} + \Delta t \left(\frac{U - K(H_{t-1}) \frac{H_{t-1}^2}{L_{t-1}^2}}{s} \right) \tag{5.1}$$

where U is net rainfall rate (precipitation minus evapotranspiration; L T^{-1}), K is depth-averaged hydraulic conductivity below the water table (L T^{-1}), L is the assumed lateral extent of the modelled bog, from its centre to its margin (L), and s is effective porosity (-). It should be noted that, as in Chapters 2 and 3, depth-averaged hydraulic conductivity is a

function of water-table height, thereby allowing depth-variant peat properties. However, the hydrological submodel described in Equation 5.1 features a significant difference from the model described in Chapter 2. Rather than using a derivative of Darcy's Law to calculate drainage to the bog's boundaries, Ingram's (1982) model has been adapted for use in calculating drainage losses from the 1-D version of **DigiBog**. The GMH by Ingram (1982) describes the behaviour of water-table position in the centre of a raised bog in response to drainage through an elliptical aquifer. While the Darcian solution of **DigiBog_Hydro** could have been used to represent this situation, the entire bog would have had to have been represented by a single column of peat, meaning that the calculation of hydraulic gradient and thickness of flow would have been subject to large errors. In this specific case of using **DigiBog** to represent a (hemi-elliptical) raised bog in one spatial dimension, Equation 5.1 gives a truer representation of water-table behaviour, although the solution still contains errors because Ingram's (1982) GMH was developed strictly for use in situations where K is uniform with depth. Water-table level is not allowed to fall below the base of the peat column (*i.e.*, the mineral substrate was assumed impermeable), nor was it allowed to rise above the current peat surface (representing loss of water via rapid overland flow).

5.2.3. Productivity submodel

The productivity submodel activates a new computational layer at the top of the bog at the beginning of each timestep, representing a cohort of newly-formed peat. A parameter, p, is used to represent the rate of addition of fresh litter below the live vegetation layer, and does not take into account any decay losses. Therefore, p represents the input of peat mass to the model, and has dimensions of $M\ L^{-2}\ T^{-1}$. In the simple model, p is assumed constant, such that new layers are simply assigned a peat mass equal to timestep-integrated p.

5.2.4. Decay submodel

The decay submodel adopts an approach similar to that of Hilbert *et al*. (2000). Peat mass is lost from all depths at a rate dependent upon water-table level. The peat mass m of each old layer at timestep t is given by:

$$m_t = m_{t-1}(1-(\Delta t \cdot ox_{t-1}\alpha_{ox})-(\Delta t \cdot an_{t-1}\alpha_{an})) \quad (5.2)$$

where Δt is timestep length, *ox* is the proportion of a layer which is above the water table during *t*-1 and so subject to oxic decay at the specific rate α_{ox}, and *an* is the proportion of a layer which is below the water table during *t*-1 and so subject to anoxic decay at the specific rate α_{an}.

5.2.5. Model testing

In order to ensure that the **DigiBog** solution to Equation (5.2) works correctly, it was parameterised so as to replicate the BGM of Clymo (1984). Much like the testing of the 2½-D version of the hydrological model in Chapter 2, DBEH2's solutions to three simple scenarios were compared to the exact analytical solution provided by the BGM. In its simplest form, the BGM predicts the growth of a single layer of peat, which may be taken to be the anoxic zone. The peat which constitutes the growing bog consists of a single biogeochemical component, the decomposability of which does not change with cumulative decay. This simple version of the BGM assumes a single, constant value for the rate of formation of new peat, *p*, and a single rate of specific decay in the anoxic zone, α_{an}. In this case, the temporal behaviour of the BGM is given by Equation 1.3. Furthermore, the BGM predicts an asymptotic limit to bog growth, in terms of peat mass per unit area, equal to p/α_{an} (Clymo, 1984).

DBEH2 was parameterised so as to replicate this simple version of the BGM, for which purpose the hydrological submodel was deactivated and all layers were subject to the anoxic decay rate. Timesteps of 1 year were used and the model was allowed to run for 10,000 simulated years. The model was run with three combinations of *p* and α_{an}. The first parameter set was the same as that used by Clymo (1984), with p = 0.0045 g cm^{-2} yr^{-1} and α_{an} = 0.0005 yr^{-1}, giving a limit to growth of 9 g cm^{-2}. In the second parameter set, both *p* and specific decay rate were increased by an order of magnitude from set 1, so that p = 0.045 g cm^{-2} yr^{-1} and α_{an} = 0.005 yr^{-1}. In this case, the limit to growth predicted by the BGM is still 9 g cm^{-2}, but the higher process rates meant that DBEH2's solution should converge much more quickly upon the limit. In the third parameter set, the rate of

formation of new peat was informed by Belyea and Clymo (2001), who fitted a polynomial regression function to their field data. When considering all SL1 unit types together for a bog site in south-western Scotland, their analysis predicted that a maximum productivity of 0.0864 g cm^{-2} yr^{-1} occurred at an optimum water-table depth of 30.2 cm. Thus, for the third parameter set, p = 0.0864 g cm^{-2} yr^{-1} and α_{an} was left at 0.005 yr^{-1}. For this combination, the BGM predicts a limit to growth of 17.3 g cm^{-2}.

The temporal behaviour of each of the three test simulations, in terms of both mass per unit area and bog height (assuming a constant peat density of 0.1 g cm^{-3}, like Clymo, 1984) can be seen in Figure 5.1 (a). As expected, all tests demonstrated an asymptotic approach to the predicted limits and their deviation from Equation 1.3 would be indistinguishable in Figure 5.1 (a) if the trajectories of both models had been plotted together. Figure 5.1 (b) shows the temporal development of error in **DigiBog**'s predictions, expressed as a percentage of the true value given by the BGM for each point in model time (Equation 1.3). Error decreases with time for all runs, and is initially larger for those runs with higher p and α_{an}, but decreases at a more rapid rate than for slower p and α_{an}. Error for parameter set 2 is equal to that for set 3 at all points in model time, suggesting that percentage error is controlled by α_{an}. By 774 simulated years, error for parameter sets 2 and 3 has decreased to below that of parameter set 1. Part of the error in the **DigiBog** solution for each point in time arises due to the fact that each newly-activated layer receives fresh peat mass which is not subject to decay in the first timestep, a simple numerical diffusion effect. Part of the reason for the decrease in error with time, therefore, is the fact that the mass of the newly-activated layer represents a progressively smaller proportion of the bog's total mass per unit area. However, even for old peat layers, the numerical solution employed will still deviate from the analytical solution, and the Euler integration employed means that the solution is biased towards process rates at the start of each timestep.

For parameter sets 2 and 3, there was no discernible error between **DigiBog**'s solution after 10,000 years of simulated time and the limit according to the BGM (at least according to **DigiBog**'s double-precision representation of real numbers). For parameter set 1, however, **DigiBog**'s convergence upon the limit of 9 g cm^{-2} was slower than that of

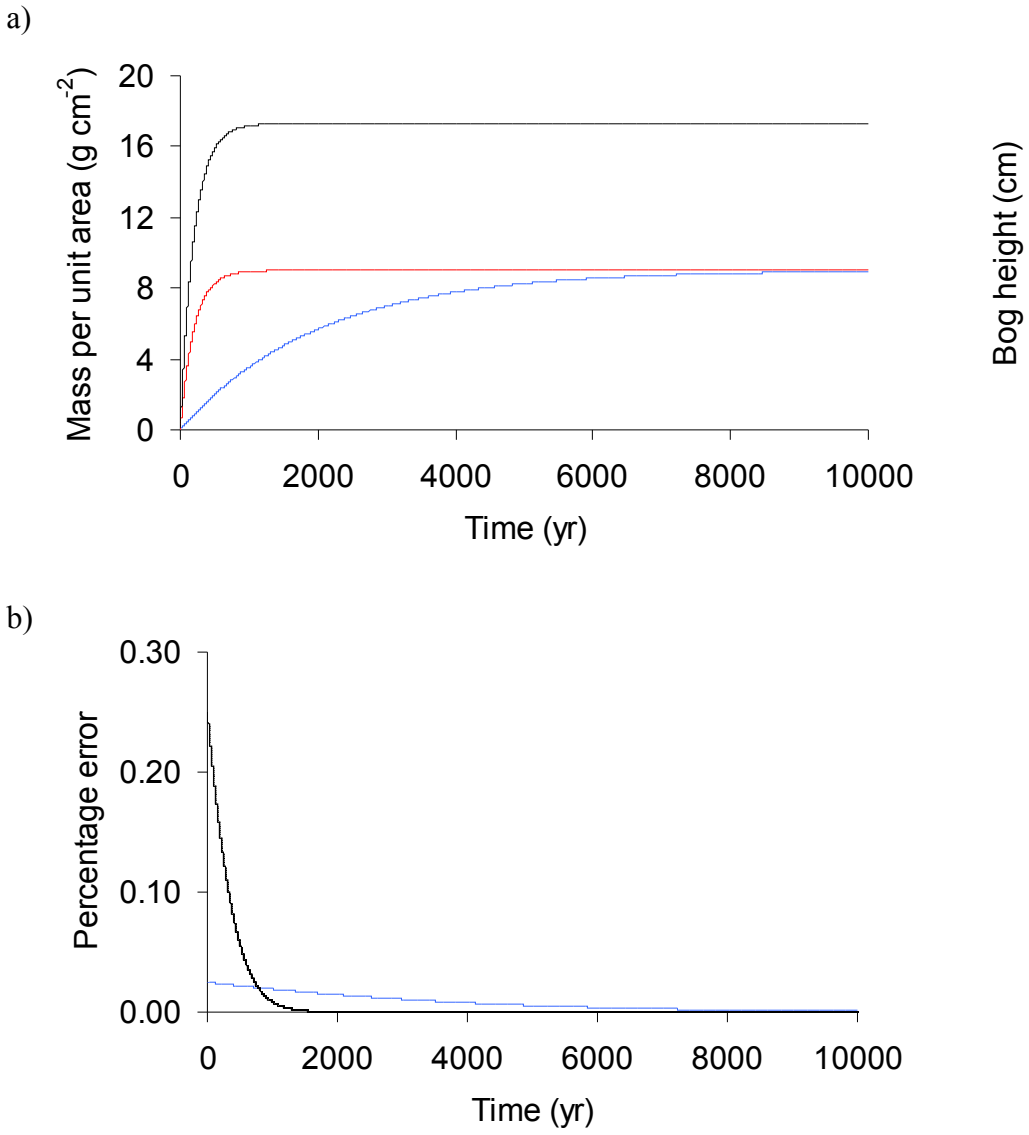

*Figure 5.1: Plot showing temporal development of a) modelled peatland mass per unit area and height for tests of DBEH2 1D; and b) percentage error relative to the BGM, calculated as 100(***DigiBog** - BGM*)/*BGM. *Blue line shows parameter set 1, red line shows parameter set 2,black line shows parameter set 3.* N.B., *in panel b), parameter sets 2 and 3 are indistinguishable from one another.*

parameter set 2 due to lower parameter values. After 10,000 simulated years the **DigiBog** solution to parameter set 1 underestimates the true limit, given by the BGM, by 0.67 % of the true limit, a small but nonetheless noteworthy error. Clearly, running the model for longer than 10,000 simulated years would give a closer approximation of the limit. While parameter sets 2 and 3 converged upon a solution very rapidly, it should be noted that even 10,000 years of simulated time may not yield steady-state behaviour when process rates are assumed to be low.

Secondly, the full version of the simple model was tested for numerical stability in response to changing timestep length. That is, the temporal development of both bog height and water-table position were both simulated (unlike the testing of the ecological model alone, described above, in which the hydrological model was deactivated) using varying timestep lengths but assuming the same parameter combination each time: U = 30 cm yr^{-1}; K = 200,000 cm yr^{-1}; L = 50,000 cm; p = 0.0864 g cm^{-2} yr^{-1}; α_{ox} = 0.015 yr^{-1}; α_{an} = 0.005. This parameter combination was repeatedly experimented with, using timesteps of 1, 10, 50 and 200 years.

The results of the testing, illustrated in Figure 5.2, indicate that timesteps of 1, 10 and even 50 years produce stable model behaviour, with both bog height and water-table height exhibiting a smooth, curved trajectory through time. Timesteps of 200 years, however, appear to exhibit unstable behaviour, evident in Figure 5.2 as oscillations, spikes or other abrupt changes in model temporal dynamics. A timestep of one year was decided upon as an appropriate and safe value. While much longer timesteps still appear to give stable behaviour, therefore suggesting that 1 year is an overly cautious choice, important short-term variability would likely be missed with timesteps as long as 50 years.

5.2.6. Demonstration of simple model

Having established that the DBEH2 productivity and decay submodels were working correctly, the hydrological submodel described in section *5.2.2.* was activated so as to demonstrate the behaviour of the simple ecohydrological model and to examine briefly its sensitivity to hydrological and ecological parameter values. The simple model may be

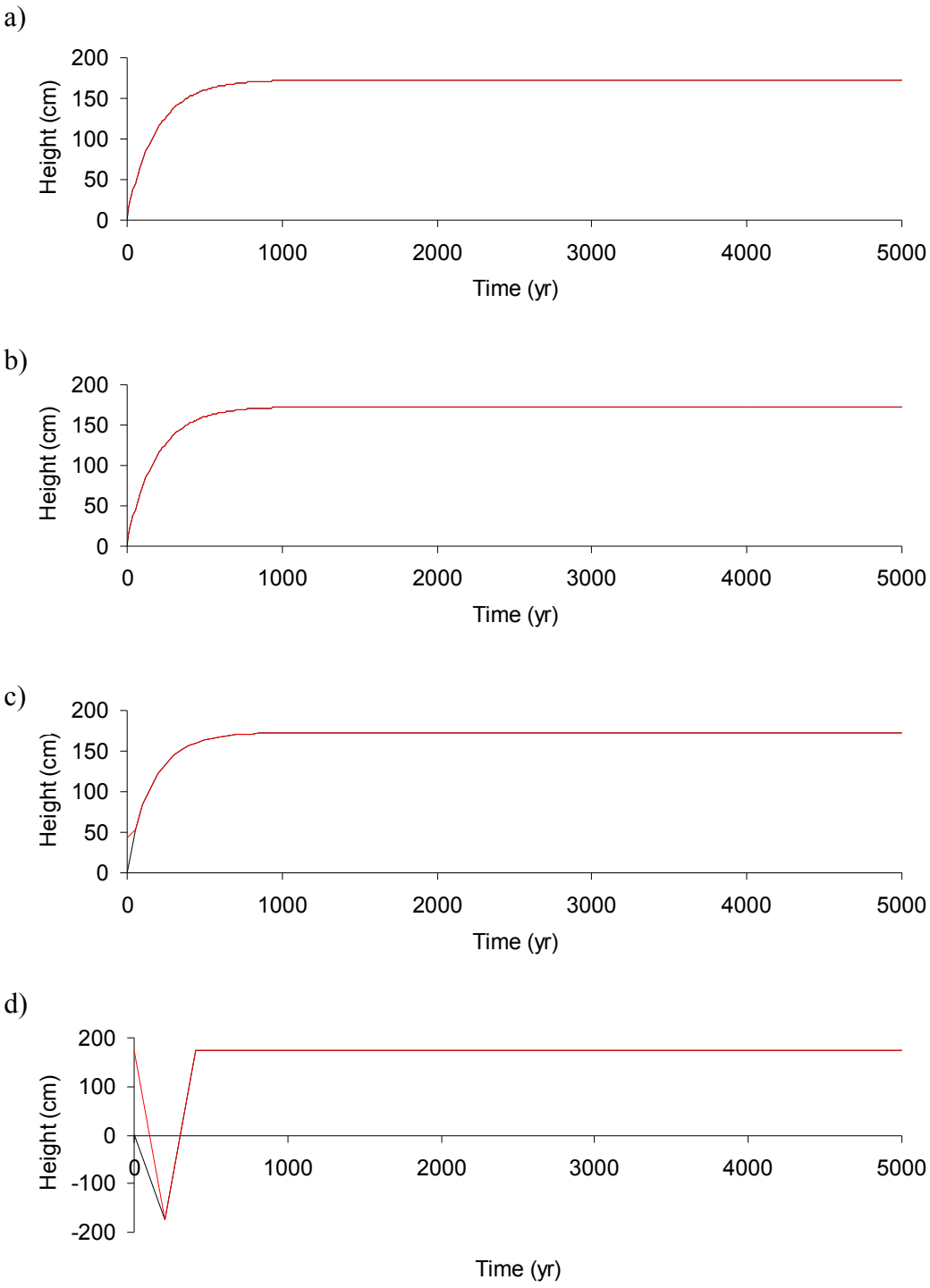

Figure 5.2: plots showing temporal behaviour of bog height (red line) and water-table height (black line) for timesteps of: a) 1 year; b) 10 years; c) 50 years; d) 200 years. See text for full description of parameter sets. Note that in panels (a) and (b), bog height and water-table height are indistinguishable from one another, indicating water tables are at the surface and the model is losing water via overland flow.

thought of as possessing a level of complexity somewhere between that of the BGM and that of the PDM. Although the model simulates a dynamic water table, hydraulic conductivity and the rate of formation of new peat are assumed constant. Two partial factorial experimental designs were used to test the model's sensitivity to net rainfall rate, the rate of formation of new peat, anoxic decay rate and the ratio between oxic and anoxic decay rates.

In the first set of simulations, the two factors experimented with were net rainfall rate (treatments of 5, 10, 15, 20, 30, 40, 50, 75, and 100 cm yr^{-1}) and the oxic specific decay rate (anoxic decay rate was maintained at 0.0001 yr^{-1} while oxic decay rate was set to values of 0.005, 0.015, or 0.05 yr^{-1}). In the second set of experiments, the two factors changed were p (Belyea and Clymo's (2001) peak value of 0.086 g cm^{-2} yr^{-1} was assumed, as well as 90 % and 75 % of this value) and anoxic decay rate (values between 0.001 and 0.00001 yr^{-1} were assumed; oxic decay rate maintained at 0.01 yr^{-1} for all runs, and U was assumed to be 30 cm yr^{-1}). In all simulations with the simple model, the following constants were assumed: K = 200,000 cm yr^{-1} (Baird *et al*., 2008); s = 0.3; lateral extent = 50,000 cm. The algorithmic structure of the hydrological submodel means that increasing the net rainfall rate has the same effect upon the groundwater mound as decreasing hydraulic conductivity or increasing lateral extent (*c.f.* Ingram, 1982). Hence, only net rainfall was manipulated. All simulations were run for 5,000 years of model time, with timesteps of 1 year. As shown in section *5.2.5.*, 5,000 years may not necessarily be enough to achieve a genuine steady state, although such a runtime is representative of a large proportion of northern peatlands (*cf.* MacDonald *et al*., 2006; Yu *et al*., 2009).

The results of the experimentation with the simple model are illustrated in Figures 5.3. The most striking result, shown in Figure 5.3 (a), is that bog height after 5,000 simulated years increases in a logarithmic manner with increasing net rainfall rate. For net rainfall rates of 5 cm yr^{-1}, bog height is between 267 and 418 cm, depending on the anoxic decay rate, increasing to between 1133 and 1269 cm for U = 100 cm yr^{-1}. High net rainfall rates allow a high groundwater mound to develop, thereby ensuring that a greater thickness of peat is 'preserved' by the low rate of decay in the anoxic zone. Bog height appears to decrease

a)

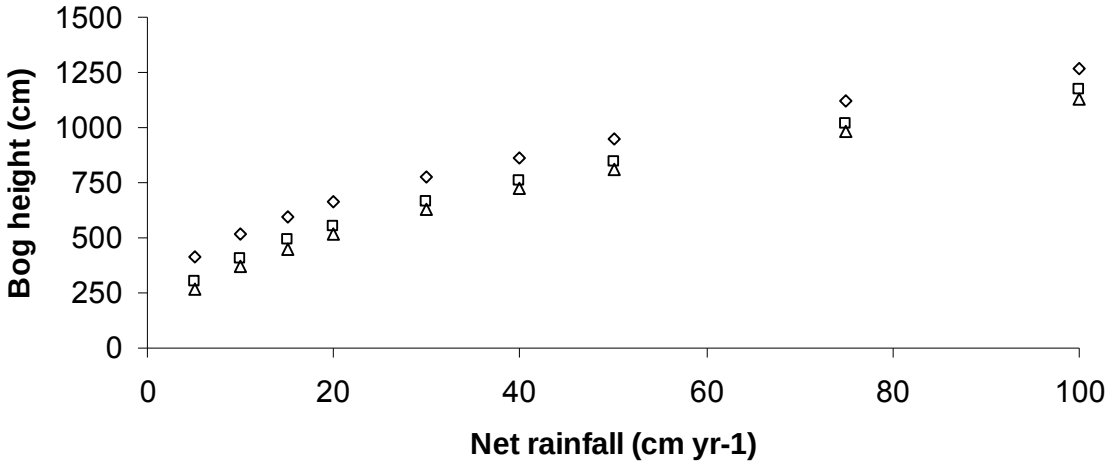

b)

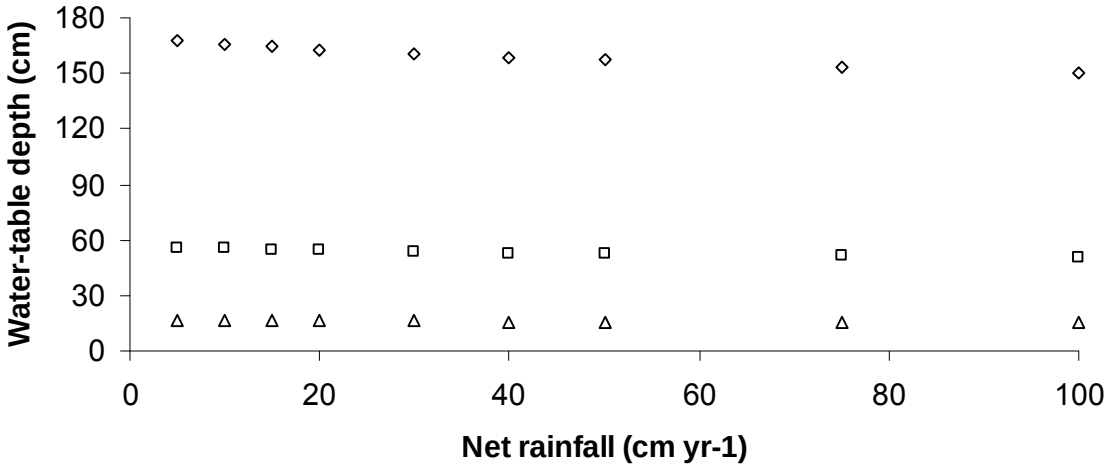

Figure 5.3 (continued on following page): plots demonstrating sensitivity of simple model to: a), b) net rainfall rate and oxic specific decay rates (◊ 0.005 yr^{-1}, □ 0.015 yr^{-1}, Δ 0.05 yr^{-1}).

strongly with increasing oxic decay rate, particularly when U is low. The difference in bog height between the lowest and highest oxic decay rates is 151 cm for net rainfall rate of 5 cm yr^{-1}, decreasing logarithmically to 135 cm difference for U = 100 cm yr^{-1}. At low rainfall rates, for which absolute bog heights are small, varying oxic decay rate causes large relative changes in final predicted bog height. At higher net rainfall rates when bog heights are greater, both the absolute and relative changes in bog height caused by varying oxic decay rate are reduced.

c)

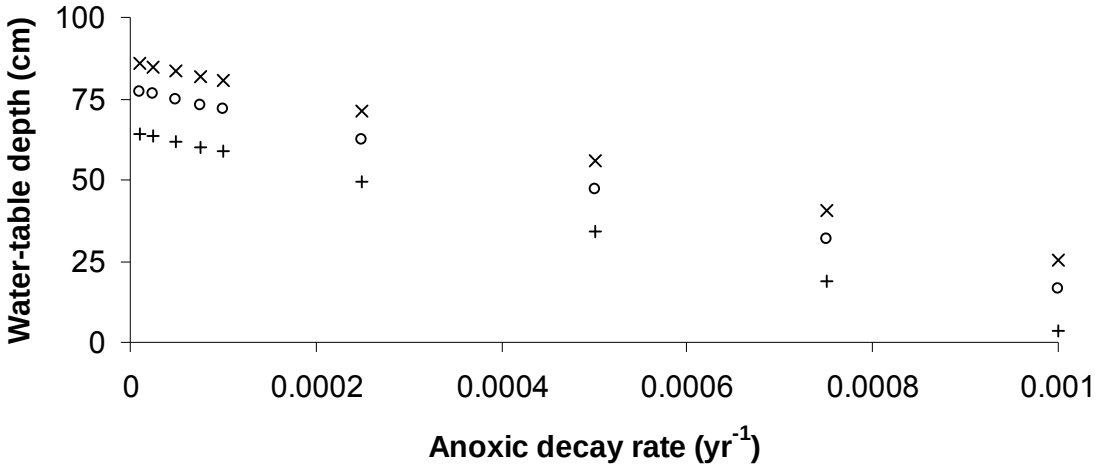

d)

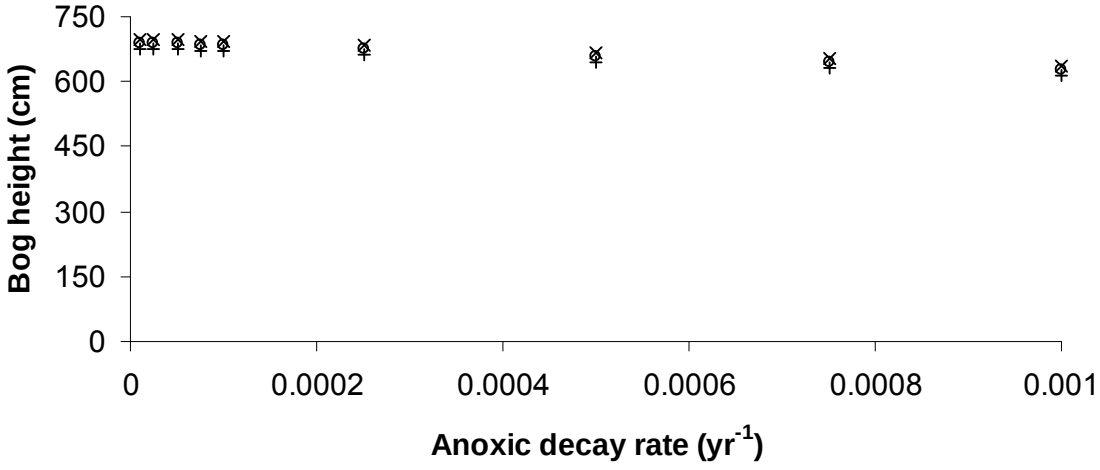

Figure 5.3 (continued from previous page): plots demonstrating sensitivity of simple model to: c) and d) anoxic specific decay rate and p *(× 0.086 g cm^{-2} yr^{-1}, ○ 0.077 g cm^{-2} yr^{-1}, + 0.065 g cm^{-2} yr^{-1}).*

Water-table depth (*i.e.*, oxic zone thickness) decreased in an approximately logarithmic manner with increasing oxic decay (see Figure 5.3 (b)), from between 151 and 168 cm when α_{ox} = 0.005 yr^{-1} to between 15.1 and 16.8 cm when α_{ox} = 0.0005 yr^{-1}, representing an order of magnitude decrease in water-table depth in response to an order of magnitude increase in α_{ox}. Water-table depth appears to increase linearly with increasing p (Figure 5.3 (c)). That is, for any given value of anoxic specific decay rate, reductions in p of 10 % or 25 % relative to the highest assumed value of p = 0.086 g cm yr^{-1} causes water-table depth

to decrease by the same percentage. By contrast, water-table depth exhibited little variation, relative or absolute, in response to changing rainfall rates, suggesting that, all other things being equal, the thickness of the oxic zone is controlled almost entirely by the simple ratio of p to α_{ox}, as observed by Clymo (1984) in his consideration of an isolated oxic zone. However, Figure 5.3 (c) also indicates that water-table depth decreases linearly with increasing anoxic decay rate, from between 64.2 and 85.8 cm when α_{an} = 0.00001 yr^{-1} to between 3.59 and 25.2 cm when α_{an} = 0.001 yr^{-1}. This initially surprising result is explained by the fact that, as long as the water table remains below the bog surface (*i.e.*, as long as water-table depth is strictly positive, as is the case for all runs with the simple model), water-table height is determined entirely by net rainfall rate, at least when K and bog shape are held constant. Therefore, as bog height decreases with increasing anoxic decay rate (see Figure 5.3 (d)), so the height of the bog is reduced and brought closer to the water table, thereby reducing water-table depth.

Surprisingly, bog height generally appeared to be insensitive to anoxic specific decay rate or p, at least within the range of values assumed here (see Figure 5.3d), probably reflecting the fact that because anoxic decay rates are so low, the majority of peat is preserved once it is submerged by the water table, regardless of the rate at which litter is produced at the bog surface. As such, net rainfall rate exerts much stronger control over the long-term rate of peat accumulation than do α_{an} or p; U indirectly determines the thickness of the oxic zone, and therefore how much peat is transferred into the anoxic zone. Rainfall rate therefore exhibits a strong control over model behaviour, but in a somewhat unrealistic manner. In real bogs, it is unlikely that water-table height would be invariant in response to changing decay rates, because increased varying rates of peat decay would in turn affect changes in hydraulic properties and so rates of drainage (see Chapter 4).

It should be remembered that if the anoxic decay rate is to act upon any substantial depth of peat, then saturated conditions are required such that water tables are close to the bog surface. A negative relationship between hydraulic conductivity and either depth or cumulative decomposition, such as that observed in Chapter 4 and advocated in section **5.1.**, above, might serve to maintain higher water tables. As such, it is hypothesised that

the inclusion of this kind of decay-dependent hydraulic conductivity will lead to greater model sensitivity to anoxic decay rate. The fact that bog height was generally not sensitive to p reflects the fact that, for most parameter combinations, the thickness of the oxic zone represents only a small proportion of total bog height. While s was assumed a constant, sensitivity of water-table position and bog height to net rainfall rate would likely increase with decreasing effective porosity, because alterations to UL^2/K would cause greater variation in water-table position.

When interpreting the predictions of the simple model, it should be noted that some points in model parameter space do not represent realistic manifestations of peatlands, but are just artefacts of an arguably simplistic model algorithm. In particular, it is difficult to imagine what kind of peatlands are represented by the runs with low rainfall rates and low oxic decay rates, where predicted water-table depth may be more than 150 cm below the surface (see Figure 5.3 (b)). In such situations, highly-adapted peatland plants such as *Sphagnum* would almost certainly be out-competed and succeeded by other vegetation, which would in turn have caused further drying of any peat deposit (van Breemen, 1995). As with other models such as the PDM of Hilbert *et al*. (2000), the predictions of the simple model presented here were largely dictated by net rainfall rate or, more correctly, the quotient UL^2/K (*cf.* Ingram, 1982).

5.3. Simulating Water-Table-Dependent Peat Formation

In line with objective (ii) identified in section *5.1.2.*, the simple model described in **5.2.** was altered such that the rate of addition of fresh peat, *p*, was predicted on the basis of water-table depth. Whilst simulating a dynamic water table and variable *p*, **DigiBog** still assumed constant values of hydraulic conductivity and lateral peatland extent. As such, this new model may be thought of as possessing an intermediate level of complexity. The intermediate model is very similar in terms of conceptual structure to the PDM, and so findings were expected to be qualitatively similar to those of Hilbert *et al*. (2000). While those authors assumed a simple and seemingly arbitrarily chosen quadratic equation to predict production of peat as a function of water-table depth, it was deemed desirable by the current author to inform model behaviour using the most appropriate available empirical data. Belyea and Clymo (2001) observed a humpback relationship between oxic zone thickness (which may be taken to be equivalent to water-table depth) and productivity of both above-ground plant tissue and root material. Part of their analysis involved fitting the following fourth-order polynomial function to their data:

$$p = 0.0001\left(9.3 + 1.33d - 0.022d^2\right)^2 \tag{5.3}$$

where p is the rate of formation of new peat material (g cm^{-2} yr^{-1}) and d is water-table depth (cm). The productivity submodel described in section *5.2.3.* was altered so as to solve Equation 5.3 for p during each timestep, and the relationship is illustrated in Figure 5.4. There is a key difference between the description of productivity assumed by Hilbert *et al*. (2000) and that given in Equation 5.3. In the PDM, addition of new peat becomes zero when water-table depth is either too deep or too shallow. In the intermediate version of DBEH2, however, Equation 5.3 predicts a non-zero value of p when water-table depth is zero. Some peatland plants such *S. cuspidatum* occupy a very wet niche and are able to photosynthesise even when water-tables are at or marginally above the peatland surface (Robröek, *et al*., 2007b), a fact reflected in the empirical data of Belyea and Clymo (2001).

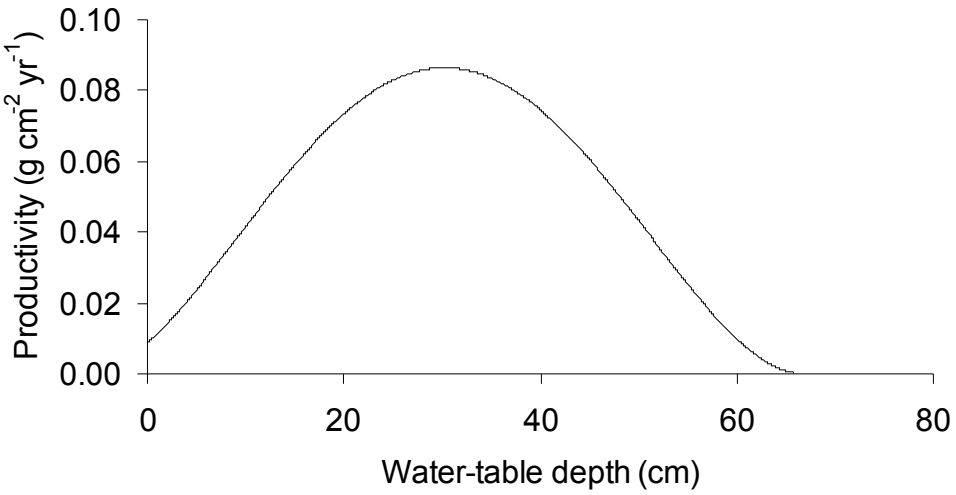

Figure 5.4: plot illustrating function used to predict p *as a function of water-table depth. Adapted from Belyea and Clymo (2001).*

Model behaviour was analysed using an experimental design that was intended to be as similar as possible to the one used for the simple model (see section *5.2.6.*, above). Two sets of experiments were again performed, the first using a factorial combination of net rainfall rates (treatments of U = 5, 10, 15, 20, 30, 40, 50, 75, and 100 cm yr^{-1}) and oxic decay rates (treatments of α_{ox} = 0.005, 0.015, and 0.05 yr^{-1}). Where the model demonstrated threshold behaviour, additional simulations were run with rainfall rates other than those listed above, chosen in a post-hoc manner, to examine more closely those areas of parameter space which give rise to interesting behaviour. The fact that the intermediate model predicts p as a function of water-table depth meant that one less parameter value must be defined, and so the second set of experiments was necessarily reduced from that performed with the simple model. Anoxic decay rate α_{an} was manipulated in isolation (a range of rates between 0.001 and 0.00001 yr^{-1} was assumed) while other parameters were maintained as follows: U = 30 cm yr^{-1}; α_{ox} = 0.015 yr^{-1}. Finally, the following constants were assumed for all runs with the intermediate model, identical to those used for the simple model: L = 50,000 cm; *runtime* = 5,000 yr; K = 200,000 cm yr^{-1}; s = 0.3.

Results of the experimentation with the intermediate model generally agreed with the findings of Hilbert *et al*. (2000). The representation of water-table depth-dependent p

caused **DigiBog** to be sensitive to net rainfall rate, predicting one of two possible peatland forms depending on net rainfall rate: either a shallow, wet peatland with water tables at the surface, or a thick, drier peatland, with water tables approximately 40 to 50 cm below the surface. As illustrated in Figure 5.5, model behaviour demonstrated interesting and complex behaviour; the state variables bog height and water-table depth bifurcate and anastomose within parameter space. Interestingly, model behaviour was both quantitatively and qualitatively different from that of the simple model. Figure 5.5 (a) shows that, as net rainfall increases up to approximately 9 cm yr^{-1}, bog height increases approximately linearly, to a maximum height of between 328 and 382 cm (substantially lower than for the same rainfall rate in the simple model – see Figure 5.3, above). However, a threshold appears to exist at around U = 9 cm yr^{-1}, and for rainfall rates above this, bog height either drops abruptly to between 337 and 348 cm (for α_{ox} = 0.005 and 0.015 yr^{-1}) or levels off at approximately 328 cm (for α_{ox} = 0.05 yr^{-1}). Bog height appears to be invariant in response to further increases in U above this apparent threshold. This is in sharp contrast to the predictions of the simple model, which predicts that bog height would continue to increase logarithmically with increasing net rainfall for all assumed values of U. Indeed, the simple model predicts bog heights of between 1133 and 1268 cm when U = 100 cm yr^{-1}, equivalent to between 3 and 4 times higher than for the same parameter sets in the intermediate model.

Figure 5.5 (b) illustrates a different manifestation of the threshold behaviour of the intermediate model, showing water-table depths between 3.2 and 54 cm for rainfall rates below the threshold of approximately 9 cm yr^{-1}. Unlike the simple model, variable rainfall rates below the threshold do not appear to cause variations in water-table depth for any of the three combinations of decay rates illustrated in Figure 5.5 (b). As the rainfall rate was increased past the threshold value, water-table depths fell abruptly to approximately 0.05 cm and, as with bog height, appear to be invariant in response to further increases in U. Unlike the simple model, in which water-table depth appears to be controlled by the simple ratio of p to α_{ox} (see section *5.2.6.*, above), water-table depth in the intermediate model exhibits an apparent homeostasis for rainfall rates within certain bounds. As noted by

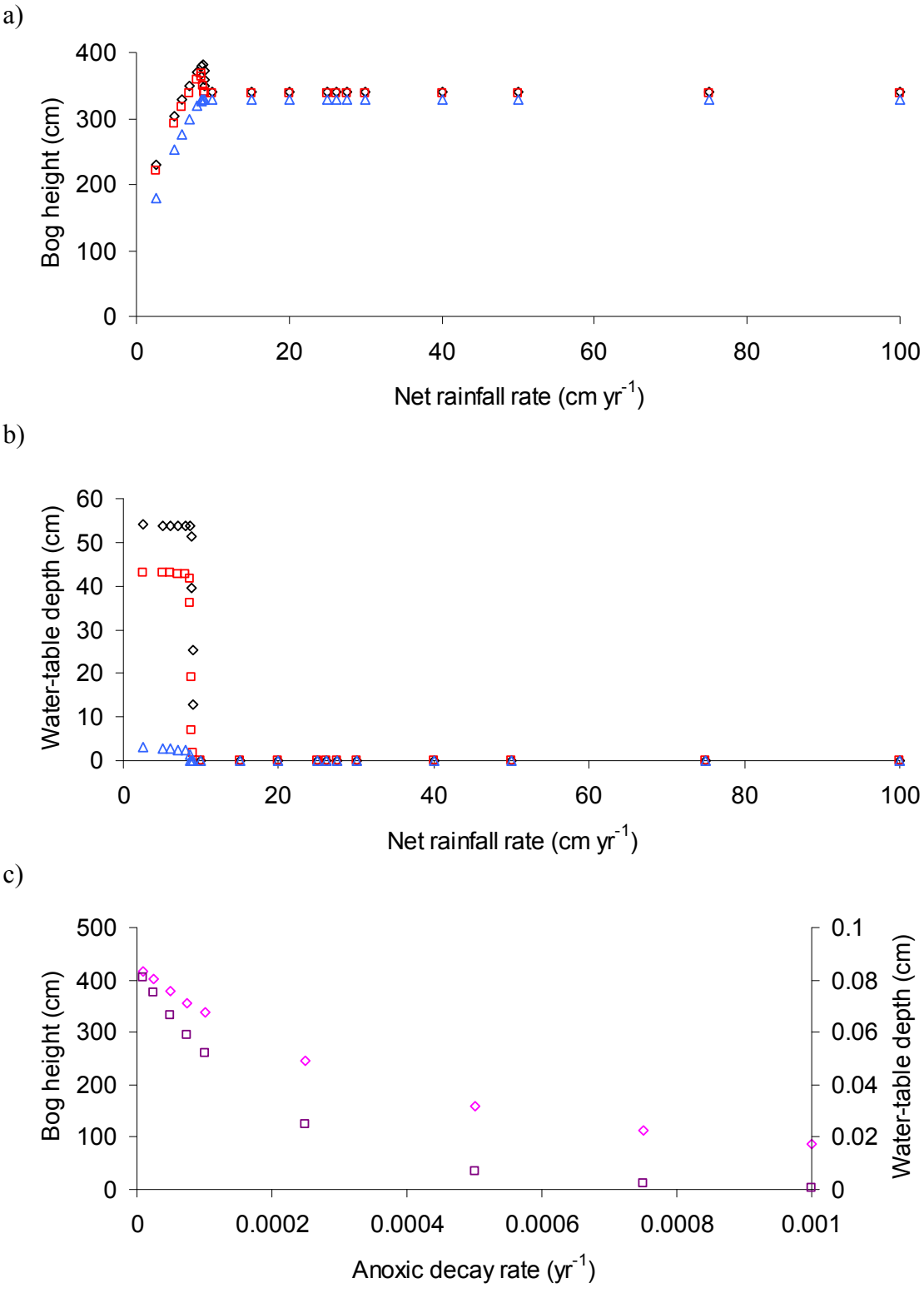

Figure 5.5: Plots showing behaviour of intermediate model under various parameter combinations: in panels (a) and (b), oxic decay rate = 0.005 yr^{-1} (◊), 0.015 yr^{-1} (□), 0.05 yr^{-1} (Δ). Panel (c) shows both bog height (◊) and water-table depth (□). See text for full description of parameter sets.

Hilbert *et al*. (2000), this homeostasis is likely controlled by a more complex interaction between rainfall rate, oxic decay rate and the relationship described by Equation 5.3.

Figure 5.5 (c) shows that, as hypothesised, the response of bog height to changing anoxic decay rates was much more pronounced for the intermediate model than for the simple model. Bog height decreased logarithmically with increasing anoxic decay rates, from 417 cm when α_{an} = 0.00001 yr^{-1} to 86 cm when α_{an} = 0.001 yr^{-1}. This compares to a maximum bog height of 698 cm and a minimum of 616 cm across the full range of parameters assumed for the second set of experiments with the simple model. All runs in the second set of experiments with the intermediate model predicted the wet system state (assuming U = 30 cm yr^{-1}).

The predictions of this intermediate model are easier to interpret as real peatlands than those of the simple model. The humpback relationship between water-table depth and p leads to two possible water-table depths, 0.05 cm and 54 cm, with a range of values in-between for a very narrow range of net rainfall rates close to the threshold. These predicted water-table depths are within realistic bounds for northern peatlands. Model predictions for rainfall rates both above and below the transition threshold may be interpreted as raised bogs, with peat thicknesses and water-table depths within realistic bounds for these systems. While the findings presented in this section are qualitatively similar to those of Hilbert *et al*. (2000), it is important to note that, as model complexity and, arguably, model realism, were increased from the simple model to the intermediate model, the predicted response of both peat accumulation rates and water-table depths (which may be thought of as a surrogate for surface wetness – *cf*. Hayward and Clymo, 1981) to varying rainfall rates was greatly altered. In particular, for any of the combinations of decay rates experimented with, the state variables bog height and water-table depth responded in a highly non-linear and non-intuitive manner to changes in net rainfall rate. A wetter climate did not necessarily lead to a wetter modelled bog, a result which could have implications for palaeoclimatic studies in which testate amoebae and plant macrofossil assemblages in peat deposits are used to reconstruct past climates (e.g. Sillasoo *et al*., 2007). This issue is picked up again later in this chapter.

The fact that the wet and dry model states are determined by an allogenic factor (net rainfall rate) rather than autogenic mechanisms suggests that the model may still be missing important feedbacks. While sudden changes in peat stratigraphy have sometimes been interpreted in environmental reconstruction studies as responses to changing climate (e.g. Wells and Wheeler, 1999; Hughes, 2000; Hughes *et al*., 2000), the so called "fen-bog transition" and abrupt changes in peatland vegetation types are commonly accepted to be a natural phase of peatland development resulting from internal ecohydrological and biochemical feedbacks (*cf.* Belyea and Malmer, 2004; Zobel, 1988). While a full exploration of model parameter space was not undertaken, the work presented here, strongly supported by Hilbert *et al*. (2000), suggests that only two water-table depths are possible for any combination of α_{an} and α_{ox}, indicating that model behaviour is too highly constrained.

5.4. Simulating Decay-Dependent Hydraulic Conductivity

In keeping with objective (iii) identified in section *5.1.2.*, as well as the literature synthesis and experimental findings from Chapter 4, the intermediate version of DBEH2 described in section **5.3.** (above) was altered so as to simulate decay-dependent hydraulic conductivity. This new version of DBEH2 is henceforth referred to as the "complex" version. In order to represent hydraulic conductivity K as a function of proportional remaining mass m, a new submodel was added to the existing structure of DBEH2, called the hydrophysical submodel. The empirical work in Chapter 4 showed that K may be assumed, for shallow peat at least, to increase in a non-linear manner with m. The work in Chapter 4 indicated that depth was a stronger control over K than was m, and there is an argument that **DigiBog** should be parameterised using Equation 4.3. This approach was deemed inappropriate, because Equation 4.3 may only be taken as representative of shallow peat (< 50 cm depth) at a single raised bog site, and extrapolation of this relationship to depths of several metres is unjustifiable without sound physical reasons for doing so, especially given that this approach would generate negative values of K. Failing the use of Equation 4.3 to inform **DigiBog** directly, there is very little other available evidence on the small-scale variation of K with depth, although Baird *et al*. (2008) showed that this relationship is likely to be highly complex and non-linear. The covariance of m with depth (see Equation 4.5) means that it seems reasonable to predict K on the basis of m alone, thereby ignoring the explicit influence of depth. However, it also seems unreasonable to use Equation 4.4 to inform **DigiBog**, because it too was generated from data that represent only shallow peat at a single site. As such, the use of a non-empirically informed, and somewhat arbitrarily chosen, relationship which describes K as a function of m is a justifiable and parsimonious alternative. An exponential function, the general form of which is given in Equation 5.4, was used in the new submodel:

$$K = ae^{(bm)} \tag{5.4}$$

where K is hydraulic conductivity (cm s^{-1}), and a and b are parameter values which describe the shape of the relationship. For the simulations presented here, it was assumed that a = 0.001 and b = 8. These parameter values lead to a conservative decline in K with decreasing m, where a power function would have led to a steeper relationship, giving

unrealistically low K values for old, highly decomposed peat with low m values. Furthermore, these choices of values for a and b lead to near-surface K values (fresh litter; high values of m) which are arguably lower than would usually be expected, and deep K values (highly-decomposed peat; low values of m) which are higher than might be expected for highly decomposed peat (Baird *et al*., 2008). The values chosen therefore likely represent a conservative decrease in K with decreasing m, so as not to exaggerate the effect of this relationship. The behaviour of all models presented in this chapter should be taken to represent general behavioural trends, rather than accurate predictions of peat accumulation rates, but this is especially true of the complex model, given the arbitrarily-chosen nature of Equation 5.4.

For fresh peat with values of m of close to unity, Equation 5.4 predicts values of K of nearly 3 cm s^{-1}, much higher than the uniform value of 0.006 cm s^{-1} used previously in the simple and intermediate models. As such, it was deemed likely that the length of the model timestep would need to be reduced in order to maintain model stability. A series of preliminary runs were performed on the complex model, with timesteps of 1, 0.5, 0.4, 0.3 and 0.2 years, in order to select a suitable stable timestep for the remainder of simulations. The following parameter values were assumed for all preliminary runs: U = 30 cm yr^{-1}; α_{ox} = 0.015 yr^{-1}; α_{an} = 0.0001 yr^{-1}; L = 50,000 cm; s = 0.3. The results of the preliminary runs are illustrated in Figure 5.6, and show that extreme instability is present when Δt = 1 year, and that much less pronounced instability is also present for timesteps of 0.5 and 0.4 years. Instability is manifest as oscillatory behaviour in the water table between successive timesteps, and can be seen in Figures 5.6 (a), (b) and (c) as a 'thicker' line. For timesteps of 0.3 and 0.2 years, no instability was evident, and so 0.3 years was chosen as an appropriate timestep for the remainder of the simulations with the complex model.

Model behaviour was analysed using the same experimental design as that used for the intermediate model (see section **5.3.**, above), so as to compare directly the behaviour of all three models. Two sets of experiments were again performed, the first using a factorial combination of rainfall rates (treatments of U = 5, 10, 15, 20, 30, 40, 50, 75, and 100 cm yr^{-1}) and oxic decay rates (treatments of α_{ox} = 0.005, 0.015, and 0.05 yr^{-1}). Again, additional simulations were run with rainfall rates other than those listed above, chosen in a post-hoc manner, to examine more closely those areas of parameter space which give rise to

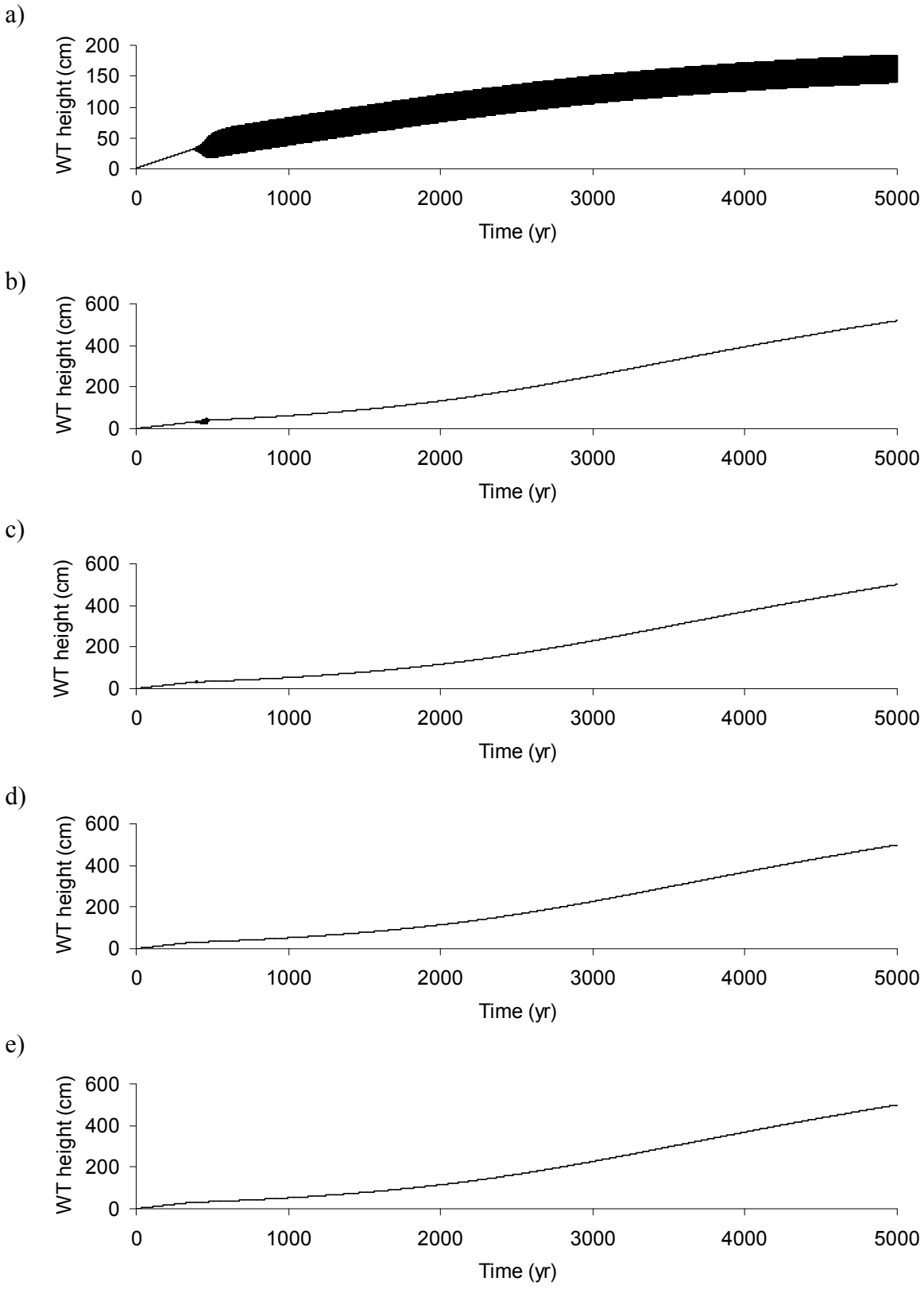

Figure 5.6: plots illustrating development of water-table height (abbreviated on vertical axes labels to WT height) for complex model run, using timesteps of: (a) 1 year; (b) 0.5 years; (c) 0.4 years; (d) 0.3 years; (e) 0.2 years.

interesting behaviour. In the second set of experiments, anoxic decay rate α_{an} was again manipulated in isolation (a range of rates between 0.001 and 0.00001 yr^{-1} were assumed) while other parameters were maintained as follows: U = 30 cm yr^{-1}; α_{ox} = 0.015 yr^{-1}. Finally, the following constants were assumed for all runs with the complex model, identical to those used for the simple and intermediate models: L = 50,000 cm; *runtime* = 5,000 yr; s = 0.3. Note that, because hydraulic conductivity was now predicted by the model according to Equation 5.4, K need no longer be defined as part of a parameter set.

Figure 5.7 shows model behaviour in the two sets of numerical experiments outlined immediately above. Figures 5.7 (a) and (b) show the behaviour of bog height and water-table depth in response to varying rates of oxic decay and net rainfall to be qualitatively very different from that of the intermediate model, but are similar to those observed in the simple model. For the parameters assumed here, the complex model does not appear to exhibit a rainfall threshold above which the behaviour of bog height and water-table depth switches abruptly. Rather, bog height increased logarithmically with increasing U, from heights of between 163 and 268 cm when U = 5 cm yr^{-1}, to between 281 and 635 cm when U = 100 cm yr^{-1}. These heights are between approximately a quarter and a half of the heights observed for the same parameter combinations in the first set of experiments with the simple model. For the complex model, both bog height and water-table depth appear to decrease logarithmically with increasing oxic decay rate, again in a similar manner to that in the simple model. Increasing oxic decay rate by an order of magnitude (from 0.005 to 0.05 yr^{-1}) caused a decrease in water-table depth of more than an order of magnitude, suggesting a strong control of α_{ox} over the characteristics of the oxic zone, but in a more complex manner than seen in the simple model, where water-table depth appeared to be controlled entirely by the simple ratio of p/α_{ox} (see section *5.2.6.*, above). The apparent lack of threshold behaviour in the complex model in response to varying rainfall rates suggests that the inclusion of decay-dependent hydraulic conductivity had introduced a certain stability to the model, thereby counteracting the seeming instability in the intermediate model. Caution must be urged at this point in the discussion, however. It should be remembered that only a small (albeit realistic) domain of parameter space has been explored here, and the complex model may well exhibit unstable or threshold behaviour for other realistic parameter combinations.

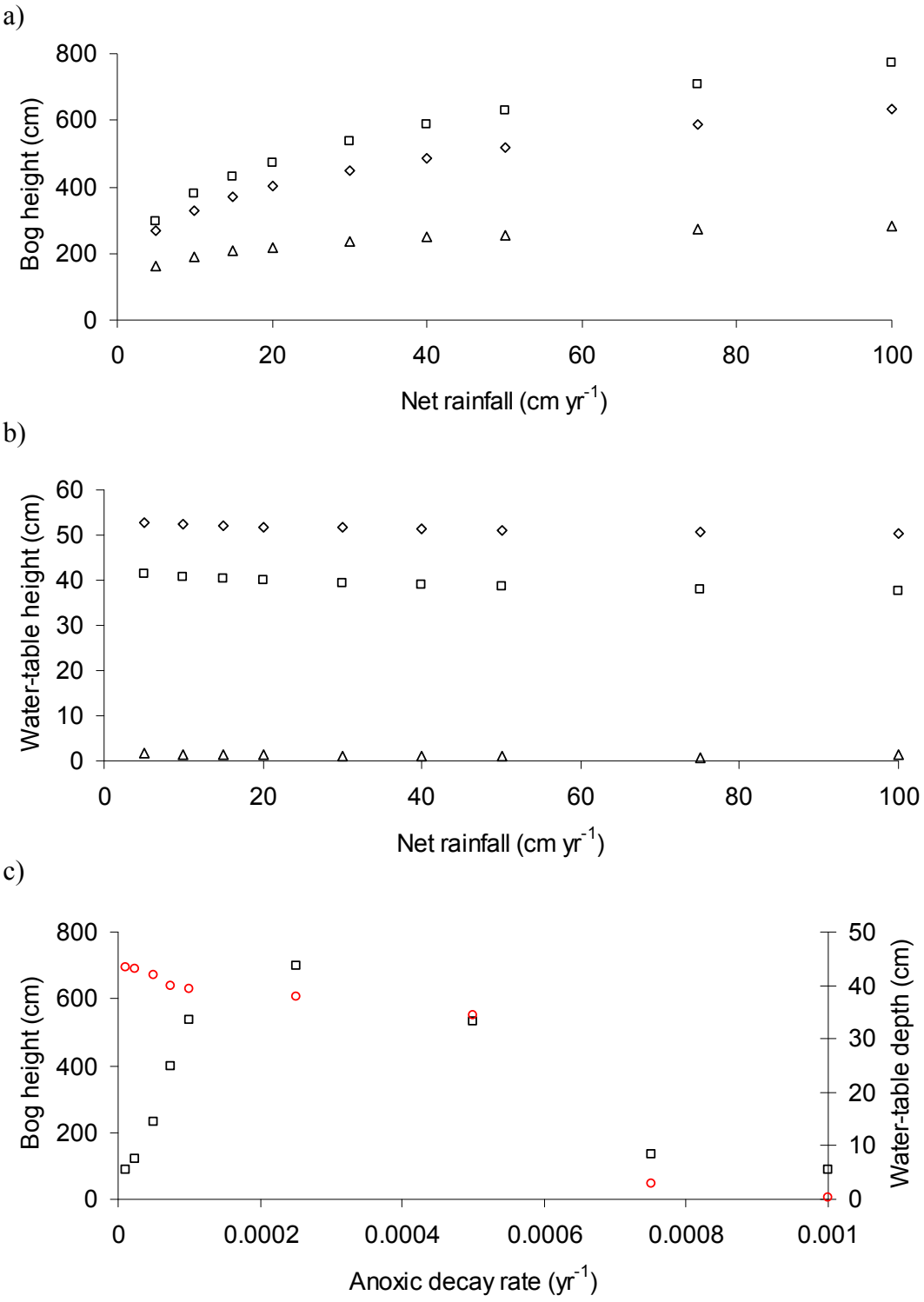

Figure 5.7: Plots showing behaviour of complex model under various parameter combinations: a), b) oxic decay rate = 0.005 yr^{-1} (◊), 0.015 yr^{-1} (□), 0.05 yr^{-1} (Δ). Panel (a) shows bog height, (b) shows water-table depth, (c) shows both bog height (□) and water-table depth (○). See text for full description of parameter sets.

Figure 5.7 (c) illustrates perhaps the most important difference between the complex model and the intermediate and simple models. As the anoxic decay rate was increased from 0.00001 to 0.00025 yr^{-1}, bog height increased in a non-linear manner from 87 to 700 cm. However, as α_{an} was increased past 0.00025 yr^{-1}, bog height began to decrease gradually, to a height of 88 cm when α_{an} = 0.001 yr^{-1}. In the simple and intermediate models, bog height decreased logarithmically (albeit only weakly for the simple model) with increasing anoxic decay rate, whereas the complex model appears to suggest an optimum value of α_{an} for which peat accumulation rate is greatest. This intriguing finding would appear to arise from the lowest anoxic decay rates used here leading to well preserved peat (high m values) which, according to Equation 5.4, leads to highly permeable peat. The result was that the model drained rapidly, preventing a large groundwater mound from developing, which in turn limited the vertical growth of the peat dome itself. Conversely, at high anoxic decay rates, bog height is limited simply by the fact that a high proportion of material is lost from the anoxic zone during each timestep (see section *5.2.6.*, above).

Another potentially important finding from the complex model is illustrated in Figure 5.8, which shows a profile of peat age against proportional mass remaining m at the end of a typical complex model run (U = 30 cm yr^{-1}; α_{ox} = 0.015 yr^{-1}; α_{an} = 0.0001 yr^{-1}; L = 50,000; s = 0.3). The plot shows highly complex and entirely unforeseeable patterns of m with depth (or peat age). Figure 5.8 appears to show an early period of low decay rates for approximately the first 500 years of model development, followed by a brief (< 100 years) period of much higher decay rates and/or low rates of peat formation, probably representing the development of an oxic zone. The well preserved nature of the oldest peat is probably only plausible if the influence of higher-pH water at the base of the peat deposit is ignored. Thus, in real peatlands, the deep, narrow zone of poorly-decomposed peat may not exist because decay here would likely be enhanced by higher pH values. For instance, Yu *et al*. (2003) found long term average specific decay rates of 0.00056 yr^{-1} to be reasonable for minerotrophic fens in western Canada, five times higher than those acting upon the base of the peat deposit shown in Figure 5.8. Peat between the ages of approximately 500 and 4,900 years decreases in cumulative decay with decreasing age, although in a non-constant and complex manner. The youngest peat of less than 100 or so years shows a very

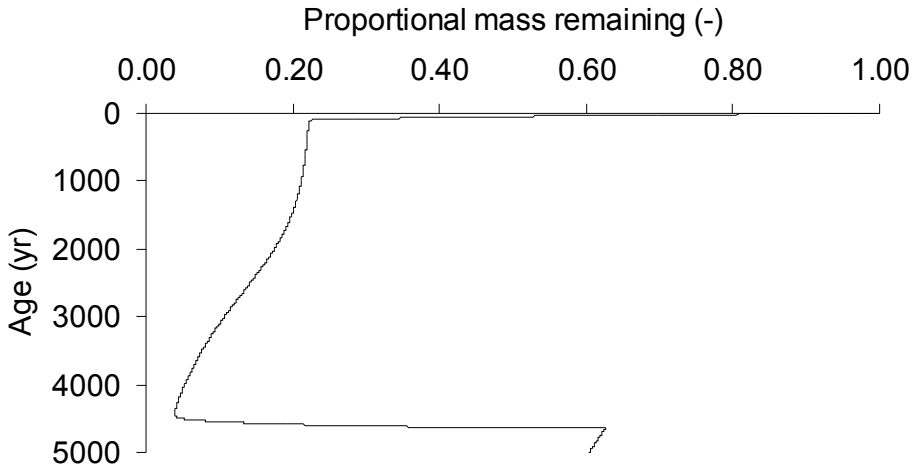

Figure 5.8: plot showing typical profile of peat age against proportional mass remaining, m, for all peat layers at the end of a 5,000 model run using the complex version of DBEH2 (parameter values: U = *30 cm* yr^{-1}, α_{ox} = *0.015* yr^{-1}, α_{an} = *0.0001* yr^{-1}*).*

rapid decay, representing the fact that it is yet to pass into the anoxic zone. While it is not clear whether such predictions represent genuine features of peatland behaviour, they arose from cross-scale interactions between simple rulesets and seem perfectly plausible. Highly complex cumulative decay profiles such as those illustrated in Figure 5.8 might help to explain some of the natural variation observed in empirical studies which would otherwise likely be interpreted as noise due to measurement error (*cf*. Chapter 4, this thesis) or climatic variability (*cf*. Sillasoo *et al*., 2007). Importantly, the profile shown in Figure 5.8 occurred under conditions of constant net rainfall rate. This fact, combined with an almost invariant water-table depth despite a 20-fold increase in net rainfall rate (see Figure 5.7 (b)), call into question the reliability of assemblages of plant and testate amoebae fossils in peat layers as indicators of past climate. Many previous palaeoclimatic studies such as that by Sillasoo *et al*. (2007) have assumed that: i) peatland surface wetness (estimated by proxy using fossil assemblages) responds in a simple and positive manner to increasing net rainfall; and ii) periods of high rates of peat decay can be identified as layers in which net peat accumulation rates were low. While such assumption may be justifiable in terms of simple, static models such the GMH of Ingram (1982) and the BGM of Clymo (1984), it is clear that these assumptions may be violated when a number of ecohydrological feedbacks

are taken into account. The literature synthesis in section **5.1.** called both of these assumptions into question, an argument which appears to be strongly supported by the experimental work presented in the rest of this chapter.

5.5. Simulating Peatland Lateral Expansion

In keeping with objective (iv) identified in section *5.1.2.*, above, a new submodel was added to the complex model described in section **5.4.**, above, in order to simulate changes in the lateral extent L of the modelled peatland as a function of model time. Raised bogs expand laterally chiefly by the process of paludification (*cf.* Anderson *et al*., 2003) in which mineral soils at the edge of the bog become saturated by outflow from the bog, providing a wet niche suitable for the establishment of *Sphagnum* and other peatland plants. While the processes of paludification are poorly understood, it seems likely that the rate of expansion of raised bogs by paludification is determined largely by the local, small-scale topography of the mineral soil at the edge of the bog (Anderson *et al*., 2003). However, taking account of such small-scale spatial variability is beyond the scope of the current work, and so L was described as a number of simple functions of time. As such, the intention here is merely to provide a brief consideration of the general types of behaviour that may be attributable to a laterally expanding bog.

Three model runs were performed, each with L described as a different function of time. For each run, an initial condition of L = 10,000 cm was assumed, and functions were chosen so as to give the same long-term rate of expansion; after a runtime of 5,000 years L had increased to a final value of 50,000 cm in all runs. Linear, logarithmic and step-like functions were used to describe the change of L with time, illustrated in Figure 5.9 (a). The following parameter values were assumed for all runs: U = 30 cm yr^{-1}; α_{ox} = 0.015 yr^{-1}; α_{an} = 0.0001 yr^{-1}; s = 0.3.

The behaviour of the three model runs with variable lateral extent can be seen compared to the behaviour of the complex model with the same parameter set (L = 50,000 cm) in Figures 5.9. All models with variable L predicted a greater rate of peat accumulation than did the model with constant L. The model with a linearly increasing lateral extent gave the greatest rate of peat accumulation over the 5,000 simulated years, with a final bog height of 659 cm, compared to 538 cm for the model with constant L. The mode of lateral expansion also appears to be highly influential upon temporal dynamics of peat accumulation, and the functions used to describe L are clearly expressed in the temporal trends in bog height. In

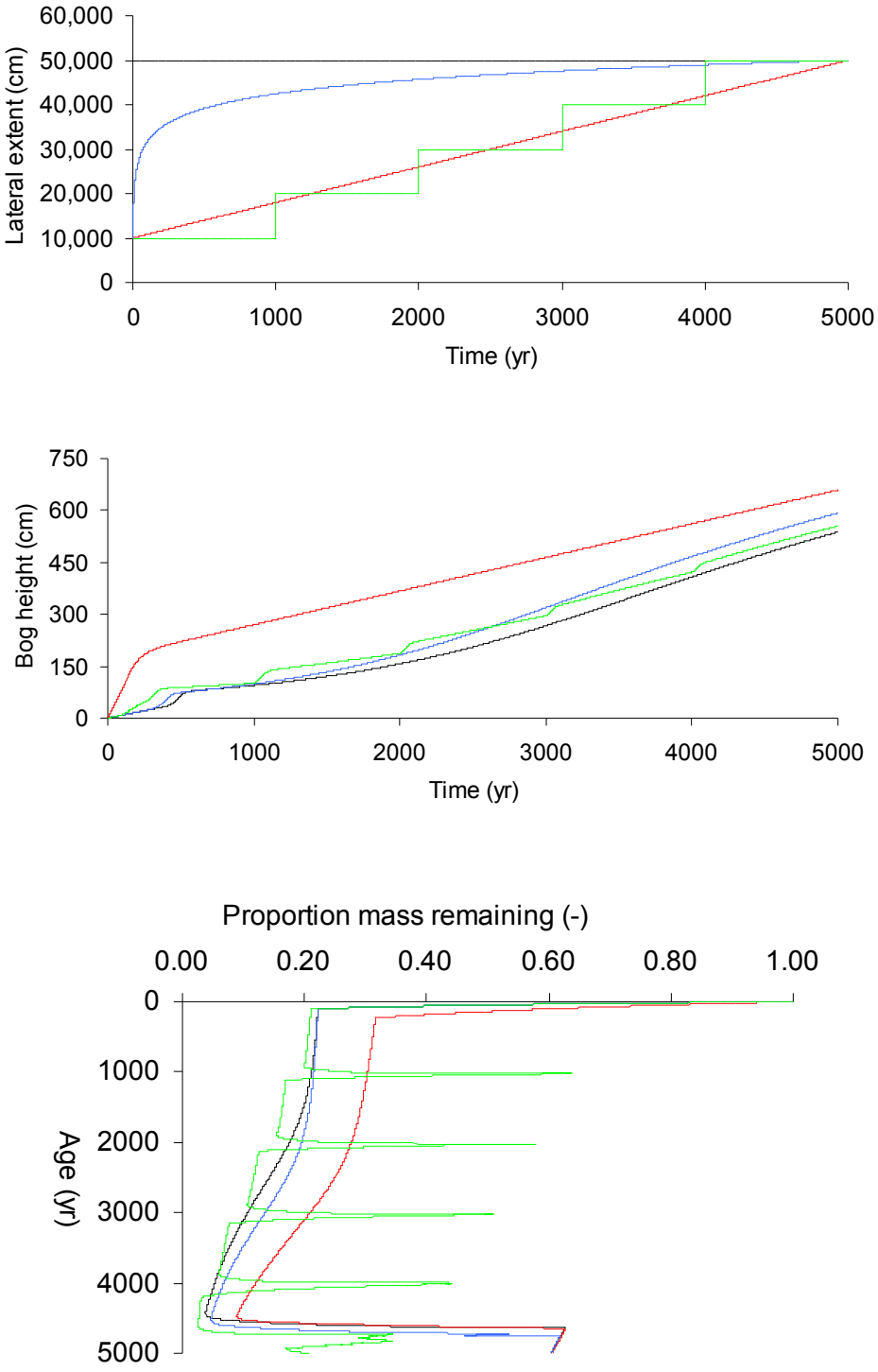

*Figure 5.9: plots illustrating changes in: (a) lateral extent; and (b) bog height, as well as (c) profile of proportional mass remaining (*m*) for runs with lateral extents which are: constant (black line); linearly expanding (red line); logarithmically expanding (blue line); and step-wise expanding (green line).*

particular, the model run in which *L* increased in a step-like manner also exhibited step-like increases in bog height and sharp spikes in the final *m* profile. Step-like expansion of a bog's lateral extent might occur in situations where the mineral substrate onto which the bog expands is topographically undulating or otherwise variable, or where adjacent bog domes coalesce, thereby causing abrupt changes in the effective drainage boundary positions (*cf.* Comas *et al*., 2005). As with some of the abrupt changes observed with the complex model (see Figure 5.8), some of the changes in rates of peat accumulation that are clearly attributable to changes in *L* in these simulations could, if observed in peat cores, be mistaken for palaeoclimatic signals.

While the experiments here are simple, and the rulesets used to describe lateral expansion are arguably over-simplified, the work nonetheless highlights that an understanding of past rates of lateral expansion may be highly important to understanding past climates from peat records. The expansion of bogs is a poorly understood area of peatland science, and the brief discussion here would seem to add weight to the argument for more research to elucidate the matter further.

5.6. Conclusions

Starting with a very simple model of peat accumulation, and adding complexity in an incremental manner gave rise to both quantitative and qualitative differences in rates of peat accumulation and surface wetness under identical realistic parameter sets. Importantly, in many cases, increases in net rainfall did not always cause increases in surface wetness in the complex model, and isolated increases in decay rates did not always lead to lower net rates of peat accumulation. Indeed, the complex model appears to suggest that, for some parameter combinations, maximum peat accumulation rates occur at an optimum, intermediate decay rate. The work presented here suggests that the connection between water-table depth (commonly taken to be indicated by biological proxies) and climate is not necessarily linear or simple. Highly complex, unpredictable patterns of proportional mass loss through time were generated by the interactions between water-table depth, the rate of addition of new peat, peat decay and changes in hydraulic conductivity under constant climatic conditions. The possibility of such behaviour arising under constant climatic conditions brings into question the reliability of many palaeoenvironmental reconstruction studies based on proxies such as peat humification (see, for example: Blundell *et al*., 2008; Charman *et al*., 2006). Rather than representing shifts in allogenic climatic influences, abrupt downcore changes in peat humification may, in some cases, be nothing more than artefacts of peatland development under a steady climate. Care must be taken at this point not to overstate these findings; the suggestion that complex variation in peat profiles may occur under steady climatic conditions is no more than that, but the area certainly warrants further investigation.

The brief experiments presented in section **5.5.**, in which the lateral extent of the modelled bog changed through time, give an indication that the mode, as well as the overall rate, of lateral expansion may be important in determining rates of peat accumulation. In particular, any abrupt changes in the effective positions of a bog's boundaries, which might be caused by the merger of adjacent, expanding bog domes, during the course of its development, are likely to be observable in peat records as abrupt changes in rates of peat accumulation. If past climatic changes are to be inferred with any accuracy from peat records, it seems that the history of peatland lateral growth must be understood, in outline at least. Furthermore, given that a variable hydraulic conductivity appears to be highly influential upon model predictions of peat accumulation rates, a better understanding of the

controls over hydraulic conductivity is highly desirable. While the work presented in Chapter 4 gave an interesting early insight into the issue, the data were largely unsuitable for parameterisation of DBEH2 due to the shallow nature of the cores taken.

The possibility of maximum long-term peat accumulation occurring under conditions of intermediate decay rates is an intriguing one, and would help to explain a number of previously confusing observational findings. For instance, Belyea and Malmer (2004) were unable to explain why one of the wettest periods at their study site in Sweden (during which one might reasonably expect a prevalence of slow, anoxic decay rates in saturated peat soils), as inferred from lake-level data, coincided with a period of relatively low rates of peat accumulation. The complex version of DBEH2 suggests a complex and seemingly emergent relationship between specific rates of anoxic decay and peat accumulation and offers a potential explanation for such situations. All simulations performed in this chapter assumed a constant climatic influence, in the form of net rainfall rate. It would be interesting to examine the effects of a variable climate, particularly given that models of peat accumulation are commonly applied to resolving palaeoclimatic signals in peat deposits. It may be that the representation of decay-dependent hydraulic conductivity and water-table depth-dependent p provide stability against a backdrop of short- to medium-term changes in climate, rather than millennia of extremely high or low net rainfall rates.

The hydrophysical submodel described by equation 5.4 is a simple one, and a number of justifiable alterations may give rise to qualitatively different predictions in future modelling work. Firstly, Equation 5.4 predicts changes in K solely on the basis of proportional mass loss through microbial decay. In reality, the biochemical decay of peat merely reduces the structural integrity of peat fibres; it is compression due to the weight of younger, overlying peat that causes a narrowing and closing of pore spaces (Boelter, 1969). The work presented in Chapter 4 suggests that depth may be a stronger control over K, and mechanical compression of peat is currently not explicitly represented within the **DigiBog** scheme. Perhaps more importantly, **DigiBog** takes no account of changes in effective porosity, s, with cumulative peat decay. The s of 0.3 used throughout this chapter, while plausible for shallow peat, is higher than might reasonably be expected for deep, highly-decomposed peat. Vorob'ev (1963) found deep peat samples from what he described as "*Sphagnum*-shrub high-lying swamps" to exhibit s values of less than 0.1, although he also

found surface values approaching 0.5. The high *s* assumed in the current study likely acted to buffer the effects of a changing water balance, as would the tendency for peat formed by hollows to float (*cf.* Strack *et al*., 2004). Conversely, the assumption of a lower *s* at depth, such as that observed by Vorob'ev (1963), might have led to more dramatic differences between model runs with different assumed net rainfall rates.

Traditional models which are linear or highly constrained in nature usually represent complex cross-scale interactions between system elements in a black-box fashion, making them parameter-sensitive and liable to misrepresent non-linear processes. On the other hand, self-organising models such as the complex version of DBEH2 may prove to be sensitive to the exact nature of the rulesets assumed to control model behaviour. For example, in relation to parameterising DBEH2 so as to represent distinct SL1 unit types, a detailed knowledge of the abundance and leaf area for individual peatland communities may be necessary (Riutta *et al*., 2007a), thereby requiring extensive parameterisation. Multiple possibilities for expanding and improving DBEH2 are suggested above, and there is a danger that, in attempting to predict increasingly complex and intricate behaviour in natural systems such as peatlands, minimalism and general applicability may be sacrificed. Alternatively, it may be that real peatlands occupy only a narrow window within parameter space and that it is an error of the current work to suggest otherwise.

Chapter 6: Modelling Peatland Dynamics in Two Dimensions

In this chapter, the 1-D DBEH2 from Chapter 5 was modified slightly so as to represent a 2-D profile of a developing bog, thereby allowing interactions between neighbouring columns. The new model is called **`DigiBog_EcoHydro3`** (DBEH3) Bog development was again simulated over 5,000 years whilst assuming the same realistic parameter combinations as in Chapter 5. The Fortran 95 code for DBEH3 can be found as two separate text files on the supplementary CD.

6.1. Introduction

6.1.1. Synthesis

The increasingly complex models presented in Chapter 5 demonstrated that the inclusion of different, realistic peatland processes generated qualitatively and quantitatively different predictions of rates of peat accumulation in a single spatial dimension. As noted in section **5.1.**, however, such 1-D models necessarily neglect a number of potentially important processes and feedbacks which operate in a horizontal direction between the centre and margin of a raised bog. A diverse range of existing work, including theoretical, modelling, and empirical studies, suggests that a consideration of planimetric variation in peat properties and process rates may be important to an accurate understanding of peatland development, and that 1-D models of peat accumulation may be of limited applicability to real systems.

Ingram's (1982) GMH (see Chapter 1) predicted a bog that was elliptical in profile, in response to a constant rainfall rate and a uniform distribution of hydraulic conductivity. In a mathematical modelling exercise, Armstrong (1995) assumed hydraulic conductivity to vary exponentially with increasing depth beneath the bog surface, leading in turn to a depth-averaged hydraulic conductivity that varied in plan below a curved bog surface. Armstrong (1995) demonstrated that the rate of decline of K with depth was highly influential upon the shape of the bog predicted by a model similar in concept to Ingram's (1982). In particular, a depth-dependent K led to a greater thickness of peat at the centre of the modelled bog and a less pronounced 'shoulder' at the margin of the bog than did uniform distributions. The latter finding, as well as its implications for the planimetric and depth distributions of hydraulic conductivity, is the kind of prediction which simply cannot be made by 1-D peat accumulation models.

Lapen *et al*. (2005) modelled steady-state flow regimes in a blanket peat complex in Newfoundland, Canada. They found that increases in K near the model's boundary caused large decreases in steady-state water-table heights, and suggested that a low-K rand at the margins may help to maintain high water tables at the centre of a bog. It may be that a low-K margin of this type is a common feature of large peatlands and that such a feature exerts a strong influence on bog development. It should be noted however, that in the model of Lapen *et al*. (2005), the variable bottom-topography of the mineral substrate meant that

flow at the margin is effectively 'pinched' by very shallow peat, which may have contributed to the model's sensitivity to hydraulic conductivity at the margin. Simulating such variable bottom topography is beyond the scope of the work in this chapter, however, and the influence of a low-*K* margin may be reduced in a model with flat bottom topography.

The suggestion of low-*K* margins being important to the development of large peat deposits is also seemingly supported by the empirical work of Baird *et al*. (2008), who found significant differences in *K* between central and marginal areas of Cors Fochno, a partially-cutover and restored raised bog in western mid Wales, UK (see Chapter 2 of this thesis). Their piezometer data from 107 locations showed that depth and location on the bog (*i.e.*, margin or central) exerted strong, complex and interacting controls over *K*. Despite the complexity in their results, the measurements taken by Baird *et al*. (2008) clearly showed that, for most depths, hydraulic conductivity was substantially lower in the marginal areas at their site than in central areas.

The possibility of planimetric variation in hydraulic conductivity also has support from the theoretical study of Belyea and Baird (2006), which showed that transmissivity and water-table depth are almost certain to exhibit systematic horizontal variation as a consequence of bog spatio-temporal development. As recognised by Belyea and Malmer (2004), dynamic water tables during bog development will lead to variability in oxic/anoxic conditions and water availability, leading in turn to variable rates of decay and formation of fresh peat, as well as changes in plant community and, therefore, the types of litter being laid down.

Another quandary arises when one considers the interactions and feedbacks between the spatially-distributed agents in such a system. To the author's knowledge, there are very few attempts to model spatial variability and complexity in peat accumulation, although the model of Borren and Bleuten (2006) goes some way towards this aim. The assumptions, capabilities and limitations of Borren and Bleuten's (2006) model, are also discussed in section *1.2.5.*, but there are a number of points relating to the model which are relevant to the current discussion. Firstly, a number of limitations in the model's conceptual and algorithmic structure mean that, while it is a spatially-distributed, 3-D, ecohydrological model of peatland development, it differs substantially from the conceptual model around

which DBEH2 (see Chapter 5) and DBEH3 (this chapter) are based. In Borren and Bleuten's (2006) model, hydraulic conductivity is almost entirely constrained and does not alter with increasing peat age, decomposition or depth. Furthermore, the model's horizontal spatial resolution of 200 m is likely so coarse as to inhibit the model from faithfully representing potentially important small-scale spatial variation, while timesteps of 50, 25 and 10 years are arguably too long and likely lead to important short-term, non-linear feedbacks being misrepresented by the model's numerical solution. Also, Borren and Bleuten (2006) performed only a limited sensitivity analysis – parameter values were manipulated by ± 10 % of the default value, although hydraulic conductivity of deep peat was increased by an order of magnitude. These manipulations were likely not sufficiently well targeted nor of sufficient magnitude to give a full picture of the model's sensitivities. This limited sensitivity analysis was, however, in keeping with the objectives of the paper.

In Borren and Bleuten's (2006) model, bog size and shape is controlled almost entirely by water-table position in a simple manner, due to a lack of model feedbacks between hydrological and ecological processes. Despite its limitations, however, the model of Borren and Bleuten (2006) did feature a certain amount of spatial complexity. Surficial peat layers exhibit variation in K according to their mire-type designation as either "bog", "fen" or "through-flow fen", and neighbouring columns are able to interact with one another through groundwater movements according to local hydraulic gradients and transmissivity. Without a fuller exploration of the model than that given by Borren and Bleuten (2006), however, it is not possible to tell how important these spatial interactions are to their model's predictions.

A much earlier model was that by Wildi (1978), who used interacting submodels to represent five aspects of peatland development: water balance, peat dry mass balance, plant community type, nutrients, and initial/boundary conditions. Wildi (1978) assumed various imposed hillslopes, and modelled the effects of those slopes upon the accumulation of thin blanket peat for a range of sites in the Swiss Alps. Results of his simulations demonstrated the potential importance of including along-slope spatial variability in the model. Wildi (1978) noted the importance of a consideration of spatial interactions in models of peat accumulation, mainly due to hydrological and hydro-chemical interactions occurring between neighbouring sites along a hydraulic head gradient. That is, the predominantly

downslope movement of water in Wildi's (1978) model caused ecohydrological interactions (such as the uptake of nutrients) at upslope locations to affect ecological interactions at locations further downslope (via an altered concentration of nutrients in groundwater, for instance). In the case of DBEH2, the rate of formation p of fresh litter, the balance between oxic and anoxic decay rates, and the hydraulic conductivity K of peat are all affected (whether directly or indirectly) by water-table depth. Therefore, in a spatially distributed version of DBEH2, the hydraulic properties of peat in upslope columns, and so the rate of groundwater flow, would likely affect the rate and nature of peat accumulation at downslope locations.

6.1.2. Rationale

Much of the rationale for this chapter overlaps with that for Chapter 5; that is, peatlands are highly concentrated and potentially fragile terrestrial stores of organic carbon, and an understanding of the mechanisms responsible for peat accumulation is likely to be of importance to the climate-change debate during the 21st century. Rather than repeating the rationale for modelling long-term peatland dynamics, the reader is instead referred to section *5.1.1.* of this thesis.

In common with a number of previous modelling studies (e.g. Clymo, 1984; Hilbert *et al*., 2000; Frolking *et al*., 2001), DBEH2 represents the accumulation of peat in just a single spatial dimension. However, it is apparent from the literature synthesis in section *6.1.1.* above, that a consideration of an extra (horizontal) spatial dimension may have a significant effect upon the predictions of 1-D models such as DBEH2. Furthermore, a spatially-distributed version of DBEH2 will predict a number of spatial patterns, such as distributions of hydraulic properties and proportional remaining mass, which a 1-D model simply cannot represent.

6.1.3. Chapter aim, objectives

The overall aim of Chapter 6 is to provide a brief, early assessment of the effects of the inclusion of a horizontal spatial dimension upon the qualitative and quantitative predictions of a simulation model of peat accumulation. The 1-D DBEH2 described in Chapter 5 was altered so as to consider the variation of peat properties and process rates in an along-slope

direction. Within this broad aim, three specific research questions have been developed from the literature synthesis above, and form objectives for the rest of the chapter:

i) What shapes of bog, in profile, are predicted by the new, spatially-distributed model?

ii) Do the long-term rates of peat accumulation predicted at the centre of the new model differ from those of the 1-D DBEH2 reported in Chapter 5, when the same parameter values are assumed? That is, does the inclusion of an extra spatial dimension have a substantial effect upon model behaviour?

iii) What spatial distributions, both vertical and horizontal, of hydraulic conductivity and proportional mass remaining are predicted by the new model? In particular, does the model predict a zone of low-*K* peat towards the edge of a raised bog, as suggested by certain sources from the literature?

6.2. Model Description

6.2.1. Algorithmic structure

A new model, **DigiBog_EcoHydro3** (DBEH3), was developed in order to address the objectives identified in section *6.1.3.*, above. Like the hydrological model DBH (see Chapter 2), DBEH3 represents a bog as a series of spatially-distributed columns of peat, each of which consists of a number of layers. Each column is treated in a very similar manner to that of the complex version of DBEH2 described in Chapter 5, with the same functions used to describe formation of new peat, decay of existing peat and alterations to *K*. The main difference between DBEH2 and DBEH3 is that the multiple columns in DBEH3 interact locally with one another through groundwater movements according to DBH.

The new model uses a nested timestep in order to ensure stable numerical solutions while keeping processing times manageable (where processing time is defined as the length of real time that it takes to complete a DBEH3 run, as opposed to the variable *runtime*, which is the length of time simulated by the model). That is, ecological time proceeds in increments (or "timesteps") of 10 years, whereas hydrological time proceeds in much smaller increments. Note that the spatially distributed nature of DBEH3 meant that it is more computationally demanding than DBEH2, thereby necessitating longer timesteps in order to maintain practical processing times. During each 10-year ecological timestep, a steady-state water-table configuration, with respect to the spatial distribution of *K*, net rainfall rate, and the model's boundaries, is calculated iteratively using short timesteps of a few minutes. Like the 1-D DBEH2 (see Chapter 5), DBEH3 consists of a number of submodels, each of which deals with a different aspect of simulated peatland behaviour. The submodels are described in sections *6.2.2.* to *6.2.5*.

6.2.2. Hydrological submodel

The 2-D DBEH3 uses a slightly modified version of **DigiBog_Hydro** (DBH; see Chapter 2) as its hydrological submodel, in order to calculate steady-state water-table positions for each ecological timestep. At the beginning of each timestep, water-table depth *d* (from the bog surface) and height *H* (relative to the impermeable base) are recalculated. Unlike that used in the 1-D DBEH2 (see Chapter 5), the hydrological submodel used in DBEH3 employs a solution to the Boussinesq Equation (Equation 2.2) in

order to calculate steady-state water-table positions. Given that a modelled bog in DBEH3 consists of just a single strip of columns, however, flow in the *x* (across slope) direction was disabled, meaning that flow occurs in a single horizontal dimension (*y*) only. As with the normal version of DBH described in Chapter 2, hydraulic conductivity *K* and effective porosity *s* are able to vary with depth and in plan.

6.2.3. Productivity submodel

Once steady-state water tables have been calculated for an ecological timestep, the productivity submodel activates a new layer at the top of each active column, in much the same way as the productivity submodel in DBEH2 (see Chapter 5). The rate of formation of peat mass in the new layer in each column is calculated using Equation 5.3 and integrated with respect to the ten-year ecological timestep. Unlike in DBEH2, however, peat in newly formed layers is subject to oxic decay during the first timestep (see section *6.2.4.*, below), regardless of water-table position. This measure was deemed necessary in order to reduce the numerical diffusion error associated with a ten-year timestep.

6.2.4. Decay submodel

The decay submodel used in DBEH3 was similar in concept to that used by DBEH2 (see Chapter 5), although it was different in implementation. After steady-state water-table positions had been calculated for all columns, all layers wholly above the water table lost a proportion of their mass equal to the oxic specific decay rate α_{ox} (yr^{-1}), integrated with respect to timestep length, while layers wholly below the water table lost mass at the anoxic specific decay rate α_{an} (yr^{-1}). As with DBEH2, those layers within which the water table resided were accounted for with an appropriate combination of oxic and anoxic decay rates. While DBEH2 used a simple Euler integration to calculate the amounts of mass lost through decay (see Equation 5.2), the use of a ten-year ecological timestep for the decay model would have led to large errors if an Euler method had been employed in DBEH3. Instead, the following equation was used to calculate the decay of each peat layer:

$$m_t = m_{t-1}(ox \cdot e^{-\Delta t_e \alpha_{ox}}) + m_{t-1}(an \cdot e^{-\Delta t_e \alpha_{an}}) \qquad (6.1)$$

where m is the peat mass (M) in any layer during timestep t (-), ox is the proportion of that layer which is above the steady-state water table during the previous timestep (-), an is the proportion of that layer which is below the steady-state water table during the previous timestep (-), and Δt_e is the length of the ecological timestep (T) which, as stated above, is equal to 10 years for all runs in this chapter. Equation 6.1 gives the integral of the exact solution to Equation 5.2, thereby greatly reducing numerical error that would otherwise have been associated with a 10-year timestep.

In the special case of new peat layers formed during the current timestep, another technique was employed so as to reduce error. In DBEH2, peat layers formed during the current timestep are not subject to decay losses. With a 10-year timestep in DBEH3, however, this would have meant that values of proportional mass remaining and hydraulic conductivity in shallow layers overestimated the true solutions to the appropriate submodels by unacceptably large amounts. This could have led to high sensitivity and even instability in the hydrological model, given the already high-K nature of shallow peat layers. Thus, each ten-year cohort was conceptually split into ten annual sub-cohorts during the timestep in which the layer came into existence, each sub-cohort representing a single year's worth of new peat. All sub-cohorts were assumed to receive an initial mass equal to p according to Equation 5.3, and the steady-state water-table during the previous 10-year timestep. The youngest sub-cohort was assumed to experience no decay during the its first timestep, the second youngest sub-cohort was assumed to experience one year's decay at the oxic rate, the third youngest sub-cohort was assumed to experience two years' decay at the oxic rate, and so on. Formally:

$$m^* = p\,(e^{-\alpha_{ox}} + e^{-2\alpha_{ox}} + \cdots + e^{-9\alpha_{ox}}) \tag{6.2}$$

where m^* is the amount of mass added to a new layer during the timestep in which it is activated. It should be noted that, due to the way in which Belyea and Clymo's (2001) equation for p (represented by Equation 5.3) was developed, there was no need to adopt sub-annual timesteps. That is, the annual increments of 'production' as measured by Belyea and Clymo necessarily include an annual integration of productivity and decay. Therefore, using more than ten sub-cohorts to represent each ten-year timestep in Equation

6.2 would have led to no less numerical diffusion and so no less danger of instability. The reason that sub-annual timesteps were used in section **5.4.** was because the high values of hydraulic conductivity predicted by Equation 5.4 would have caused instabilities in the hydrological submodel with timesteps of longer than 0.3 yr.

6.2.5. Hydrophysical submodel

The hydrophysical submodel used in DBEH3 is identical to that used in DBEH2, such that the hydraulic conductivity K of each layer is calculated as a function of its proportional remaining mass m, according to Equation 5.4, again with the parameter values $a = 0.001$ and $b = 8$. As with DBEH2 (see Chapter 5), a constant peat density of 0.1 g cm^{-3} was assumed for all layers (*cf.* Wildi, 1978), as well as a constant s of 0.3 (*cf.* Vorob'ev, 1963).

6.2.6. Model time trials

Two questions were posed before a full experimental design could be completed:

1) What is the maximum hydrological timestep length that will yield stable model behaviour with the kinds of K distributions that are likely to occur in DBEH3 runs?
2) For how long should the hydrological model run in order to generate what may reasonably be taken to be steady-state behaviour?

A number of tests were performed using the standalone hydrological model **`DigiBog_Hydro`** (DBH) in order to assess the likely numerical stability of DBEH3 in response to hydrological timestep length, thereby giving an indication of processing times for DBEH3 runs. DBH was parameterised with grid dimensions of 5 (x) by 54 (y) columns, a total of 270 columns. The outer 114 columns were deactivated, and a further 106 columns were nominated as boundary columns. This left 50 active columns arranged in a strip of single column width, representing a peat deposit in profile underlain by a flat, impermeable base layer of mineral soil or bedrock. All columns had a width of 10 m, giving an aquifer of length 500 m, as assumed in Chapter 5.

The highest K that can be predicted by the hydrophysical submodel in Chapter 5 was approximately 3 cm s^{-1}, although the greatest transmissivity values (the product of the thickness of flow and depth-averaged hydraulic conductivity) were generated when depth-averaged K was approximately 2.15 cm s^{-1} and the thickness of flow at the centre of the bog

was approximately 60 cm. Each active column consisted of 500 active layers, each 0.12 cm thick (giving a total bog height of 60 cm), giving the same number of computational entities as would be required for a 5,000 year run with DBEH3, and the same transmissivity as the highest observed in Chapter 5. In keeping with the parameterisation of DBEH2, effective porosity *s* was assumed to be 0.3 (-). Net rainfall rate was assumed to be zero, meaning that flow through the model was motivated solely by the hydraulic gradient between the upslope and downslope boundaries. All boundaries were assumed to be impermeable (reflective), apart from one boundary column at the down-flow end of the model and one at the up-flow end, which were assumed to be Dirichlet boundaries with constant water-table heights of 10 and 60 cm above the impermeable base, respectively. This configuration, under a zero net rainfall rate, caused the development of a water-table drawdown between the upper and lower ends of the model, similar to the parallel ditch geometry of Youngs (1990; see Chapter 2 of this thesis).

Timesteps of longer than 1,200 seconds produced numerical instability in model behaviour, so 1,000 s was chosen as a safe timestep length in the full version of DBEH3. In order to determine a satisfactory steady-state criterion for the model, two time trial model runs were performed. Each run was for a total of 1,000 days of simulated time, one with a uniform K of 2.15 cm s^{-1} (representing the highest K value from the Chapter 5 simulations; see above) and the other with K = 0.009 cm s^{-1} (the lowest depth-averaged K from Chapter 5). The high-K run reached a suitably steady state much more quickly than did the lower-K run. After 1,000 simulated days, the average absolute change in water-table position per column had fallen from 158 (high K) or 0.661 (low K) cm per column per year to 1.91×10^{-5} (high K) or 0.301 (low K) cm per column per year. After 500 days of simulated time, water table movements were 0.00510017 (high K) or 0.370 (low K) cm per column per year. As such, 500 days of simulated time were deemed sufficient to predict steady-state behaviour for the hydrological model. Projected processing times for 5,000-year runs with 10-year timesteps were estimated to be approximately 76 hours.

6.2.7. Experimental design

A simple experimental design was formulated in order to examine the model's behaviour under variable: i) net rainfall rates; and ii) anoxic decay rates. The two most important findings from Chapter 5 were that the 1-D DBEH2 appeared to be resistant, at least for the

parameter combinations assumed, to varying rainfall rates, and that peat accumulation rates peak for an intermediate optimum decay rate. The experimental design for the current chapter aimed to examine briefly whether these findings hold for a 3-D version of what is essentially the same model, or whether the interactions of spatially-distributed columns within a bog profile gave rise to different behaviour. Two sets of four experiments were performed, and parameter values were selected so as to enable as direct a comparison as possible between the 1-D and 2-D models. In the first set of experiments, net rainfall U was manipulated in isolation (treatments of U = 5, 30, 50, and 100 cm yr^{-1}) while all other parameter values were maintained as follows: α_{ox} = 0.015 yr^{-1}; α_{an} = 0.0001 yr^{-1}; runtime = 5,000 yr. Note that these parameter sets are equivalent to those assumed in Chapter 5, and that L need no longer be specified as a parameter because the lateral extent of the bog is implicitly specified by the size of the 1 × 50 column grid and the spatial resolution of 10 m (giving a length of 500 m, again as in Chapter 5). In the second set of experiments, again in keeping with Chapter 5, α_{an} was manipulated in isolation (treatments of 0.00001, 0.0001, 0.001 yr^{-1}), while: α_{ox} = 0.015 yr^{-1}; U = 30 cm yr^{-1}; runtime = 5,000 year. For all runs, the upslope boundary was ssumed impermeable, representing a drainage divide along the central axis of a hemi-elliptical bog, as with Chapter 3, and the downstream boundary was assumed to contain a constant water-table height of 0.1 cm, thereby representing a marginal ditch to which the rest of the model drains.

6.3. Results

The results of the simulations with DBEH3 show very clearly that the 2-D model behaves differently, both in quantitative and qualitative terms, from DBEH2. Peat accumulation rates predicted by DBEH3 were generally much lower than those of DBEH2 under comparable parameter sets. Peat accumulation rates at the centre of the modelled bog were entirely invariant in response to varying net rainfall rates, at least with the model's other parameter values set to α_{ox} = 0.015 yr^{-1} and α_{an} = 0.0005 yr^{-1}. All runs in the first set of experiments, in which net rainfall was manipulated whilst other parameter values were held constant, predicted final central bog heights of 150 cm, with water tables at the surface in all cases. This is in sharp contrast to the response of DBEH2 to varying rainfall rates: the 1-D model predicted bog heights that increased in a complex and non-linear manner with increasing net rainfall rates, as well as non-zero water-table depths which decreased (*i.e.*, became shallower) weakly with increasing net rainfall rates.

From the second set of experiments, anoxic decay rate appears to exert a strong and complex control over peat accumulation rates, with the greatest final central bog height of 196 cm occurring when α_{an} = 0.00005 yr^{-1} (see Figure 6.1). As with DBEH2, it seems that this maximum rate of peat accumulation occurs at an intermediate value of α_{an}, because the lowest anoxic decay rate, 0.000005 yr^{-1}, led to a bog height of only 130 cm, while the highest rate of anoxic decay, 0.005 yr^{-1}, led to a final central bog height of just 16.6 cm. The maximum bog height of 196 cm predicted by DBEH3 (when α_{an} = 0.00005 yr^{-1}) is much smaller than the maximum height of 700 cm predicted by DBEH2 (when α_{an} = 0.00025 yr^{-1}), although it remains to be seen whether a more comprehensive exploration of model parameter space would have revealed thicker bogs.

Final predicted water-table depths, illustrated in Figure 6.1, appear to show reliance upon anoxic specific decay rate α_{ox}. All runs in which α_{ox} was assumed to be equal to or greater than 0.0005 yr^{-1} predicted a final water table depth, after 5,000 simulated years, of 0.0 cm, *i.e.* the water table was at the surface and water was being lost from the model's solution, representing overland runoff. For the two runs with α_{ox} = 0.00005 and 0.000005 yr^{-1}, however, final central water-table depths were 42.7 and 43.6 cm below the bog surface, respectively.

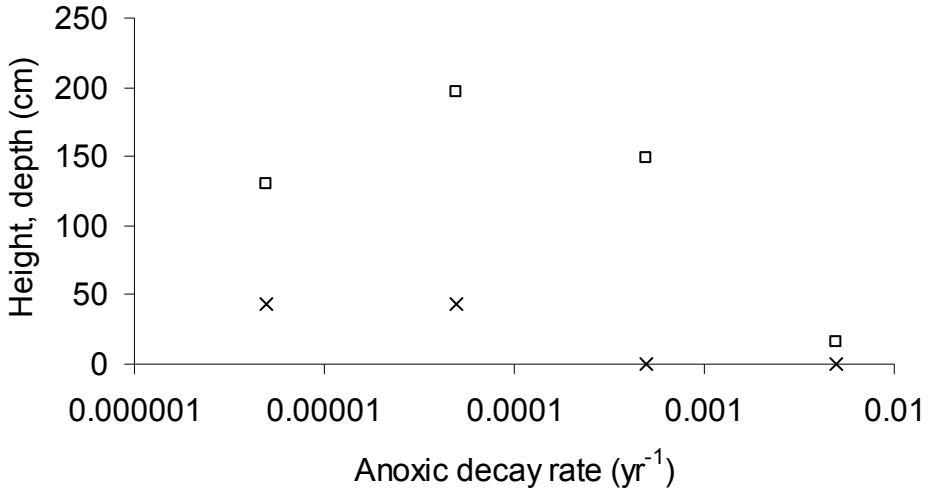

Figure 6.1: plot showing final central bog heights (open squares) and water-table depths (crosses) for the second set of experiments with DBEH3, in which anoxic decay rate was manipulated in isolation. See text for full description of parameter sets. Note the logarithmic scale on horizontal axis.

The profile plots showing final predicted distributions of hydraulic conductivity *K* (Figure 6.2) and proportional mass remaining *m* (Figure 6.3) illustrate a number of interesting and odd predictions of DBEH3 not evident from the summary data on central bog heights and water-table depths. In the runs with anoxic decay rates greater than 0.00005 yr^{-1}, including all runs in the first set of experiments in which net rainfall rate was manipulated, the final predicted bog shape consisted of a flat plateau extending from the centre of the bog to between approximately 30 and 110 m from the margin. Beyond this plateau, adjacent to the margin, the model predicts a hump, between approximately 30 and 110 m wide and raised above the low, central plateau by up to 100 cm. The prediction of this raised rand means that, contrary to original expectations, the state variable central bog height (see Figure 6.1) does not necessarily give the highest point on the bog profile. It also means that water-table depth, at least for some parameter combinations, is far from spatially uniform, nor does it necessarily decline simply or monotonically with distance from the central axis of the bog.

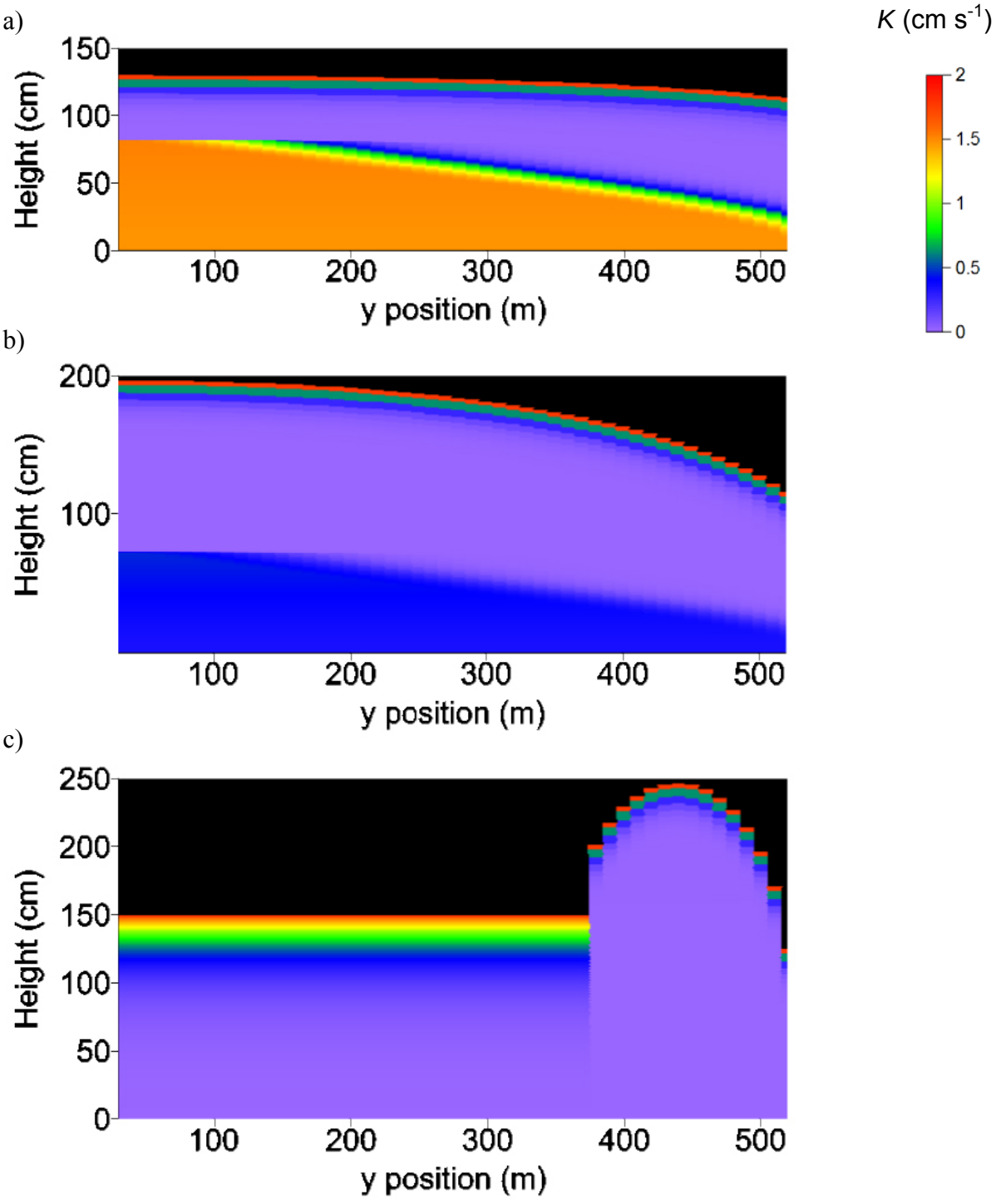

Figure 6.2: hydraulic conductivity profiles for model runs from the second set of experiments with DBEH3, in which anoxic decay rate was manipulated in isolation: a) α_{an} *= 0.000005 yr*$^{-1}$*; b)* α_{an} *= 0.00005 yr*$^{-1}$*; c)* α_{an} *= 0.0005 yr*$^{-1}$*.*

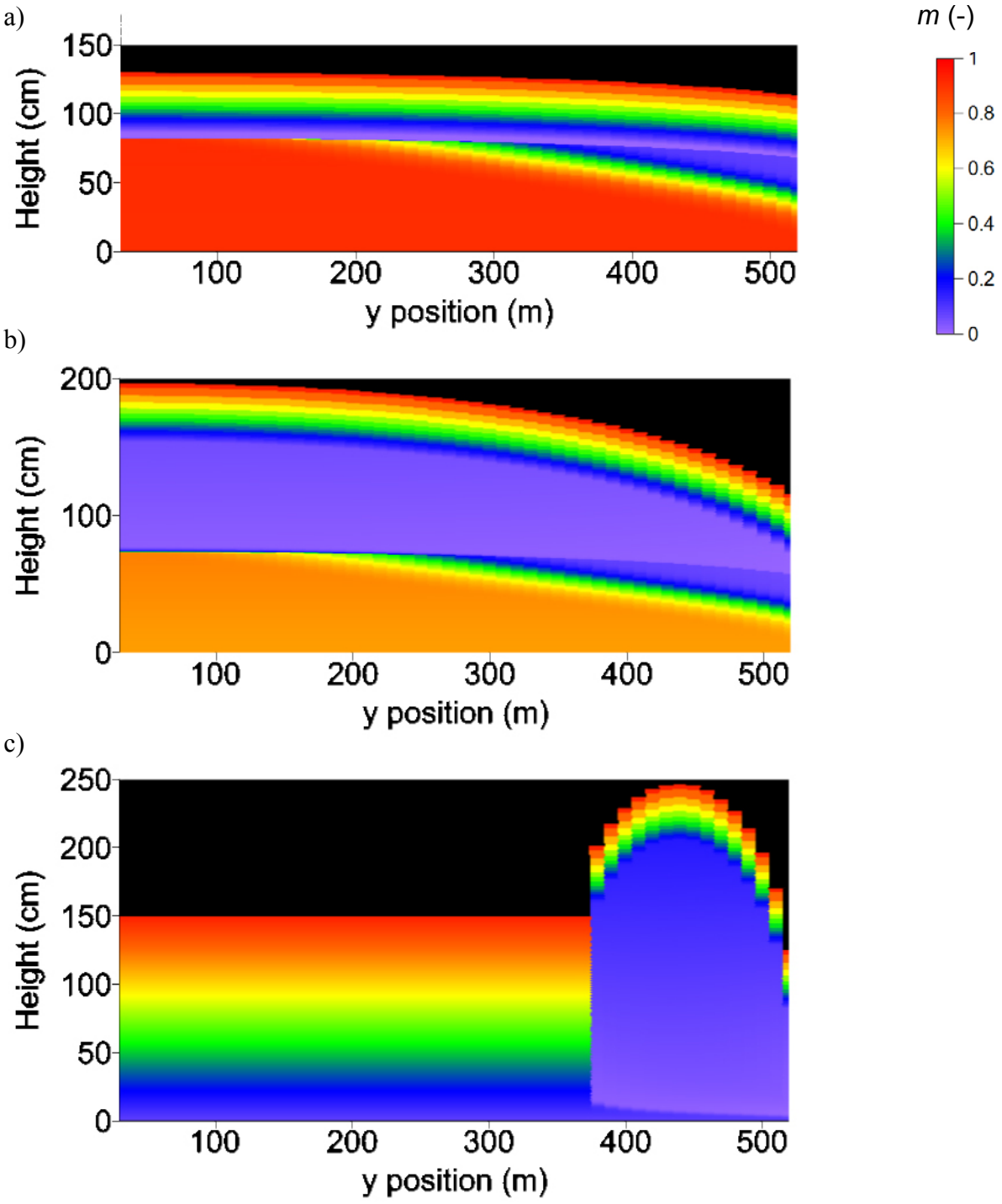

Figure 6.3: proportional remaining mass profiles for model runs from the second set of experiments with DBEH3, in which anoxic decay rate was manipulated in isolation: a) α_{an} *= 0.000005* yr^{-1}*; b)* α_{an} *= 0.00005* yr^{-1}*; c)* α_{an} *= 0.0005* yr^{-1}*.*

Runs with lower anoxic decay rates of 0.00005 yr^{-1} and 0.000005 yr^{-1} exhibited an entirely different bog shape, with neither a low central plateau nor a marginal hump. Rather, the two runs with low anoxic decay rates predicted a curved, dome-shaped landform which was highest at the bog's central axis and lowest at the margin (see Figures 6.2 and 6.3).

Figure 6.2 shows that final predicted distributions of hydraulic conductivity *K* for all model runs with DBEH3 demonstrate interesting spatial patterns both vertically and horizontally. It is evident that those runs with anoxic specific decay rates of 0.0005 yr^{-1} or greater feature a very obvious and well-defined curtain of low *K* at the model's margin, seemingly coincident with the marginal humps also predicted by those runs. By contrast, and contrary to evidence provided by Lapen *et al*. (2005) and Baird *et al*. (2008), the runs with α_{an} = 0.00005 or 0.000005 yr^{-1} exhibit a more gentle horizontal gradient in *K* near the boundary, with no sharp step apparent. Nonetheless, even in the runs with the lowest values of α_{an}, the deep layers of well preserved, higher-*K* peat thins almost to nothing near the model's downslope boundary, affording almost a twofold difference in depth-averaged hydraulic conductivity below the water table in the run with α_{an} = 0.00005 yr^{-1}, from 0.187 cm s^{-1} at the centre of the bog to 0.0958 cm s^{-1} at the margin. In the run with α_{an} = 0.000005 yr^{-1}, the anoxic decay rate is so low that the deepest layers of peat, which have been below the water table at all times during the simulation, have barely decayed at all from their fresh state and exhibit *m* values of approximately 0.92 (see Figure 6.3 (a)), seemingly unrealistically high for deep, 5,000 year-old bog peat.

Figure 6.4 shows the development of the model's dynamics though time for two runs from the first set of experiments: one with α_{an} = 0.00005 yr^{-1} and the other with α_{an} = 0.0005 yr^{-1}. These snapshots of the model's temporal development elucidate much about the final distributions of *K* and *m* seen in Figure 6.2 (b, c) and 6.3 (b, c). For all points in model time after 500 yr, Figure 6.4 (a) shows that in the model run with α_{an} = 0.00005 yr^{-1}, water-table depth has been maintained at approximately 43 cm below the bog surface, along the entire length of the model. At 500 years, the water table is at the bog surface in the centre of the model, while there is also a marginal hump, up to 41 cm at its thickest, which is not apparent during later timesteps. The model has undergone a hydrological regime transition at some point between 500 and 1,250 years of simulated time, from a wet state similar to

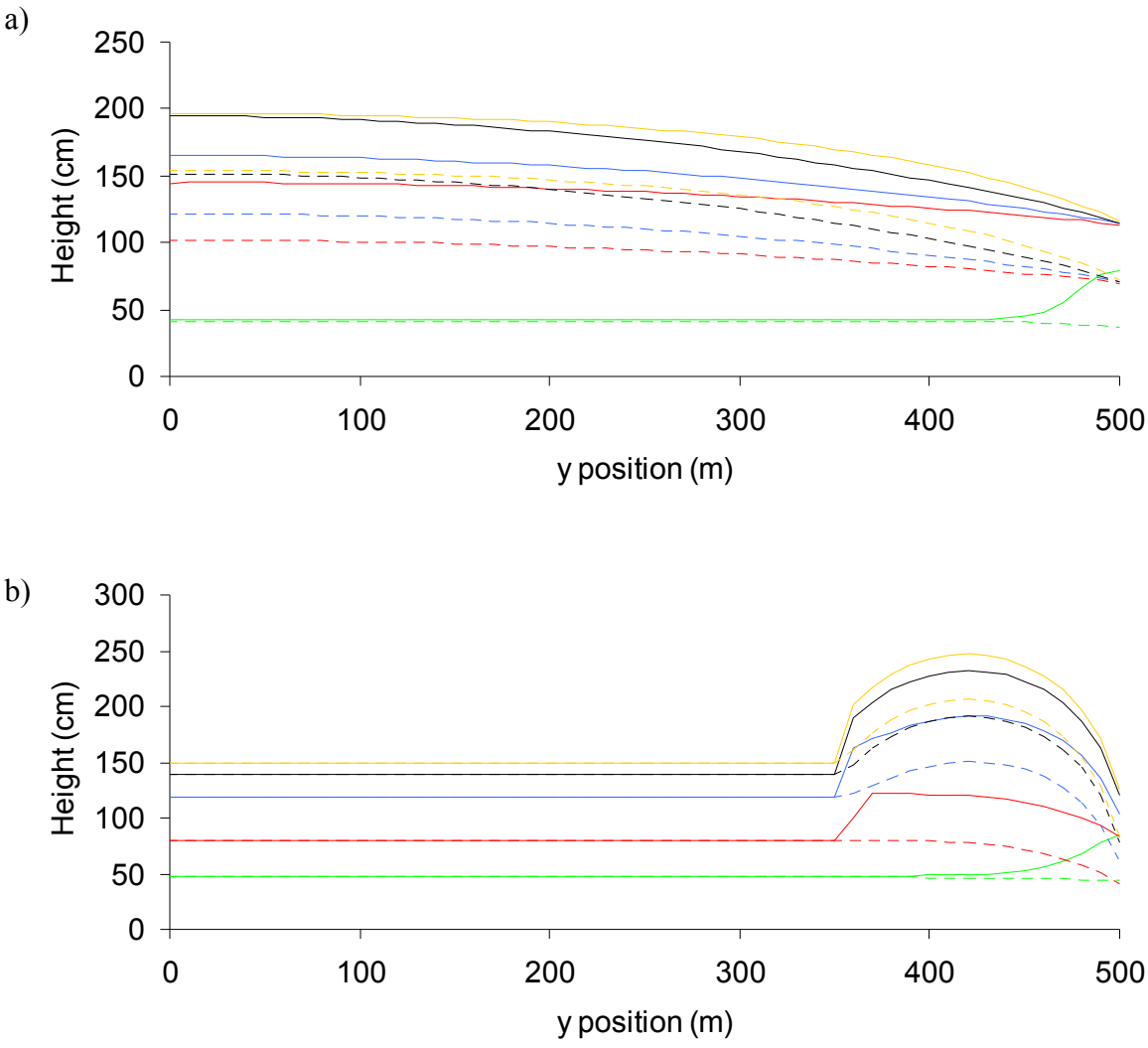

Figure 6.4: Plots showing temporal development of water-table heights (broken lines) and bog surface heights (solid lines), in profile, after 500 (green), 1,250 (red), 2,500 (blue), 3,750 (black) and 5,000 (gold) simulated years, for two runs from the first set of experiments with DBEH3. Anoxic specific decay rates: (a) α_{an} *= 0.00005 yr*$^{-1}$*; (b)* α_{an} *= 0.0005 yr*$^{-1}$*. Note the different scales of vertical axes between the two panels. See text for full description of parameter sets.*

those evident in the runs with a higher α_{an}, to a later, drier state with a deeper water table. While the height and profile shape of the bog changed through time after the transition, the water table appears to have followed these changes exactly and stayed at 43 cm below the surface. Figure 6.4 (b) shows that the run with α_{an} = 0.0005 yr^{-1} possessed its marginal hump and a wet state in all five of the chosen points in time, and did not undergo a

hydrological regime change. Furthermore, water-table depth across the entire hump is approximately 43 cm at all points in time other than 500 yr. While the width (extent in the *y* direction) and water-table depth in the hump appear to have been constant throughout the model run, the profile shape of the hump has changed throughout model time. Whilst almost flat and plateau-like after 1,250 simulated years, the hump became more convex throughout model time. To the left of Figure 6.4 (b), before the hump, the flat, wet plateau appears to have been maintained throughout the entire model run, with the water table at the surface at all five points in time.

Figures 6.3 (a) and (b) show sharp, sub-horizontal divisions between contrastingly well- and poorly-decomposed peat layers. These seem almost certain to be artefacts of the kind of hydrological regime changes indicated in Figure 6.4a, as discussed above, and as predicted by Belyea and Malmer (2004). That is, when the model has possessed a wet state at the beginning of the simulation, all peat layers were below the surface, and therefore subject to the low, anoxic decay rate, leaving the deepest peat in a well-preserved state. When the model changed to a dry state (at some point between 500 and 1,250 years, in the run where α_{an} = 0.00005 yr^{-1}: see Figure 6.4a), and the bog surface rose up above the water table, the upper ~43 cm of the peat profile became exposed to the faster, oxic decay rate, meaning that peat formed after the transition was already well-decomposed before it was submerged by the rising water table. This situation has not occurred in the model runs with anoxic specific decay rates of 0.0005 yr^{-1} or higher, because the water table was at the bog surface for the duration of the simulation.

A closer examination of Figures 6.3 (a) and (b) indicates that there are further interesting features of the final peat profile. After 5,000 simulated years, there appears to be more than one unconformity in peat quality (represented by *m*) at the right-hand side (high *y* values) of Figures 6.3 (a) and (b). The multiple vertical transitions in *m* are artefacts of a former marginal hump which existed early in the simulation, and which has been eradicated from the final bog profile, as shown in Figure 6.4 (a), after a hydrological regime transition. The marginal humps which existed during the wet phase at the beginning of the runs with α_{an} = 0.000005 yr^{-1} and α_{an} = 0.00005 yr^{-1} were taller than the rest of the model and were raised above the water table, meaning that they were subject to oxic decay rates early in the model's development. The regime change then brought the bog surface up above the water

table and left an isolated area of well decomposed peat – the former hump – within an otherwise poorly decomposed area of the peat profile. A vertical unconformity in *m* is also evident in the runs with anoxic decay rates of 0.0005 yr^{-1} or higher, at the right-hand side (downslope end) of figure 6.3c. This vertical unconformity is an artefact of a persistent marginal hump which has been present throughout the 5,000-year model run, and where decay regime has been different from that in the neighbouring (upslope) area, which has possessed the dry system state throughout the simulation.

Another notable feature of all runs with DBEH3, evident in figures 6.2 and 6.3 is that the thickness of the modelled peat deposit does not thin to zero at the boundary, and many of the model runs demonstrate a peat thickness of over a meter in the column immediately adjacent to the downslope boundary.

6.4. Discussion

DBEH3, in common with DBEH2, still seems to exhibit an optimum decay rate which produces maximum peat accumulation rate, at least at the centre of the modelled bog, although this optimum rate would seem to possess different values between the two models. As with DBEH2, the fact that the greatest rate of peat accumulation does not occur under the lowest assumed value of α_{an} is easy to understand. The lowest anoxic specific decay rate of 0.000005 yr^{-1} has led to poorly decomposed peat with high K values (see Figures 6.2a and 6.3a) which causes the bog to drain efficiently, thereby preventing a high groundwater mound from developing, which in turn limits peat accumulation.

The large differences between the predictions of the 1-D DBEH2 and the 2-D DBEH3 are likely due, in part, to differences in the hydrological submodel used to calculate steady-state water tables. Small variations in water tables between the two models, due to a number of factors arising from differences in calculation of steady-state water tables, may be amplified by feedbacks within the productivity and decay submodels. In particular, Ingram's (1982) GMH, used to calculate water-table behaviour in DBEH2 (see section 5.2.2), assumes K to be uniform with depth (which it is in neither DBEH2 nor DBEH3) and that depth-averaged K is uniform in plan (which is the case in DBEH2, but not in DBEH3).

DBEH3 apparently exhibits a narrower window in parameter space within which realistic peatlands are predicted than does DBEH2, with higher decay rates leading to oddly shaped peat deposits, seemingly not realistic manifestations of peatlands. It is interesting to see how the inclusion of an extra spatial dimension can so drastically alter the predictions of a model, through the hydrological interactions between neighbouring columns. The large, raised humps at the edge of model runs with higher anoxic specific decay rates, whilst surprising at first, are easily explained. The central area of the model will be subject to extremely low hydraulic gradients at the beginning of a simulation. Even with low net rainfall rates, the low hydraulic gradients lead to water tables close to the bog surface, because only very slow rates of lateral flow occur. When water-table depth is equal to zero, the entire column is subject to the anoxic decay rate, while the rate of formation of fresh peat, according to Equation 5.3, is equal to 0.0093 g cm^{-2} yr^{-1}. If this condition of *water-table depth* = 0 cm is maintained throughout the duration of the simulation then, according to Clymo (1984), bog height in those columns will approach the asymptotic limit of:

$$bog\ height = \frac{0.0093}{\rho \alpha_{an}} \tag{6.3}$$

where ρ is peat dry bulk density (g cm^{-3}; assumed throughout this chapter to be equal to 0.1 g cm^{-3}). An examination of the temporal trajectories of central bog heights in the runs with α_{an} = 0.0005 and 0.005 yr^{-1}, particularly the latter, which appears to have reached a steady state well before the end of the simulation, suggest that the limit predicted by DBEH3 is slightly lower than that given in Equation 6.3. Given that central water-table depth was equal to 0 cm throughout the entire course of both simulations, this lower figure is likely attributable to the oxic decay rate experienced by all layers during the timestep in which they are activated (see section *6.2.4.*, above), even when a column's water table is at the bog surface. This combination of feedbacks would also explain why a twenty-fold increase in net rainfall rate failed to have any effect upon predicted central bog height in the first set of experiments. The height of both the bog surface and the water table in the central portion of the bog are essentially controlled by the anoxic specific decay rate, and increasing rainfall is simply lost by the model solution, assumed to be overland runoff. Higher net rainfall rates lead to a wider central flat plateau than do lower rainfall rates, because high rainfall rates cause more columns to be saturated and a narrower, steeper drawdown zone at the model's boundary.

The complex version of the 1-D DBEH2 appeared to exhibit a non-linear decrease in water-table depth with increasing anoxic specific decay rate α_{an} (see Figure 5.7c), although not such a sharp, threshold change as exhibited by the intermediate 1-D model. In a similar manner, some runs with the spatially-distributed version of that model, DBEH3, appear to exhibit a similar non-linear change in water table depth (or anoxic-zone thickness) in horizontal space, rather than in parameter space. This is evident in the runs with α_{an} = 0.0005 and 0.005 yr^{-1}, which predict a marginal hump in the zone of water-table drawdown.

It should be remembered that, as with the DBHE2 presented in Chapter 5, all of the interesting behaviour exhibited by DBEH3, in particular the unconformities in the final peat-quality profiles, were generated under a constant climatic influence (*i.e.*, constant net rainfall). The work in this chapter provides much more convincing evidence than that in

the previous chapter that the kinds of hydrological regime changes predicted by Belyea and Malmer (2004) may occur as a natural part of bog spatio-temporal development. A corollary is that, contrary to the assumptions of well established works such as those by Barber (1981) and Charman *et al*. (1999), any such changes observed in real peat deposits may not represent climatic changes.

At raised bog sites such as Ryggmossen in Sweden (see section *4.2.1.* for full site description) and Cors Fochno (at least in its natural state, before it was cut for fuel and land reclamation; see section *2.6.1.*), the peat soil at the edge of the bog gradually thins to almost nothing, and the bog is surrounded by mineral soil deposits. No model runs with DBEH3 predicted such a realistic thinning of peat soils to zero thickness at the edge of the bog. This finding almost certainly reflects the fact that Equation 5.3, which determines p on basis of water-table depth, was developed by Belyea and Clymo (2001) from data on bog species and is therefore unlikely to be representative of lagg fen communities such as those that would be expected at the margin of a raised bog. Maybe, therefore, we should not assume that **DigiBog** is able to represent the development of an entire raised bog, up to and including the lagg fen. High m and K values at depth are also indicators of a limited model ruleset, because DBEH2 and DBEH3 fail to take account of potential reactions with mineral substrates. As mentioned in Chapter 5, Yu *et al*. (2003) observed decay rates of greater than 0.0005 yr^{-1} in Canadian minerotrophic fens, two orders of magnitude higher than that acting at the bottom of the simulation illustrated in Figure 6.3a. **DigiBog** considers a raised bog to develop within a hydrologically and biologically inactive, chemically inert environment, in that it ignores any influence that the diffusion of dissolved minerals may have on rates of decay, pH and peat properties at the base of the peat deposit, and the modelled bog does expand laterally through time. The work in this chapter suggests that, as well as internal rulesets which govern the formation and decay of peat and the movements of water, accurate modelling of peatland spatio-temporal dynamics may require a consideration of the hydrological, ecological and chemical interactions between the growing peat deposit and its surroundings, including mineral soils.

The potential importance of lateral expansion to accurate modelling of peatland dynamics was demonstrated in Chapter 5, and that argument is reinforced by the work presented here. If it is necessary to represent vegetation succession in response to moisture availability, pH,

nutrient availability, *etc.*, as argued above, then it is also necessary to model the lateral expansion of a growing bog, for which the paludification of mineral soils at the edge of the bog is an important process (Anderson *et al*., 2003; Foster *et al*., 1988). Where the peat-mineral soil interface has advanced away from the centre of an expanding domed bog, vegetation composition at any point in the path of the advancing peat front will have undergone succession from mineral-soil bog forest, through lagg fen, to ombrotrophic raised bog. A record of this succession would be left within the peat deposit in terms of the botanical composition, biochemistry and physical structure of the peat. Furthermore, changes in vegetation attributable to an advancing paludification front would cause spatial and temporal changes in the rates of formation of new peat, decay regime, and peat hydrophysical properties (Foster and Wright, 1990; Foster *et al*., 1988), in turn leading to changes in the overall shape of the peat deposit.

6.5. Conclusions

It is clear that the inclusion of a second spatial dimension within the **DigiBog** algorithm caused model predictions to vary greatly from those of the 1-D version. While some differences between the two models are likely attributable to subtle differences in the solutions to the models' equations, the spatial variability of properties and process rates was undoubtedly important.

While **DigiBog** is not the first model to utilise a spatially-distributed, finite-difference approach to modelling peatland dynamics (*cf*. Borren and Bleuten, 2006), the work here is an example of a paradigm shift away from traditional, static, aspatial models such as the BGM and GMH. In particular, the bog profile plots showing K and m distributions (Figures 6.2 and 6.3) demonstrate the excellent ability of the DigiBog framework, if not necessarily the specific model rulesets used here, in predicting and visualising spatio-temporal dynamics in bog development. Predicting and plotting soil properties in profile in this way is a highly powerful visual tool for understanding complex processes.

Several limitations of the complex model, implemented in one dimension in Chapter 5, were not evident until that model was implemented in two dimensions. It would be interesting, therefore, to examine what effects, if any, a similar 2-D treatment would have upon the predictions of other 1-D models of peat accumulation, such as the PDM of Hilbert *et al*. (2000) and the PAM of Frolking *et al*. (2001). DBEH3 produced some odd results, in particular some unrealistic bog shapes with flat central plateaus and large, raised humps at the margin. The two most likely possibilities seem to be that either the conceptual model represented by DBEH3 is flawed, or that real peatlands genuinely do occupy a very narrow area in parameter space. An alternative, although not necessarily exclusive, possibility is that some important processes are still missing from DBEH3's conceptual and algorithmic structure. For example, peat bulk density and effective porosity were assumed to be constants in the current work, but there is strong evidence from the literature that they vary with peat cumulative decomposition or depth (Vorob'ev, 1963; Ivanov, 1981). While the assumption of constant peat density has some empirical support (Borren *et al*., 2004), there is also plentiful evidence to the contrary (*cf*. Johnson *et* al., 1990; Damman, 1988; Kennedy and Price, 2005). Furthermore, the assumption of constant peat density is difficult to justify from first principles, because older, more highly-decayed peat is structurally weaker than

fresh peat. By virtue of its greater depth, old peat is also subject to greater compression due to the weight of overlying material. While the assumption of constant peat bulk density represents a parsimonious starting point for the current work, it may be that this assumption is partly responsible for some of DBEH3's odd predictions. Peat bulk density might be assumed to increase with decreasing *m*, representing the compression of older, weaker peat, in a similar manner to the relationship between *m* and *K*. Then, the large humps at the edge of the modelled bog would likely not have the chance to develop, because they would be compressed by the high decay rates in the oxic zone.

Despite the fact that this work possibly identifies limitations in DBEH3's conceptual model, therein lies arguably the greatest strength of the modelling approach used here. The fact that the spatially-distributed version of the model produced some odd and unrealistic results calls into question the reliability of the conceptual model upon which the computer model is based, and forces a re-examination of the rulesets assumed to represent peatland behaviour. In particular, the equations which describe *p* as a function of water-table depth and *K* as a function of *m* may be need of refinement. It should be remembered, too, that the current model takes no account of high latitude processes such as freezing/thawing and snowmelt, which may have significant effects upon model hydrology and hydrophysics in possible future expansions of the **`DigiBog`** suite.

This early work with the spatially distributed version of DigiBog has generated some fascinating results, and represents, to the author's knowledge, the first model of its kind to predict profiles of multiple peat properties such as age, hydraulic conductivity, and quality. Possibilities for future work with DBEH3 are seemingly plentiful and the modular structure of the program code allows for easy addition of future submodels. In particular, the current inability of the model to predict lateral expansion of a developing peatland, or succession between plant communities in response to changing hydrology and/or soilwater chemistry, have caused DBEH3 to predict some odd results, and these areas seem likely to be most in need of improvement.

The Holocene Peat Model (HPM) currently being developed by Steve Frolking (University of New Hampshire, Durham, NH), Nigel Roulet (McGill University, Montreal, QC) and co-workers will address some of the above issues and is a development of the PAM and the

PDM. The HPM will include continuous succession between plant communities based on water-table depth, and complex, species-abundance-dependent relationships between: water table and rate of new peat formation; water-table position and decay rates; cumulative decay and peat bulk density; peat bulk density and hydraulic properties (N.T. Roulet, pers. comm.). The HPM, while still a 1-D model of a single point at the centre of a bog, in a similar manner to DBEH2, may prove to be more suitable for expansion into two or three spatial dimensions due to its ability to represent a gradient of plant communities. HPM is an alternative approach to that of **DigiBog**, and uses a great deal of empirical data to inform its various algorithmic relationships. By contrast, the approach advocated here is to start with the simplest possible model, and to increase complexity and realism gradually as and when model behaviour suggests that such alterations are necessary. A full critique of the HPM is clearly not possible, however, until the model is formally reported in the public domain. The possibility of a new modelling approach that appears to feature a higher degree of sophistication should certainly not be seen as reason to abandon the **DigiBog** suite, especially given its success thus far in allowing exploration of complex peatland behaviour.

The **DigiBog** approach of starting with the simplest, most minimal model possible, and only gradually increasing complexity, allows identification of peatland system components and scales of consideration which are key to understanding holistic system behaviour (Goldenfeld and Kadanoff, 1999). This approach may be seen as the reason for not having implemented the micro-succession model identified in Figure 1.3 and the conceptual model description given in section *1.4.1*. Many interesting findings have been made using DBEH2 and DBEH3, models which do not include micro-succession. Including a micro-succession submodel from the beginning would have prevented comparison against simpler models and would, therefore, have caused a powerful experimental control to be lost. However, the work with DBEH3 presented in this chapter indicates that not all of the essential peatland-system components necessary to a full description of system behaviour have been represented, and that a micro-succession submodel may now be a desirable addition to the model algorithm. This issue is discussed in more detail in Chapter 7.

Chapter 7: Thesis Conclusions

In this the final chapter, the success of the thesis in addressing the aim and objectives identified in Chapter 1 is assessed, before an agenda for future work is presented.

7.1. Success of Thesis in Addressing Aim and Objectives

7.1.1. Hydrological modelling

The work presented in Chapter 2 was generally a very successful area of the thesis, and succeeded in creating a powerful and flexible new hydrological computer model which offers an alternative to Modflow for simulating peatland aquifers. DBH is particularly suited to modelling peatland hydrological behaviour, due to its ability to represent small-scale variability in peat properties. In this respect it is able to overcome certain problems associated with small-scale variation in peat properties which Modflow is subject to (Doherty, 2001). Success is reflected in the model having been commissioned for use in a consultancy project at Cors Fochno (Baird *et al*., 2009).

The main purpose for the construction of DBH, however, was in order to use it as a building block for DBEH1 and DBEH3 (DBEH2 used its own, simple, purpose-built hydrological submodel). The true success of the hydrological model, therefore, should be measured in terms of the success of the ecohydrological models. One possible criticism of the hydrological submodel is that, due to its first-order numerical solution to the Boussinesq Equation, it is prone to numerical instability. DBH therefore requires short timesteps in order to maintain model stability, especially in DBEH3 where high values of hydraulic conductivity were assumed for young peat. All other things being equal, short timesteps lead to longer processing times, meaning that **`DigiBog`** is computationally intensive compared to other, simpler, hydrological models which ignore vertical variations in K, such as those employed by Swanson and Grigal (1988), Couwenberg(2005) and Couwenberg and Joosten (2005). Certainly, the calculation of steady-state water tables is by far the most computationally demanding part of a developmental step in DBEH1 or a timestep in DBEH3. However, it is the detailed and comprehensive treatment of groundwater hydrology adopted in this thesis which led to one of its most important findings. Without a careful and thoughtful approach to hydrology, the ponding model would likely not have been run to a genuine steady state, and so the finding of its failure to predict patterning in steady-state would likely not have been made.

7.1.2. Peatland patterning modelling

Chapter 3 presented an in-depth and largely successful exploration of a variety of patterning models, and DBEH1 is the only model in the thesis that incorporates a micro-

succession submodel, which was identified as a potentially key linkage in the conceptual model of peatland dynamics in section *1.4.1.* (see also Figure 1.3). While none of the patterning models presented in the thesis was able to offer an improvement over the existing nutrient-scarcity model of Rietkerk *et al*. (2004a, b), this is an important and original finding in itself and should certainly not be viewed as a failure of the current work. The modified ponding model, the water-scarcity model, and the ponding model with ecological memory were all developed from justifiable first principles, with the hypothesis that they would predict stable, realistic, across-slope striped patterning under steady-state hydrology. The recognition that none of the new models was able to predict such patterning may be thought of as the adoption of the null hypotheses.

Possibly the most intriguing and important finding from Chapter 3 is that the revised ponding model did not predict across-slope stripes in the manner reported by Swanson and Grigal (1988), Couwenberg (2005) and Couwenberg and Joosten (2005). It is not entirely clear why previous authors reported that the steady-state ponding model predicted patterning under steady-state behaviour. However, the fact that the model predicts strong, closely-spaced, across-slope stripes under non-steady hydrology, and that these stripes move rapidly downslope, is strongly suggestive that those previous authors had used a non-conservative steady-state criterion.

7.1.3. Laboratory investigation of the controls on peat hydraulic conductivity

The work presented in Chapter 4 represents arguably the least successful area of the thesis. Problems with the work were mainly due to a somewhat inflexible approach to core selection, arising in turn from the author's own inexperience. Unfortunately, these problems meant that the statistical model developed from laboratory data was unsuitable for the parameterisation of DBEH2 and DBEH3. Given that this was the main aim of Chapter 4, it would be easy to judge Chapter 4 as unsuccessful. However, there were a number of interesting and surprising secondary findings from the chapter, meaning that the work may still be viewed as a partial success.

The selection of paired cores introduced a dependency into the data set, in that data from any given hollow location were not independent from the data from the hummock which that hollow was paired with. The binary factorial treatments *habitat* and *position*

introduced a further dependency, in that all data points with the same treatment in either factor were not independent of one another. Furthermore, multiple depth intervals were used from the same cores, introducing yet another, albeit commonly ignored, dependency in the dataset. While these dependencies were all overcome by the use of hierarchical regression modelling, a more problematic issue was that the peat cores were not deep enough to allow comparison of peat from contiguous depths from hummocks and hollows, thereby preventing like for like comparisons for given depth intervals. As a result, the hummock samples almost exclusively represent oxic-zone peat, which is rarely, if ever, subject to saturated flow.

The dependency between data points from different depth intervals within the same core could be overcome by taking only a single sample from each location. This would, however, make data collection much more time-consuming because many more cores would have to be taken in order to generate a dataset of similar size. The dependencies caused by binary treatments such as *hummock* or *hollow* are less easy to overcome, and generally require separate regression models to be developed for each factorial combination of treatments, as implemented in Equations 4.3 and 4.4. However, such dependencies should not be viewed as limitations to a dataset, because they can be overcome using appropriate selection of statistical techniques, the adoption of which means that fieldwork can be conducted more efficiently.

While measurement of hydraulic conductivity K was relatively straightforward and was undertaken using reliable methods (*cf.* Beckwith *et al*., 2003a; Surridge *et al*., 2005), the estimation of m proved much more challenging, and the reliability of using C to N ratios for this purpose is not clear. In section *7.2.3.*, below, a number of alternative methods are suggested for estimating m in similar studies in future

Nonetheless, Chapter 4 represents what is, to the author's knowledge, the first attempt to predict hydraulic conductivity as a function of peat cumulative decomposition using fully reproducible protocols, and the suggestion of a linear relationship between m and K is intriguing, even if this represents only the nearly-linear beginning of a curve. Furthermore, the unexpected finding of higher near-surface hydraulic conductivity in hummocks than in hollows ($p = 0.002$) is an interesting and original one, even if it was not of direct relevance

to the work in Chapters 5 and 6, and may be used to direct protocols for future work on similar experiments (see section *7.2.3.*, below).

7.1.4. Modelling peat accumulation in 1-D and 2-D

The work presented in Chapters 5 and 6 represents arguably the most successful part of the thesis, despite the fact that the micro-succession submodel was not included, as required by objective (i) identified in section *1.4.2.*

The work showed that the inclusion of extra levels of complexity dramatically alters the predictions of models of peat accumulation. In particular, relationships which describe the rate of formation of new peat as a function of water-table depth, and hydraulic conductivity as a function of peat quality, are of central importance to model predictions, rather than merely adding trivial detail. Similarly, the predictions of the peat accumulation model were significantly altered by the consideration of an extra spatial (plan) dimension in Chapter 6, which allowed the interaction of neighbouring columns via groundwater movements.

The hydrophysical submodel, which describes hydraulic conductivity as a function of peat quality, affords DBEH2 and DBEH3 Type II Strong Memory, as discussed in Chapter 3. Through this mechanism, the individual agents which constitute the complex version of DBEH2 and DBEH3 (*i.e.*, each peat layer) adapt to their own individual histories, as well as the history of the model as a whole.

Chapter 6, more so than Chapter 5, demonstrates the excellent potential for the **DigiBog** approach in not only simulating peatland developmental dynamics, but also for visualising the results of these simulations. In particular, the profile plots from Chapter 6 showing horizontal and vertical distributions of peat cumulative decay, m, explained much about the model's spatio-temporal development.

At least in its current format, the rule-based, high- (spatial) resolution **DigiBog** model suite seems a long way from being of direct use in informing process-based, coarse resolution of models of peatland-atmosphere exchanges of carbon gases, such as those described by Schaphoff *et al*. (2006). However, the current thesis was justified largely on the basis of the role of peatlands in the global carbon cycle (see section *1.1.2.*), so it is only

prudent to mention the place of the current work within the carbon gas debate. Given that they represent peat thickness and include an assumed peat density, DBEH2 and DBEH3 implicitly include a mass-balance scheme for peat. Thus, they predict the rate at which atmospheric carbon is fixed by peatland plants and turned into fresh peat, and the rate at which carbon is returned to the atmosphere by decomposers as both CO_2 (broadly, via oxic decay) and CH_4 (from anoxic decay). DBEH2 and DBEH could, therefore, be altered with a minimum of difficulty to predict peatland carbon balance terms over long timescale, in a similar manner to the model of Frolking *et al.* (2002).

However, as Baird *et al*. (2009) recognise, the land surface schemes (LSS) used in global circulation models (GCMs) have such coarse horizontal resolution (typically 2-3˚ latitude 2-3˚ longitude) that they are currently only able to represent peatlands as uniform 'slabs' of soil in a landscape, and with aspatial 'bucket' hydrology. It may be more helpful, therefore, to think of the disparity between **`DigiBog`**'s high-resolution, spatially-distributed scheme and the requirements of LSSs as a limitation of the latter rather than the former. Chapters 5 and 6 showed how incremental increases in model complexity led to both qualitatively and quantitatively different model behaviours. In the complex model, the inclusion of realistic feedbacks even altered the direction of response of state variables such as bog height and water-table depth to predictors such as anoxic decay rate and net rainfall rate. Therefore, arguably the greatest worth of the work presented in Chapters 5 and 6 lies in demonstrating the potential error associated with the current representation of peatlands as uniform 'bucket-and-slab' landscape units, assumption upon which the findings of the IPCC (Randall *et al.*, 2007) are largely based.

7.2. Agenda for Future Research

7.2.1. Hydrological modelling

The standalone hydrological model, DBH, has application to almost any peatland aquifer, possibly with small alterations to code, so as to represent things like special boundary conditions. The application of DBH to real aquifers may be limited in some cases by the availability of K and s data with which to parameterise the model, but this problem is true of any similar type of model.

One exciting possibility for the future development of DBH involves the implementation of a hexagonal, rather than square, grid, in order to reduce numerical diffusion. In a regular hexagonal grid, any cell has six neighbours, with each of which it shares a boundary of finite length. Unlike **DigiBog**'s square grid, hexagonal cells do not have neighbours with which they only share a vertex. A hexagonal grid would improve the efficiency with which water is able to move through the model and would lead to more accurate water-table depths under the D-F approximation, which may be of use to ecological studies or future ecohydrological models which are sensitive to fine accuracy in water-table position. A hexagonal grid would be more challenging to code and to conceptualise than a square grid, and would possibly cause compatibility problems with input dataset that utilise a more conventional square grid.

The work which simulated Cors Fochno in Chapter 2 demonstrated that the representation of cracks and macropores may be a desirable addition to the DBH code, especially if the model is to be used to simulate degraded peatlands. Macropores can form in peat due to drying, slumping, and cracking, in degraded peatlands. Macropores form highly preferential pathways for flow, and cannot be described using Darcy's law or, therefore, **DigiBog**'s representation of the Boussinesq Equation (Holden, 2009).

One of the main omissions from DBH at present is the lack of any representation of the unsaturated zone. It was judged that, for the purposes of the current work, a representation of saturated hydrology alone would suffice, with certain ecological processes (*i.e.* SL1 transition in Chapter 3, and the calculation of p in Chapters 5 and 6) predicted as functions of depth to the water table. However, there are multiple possibilities for a future representation of the unsaturated zone, as well as multiple reasons why such an inclusion

may be desirable. Unsaturated dynamics could be represented simply using a curvilinear relationship to describe soil wetness in the unsaturated zone as some function of water-table depth (e.g. Hayward and Clymo, 1982; Kettridge and Baird, 2007), or a full consideration of unsaturated flux and storage could be taken, using the Richards Equation (Fetter, 1999).

Simulating peat water content in the unsaturated zone will be of great importance to a planned future study of wildfire in peat soils. The **DigiBog** hydrological model will be used to predict water content in the unsaturated zone in response to antecedent drought conditions. The model will be informed by empirical work currently being conducted by Dan Thompson (McMaster University, Hamilton, ON), Merritt Turetsky and Brian Benscoter (University of Guelph, Guelph, ON) as to how much energy is required to combust peat which possesses a given water content. Using a spatially-distributed grid scheme, such as those employed in Chapters 2, 3 and 6, it is intended to use this new **DigiBog** model to predict the areal extent and depth of peat that would burn during a fire of a given heat. In this way, DBH will again form the building blocks for another **DigiBog** model.

In addition to modelling the spread of wildfire in peat soils, the accurate modelling of peat water content in the unsaturated zone may be of use in future ecohydrological models. Particularly in tall hummocks, which are elevated several decimetres above the surrounding water table (Nungesser, 2003), live vegetation draws up water for photosynthesis from the unsaturated zone (Rydin and Jeglum, 2006). Representing this important zone with greater fidelity than the simple water-table depth scheme in Chapters 3, 5 and 6 may prove necessary to future models which predict plant community succession, partially-oxic decay (*cf.* Clymo and Bryant, 2008), and rates of plant productivity.

7.2.2. Peatland patterning

A number of possibilities for future work on understanding peatland patterning were mentioned in the conclusions to Chapter 3 (see section **3.6.**, above). These include a number of new cellular computer models, some based on the **DigiBog** architecture.

One interesting possibility for future work on patterning would involve a field study of peatland macrofossil records, in an attempt to falsify the predictions of downslope movement of patterning made by the non-steady-state ponding model. If SL2 units were migrating consistently downslope then a plant macrofossil record of the previous locations of hummocks and hollows would be left in the peat deposit. While it was claimed at the end of Chapter 3 that the non-steady-state ponding model should be abandoned based on the evidence of the current modelling work, strong field evidence in favour of downslope pattern migration would force a reassessment of that claim.

It may be that the currently popular approach to peatland patterning modelling, where patterning entities are superimposed onto a static peat landform and self-organise in two dimensions, is not the most appropriate. It may be that the most accurate model of peatland patterning requires the peatland as a whole, and its constituent hummocks, hollows and lawns to grow and decay autonomously. That is, the incorporation of a micro-succession model into the existing DBEH3 may lead to realistic peatland patterning, with community-dependent relationships between moisture availability, productivity and decay, and changes in peat hydrophysical properties. Such an approach may lead to the unification of models of peat accumulation and peatland patterning, because in such a model scheme, the modelling of each of those two aspects of peatland dynamics would necessarily require a consideration of the other.

7.2.3. Controls on peat hydraulic conductivity

Many possibilities present themselves for the improvement and expansion of the current work. One of the main challenges associated with the work presented in Chapter 4, aside from the oversights with regard to core selection, arose from difficulties in estimating proportional mass remaining, *m*. One of the most obvious areas for future work on this topic, therefore, should be to develop a reliable and reproducible method for estimating *m*.

An alternative biogeochemical approach, as mentioned at the end of Chapter 4, would be to adopt the method of Turetsky *et al*. (2008), in which the ratio of metabolic to structural carbohydrates is used to estimate *m*. Still another biogeochemical technique was presented by Davydik (1987), in which the degree of decomposition of a peat sample is calculated from the concentrations of elemental carbon and oxygen. The method is based on the

assumption that the C to O ratio increases with cumulative decay of organic matter. The possibility of using a microtomographic scanner to estimate stem lengths, thereby reducing user error in the stem-length method (Johnson *et al*., 1990), was also mentioned at the end of Chapter 4. However, the problem of species identification, especially in well-decomposed samples, would still limit the method's application to highly-decomposed samples.

A range of methods for estimating *m*, including those mentioned above, and others such as the von Post scale (von Post and Granlund, 1926), the fibre content (Boelter, 1969) method, and the C:N method used in Chapter 4 could be assessed using laboratory analyses of peat samples which had undergone a known, and possibly manipulated, amount of decomposition. It may be that the von Post scale, for example, does indeed exhibit a linear relationship with cumulative decay. Samples of fresh peat (*i.e.*, those with close to unity proportional remaining mass) might be incubated or chemically treated so as to accelerate decomposition to chosen levels. A comparison of the various methods could then be conducted, by comparing the estimated values of *m* to the known manipulated values of *m*. The incubation of peat samples at high temperatures, as well as chemical treatments would, however, likely result in biases in the estimates of *m* generated using chemical analyses. This work is currently only at a concept stage, but could prove an exciting pathway to devising reliable, reproducible and widely-available protocols for the laboratory determination of *m*.

7.2.4. Modelling peat accumulation

The modelling of peat accumulation over long timescales represents arguably the most exciting area for future work that the current thesis has highlighted, with the widest range of possibilities. Work in both Chapters 5 and 6 is strongly suggestive that accurate modelling of peat accumulation requires a consideration of lateral expansion of the peatland. Currently, DBEH3 does not feature a submodel which can predict the lateral expansion of a bog, and the lateral expansion submodel for DBEH2 reported in section **5.5**., above, is likely oversimplified and is not physically-based. Existing studies have indicated that lateral expansion is not a simple process, nor one which can be easily described using generally applicable rulesets (Anderson *et al*., 2003).

One of the most exciting possibilities for future work involves the inclusion of a third spatial dimension to the **DigiBog** model of long-term peat accumulation. While the 2-D profile modelling with DBEH3 (see Chapter 6) generated some interesting findings, the model is still a highly idealised representation, and is therefore abstract in a way which prevents an accurate representation of real peatlands.

The inclusion of the third spatial dimension would have little additional effect to that of the second spatial dimension (as in DBEH3), without plan (x, y) variation in initial conditions, bottom topography, or an irregularly-shaped boundary, so as to lead to rates of peat accumulation and water-table behaviour which were initially spatially non-uniform. For instance, variable bottom topography would allow peat to grow up and out of small-scale depression in the mineral substrate where runoff collects. Small, isolated patches of peat would be modelled to initiate in the depressions (*cf*. Belyea and Baird, 2006; Anderson *et al*., 2003) and these small, proto-peatlands would accumulate vertically in a manner similar to DBEH3, but they would also expand laterally onto the surrounding mineral soil. Clearly, the lateral expansion of each patch of peat would require the development of a suitable ruleset (see above). One of the main issues associated with the representation of a laterally expanding bog is the movement of model boundaries, currently not possible within the **DigiBog** scheme.

Through variable bottom topography and/or initial conditions, the modelled rates and nature of peat accumulation would become spatially heterogeneous, in a manner more complex than simply a monotonic decrease in bog height with proximity to the margin (see Figures 6.4a). The representation of distinct plant communities (as opposed to a continuous productivity curve to represent the entire spectrum of peatland species, such as that used in Chapters 5 and 6: see Equation 5.3) would introduce a further set of interesting feedbacks, the effects of which are almost entirely unforeseeable at this stage due to the complex nature of the model. It is through this scheme that the unification of peatland patterning models and peat accumulation models, as mentioned in section *7.2.2.*, above, may occur. Under such a model scheme, individual hummocks, hollows and lawns would grow up out of the digitised bog surface, and possibly self organise into patterns. The development of a unified model of peatland dynamics represents the ultimate goal for the work begun in this thesis.

There are a number of types of peatland aside from temperate, northern-hemisphere raised bogs which, in its current format, **DigiBog** is not capable of simulating. Examples of such systems include tropical raised bogs, minerotrophic fens, and high-latitude peatlands with permafrost. The representation of each would begin with a 1-D consideration of the new system (in the style of DBEH2), before spatial variability was included (like in DBEH3). The representation of tropical raised bogs and minerotrophic fens would require new relationships between: i) water-table depth and p, because the one given in Equation 5.3 describes the raised bog species examined by Belyea and Clymo (2001); and ii) cumulative decay and hydraulic conductivity, because the one given in Equation 5.4 was parameterised so as to represent temperate raised bog peat. The parameterisation of **DigiBog** to represent minerotrophic fens should not prove overly challenging, because the literature contains plentiful data on parameters such as decay rates and long term rates of peat accumulation in fens (see, for example: Yu *et al*., 2003; Farrish and Grigal, 1988).

Tropical raised bogs are, in common with northern peatlands, highly concentrated and possibly fragile carbon stores in south-eastern Asia, South America and Oceania, and many are under severe pressure from deforestation, drainage and fire (Page *et al*., 2002). Process rates in tropical raised bogs are much less well documented than in northern peatlands, although the works of Page *et al*. (2004) and Chimner (2004) may be taken as starting points for parameterising **DigiBog** to represent these important systems.

High-latitude peatlands with permafrost, as well as those which receive a large proportion of their annual precipitation as snowfall, present hydrological situations that the **DigiBog** algorithmic structure is currently not capable of representing. Peatlands which receive high annual snowfall possess what may be conceptualised as an above-ground store of water as a layer of snow accumulates above the peat surface during the winter, and which is suddenly added to the aquifer during spring snowmelt. **DigiBog** could easily be altered so as to represent a temporally-variable net rainfall rate, such as the seasonal addition of snow meltwater. A surficial snow would, however, create a frost table, thereby reducing permeability of the frozen layers. As such, a thermal model would also be required, so as

to account for the phase changes in groundwater at different depths. A similar problem arises when one considers the representation of permafrost.

To conclude, then, while the work on DBEH3 in Chapter 6 produced some fascinating results, these seem likely to represent just the beginning for the spatially-distributed modelling of long-term peatland dynamics.

Acknowledgements

Firstly I must thank my supervisors, Andy Baird and Lisa Belyea, for all of their time, advice and encouragement during the last four years.

This project was funded principally by a Queen Mary, University of London studentship. Andy Baird also provided financial assistance via the use of a separate research account for the purchase of equipment, travel and subsistence on multiple occasions.

The hierarchical regression model presented in Chapter 4 was developed by Islay Gemmell of Remstat Consultants using primary laboratory data supplied by the author.

Professional acknowledgements also go to Simon Dobinson, Laura Shotbolt, Håkan Rydin, and Ed Oliver.

Uppland County Council, Sweden, granted my permission to conduct two weeks of fieldwork on the Ryggmossen nature reserve and raised bog, during September 2006.

On a personal note, I must thank all of my postgraduate colleagues at Queen Mary – in particular my office mates, Steve Forden and Imelda Stamp – for their role in making my three years in London an enjoyable and sociable time.

Thanks to Trevor and Ruth Collins for allowing me to live and work in their beautiful home while I wrote the thesis.

Thanks to my mum Val for her love, support and encouragement during the past four years, as ever, as well as for her considerable financial assistance towards the end of the project. And yes, Mum, I promise this is the end of the studying now.

Lastly but by no means least, I must thank Michelle for her unfailing love, support and confidence in me, as well as for her assistance in the office and the laboratory, including some very late nights coating cubes of Swedish peat in paraffin wax, proof reading my thesis chapters, and for keeping me organised, sane and smiling.

References

Aaviksoo, K., Ilomets, M. and Zobel, M. (1993) Dynamics of mire communities: a Markovian approach (Estonia). In: Patten, B.C., Jørgensen, S.E. and Dumont, H. (Editors), *Wetlands and Shallow Continental Water Bodies*, Volume 2: Case Studies, SPB Academic Publishing, The Hague, pp. 23-43.

Abbot, R. (2006) Emergence explained: abstractions, *Complexity*, **12**, 13-26.

Aber, J. S. and Aber, S. W. (2001) Potential of kite aerial photography for peatland investigations with examples from Estonia, *Suo*, **52**, 45-56.

Aber, J. S., Aaviksoo, K., Karofeld, E. and Aber, S. W. (2002) Patterns in Estonian bogs as depicted in color kite aerial photographs, *Suo*, **53**, 1-15.

Ågren, G. I. and Bosatta, E. (1996) Quality: a bridge between theory and experiment in soil organic matter studies, *Oikos*, **76**, 522-528.

Almendinger, J. E. and Leete, J. H. (1998) Regional and local hydrogeology of calcareous fens in the Minnesota River Basin, USA, *Wetlands*, **18**, 184-202.

Almquist-Jacobson, H. and Foster, D. R. (1995) Toward an integrated model for raised bog development: theory and field evidence, *Ecology*, **76**, 2503-2516.

Alonso-Sanz, R. (2007) A structurally dynamic cellular automaton with memory in the triangular tessellation, *Complex Systems*, **17**, 1-15.

Anderson, R. L., Foster, D. R. and Motzkin, G. (2003) Integrating lateral expansion into models of peatland development in temperate New England, *Journal of Ecology*, **91**, 68-76.

Armstrong, A. C. (1995) Hydrological model of peat-mound form with vertically varying hydraulic conductivity, *Earth Surface Processes and Landforms*, **20**, 473-477.

Austin, P. C., Goel, V. and van Walraven, C. (2001) An introduction to multilevel regression models, *Revue Canadienne de Santé Publique*, **92**, 150-154.

Backéus, I. (1972) Bog vegetation re-mapped after sixty years: Studies on Skagershultamossen, central Sweden, *Oikos*, **23**, 384-393.

Baird, A. J., Belyea, L. R. and Morris, P. J. (2009) Upscaling peatland-atmosphere fluxes of carbon gases: small-scale heterogeneity in process rates and the pitfalls of 'bucket-and-slab' models. In: Baird, A. J., Belyea, L. R., Comas, X., Reeve, A. and Slater, L. (eds) *Northern Peatlands and Carbon Cycling*, American Geophysical Union Monograph.

Baird, A. J., Eades, P. A. and Surridge, B. J. W. (2008) The hydraulic structure of a raised bog and its implications for ecohydrological modelling of bog development, *Ecohydrology*, **1**, 289-298.

Baird, A. J., Eades, P. A., Surridge, B. W. J., and Harris, A. (2006) Cors Fochno Hydrological Research and Management Study: Final Report of Theme 1. Report No. 718, Countryside Council for Wales Contract Science, Bangor, 74 pp.

Barber, K. E. (1981) *Peat Stratigraphy and Climate Change: A Palaeoecological Test of the Theory of Cyclic Peat Bog Regeneration*, Balkema, Rotterdam, 219 pp.

Beckwith, C. W., Baird, A. J. and Heathwaite, A. L. (2003a) Anisotropy and depth-related heterogeneity of hydraulic conductivity in bog peat. I: laboratory measurements, *Hydrological Processes*, **17**, 89-101.

Beckwith, C. W., Baird, A. J. and Heathwaite, A. L. (2003b) Anisotropy and depth-related heterogeneity of hydraulic conductivity in bog peat. II: modelling the effects on groundwater flow, *Hydrological Processes*, **17**, 103-113.

Beltrami, E. and Carroll, T. O. (1994) Modeling the role of viral disease in recurrent phytoplankton blooms, *Journal of Mathematical Ecology*, **32**, 857-863.

Belyea, L. R. (2007) Climatic and topographic limits to the abundance of bog pools, *Hydrological Processes*, **21**, 675-687

Belyea, L. R. and Baird, A. J. (2006) Beyond "the limits to peat bog growth": cross-scale feedback in peatland development, *Ecological Monographs*, **76**, 299-322.

Belyea, L. R. and Clymo, R. S. (2001) Feedback control of the rate of peat formation, *Proceedings of the Royal Society of London B*, **268**, 1,315-1,321.

Belyea, L. R. and Lancaster, J. (2002) Inferring landscape dynamics of bog pools from scaling relationships and spatial patterns, *Journal of Ecology*, **90**, 223-234.

Belyea L. R. and Malmer N. (2004) Carbon sequestration in peatland: patterns and mechanisms of response to climate change, *Global Change Biology*, **10**, 1,043-1,052.

Belyea, L. R. and Warner, B. G. (1996) Temporal scale and the accumulation of peat in a *Sphagnum* bog, *Canadian Journal of Botany,* **74**, 366-377.

Betró, B. and Ladelli, L. (1990) A Markov chain model for traffic queue evolution at an intersection, *Stochastic Models*, **6**, 367-382.

Blundell, A., Charman, D. J., and Barber, K. (2008) Multiproxy late Holocene peat records from Ireland: towards a regional palaeoclimate curve, *Journal of Quaternary Science*, **23**, 59-71.

Boelter, D. H. (1969) Physical properties of peats as related to degree of decomposition, *Soil Science Society of America Journal*, **33**, 606-609.

Borren, W. and Bleuten, W. (2006) Modelling Holocene carbon accumulation in a western Siberian watershed mire using a three-dimensional dynamic modelling approach, *Water Resources Research*, **42**, W12413, doi:10.1029/2006WR004885

Bragazza, L. and Gerdol, R. (1996) Response surfaces of plant species along water-table depth and pH gradients in a poor mire on the southern Alps (Italy), *Annales Botanici Fennici*, **33**, 11-20.

Bubier, J. L. (1995) The relationship of vegetation to methane emission and hydrochemical gradients in northern peatlands, *Journal of Ecology*, **83**, 403–420.

Bubier, J., Costello, A., Moore, T. R., Roulet, N. T. and Savage, K. (1993) Microtopography and methane flux in boreal peatlands, northern Ontario, Canada, *Canadian Journal of Botany*, **71**, 1056–1063.

Bubier, J. L., Moore, T. R., Bellisario, L., Comer, N. T. and Crill, P. M. (1995) Ecological controls on methane emissions from a northern peatland complex in the zone of discontinuous permafrost, Manitoba, Canada, *Global Biogeochemical Cycles*, **9**, 455–470.

Charman, D. J., Blundell, A., Chiverrell, R. C., Hendon, D. and Langdon, P. G. (2006) Compilation of non-annually resolved Holocene peatland palaeo-water table reconstructions from northern Britain, *Quaternary Science Reviews*, **25**, 336-350.

Charman, D. J., Hendon, D. and Packman, S. (1999) Multiproxy surface wetness records from replicate cores on an ombrotrophic mire: implications for Holocene palaeoclimate records, *Journal of Quaternary Science*, **14**, 451-463.

Childs, E. C. and Youngs, E. G. (1961) A study of some three-dimensional field-drainage problems, *Soil Science*, **92**, 15-24

Chimner, R. A. (2004) Soil respiration rates of tropical peatlands in Micronesia and Hawaii, *Wetlands*, **24**, 51-56.

Clymo, R. S. (1992) Models of peat growth, *Suo*, **43**, 127-136.

Clymo, R. S. (1984) The limits to peat bog growth, *Philosophical Transactions of the Royal Society of London*, **B303**, 605-654.

Clymo, R. S. and Bryant, C. L. (2008) Diffusion and mass flow of dissolved carbon dioxide, methane, and dissolved organic carbon in a 7-m deep raised peat bog, *Geochemica et Cosmochimica Acta*, **72**, 2048-2066.

Clymo, R. S. and Hayward, P. M. (1982) The ecology of *Sphagnum*, in Smith, A. J. E. (ed), *Bryophyte Ecology*, Chapman and Hall, London, 511 pp.

Comas, X., Slater, L. and Reeve, A. (2005) Stratigraphic controls on pool formation in a domed bog inferred from ground penetrating radar (GPR), *Journal of Hydrology*, **315**, 40-51.

Comas, X., Slater, L. and Reeve, A. (2004) Geophysical evidence for peat basin morphology and stratigraphic controls on vegetation observed in a Northern Peatland, *Journal of Hydrology*, **295**, 173-184.

Cook, B. I., Bonan, G. B., Levis, S. and Epstein, H. E. (2008) The thermoinsulation effect of snow cover within a climate model, *Climate Dynamics*, **31**, 107-124.

Couwenberg, J. (2005) A simulation model of mire patterning – revisited, *Ecography*, **28**, 653-661.

Couwenberg, J. and Joosten, H. (2005) Self-organization in raised bog patterning: the origin of microtope zonation and mesotope diversity, *Journal of Ecology*, **93**, 1,238-1,248.

Damman, A. W. H. (1988) Regulation of nitrogen and retention in *Sphagnum* bogs and other peatlands, *Oikos*, **51**, 291-305.

Davydik, I. I. (1987) An approach to the determination of the state of decomposition of peat and other organic substances, *International Peat Journal*, **2**, 19-27.

Dise, N. B., Gorham, E. and Verry, E. S. (1993) Environmental factors controlling methane emissions from peatlands in northern Minnesota, *Journal of Geophysical Research*, **98 (D6)**, 10,583-10,594.

Doherty, J. (2001) Improved calculations for dewatered cells in Modflow, *Ground Water*, **39**, 863-869.

Dutta, K., Schuur, E. A. G., Neff, J. C. and Zimov, S. A. (2006) Potential carbon release from permafrost soils of Northeastern Siberia, *Global Change Biology*, **12**, 2,336-2,351.

E-Daoushy, F., Tolonen, K. and Rosenberg, R. (1982) Lead ^{210}Pb and moss-increment dating of two Finnish *Sphagnum* hummocks, *Nature*, **296**, 429.

Eppinga, M. B., Rietkerk, M., Borren, W., Lapshina, E. D., Bleuten, W. and Wassen, M. J. (2008) Regular surface patterning of peatlands: Confronting theory with field data, *Ecosystems*, **11**, 520-536.

Farrish, K. W. and Grigal, D. F. (1988), Decomposition in an ombrotrophic bog and a minerotrophic fen in Minnesota, *Soil Science*, **145**, 353-358.

Fetter, C. W. (1999) *Contaminant Hydrogeology*, 2nd edition, Prentice Hall, New Jersey, 500 pp.

Foster, D. R. and Fritz, S. C. (1987) Mire development, pool formation and landscape processes on patterned fens in Dalarna, central Sweden, *Journal of Ecology*, **75**, 409-437.

Foster, D. R. and Wright, H. E. Jr. (1990) Role of ecosystem development and climate change in bog formation in central Sweden, *Ecology*, **71**, 450-463.

Foster, D. R., Wright, H. E. Jr., Thelaus, M. and King, G. A. (1988) Bog development and landform dynamics in central Sweden and south-eastern Labrador, Canada, *Journal of Ecology*, **76**, 1164-1185.

Freeze, R. A. and Cherry, J. A. (1979) *Groundwater*, Prentice Hall, Englewood Cliffs, New Jersey, 604 pp.

Frey, K. E. and Smith, L. C. (2005) Amplified carbon release from vast West Siberian peatlands by 2100, *Geophysical Research Letters*, **32**, L09401, doi:10.1029/2004GL022025

Frolking, S., Roulet, N. T., Moore, T. R., Richard, Lafleur, P. M., Bubier, J. L. and Crill, P. M. (2002) Modeling seasonal to annual carbon balance of Mer Bleue Bog, Ontario, Canada, *Global Biogeochemical Cycles*, **16**, doi: 10.1029/2001GB001457

Frolking, S., Roulet, N. T., Moore, T. R., Richard, P. J. H., Lavoie, M. and Muller, S. D. (2001) Modelling northern peatland decomposition and peat accumulation, *Ecosystems*, **4**, 479-498.

Gallagher, R. and Appenzeller, T. (1999) Beyond Reductionism, *Science*, **284**, 79.

Gelman, A. (2005) Multilevel (hierarchical) modeling: what it can and can't do, (unpublished research paper).

Gilmer, A. J. (2001) *Carbon Cycling in a Developing Fen-raised Bog Complex: A Modelling Approach*, PhD Thesis, National University of Ireland, University College Dublin, Faculty of Engineering and Architecture, Department of Agricultural and Food Engineering, Earlsfort Terrace, Dublin, Ireland.

Givelet, N., Le Roux, G., Cheburkin, A., Chen, B., Frank, J., Goodsite, M. E., Kempter, H., Krachler, M., Noernberg, T., Rausch, N., Rheinberger, S., Roos-Barraclough, F., Sapkota, A., Scholz, C. and Shotyk, W. (2004) Suggested protocol for collecting, handling and preparing peat cores and peat samples for physical, chemical,

mineralogical and isotopic analyses, *Journal of Environmental Monitoring*, **6**, 481-492.

Goldenfeld, N. and Kadanoff, L. P. (1999) Simple lessons from complexity, *Science*, **284**, 87-89.

Gorham, E. (1991) Northern peatlands: role in the carbon cycle and probable responses to climatic warming, *Ecological Applications*, **1**, 182-195.

Gorham, E., Bayley, S. E. and Schindler, D. W. (1984) Ecological effects of acid deposition upon peatlands – a neglected field in acid-rain research, *Canadian Journal of Fisheries and Aquatic Sciences*, **41**, 1,256-1,268.

Grimm, V., Revilla, E., Berger, U., Jeltsch, F., Mooij, W. M., Railsback, S. F., Thulke, H., Weiner, J., Wiegand, T. and DeAngelis, D. L. (2005) Pattern-oriented modeling of agent-based complex systems: lessons from ecology, *Science*, **310**, 987-991.

Hastings, A. and Powell, T. (1991) Chaos in a three-species food chain, *Ecology*, **72**, 896-903.

Hayward, P. M. and Clymo, R. S. (1982) Profiles of water content and pore size in *Sphagnum* and peat, and their relation to peat bog ecology, *Proceedings of the Royal Society of London. Series B, Biological Sciences*, **215**, 299–325

Hilbert, D. W., Roulet, N. and Moore, T. (2000) Modelling and analysis of peatlands as dynamical systems, *Journal of Ecology*, **88**, 230-242.

Hilborn, R. C. (2004) Sea gulls, butterflies and grasshoppers: A brief history of the butterfly effect in nonlinear dynamics, *American Journal of Physics*, **72**, 425-427.

Hoag, R. S. and Price, J. S. (1997) The effects of matrix diffusion on solute transport and retardation in undisturbed peat in laboratory columns, *Journal of Contaminant Hydrology*, **28**, 193-205.

Holden, J. (2009) Flow through macropores of different size classes in blanket peat, *Journal of Hydrology*, **364**, 342-348.

Hughes, P. D. M. (2000) A reappraisal of the mechanisms leading to ombrotrophy in British raised mires, *Ecology Letters*, **3**, 7-9.

Hughes, P. D. M., Mauquoy, D., Barber, K. E. and Langdon, P. G. (2000) Mire-development pathways and palaeoclimatic records from a full Holocene peat archive at Walton Moss, Cumbria, England, *The Holocene*, **10**, 465-479.

Ingram, H. A. P. (1987) Ecohydrology of Scottish peatlands, *Transactions of the Royal Society of Edinburgh: Earth Sciences*, **78**, 287-296

Ingram, H. A. P. (1982) Size and shape in raised mire ecosystems: a geophysical model, *Nature*, **297**, 300-303.

Ingram, H. A. P. (1978) Soil layers in mires: function and terminology, *Journal of Soil Science*, **29**, 224-227.

Ivanov, K. E. (1981) *Water Movement in Mirelands*, translated from Russian by Thompson, A. and Ingram, H. A. P., Academic Press, London.

Johns, T. C., Carnell, R. E., Crossley, J. F., Gregory, J. M., Mitchell, J. F. B., Senior, C. A., Tett, S. F. B. and Wood, R. A. (1997) The second Hadley Centre coupled ocean-atmosphere GCM: Model description, spinup and validation, *Climate Dynamics*, **13**, 103-134.

Johnson, L. C., Damman, A. W. H. and Malmer, N. (1990) *Sphagnum* macrostructure as an indicator of decay and compaction in peat cores from an ombrotrophic south Swedish peat-bog, *Journal of Ecology*, **78**, 633-647.

Kennedy, G. W. and Price, J. S. (2005) A conceptual model of volume-change controls on the hydrology of cutover peats, *Journal of Hydrology*, **302**, 13-27.

Kettridge, N. and Baird, A. J. (2007) In situ measurements of the thermal properties of a northern peatland: Implications for peatland temperature models, *Journal of Geophysical Research*, **112**, F2, F02019, doi:10.1029/2006JF000655.

Kettridge, N. and Binley, A. (2008) X-ray computed tomography of peat soils: measuring gas content and peat structure, *Hydrological Processes*, **22**, 4,827-4,837.

Khan, I. H. (2005) *Textbook of Geotechnical Engineering*, 2nd edition, Prentice Hall of India, New Delhi, 466 pp.

Klinger, L. F., Taylor, J. A. and Franzen, L. G. (1996) The potential role of peatland dynamics in ice-age initiation, *Quaternary Research*, **45**, 89-92.

Koutaniemi, L. (1999) Twenty-one years of string movements on the Liippasuo aapa mire, Finland, *Boreas*, **28**, 521-530.

Lapen, D. R., Price, J. S. and Gilbert, R. (2005) Modelling two-dimensional steady-state groundwater flow and flow sensitivity to boundary conditions in blanket peat complexes, *Hydrological Processes*, **19**, 371-386.

Larsen, L. G., Harvey, J. W. and Crimaldi, J. P. (2007) A delicate balance: Ecohydrological feedbacks governing landscape morphology in a lotic peatland, *Ecological Monographs*, **77**, 591-614.

Levin, S. A. (1998) Ecosystems and the biosphere as complex adaptive systems, *Ecosystems*, **1**, 431-436.

Lewin, R. (2000) *Complexity: Life at the Edge of Chaos*, 1st edition, University of Chicago Press, 242 pp.

MacDonald, G. M., Beilman, D. W., Kremenetski, K. V., Sheng, Y., Smith, L. C. and Velichko, A. A. (2006) Rapid early development of circumpolar peatlands and atmospheric CH_4 and CO_2 variations, *Science*, **314**, 285-288.

Malmer, N. and Holm, E. (1984) Variation in the C/N-quotient of peat in relation to decomposition rate and age determination with ^{210}Pb, *Oikos*, **43**, 171-182.

Malmer, N. and Wallén, B. (2004) Input rates, decay losses and accumulation rates of carbon in bogs during the last millennium: internal processes and environmental changes, *The Holocene*, **14**, 111-117.

McDonald, M. G. and Harbaugh, A. W. (2005) A modular three-dimensional finite-difference ground-water flow model, [online], *U.S. Geological Survey, Techniques of Water-Resource Investigations, Book 6, Chapter A1*, http://pubs.usgs.gov/twri/twri6a1/html/pdf.html, accessed 31st January 2007.

McDonald, M. G. and Harbaugh, A. W. (2003) The history of MODFLOW, *Ground Water*, **41**, 280-283.

McDonald, M. G. and Harbaugh, A. W. (1984) A modular three-dimensional finite-difference ground-water flow model, U.S. Geological Survey Open-File Report 83-875.

Merlis, T. M. and Khatiwala, S. (2008) Fast dynamical spin-up of ocean general circulation models using Newton-Krylov methods, *Ocean Modelling*, **21**, 97-105.

Moore, T. R., Roulet, N. T. and Waddington, J. M. (1998) Uncertainty in predicting the effect of climatic change on the carbon cycling of Canadian peatlands, *Climatic Change*, **40**, 229-245.

Nungesser, M. K. (2003) Modelling microtopography in boreal peatlands: hummocks and hollows, *Ecological Modelling*, **165**, 175-207.

Ours, D. P., Siegel, D. I. and Glaser, P. H. (2007) Chemical dilation and the dual porosity of humified bog peat, *Journal of Hydrology*, **196**, 348-360.

Page, S. E., Siegert, F., Rieley, J. O., Boehm, H-D. V., Jaya, A. and Limin, S. H. (2002) The amount of carbon released from peat and forest fires in Indonesia in 1997, *Nature*, **420**, 61-65.

Page, S. E., Wüst, R.A. J., Weiss, D., Rieley, J. O., Shotyk, W. and Limin, S. H. (2004) A record of Late Pleistocene and Holocene carbon accumulation and climate change from an equatorial peat bog (Kalimantan, Indonesia): implications for past, present and future carbon dynamics, *Journal of Quaternary Science*, **19**, 625-625.

Payette, S., Delwaide, A., Caccianiga, M. and Beauchemin, M. (2004) Accelerated thawing of subarctic peatland permafrost over the last 50 years, *Geophysical Research Letters*, **31**, L18208, doi:10.1029/2004GL020358

Peterson, G. D. (2002) Contagious disturbance, ecological memory, and the emergence of landscape pattern, *Ecosystems*, **5**, 329-338.

Pfitzner, J. (1976) Poiseuille and his law, *Anaesthesia*, **31**, 273-275.

Price, J. S., Cagampan, J. and Kellner, E. (2005) Assessment of peat compressibility: is there an easy way? *Hydrological Processes*, **19**, 3,469-3,475.

Randall, D. A., Wood, R. A. Bony, S., Colman, R. Fichefet, T., Fyfe, J., Kattsov, V., Pitman, A., Shukla, J., Srinivasan, J., Stouffer, R. J., Sumi, A., and Taylor, K. E. (2007) Cilmate models and their evaluation, in Solomon, S., Qin, D., Manning, M., Chen, Z., Marquis, M., Averyt, K. B., Tignor, M., and Miller, H.L. (eds.) *Climate Change 2007: The Physical Science Basis. Contribution of Working Group I to the Fourth Assessment Report of the Intergovernmental Panel on Climate Change*, Cambridge University Press, Cambridge.

Reeve, A. S., Siegel, D. I. and Glaser, P. H. (2000) Simulating vertical flow in large peatlands, *Journal of Hydrology*, **227**, 207-217.

Rietkerk, M., Dekker, S. C., Wassen, M. J., Verkoost, A. W. M. and Bierkens, M. F. P. (2004a) A putative mechanism for bog patterning, *The American Naturalist*, **163**, 699-708.

Rietkerk, M., Dekker, S. C., de Ruiter, P. C. and van de Koppel, J. (2004b) Self-organised patchiness and catastrophic shifts in ecosystems, *Science*, **305**, 1,926-1,929.

Riutta, T., Laine, J., Aurela, M., Rinne, J., Vesala, T., Laurila, T., Haapanala, S., Pihlatie, M. and Tuittila, E. S. (2007a) Spatial variation in plant community functions regulates carbon gas dynamics in a boreal fen ecosystem, *Tellus*, **B59**, 838-852.

Riutta, T., Laine, J. and Tuittila, E. S. (2007b) Sensitivity of CO_2 exchange of fen ecosystem components to water level variation, *Ecosystems*, **10**, 718-733.

Robröek, B. J. M., Limpens, J., Breeuwer, A. and Schouten, M. G. C. (2007a) Effects of water level and temperature on four *Sphagnum* mosses, *Plant Ecology*, **190**, 97-107.

Robröek, B. J. M., Limpens, J., Breeuwer, A., Crushell, P. H. and Schouten, M. G. C. (2007b) Interspecific competition between *Sphagnum* mosses at different water tables, *Functional Ecology*, **21**, 805-812.

Rycroft, D. W., Williams, D. J. A. and Ingram, H. A. P. (1975) The transmission of water through peat: I. Review, *Journal of Ecology*, **63**, 535-556.

Rydin, H., Gunnarsson, U. and Sundberg, S. (2002) Field guide – Swedish mires, in Thingsgaard, K. and Flatberg, K. I. (eds) *Third international symposium on the biology of* Sphagnum*, Uppsala-Trondheim, August 2002: excursion guide*, Norges teknisk-naturvitenskaplige universitet, Vitenskapmuseet, Rapport Botanisk Serie 2002-2.

Rydin, H. and Jeglum, J. K. (2006) *The Biology of Peatlands*, 1st edition, Oxford University Press, Oxford, UK, 360 pp.

Rydin, H. and McDonald, A, J. S. (1985a) Tolerance of *Sphagnum* to water level, *Journal of Bryology*, 13, 571-578.

Rydin, H. and McDonald, A, J. S. (1985b) Photosynthesis in *Sphagnum* at different water contents, *Journal of Bryology*, 13, 579-584.

Schaphoff, S., Lucht, W., Gerten, D., Sitch, S., Cramer, W. and Prentice, I. C. (2006) Terrestrial biosphere carbon storage under alternative climate projections, *Climatic Change*, **74**, 97-122.

Schlotzhauer, S. M. and Price, J. S. (1999) Soil water flow dynamics in a managed cutover peat field, Quebec: Field and laboratory investigations, *Water Resources Research*, **35**, 3,675-3,683.

Sillasoo, U., Mauquoy, D., Blundell, A., Charman, D., Blaauw, M., Daniell, J.R.G., Toms, P., Newberry, J., Chambers, F.M. and Karofeld, E. (2007) Peat multi-proxy data from Männikjärve bog as indicators of late Holocene climate changes in Estonia, *Boreas*, **36**, 20-37.

Silvola, U. (1986) Carbon dioxide dynamics in mires reclaimed for forestry in eastern Finland, *Annales Botanici Fennici*, **23**, 59-67.

Smith, L. C., MacDonald, G. M., Velichko, A. A., Beilman, D. W., Borisova, O. K., Frey, K. E., Kremenetski, K. V. and Sheng, Y. (2004) Siberian peatlands a net carbon sink and global methane source since the early Holocene, *Science*, **303**, 353-356.

Stone, L. and Ezrati, S. (1996) Chaos, cycles and spatiotemporal dynamics in plant ecology, *Journal of Ecology*, **84**, 279-291.

Strack, M., Waddington, J. M. and Tuittila, E.-S. (2004) Effects of water-table drawdown on northern peatland methane dynamics: Implications for climate change, *Global Biogeochemical Cycles*, **18**, GB4003, doi:10.1029/2003GB002209

Surridge, B. W. J., Baird, A. J. and Heathwaite, A. L. (2005) Evaluating the quality of hydraulic conductivity estimates from piezometer slug tests in peat, *Hydrological Processes*, **19**, 1,227-1,244.

Swanson, D. K. and Grigal, D. F. (1988) A simulation model of mire patterning, *Oikos*, **53**, 309-314.

Tilman, D. and Wedin, D. (1991) Dynamics of nitrogen competition between successional grasses, *Ecology*, **72**, 1,038-1,049.

Tokida, T., Miyazaki, T., Mizoguchi, M. and Seki, K. (2004) '*In situ* accumulation of methane bubbles in a natural wetland soil', *European Journal of Soil Science*, **56**, 389-396.

Turetsky, M. R., Crow, S. E., Evans, R. J., Vitt, D. H. and Wieder, R. K. (2008) Trade-offs in resource allocation among moss species control decomposition in boreal peatlands, *Journal of Ecology*, **96**, 1,297-1,305.

Turunen, J. (2008) Development of Finnish peatland area and carbon storage 1950-2000, *Boreal Environment Research*, **13**, 319-334.

Turunen, J., Tomppo, E., Tolonen, K. and Reinikainen, A. (2002) Estimating carbon accumulation rates of undrained mires in Finland – application to boreal and subarctic regions, *Holocene*, **12**, 69-80.

van Breemen, N. (1995) How *Sphagnum* bogs down other plants, *Trends in Ecology and Evolution*, **10**, 270-275.

van Dam, H. (1988) Acidification of three moorland pools in The Netherlands by acid precipitation and extreme drought periods over seven decades, *Freshwater Biology*, **20**, 157-176.

Von Post, L. and Granlund, E. (1926) Sodra Sveriges Tortillangar I, *Sveriges Geologiska Undersoetning*, **C335**, 125.

Vorob'ev, P. K. (1963) Investigations of water yield of low lying swamps of Western Siberia, *Transactions of the State (Soviet Union) Hydrologic Institute*, **105**, 45-79.

Walker, D. and Walker, P.M. (1961) Stratigraphic evidence of regeneration in some Irish bogs, *Journal of Ecology*, **49**, 169-185.

Walter, K. M., Zimov, S. A., Chanton, J. P., Verbyla, D. and Chapin, F. S. III (2006) Methane bubbling from Siberian thaw lakes as a positive feedback to climate warming, *Nature*, **443**, 71-75.

Watson, A. J. and Lovelock, J. E. (1983) Biological homeostasis of the global environment: the parable of Daisyworld, *Tellus*, **35B**, 254-289.

Werner, B. T. (1999) Complexity in natural landform patterns, *Science*, **284**, 102-104.

Weider, K. R. (2001) Past, present, and future peatland carbon balance: an empirical model based on ^{210}Pb-dated cores, *Ecological Applications*, **11**, 327-342.

Wells, C. E. and Wheeler, B. D. (1999) Evidence for possible climatic forcing of late-Holocene vegetation changes in Norfolk Broadland floodplain mires, UK, *The Holocene*, **9**, 595-608.

Wildi, O. (1978) Simulating the development of peat bogs, *Vegetatio*, **37**, 1-17.

Wu, X. B., Thurow, T. L. and Whisenant, S. G. (2000) Fragmentation and changes in hydrologic function of tiger bush landscapes, south-west Niger, *Journal of Ecology*, **88**, 790-800.

Yabe, K. and Onimaru, K. (1997) Key variables controlling the vegetation of a cool-temperate mire in northern Japan, *Journal of Vegetation Science*, **8**, 29-36.

Youngs, E. G. (1965) Horizontal seepage through unconfined aquifers with hydraulic conductivity varying with depth, *Journal of Hydrology*, **3**, 283-296

Youngs, E. G. (1990) An examination of computed steady-state water-table heights in unconfined aquifers: Dupuit-Forchheimer estimates and exact analytical results, *Journal of Hydrology*, **119**, 201-214

Yu, Z., Beilman, D. W., and Jones, M. C. (2009) Sensitivity of northern peatland carbon dynamics to Holocene climate change. In Baird, A. J., Belyea, L. R., Comas, X., Reeve, A., and Slater, L. (eds) *Carbon Cycling in Northern Peatlands*, Geophysical Monograph Series, American Geophysical Union, Washington DC.

Zimmer, C. (1999) Life after chaos, *Science*, **284**, 83-86.

Zobel, M. (1988) Autogenic succession in boreal mires – a review, *Folia Geobotanica & Phytotaxonomica*, **23**, 417-445.